UNIVERSITY COLLEGE LONDON

Clinical and molecular genetics of Usher syndrome

by

Zubin Saihan

A thesis submitted in partial fulfillment for the
degree of Doctor of Philosophy

in the
Institute of Ophthalmology
UCL

April 2011

Declaration of Authorship

I, AUTHOR NAME, declare that this thesis titled, 'Clinical and molecular genetics of Usher syndrome' and the work presented in it are my own. I confirm that:

- This work was done wholly or mainly while in candidature for a research degree at this University.
- Where any part of this thesis has previously been submitted for a degree or any other qualification at this University or any other institution, this has been clearly stated.
- Where I have consulted the published work of others, this is always clearly attributed.
- Where I have quoted from the work of others, the source is always given. With the exception of such quotations, this thesis is entirely my own work.
- I have acknowledged all main sources of help.
- Where the thesis is based on work done by myself jointly with others, I have made clear exactly what was done by others and what I have contributed myself.

Signed: _____

Date: _____

"Never put off till tomorrow what you can do the day after tomorrow."

Mark Twain

UNIVERSITY COLLEGE LONDON

Abstract

Institute of Ophthalmology
UCL

Doctor of Philosophy

by Zubin Saihan

Usher syndrome (USH) is the name given to a group of recessively inherited disorders characterised by hearing loss, progressive visual loss due to a retinal degeneration termed retinitis pigmentosa (RP) and in some cases vestibular dysfunction. It is the most common form of syndromic RP and is clinically and genetically heterogeneous. There are three clinical subtypes termed USH1, USH2 and USH3, which are defined by the severity of hearing loss and vestibular dysfunction with visual loss due to RP being common to each subtype. To date, mutations in nine genes have been associated with the three clinical subtypes of Usher syndrome as well as non-syndromic hearing loss and RP. This wide spectrum of clinical and genetic variability provides challenges to clinicians in making a diagnosis of Usher syndrome and delivering prognostic information to affected individuals, whilst the genetic heterogeneity presents problems to geneticists attempting to achieve a molecular diagnosis.

This study aims to address these issues by determining the distribution of clinical and molecular subtypes of USH in the United Kingdom (UK). This study represents an original contribution to the knowledge of Usher syndrome, as it is the first prospective clinical study to sequence the coding regions of each of the nine genes associated with this disorder in 187 affected families regardless of their clinical subtype. Detailed ophthalmic phenotyping was performed in 219 individuals.

This comprehensive strategy of molecular analysis afforded the opportunity to interrogate for the possibility of digenic effects for which no evidence was found. This strategy enabled the discovery of an atypical and novel phenotype associated with the USH1C gene. A molecular diagnosis was achieved in 80% of families with Usher syndrome and the ophthalmic phenotype of a large cohort of affected individuals with Usher syndrome has been further delineated.

This study has resulted in a large cohort of UK patients with a confirmed molecular diagnosis and detailed ophthalmic phenotyping, which will provide a framework for subsequent longitudinal studies enabling the characterisation of how visual function progresses over time. Understanding the natural history of this disorder in genotyped individuals will help pave the way for subsequent gene-directed therapy studies in the future.

Acknowledgements

This study was supported financially from the generous contributions from the British Retinitis Pigmentosa Society, Big Lottery Fund and The Special Trustees of Moorfields Eye Hospital.

Thanks to my supervisors Dr Andrew Webster and Prof Tony Moore as well as to Dr Maria Bitner-Glindzicz for your support and encouragement throughout the study. It has been a pleasure working with you all and I would like to thank you all for giving me the opportunity to get involved in the study and help keep me in gainful employ over the years - much appreciated!

Extra special thanks to my lovely wife Carys for your constant encouragement and tolerance, especially around writing up time! Thanks to my friends and family for helping to simultaneously encourage and (mainly) distract me from writing up.

Thanks to Mrs Mary Guest, an inspirational lady who helped get this study off the ground. Thank you Mary for your many kind words over the years and securing funding for me to present at the 14th Deafblind International (DbI) World Conference, Perth, Australia in 2007.

Dr Polona Le Quesne Stabej helped complete the lion-share of molecular analysis in this study. It has been a real pleasure working with you Polona. Thanks also to all the other clever scientists who showed me what to do/not to do in the lab.

Thanks to Miss Liz Cook who was employed as the family coordinator on the study and also helped recruit families into the study. Liz did a great job in helping families get to London for clinical examinations as well as organising skilled sign language interpreters and hands-on signers enabling me to communicate effectively with study participants. Liz, thanks for your hard work over the years!

Thanks to the people at Moorfields Eye Hospital, Miss Felicia Ikeji and Mr Ed Jones for helping with the OCT scans, Miss Sally Falk for helping me find quiet rooms to see patients, thanks to the Medical Illustration department headed by Mr Kulwant Sehmi and thanks to Mrs Eileen Irving for her help with assisting families navigate around Moorfields.

I would like to acknowledge Prof. Karen Steel from the Sanger Centre and all her laboratory group, particularly Mr John Ambrose for collaborating with us and giving us the opportunity to use the high throughput sequencing facilities at the Sanger which allowed us to extract more genetic data than we had ever anticipated at the start of the study.

Lastly and perhaps most importantly I would like to thank all the families that gave up their time and effort to contribute to this study. It has been a great pleasure to meet you all and many of you have been a genuine source of inspiration to me.

Contents

List of Figures

List of Tables

Abbreviations

USH Ūsher syndrome

USH1 Ūsher syndrome type 1 (clinical diagnosis)

USH2 Ūsher syndrome type 2 (clinical diagnosis)

USH3 Ūsher syndrome type 3 (clinical diagnosis)

MYO7A Mȳosin VIIA gene

USH1C ŪSH1C (also known as 'Harmonin') gene

CDH23 Cādherin gene

PCDH15 Pṛotocadherin 15 gene

USH1G SĀNS gene

USH2A Ūsherin gene ***GPR98*** GṚP98 gene

WHRN Whirlin gene ***USH3A*** Clarin-1 gene

USH1A Ūsher syndrome due to USH1A locus (molecular diagnosis)

USH1B Ūsher syndrome due to *MYO7A* gene (molecular diagnosis)

USH1C Ūsher syndrome due to *USH1C* gene (molecular diagnosis)

USH1D Ūsher syndrome due to *CDH23* gene (molecular diagnosis)

USH1E Ūsher syndrome due to USH1E locus (molecular diagnosis)

USH1F Ūsher syndrome due to *PCDH15* gene (molecular diagnosis)

USH1G Ūsher syndrome due to *SANS* gene (molecular diagnosis)

USH2A Ūsher syndrome due to *USH2A* gene (molecular diagnosis)

USH2B Ūsher syndrome due to USH2B locus (molecular diagnosis)

USH2C Ūsher syndrome due to *GPR98* (previously *MASS1*) gene (molecular diagnosis)

USH2D Ūsher syndrome due to *WHRN* gene (molecular diagnosis)

USH3A Ūsher syndrome due to *USH3A* gene (molecular diagnosis)

SNHL S̄ensorineural hearing loss

RP R̄etinitis Pigmentosa

ARRP Ā utosomal Recessive Retinitis Pigmentosa

Dedicated to Purmaya

Chapter 1

Introduction

1.1 Usher syndrome

1.1.1 Definition

Usher syndrome (USH) is the name given to a group of recessively inherited disorders in which there is dual sensory impairment of the audiovestibular (hearing and balance) and visual systems. There are over 50 known human syndromes which include symptoms of combined visual and hearing loss (sometimes termed "deafblindness") of which Usher syndrome is the most common [1], representing over 50 percent of deafblind adults [2–4] [5–7].

A "syndrome" can be defined as a group of symptoms (or signs) that collectively indicate or characterize a disease. Thus Usher syndrome is often referred to as a *syndromic* form of hearing impairment or a *syndromic* form or retinitis pigmentosa (RP), as both hearing loss and RP can also occur in isolation.

1.1.2 History of Usher syndrome

Following the invention of the ophthalmoscope by German optical physiologists during the mid-nineteenth century, the occurrence of a pigmentary retinopathy with deafness was observed in three out of five siblings by the German ophthalmologist Alfred von Graefe and reported by his cousin Albrecht von Graefe in 1858 [8].

Three years later in 1861, his student Richard Liebreich reported a survey of deaf inhabitants from Berlin, in whom he noted the frequent presence of retinal pigmentation in individuals with congenital deafness [9]. Significantly he emphasised the genetic nature

of the disease by commenting on the presence of these findings in Jewish consanguineous families or in families with several members affected in different generations.

Following these reports of heritable pigmentary retinopathy and deafness the disease finally received its eponymous name from the Scottish ophthalmologist Charles Usher, who examined a cohort of 69 cases of retinitis pigmentosa reporting 19 cases with additional hearing loss. He also emphasised the heritable nature of their disease [10].

Although the name "Usher syndrome" is still used to this day, it has also been referred to as Hallgren syndrome, Usher-Hallgren syndrome, RP-dysacusis syndrome, and dystrophia retinae dysacusis syndrome by others [11][1].

The variability in the severity of hearing and visual loss has been noted since the early literature at the start of the last century [12][13] and following the confirmation of genetic heterogeneity of Usher syndrome in the early 1990s, Smith et al. [14] proposed clinical criteria that could be used to divide the syndrome in to two distinct phenotypic forms based on the severity of hearing loss. USH1 (Usher syndrome type 1) is associated with profound hearing loss preventing the attainment of language and vestibular abnormalities, whilstUSH2 (Usher syndrome type 2) is associated with moderate to severe congenital hearing loss.

USH3 (Usher syndrome type 3) is distinguished from USH1 and USH2 by onset of deafness later in life (sometimes referred to as "postlingual") progressive hearing loss, variable vestibular dysfunction and onset of RP usually in the second decade of life.

1.1.3 Clinical characterisation of Usher syndrome

Historically Usher syndrome has been divided into three clinical subtypes, USH1, USH2 and USH3, all manifesting combined sensorineural hearing loss and visual loss due to a progressive retinal degeneration termed retinitis pigmentosa (RP). Vestibular dysfunction may also be a feature for USH1 and USH3 [15]. The three subtypes are distinguished purely on the severity and progression of hearing loss and the presence or absence of vestibular dysfunction, with visual loss due to RP being common to all. It is important to appreciate that visual symptoms do not define the subtypes.

USH1 is the most severe audiovestibular phenotype, with congenital profound hearing loss and absent vestibular function (vestibular arreflexia). USH2 accounts for over a half of all Usher syndrome cases in the western world [16, 17] and is characterised by congenital moderate to severe hearing impairment, generally more severe in the higher frequencies, with normal vestibular function. In USH3 the hearing loss is progressive and the vestibular function variable. USH3 is rare in most populations apart from in

Finland [18–20] and among Ashkenazi Jews where it may be responsible for over 40 percent of USH cases in these population groups [21–23].

The onset of night-blindness, termed "nyctalopia", is generally the first visual symptom of the RP. This has been reported as occurring at an earlier age in USH1 than in USH2, however due to the overlap between the age of onset of visual symptoms in the USH subtypes, it cannot be regarded as a reliable diagnostic discriminator [24–29]

The numbers of patients affected by the three distinct USH types is unequal

During the 1990s, each of three clinical forms of USH were shown to be genetically heterogeneous. Initially USH1 was reported as being the most prevalent subtype; however this probably represented sample bias, as the groups studied were all *profoundly* deaf (thus reducing likelihood of picking up USH2 cases) [3, 13, 30].

Studies in Europe generally demonstrate that USH2 is more common than USH1, with reported percentages in the region of 56 - 75% (USH2) and 25 - 44% (USH1) [4, 6, 7, 24].

The USH3 subtype occurs in a much smaller proportion of Usher syndrome, apart from in Finnish and Ashkenazi Jewish populations, where it accounts for up to 40% of cases, due to intermarriage and "founder effects". [23, 31].

1.1.4 Reported prevalence of Usher syndrome

The "prevalence" of Usher Syndrome can be defined as the number of people affected with Usher Syndrome in a given population at any given time and reports range from 1 in 23,000 in the U.S. [3], 1 in 29,000 in Scandinavia and 1 in 12,500 in Germany [32]. The prevalence of retintis pigmentosa in the general population is estimated at about 1 in 3700 - 4450 [33]; suggesting that Usher syndrome may make up approximately 17 percent of retinitis pigmentosa cases [34].

Accurate estimates of prevalence require a high rate of diagnostic accuracy, which may prove difficult in the case of Usher syndrome. Hearing loss is extremely common and can present at any time from infancy to old age. About 1 per 1000 children in the UK is born with a permanent hearing impairment and a similar number develop this during early childhood [35]. Approximately half of all congenital hearing loss is thought to be of genetic origin[36].

Thus, Usher syndrome is found more frequently amongst those with retinitis pigmentosa than those that are deaf.

1.1.5 Importance of screening deaf children for syndromic causes of deafness

In the absence of an affected family member, a child with Usher syndrome is likely to initially receive a (mis)diagnosis of nonsyndromic congenital hearing loss, with the correct diagnosis not being considered until the onset of visual symptoms later in life. Thus, effective ophthalmological and/or genetic tests are important for children with congenital sensorineural hearing loss in order to exclude Usher syndrome.

The prevalence of hearing impairment increases with age such that by the fifth decade of life 2.3% of the population experiences hearing loss exceeding 40dB and this figure rises to 30% by the eighth decade [37, 38].

Syndromic hearing loss accounts for about a third of all cases of hearing loss with a genetic aetiology [38]. Screening hearing impaired children for *syndromic* causes of hearing loss important for a number of reasons.

1. Inheritance patterns may be known for specific syndromic causes of deafness, allowing for genetic counselling of the family in the absence of a molecular diagnosis.
2. Molecular diagnosis for many of the commoner forms of syndromic deafness may be available, which has implications for genetic counselling [38].
3. Diagnosis will allow monitoring of known complications of the syndrome, such as renal, ocular or endocrine disease [38].
4. Early diagnosis may allow preparation for the physical and emotional impact of the approaching additional sensory loss [11]. e.g. a deaf person with USH learning hands-on signing prior to the onset of severe visual impairment.

Even if no 'cure' for a genetic disease exists, it is still important for a clinican to arrive at an accurate clinical and molecular diagnosis as this may enable them to deliver important prognostic information regarding disease progression which may have a significant influence upon important career and lifestyle choices to allow for appropriate genetic counselling. This is particularly relevant in the case of Usher syndrome, where a number of other rare syndromic syndromes resulting in dual sensory loss may manifest similar symptoms.

1.2 Molecular genetics of Usher syndrome

Since the first gene for USH was discovered in 1995, a total of eleven loci including nine genes have been identified as causing the various clinical subtypes of USH [17, 21, 39–50] [51, 52]. see Table1.1

The genes that are associated with the USH phenotype code for proteins of different classes which are predicted to have different functions. Moreover there is a wide spectrum of clinical variability associated with mutations in these nine genes. Mutations in five of these genes can also give rise to isolated (non-syndromic) sensorineural hearing loss [41, 48, 53–57], and mutations in *USH2A* can produce isolated (non-syndromic) autosomal recessive RP without hearing loss [58, 59].

For three of the USH1 genes, *USH1C*, *CDH23* and *PCDH15*, a genotype-phenotype correlation exists with truncating mutations causing USH, while missense/in-frame alterations result in non-syndromic deafness [43, 45–48, 54, 60, 61] [62–65]

Although such genotype-phenotype relationships exist, monozygotic twins with disease due to the same mutations in the gene *USH2A* have also been reported to manifest different phenotypes, suggesting that the severity of disease due to some of these genes may be influenced by environmental or genetic modifiers, or stochastic factors [66, 67].

1.2.1 The Usher genes

How do mutations in the nine known Usher genes that code for proteins with such different functions, give rise to similar pathology in the inner ear and retina? Both the inner ear and retina share structural and functional similarities, in that both are highly specialised neurosensory cells and both contain non-motile cilia and ribbon synapses (see Figure 1.1).

These synapses allow continuous release of neurotransmitter from the presynaptic terminals, a property thought to be necessary for high frequency transmission needed in sensory cells [68]. The ciliary structures in both the hair cell and photoreceptor are the kinocilium and connecting cilium respectively.

The localization of the USH proteins to the common synaptic and periciliary areas of the ear and eye and the identification of a network of USH protein interactions, led to the proposal of an *USH protein interactome* model functioning at these locations, explaining the pleiotropic effects of mutant USH genes [49, 69–77].

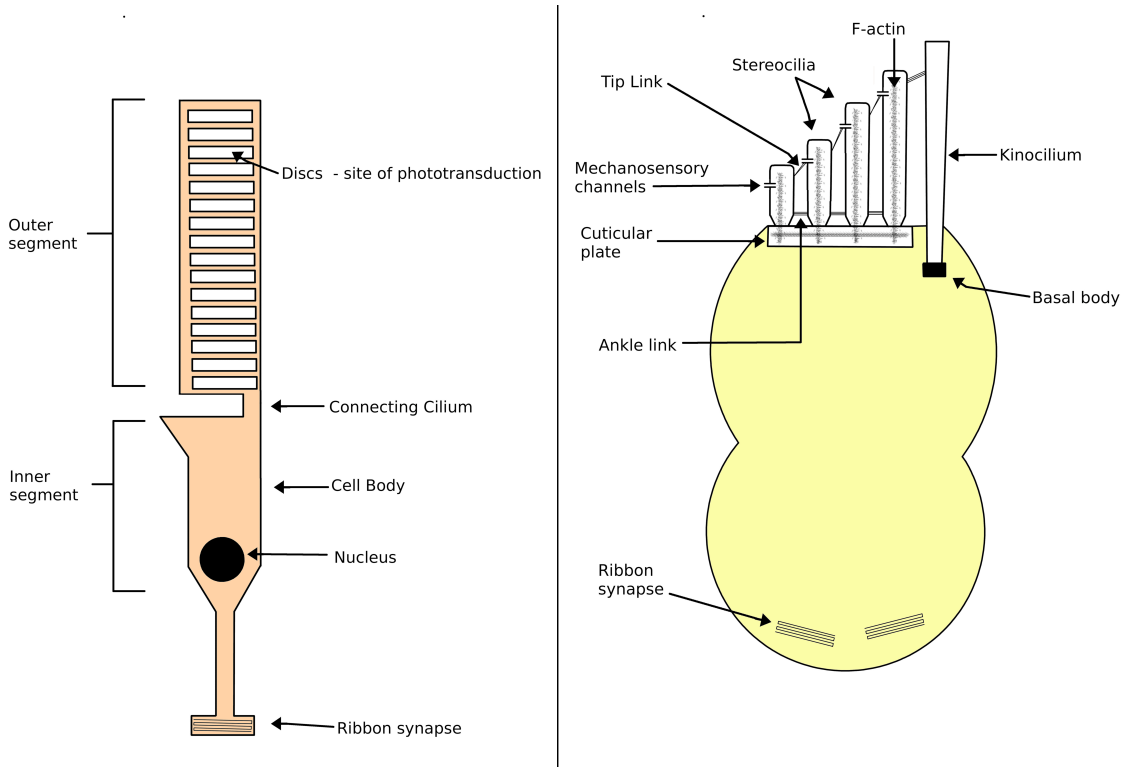

FIGURE 1.1: Schematic of (left) retinal photoreceptor cell and (right) cochlear hair cell

1.2.2 The retinal clilopathies

Usher syndrome is one of a number of inherited syndromic conditions that result in retinal degeneration secondary to dysfunction at the level of the photoreceptor connecting cilium.

A cilium is an organelle found in eukaryotic cells and are present in most human cells. There are two types of cilia, *motile* cilia (" 9+2" central configuration) and non-motile, or primary, cilia ("9+0" central configuration), which typically serve as sensory organelles.

Although USH lacks many of the systemic features associated with the more recognised *ciliopathies* such as primary ciliary dyskinesia, hydrocephalus and polycystic liver/kidney disease, it has nevertheless been classed as an example of a **"retinal ciliopathy"**, a term used to describe a retinal disorder in which the retinal connecting cilium has been shown to be involved [78]. Dysfunction of components of the photoreceptor connecting cilium are known to give rise to both syndromic and non-syndromic forms of retinal degeneration such as Retinitis Pigmentosa GTPase Regulator Interacting Protein (RPGR-IP) causing Lebers Congenital Amaurosis (LCA6) OMIM 605446 [79], and Retinitis Pigmentosa GTPase Regulator (RPGR) causing X-Linked RP (RP3) OMIM 312610 [80], which is important in photoreceptor disc morphogenesis; the Bardet-Biedl syndrome (BBS) proteins OMIM 209900, appear to play a role in intracellular transport

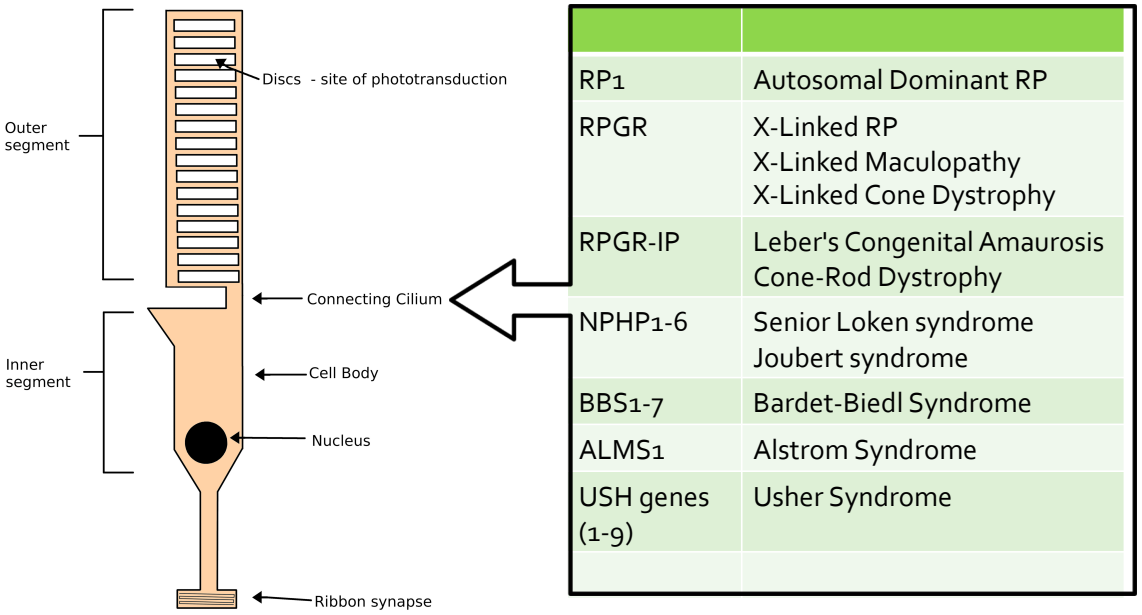

RP1	Autosomal Dominant RP
RPGR	X-Linked RP X-Linked Maculopathy X-Linked Cone Dystrophy
RPGR-IP	Leber's Congenital Amaurosis Cone-Rod Dystrophy
NPHP1-6	Senior Loken syndrome Joubert syndrome
BBS1-7	Bardet-Biedl Syndrome
ALMS1	Alstrom Syndrome
USH genes (1-9)	Usher Syndrome

FIGURE 1.2: Schematic of photoreceptor and table of the retinal ciliopathies

between the inner and outer segments of the retinal photoreceptor reviewed elsewhere [81]. Similarly to USH, the BBS proteins have recently shown to also interact forming a molecular complex, the "BBSome" that has been shown to be required for ciliogenesis [82].

1.2.3 Protein structure of the Usher genes

MYO7A, molecular subtype USH1B

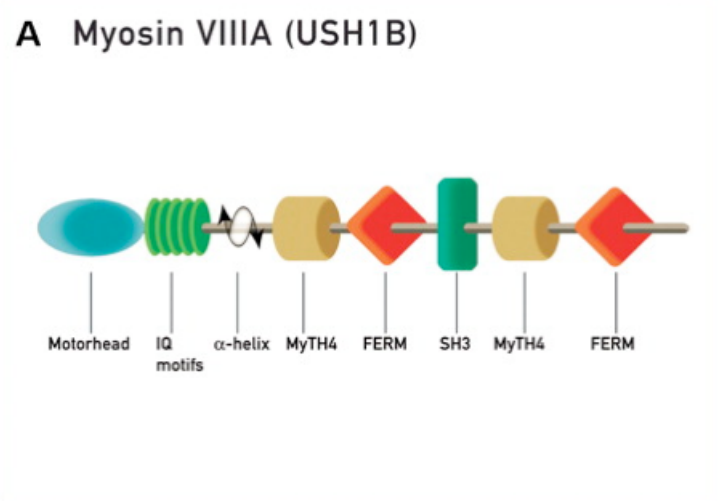

FIGURE 1.3: The Usher 1B protein, myosin 7a, consists of a motor head domain, five calmodulin binding IQ motifs, two FERM domains, two MyTH4 domains and an Src homology 3 (SRC3) domain

MYO7A (USH1B) encodes myosin 7A, an unconventional myosin, with a predicted domain structure consisting of a motor head domain, ve calmodulin-binding IQ motifs, two FERM domains, two MyTH4 domains and an Src homology 3 (SH3) domain. [83]

Mutations in *MYO7A* are responsible for Usher syndrome type 1B,[84, 85], recessively inherited atypical Usher syndrome [86, 87], autosomal recessive (DFNB2) and dominant (DFNA11) non-syndromic sensorineural deafness [88, 89]. Shaker-1 (sh1) mice have loss-of-function mutations in the orthologous gene, Myo7a, and thus serve as model of Usher 1B. Shaker-1 homozygous mice exhibit an audiovestibular but not a retinal phenotype as is found in humans with mutations in *MYO7A* [90]. Myo7a has also been shown to be important for melanosome localisation in the RPE [91].

USH1C (molecular subtype USH1C)

The USH1C gene (OMIM 605242) encodes a PDZ-containing protein called Harmonin or USH1C, which is expressed in alternatively spliced isoforms that make up three different sized subclasses [43, 44]. Mutations in this gene have been associated with Usher syndrome (the combination of generalized RP and hearing loss) [44, 92–97], as well as with non-syndromic autosomal recessive hearing loss (DFNB18) [54, 62]. *USH1C* encodes a scaffold protein that functions in the assembly of Usher protein complexes. The protein contains PDZ binding domains, which facilitates interaction with other Usher

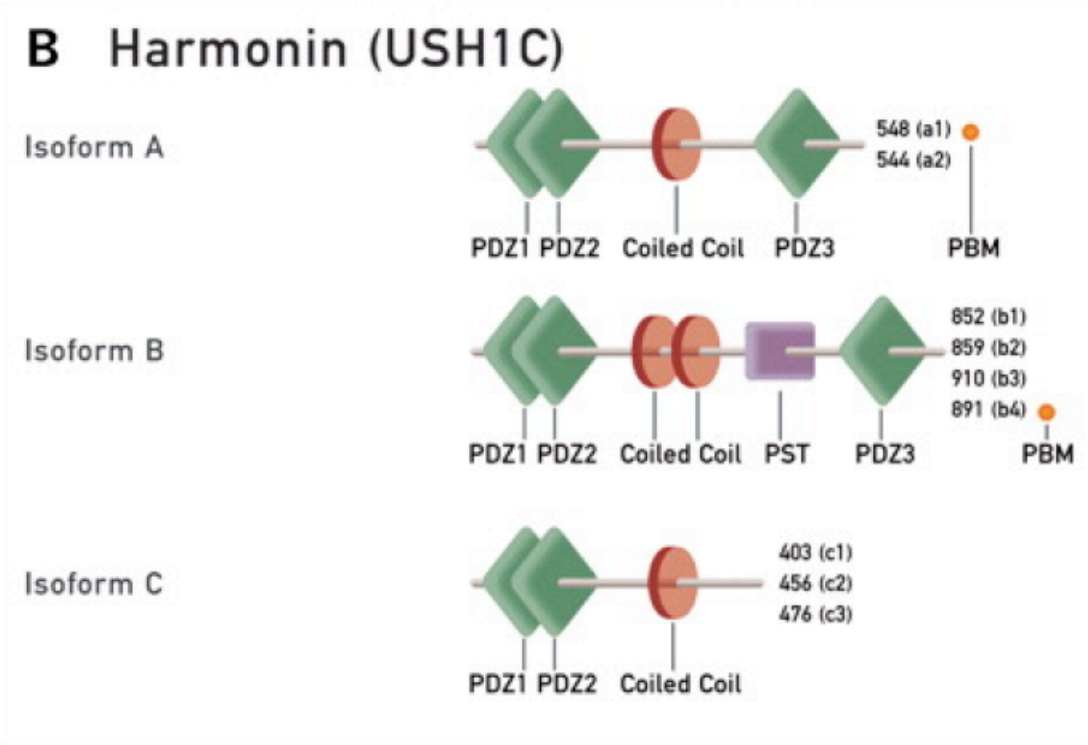

FIGURE 1.4: The USH1C protein, harmonin, of which three different classes of isoforms are identified. All three isoforms consist of two PDZ (PSD95, discs large, ZO-1) domains (PDZ1 and 2) and one coiled-coil domain. In addition, class A isoforms contain an additional PDZ domain (PDZ3). The class B isoforms contain also this third PDZ domain, a second coiled-coil domain and a proline, serine, threonine-rich region (PST). Isoforms A1 and B4 contain a C-terminal class I PDZ binding motif (PBM)

proteins, a coiled-coil region with a bipartite nuclear localization signal and a PEST degradation sequence.

There appears to be some genotype-phenotype correlation with hypomorphic alleles causing hearing loss without RP, whilst more severe truncating mutations result in hearing loss and RP [54, 62]. The audiovestibular phenotype associated with mutations in USH1C is one of prelingual profound hearing loss with absent peripheral vestibular function when associated with RP [43, 44, 97], and with normal vestibular function when associated with non-syndromic hearing loss [54, 62].

CDH23 (molecular subtype USH1D)

CDH23 is one of the two USH genes from the cadhedrin family of genes encoding calcium dependent cell-cell adhesion glycoproteins. The protein encoded by this gene is a large transmembrane protein composed of an extracellular domain and expressed in the neurosensory epithelium. Cadhedrins preferentially interact with themselves in connecting

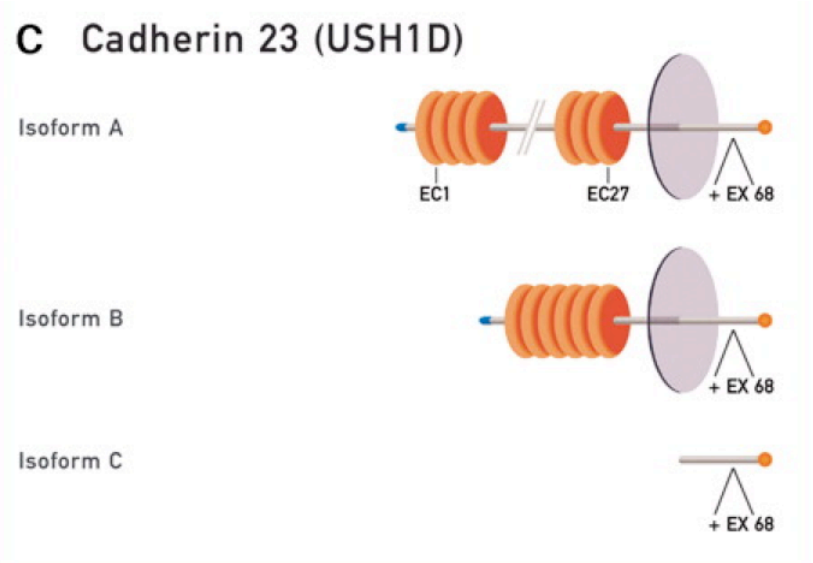

FIGURE 1.5: Cadherin 23 (USH1D) is represented by three different isoforms. Isoform A is composed of 27 Ca2+-binding extracellular cadherin domains (EC1-27), a transmembrane domain (grey disks) and a short intracellular domain with a C-terminal class I PBM. Isoform B is similar to isoform A, but only contains the last six EC domains. Isoform C only consists of the intracellular domain and C-terminal PBM.

cells and are required for establishing and/or maintaining organization of the stereocilia bundle of hair cells in the cochlea and the vestibule during late embryonic/early postnatal development. Null mutations in *CDH23* result in retinal and audiovestibular dysfunction (USH1D) whereas hypomorphic alleles may affect hearing alone (DFNB12).

Two PDZ domains in the *USH1C* encoded protein harmonin, interact with two complementary binding surfaces in the cadhedrin-23 cytoplasmic domain. As murine models of the *CDH23* ortholog Cdh-23 have splayed stereocilia, it was postulated that via their interaction with harmonin, form a transmembrane complex that connects stereocilia into a bundle, and that defects in the formation of this complex result hearing loss associated with defects in the gene [98] in mice and humans.

Kazmierczak et al. (2007) demonstrated that CDH23 and PCDH15 (605514), 2 cadherins that are linked to inherited forms of deafness in humans, interact to form tip links, extracellular filaments that connect the stereocilia and are thought to gate the mechanoelectrical transduction channel. Immunohistochemical studies using rodent hair cells demonstrated that two cadhedrin-related USH genes cadhedrin-23 and protocadherin-15 are localised to the upper and lower part of tip links, respectively.

PCDH15 (molecular subtype USH1F)

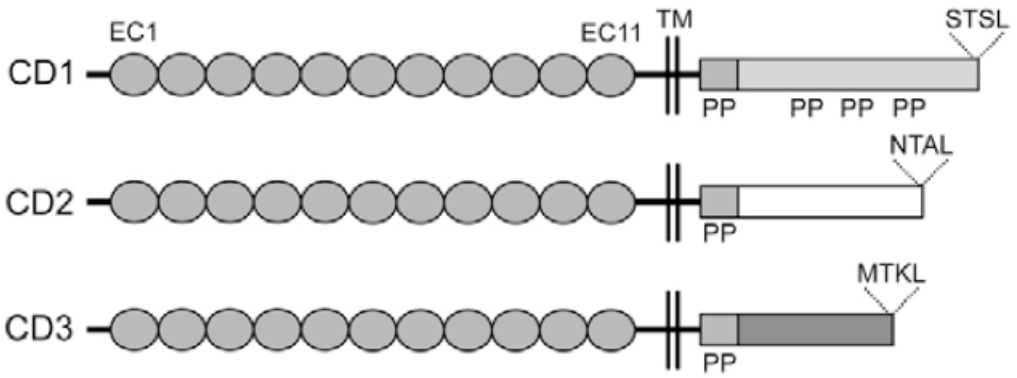

FIGURE 1.6: Like cadherin 23, the non-classical cadherin protocadherin 15 (USH1F) consists of either 11 (isoform A) or one (isoform B) EC domain, a transmembrane domain and a C-terminal class I PBM

Along with *CDH23*, *PCDH15* is the other Usher gene that is a member of the cadherin superfamily and both genes are components of kinociliary links, transient lateral links and tip links between adjacent cochlear sterocilia [73, 99–103].

RT-PCR and immunohistochemistry has demonstrated PCDH15 expression in both retina and cochlea [46], and was further localised to inner ear hair cell stereocilia and to retinal photoreceptors by immunocytochemistry [63].

Similarly to *USH1C* and *CDH23*, missense mutations in PCDH15 have been found to cause DFNB23 [104, 105], while more severe mutations (splicing, frameshift, nonsense, large deletions) cause USH1F.

PCDH15 is expressed in several isoforms differing in their cytoplasmic domains. Recent knock-out mouse model studies have shown that mice lacking PCDH15-CD2 develop tip links, but are deaf, whereas surprisingly, mice lacking PCDH15-CD1 and PCDH15-CD3 isoforms form normal hair bundles and tip links and maintain hearing function [106].

The majority of mutations identified in the PCDH15 gene have been point mutations, whereas large deletions, which can escape routine screening methods, may also form a significant proportion of PCDH15 mutations [65, 107].

USH1G (molecular subtype USH1G)

USH1G encodes a scaffolding protein that contains three ankyrin-like domains and a SAM (sterile alpha motif) domain with a class I PDZ-binding motif at its C-terminal end. USH1G is the smallest Usher gene comprising of only three exons, two of which are coding. The SANS protein interacts with harmonin, myosin VIIa and whirlin. SANS has

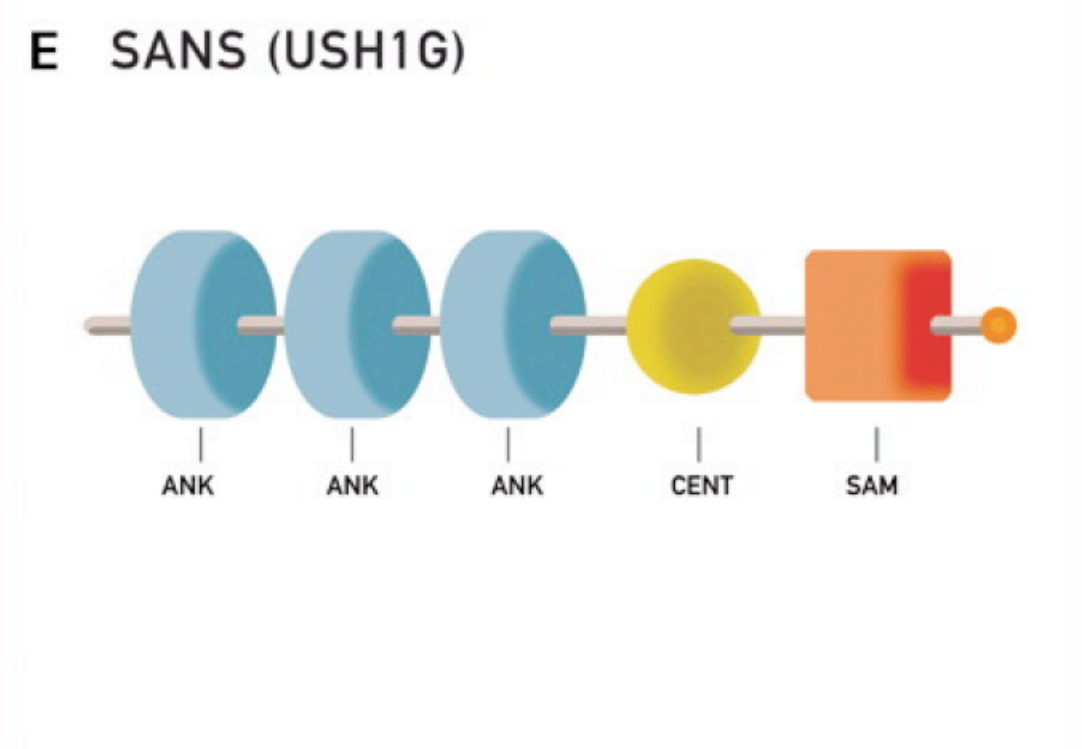

FIGURE 1.7: The scaffold protein SANS (USH1G) consists of three ankyrin domains (ANK), a central region (CENT), a sterile alpha motif (SAM) and a C-terminal class I PBM

been shown to be a critical component of the tip-link complex, a structure controlling actin polymerization in stereocilia, where it interacts with CDH23 and PCDH15 [108].

Only a handful of mutations have been identified in Usher populations across the world, suggesting that this gene makes a small contribution to the molecular cause of Usher syndrome [49, 109, 110].

USH2A (molecular subtype USH2A)

The Usherin transcript was originally reported to be 5 kb [17], encoding a 170-kDa protein which was predicted to be a secreted, extracellular protein. Since the start of the work presented in this thesis, other researchers identified a further 51 exons were discovered. This larger transcript predicted a 600-kDa protein which is predicted to be anchored on the cell membrane with a large extracellular domain and a short C-terminal PDZ-binding motif. The long Usherin isoform has been shown to be the predominant form in murine photoreceptor cells. Usherin is thought to be required in the long-term maintenance of photoreceptor cells, as USH2A null mice develop a normal retina which subsequently degenerates [111].

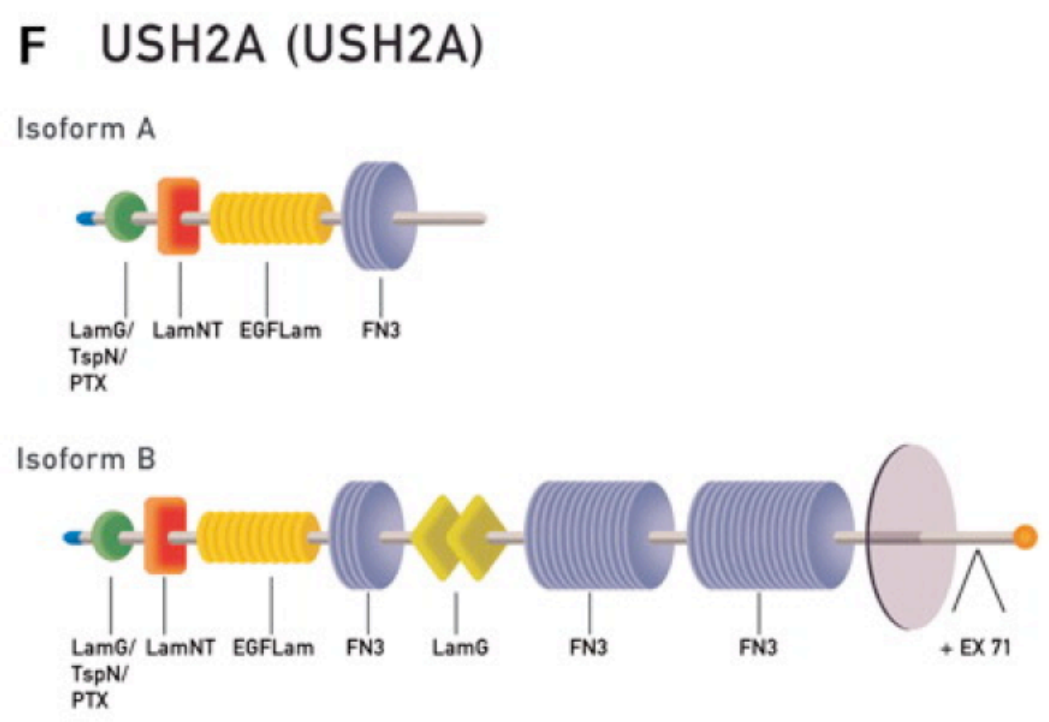

FIGURE 1.8: Isoform A of the Usher 2A protein (USH2A) contains an N-terminal thrombospondin/pentaxin/laminin G-like domain, a laminin N-terminal (LamNT) domain, ten laminin-type EGF-like (EGF Lam) and four fibronection type III (FN3) domains. In addition to this region, isoform B contains two laminin G (LamG), 28 FN3, a transmembrane domain and an intracellular domain with a C-terminal class I PBM.

Usherin is expressed transiently in murine models and is postulated to have a role in the postnatal maturation of cochlear hair cells [77, 111].

GPR98 (molecular subtype USH2C)

GPR98 is a large gene encompassing 605 kb. Three human *GPR98* mRNA isoforms are known, of which Isoform b is the largest and it contains all 90 exons. All three isoforms are expressed during the development of the central nervous system and are also found in the fetal retina. The translated *GPR98* protein is one of the largest proteins found in humans and belongs to the large N-terminal family B (LNB) of seventransmembrane segment (7TM) receptors; specifically, to the subfamily with a G-protein-coupled proteolysis site (GPS) for G-protein signalling. The protein has several domains, each with its own function [112].

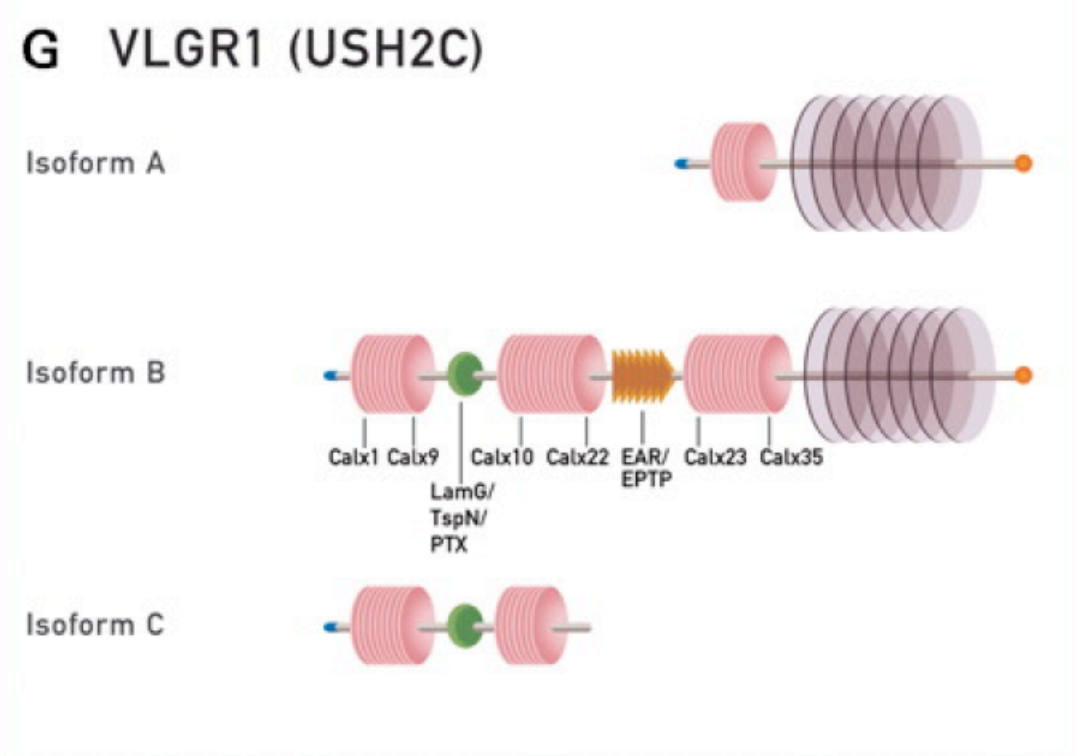

FIGURE 1.9: Isoform B of the very large G-coupled protein receptor, *GPR98* (formerly known as *VLGR1* or *MASS1*), contains a thrombospondin/pentaxin/laminin G-like domain, 35 Ca2+-binding calcium exchanger (Calx) domains, seven EAR/EPTP repeats, a seven-transmembrane region and an intracellular domain containing a C-terminal class I PBM. (H) Clarin-1, the USH3A protein, only contains four (isoform A) or one transmembrane (isoform C) domain.

WHRN (molecular subtype USH2D)

The most recent USH gene to be identified is *WHRN* that encodes the scaffold protein Whirlin, previously reported to underlie non-syndromic deafness linked to the locus *DFNB31* and to cause deafness in the whirler mouse mutant [74]. Mutations in *WHRN* (USH2D) were identified in a German USH2 family, previously excluded for all other known Usher loci [52]. Prior to the identification of pathogenic mutations in *WHRN*, it was proposed as a candidate gene for USH2 due to its reported interactions with the other two USH2 proteins, Usherin and GPR98, as well as co-localizing with these proteins in the retina and inner ear [74]. Whirlin is a PDZ scaffold protein and functions similar to *USH1C* in the Usher protein interactome. It is expressed both in the ear and the eye throughout development.

CLRN1 (molecular subtype USH3A)

CLRN1 belongs to a superfamily of four-transmembrane proteins that includes the tetraspanin and claudin families. Tetraspanins are considered to be structural proteins

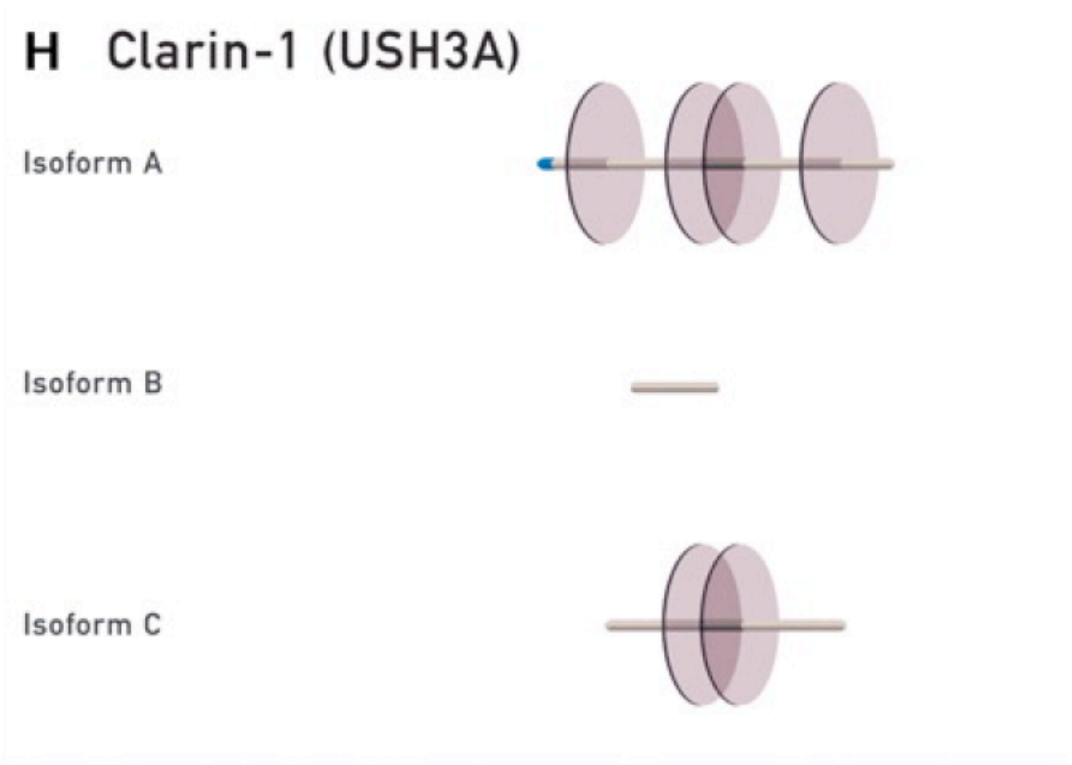

FIGURE 1.10: Clarin-1, the USH3A protein, only contains four (isoform A) or one transmembrane (isoform C) domain

that interact laterally with other membrane proteins such as ion channels, integrins, and other tetraspanins [113, 114] Despite the genetic and phenotypic characterization in humans, the molecular function of *CLRN1* remains elusive [115].

Molecular genetic advancements since the start of the study

Since the start of this study in 2003 research groups from around the world made significant breakthroughs regarding the clinical and molecular aspects of Usher syndrome. As many of these findings were significant and influenced the design of this study, some are mentioned below in reverser chronological order.

A new locus for USH1

A new locus for USH1, designated USH1H has recently been reported following genome-wide linkage scanning of a two large Pakistani consanguineous families [116]. This locus overlaps the non-syndromic deafness locus DFNB48 raising the possibility that these two disorders may be caused by the same gene, as is the case for other Usher genes see 1.1, [116].

USH Loci withdrawn

Two previously reported loci, USH1A and USH2B (3p23-24.2) were recently withdrawn by their original authors. New pedigree information and additional molecular analysis in the original French families used for the initial USH1A locus mapping studies identified *MYO7A* as the causative gene in 7 of the 9 original families [117][75]. The USH2B locus was also recently withdrawn [75].

1.2.4 The Usher "protein interactome"

The Usher genes encode proteins from different classes. The USH1 proteins include the actin-based motor protein Myosin VIIa (USH1B), the cell-cell adhesion proteins, Cadherin 23 (USH1D) and Protocadherin 15 (USH1F) and the scaffold proteins Harmonin (USH1C) which contains PDZ domains and SANS (Scaffold protein containing ANkyrin repeats and Sam domain, USH1G). The USH2 protein Whirlin (USH2D) is also a PDZ domain-containing scaffold protein whilst the remaining two USH2 proteins USH2A, termed Usherin and GPR98 (G Protein-coupled Receptor 98) representing USH loci USH2A and USH2C respectively, are large transmembrane proteins. Clarin-1 is a membrane glycoprotein with 4-transmembrane domains from the Clarin family and to date is the only molecular cause of USH3.

PDZ (Post synaptic density, Disc-large, Zo-1 protein domains) domains are protein modules that interact via C-terminal sequences in other proteins to direct protein complex assembly in multicellular organisms [118][119].

TABLE 1.1: Usher syndrome loci, genes, proteins, additional non-syndromic phenotypes and mouse models

Clinical USH phenotype	Usher syndrome locus	*Gene symbol*	Protein Name	Protein class	Chromosomal Locus	Non-syndromic sensorineural hearing loss (nsSNHL) loci	Non-syndromic retinitis pigmentosa (ARRP) loci
	USH1A*						
USH1	USH1B	*MYO7A*	Myosin VIIa	motor protein	11q13.5	DFNB2/DFNA11	
USH1	USH1C	*USH1C*	Harmonin or USH1C	'scaffold' protein	11p15.1	DFNB18	
USH1	USH1D	*CDH23*	Cadherin-23	cell-cell adhesion protein	10q21-q22	DFNB12	
USH1	USH1E	*USH1E*	Unknown		21q21		
USH1	USH1F	*PCDH15*	Protocadherin 15	cell-cell adhesion protein	10q21-q22	DFNB23	
USH1	USH1G	*USH1G*	Sans	'scaffold' protein containing ankyrin repeats and SAM domain	17q24-q25		
USH1	USH1H	*unknown*			15q22-23	DFNB31	
USH2	USH2A	*USH2A*	Usherin	transmembrane protein	1q41		RP39
USH2	USH2B**						
USH2	USH2C	*VLGR-1*	Mass1	seven transmembrane receptor protein	5q14-q21		
USH2	USH2D	*WHRN*	Whirlin	'scaffold' protein	9q32-q34	DFNB31	
USH3	USH3A	*USH3A*	Clarin1	transmembrane protein	3q21-q25		

* The proposed locus USH1A was withdrawn as Gerber et al. (2006) presented evidence that the French families ascribed to this locus harboured mutations in the MYO7A gene or mapped to other loci

** The proposed locus USH2B has been reported as withdrawn Kremer et al. (2006)

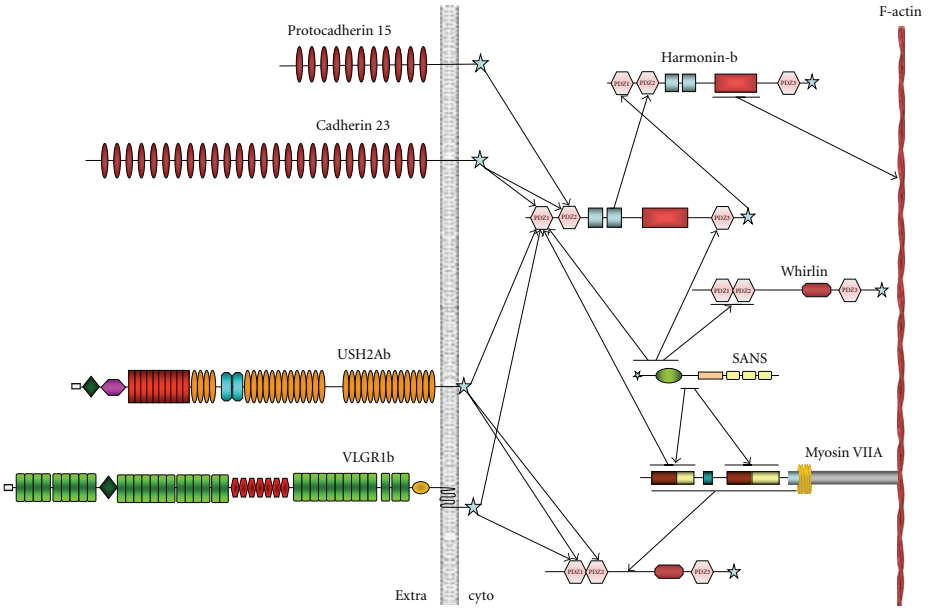

FIGURE 1.11: Schematic diagram illustrating the deciphered interactions within the USH protein network interactome adapted from van Wijk et al. 2006 courtesy of Millan et al. 2011

The PDZ containing proteins Harmonin, Whirlin and SANS are thought to facilitate such protein interactions. In the inner ear, Harmonin and Whirlin are thought to mediate these interactions whilst in the retina Whirlin and SANS appear to fulfil this role[77][69][71][72][74][75][76].

In addition, Harmonin [98][71], Whirlin [120], SANS [71] and possibly Myosin VIIa[75] also form homodimers. The existence of different protein isoforms secondary to splicing variations adds a further layer of complexity to these potential interactions, since some isoforms appear to be much more abundant in some tissues than others. The only known USH3 protein, Clarin-1 is less well understood than the other USH proteins. It is the only USH protein in which the retinal cell and subcompartment localization are unknown and does not yet fit in to the current USH interactome model [121].

1.2.5 The role of Usher proteins in the inner ear

The functional role of the Usher proteins in the inner ear concerns the morphogenesis of hair cell bundles.

The stereocilia are the mechanosensory organelles present on the apical surface of cochlear auditory and vestibular sensory hair cells, which are supported by an internal cytoskeleton of F-actin filaments. These bundles of stereocilia are neatly arranged in rows of graded height and are tethered together by a number of fibrous connections or links,

along their length (see Figure 1.1). These stereocilia are actually organelles whereas the "true" hair cell cilium is the *kinocilium*, which is transient in mammals and responsible for the orientation of the developing stereocilia. Normally, deflection of the hair cell stereocilia results in mechanical opening of channels, inflow of potassium from endolymph into the hair cell causing membrane depolarization, and release of neurotransmitter from the ribbon synapse at the basal end of the cell [122][123][124].

The USH1 proteins have been localized to the developing auditory hair bundle, specifically the growing stereocilia and/or the kinocilium in mouse models [69, 77, 101, 120, 125–127].

Protein interaction and localisation studies in mouse models have also suggested roles for some of the USH proteins in the extracellular interstereocilia links, specifically the extracellular regions of the USH1 transmembrane proteins Cadherin 23, Protocadherin 15 forming the tip links [101–103, 128, 129]. The three USH2 proteins Usherin, GPR98 and Whirlin are all transiently expressed during early cochlear development, as are the interstereocilia ankle links which are vital for the postnatal development of cochlear hair cells, supporting their involvement in the formation of a so called ankle-link molecular complex (ALC)[74, 77, 111, 130, 131]. The current model is that these extracellular interstereocilia links are anchored intracellularly by the scaffold proteins Harmonin, and Whirlin which are in turn thought to link to the actin cytoskeleton directly or via other proteins, such as Myosin VIIa (USH1B), Myosin XV, MYO1c and/or Vezatin [69, 71, 120, 129, 131, 132]. In mouse models of USH, electron microscopy of the sensory hair bundles in mutant mice demonstrate disorganised and disorientated hair cell stereocilia due to a lack their characteristic cohesion and interstereociliary links [16, 75, 76, 90, 133–136], supporting the role of the USH interactome in stereocilia development.

The actin-based motor protein Myosin VIIa (USH1B) has been hypothesised to act as a general transporter of the stereocilia USH proteins to their intended destination based on the observation that the USH proteins Harmonin [69], Protocadherin 15 [73], GPR98, Usherin, Whirlin, and Vezatin are misplaced or mislocalized in the hair bundles of the shaker-1 (MYO7A mutant) mouse model [131], and that Myosin VIIa has also been shown to interact with these proteins [132][69][71][120][131].

Unlike the other four USH1 proteins, SANS has not been localized to the stereocilia in murine models, but instead to the apical region of the outer hair cell beneath the cuticular plate at the base of the kinocilium [71]. It has been proposed that as SANS controls the traffic of USH1 proteins along microtubules and the actin cytoskeleton toward the stereocilia as it has been shown to colocalize and interacts with Myosin VIIa and/or Harmonin [71]. Although USH proteins have been localized to the hair cell

synapse, the ribbon synapse has been examined in one mouse model and found to be normal [137][75]

1.2.6 Mouse models of Usher syndrome

Mouse models of disease provide a useful tool to enable research and investigation of human disease, although the use of live animals as a research tool remains a controversial topic. Mouse models of the Usher genes have produced hearing defects analogous to those observed in human USH, with sensorineural hearing loss and impaired vestibular function, mouse models for the Usher genes have largely failed to demonstrate the visual phenotype of photoreceptor cell loss as seen in human USH (see Figure 1.1). Previous mouse models for USH display grossly normal retinas, although a mild peripheral retinal degeneration been noted histologically in the USH1C *dfcr* mutant mouse [134]. In mouse models with no gross retinal degeneration, some mutant alleles have been noted to have a mild reduction of electroretinographic responses, suggesting photoreceptor rather than synaptic dysfunction as none demonstrated an electronegative response (one in which the b-wave is smaller than the a-wave).

The reason for the lack of a convincing retinal phenotype in these rodent models is unclear, with alternative splicing of genes, functional redundancy of the Usher proteins in the murine retina and/or the slow disease progression making characterisation difficult, all proposed as theories to explain this observation [127][111]. However Liu et al. [111] recently reported the first murine model of any of the USH genes to demonstrate a clear retinal phenotype. These USH2A null mice showed an essentially normal retinal phenotype at birth but went on to develop overt photoreceptor degeneration by age 20 months, as demonstrated by light and electron microscopy and a decline in electroretinography responses [111].

1.2.7 Usher protein function in the retina

The photoreceptor cell is a highly specialized sensory neuron that is capable of phototransduction.

The connecting cilium joins the metabolically active inner segment to the photosensitive outer segment (which itself is actually a modified cilium) required for phototransduction in the outer segment are synthesised in the inner segment and then transported through the connecting cilium to the outer segment (see Figure 1.2) [138][76].

All three USH2 proteins and the USH1 proteins, with the exception of Harmonin, have been localised at/around ciliary photoreceptor structures in the retina (as well

as other ciliated tissues, such as olfactory epithelium and spermatozoa in the testis [139][140][141][21][136].

The long ectodomains of the transmembrane protiens Usherin (USH2A) and GPR98 (USH2C) have been found to extend between the photoreceptor inner segment plasma membrane and ciliary surface [111][76]. Both proteins have been proposed to form fibrous links between these two membranes which are analogous to the ankle links between adjacent stereocilia in cochlear hair cells mentioned above.

The scaffold proteins SANS (USH1G) and Whirlin (USH2D) have also been localized to the periciliary collar of the apical inner segment and the adjacent connecting cilium of murine photoreceptor cells and interact with the cytoplasmic domains of the long isoforms of the large transmembrane proteins USH2A and GPR98 [76]. SANS may be linked indirectly to microtubule-associated intracellular transport machinery [76].

There is some debate as to the localisation and function of USH proteins at the ribbon synapse

In the photoreceptor cell, hyperpolarisation leads to a reduction of neurotransmitter at the ribbon synapses in the outer plexiform layer of the retina. There have been reports of localisation of the USH proteins to both the ribbon synapse and plexiform layers of the retina [70][142][72][75][136][143][74]. However, other investigators have failed to find evidence of expression at the synapse [111][34]. Furthermore no mutant mouse phenotypes for any USH gene have demonstrated electronegative electroretinograms, as might be expected if synaptic function were compromised [34].

In vivo studies of retinal function in humans harbouring mutations in *MYO7A* (USH1B), *PCDH15* (USH1F), *USH2A* and *GPR98* (USH2C) have recently demonstrated that the primary pathology in human cases of USH due to these genes is a primary photoreceptor degeneration rather than a primary RPE or synaptic pathogenesis as has been previously suggested [144]. Evidence of synaptic dysfunction such as preserved photoreceptor layer thickness relative to impaired visual function, electronegative electroretinograms or dysplastic thickened retinas were not observed, arguing against the synapse being the major site of pathology [144]. Liu et al. [111] are the only investigators to describe an USH mouse model with a significant retinal phenotype and were unable to demonstrate Usherin immunostaining in the inner retina, RPE or the photoreceptor synapses and were unable to demonstrate defective synaptic transmission from photoreceptors to second-order retinal neurons arguing against a significant function for Usherin at the ribbon synapses.

1.3 Human molecular genetics

1.3.1 Genetic linkage

Genetic linkage mapping compares the inheritance pattern of a phenotypic trait with the inheritance pattern of chromosomal regions. By establishing pedigrees and genotyping known chromosomal regions within a family, inheritance of these loci can be traced. In a study such as this in order to determine whether certain genes might be disease causing, variable DNA sequences (polymorphic markers) within or near the gene in question one can be genotyped to help deduce inheritance within a family.

An important prerequisite for such genetic linkage analysis is that all individuals in a pedigree should have distinct (and mutually exclusive) phenotypes, namely be affected or unaffected. When employing such a strategy, an important caveat is that mendelian inheritance may not always apply. Indeed there have been reported cases of uniparental heterodisomy resulting in nonmedelian inheritance involving the gene *USH2A* [145]. Disease phenotypes may also arise from genetic mechanisms such loss of whole exon, gene or chromosome.

Assuming Usher syndrome is a monogenic disorder with mendelian recessive inheritance, the tracking of alleles in consanguineous and non-consanguineous pedigrees can be extremely useful as outlined below:

In consanguineous families

In a monogenic recessively inherited disorder in a consanguineous family, it would be anticipated that due to the shared genetic material in the pedigree, the pathogenic allele would be the same DNA sequence variant. In chromosomal terms this would mean that two copies of the same stretch of chromosome (containing this pathogenic allele) could have been inherited, resulting in two pathogenic alleles producing the disease phenotype.

If we assume that this pathogenic allele is the same, then so should a finite genetic distance of chromosome encompassing the allele. Within this area, other polymorphic sequence variants would by definition also be expected be identical, resulting in an area of homozgosity delimited by crossovers at either end. Investigating chromosomal regions that display homozygosity for alleles is termed **homozygosity mapping** and is a useful way to determine or search for areas of the genome that are homozygous and thus in consanguineous pedigrees good candidate regions for containing the putative pathogenic allele.

In non-consanguineous families

In cases where two *different* pathogenic alleles in the same gene are inherited from each parent, which would be more probable in the case of families that are non-consanguineous, the combination of different alleles inherited can be referred to as **compound heterozygosity**.

The term **haplotype** is actually a concatenation of the term "haploid genotype". It can be used to refer to the inheritance of one of the two copies of a chromosome possessed by an individual. The inheritance of the region of chromosome can be deduced by analysing polymorphic markers close to this particular locus. Within families, transmission of genetic material is organised into a limited number of haplotypes delimited by crossovers during meiosis and representing the independent assortment of stretches of genetic material across chromosomes.

1.3.2 Polymorphic SNPs and microsatellite markers

A genetic mutation can be thought of as a DNA sequence change that deviates from normal and/or that confers some form of deleterious effect. Often DNA sequence variants at a particular locus do in fact vary in the normal population. These DNA sequence variants occur commonly in a population can be referred to as genetic **polymorphisms**. In the case of polymorphisms, no single allele can be regarded as the standard DNA sequence for that species, instead there are two or more equally acceptable variations.

In terms of prevalence, mutations can also be thought of as a rare abnormal DNA sequence variant, whereas a polymorphism a more common sequence variation. The approximate frequency cut-off for a DNA sequence variant to be thought of as a common polymorphism, is often regarded as being $\sim$1%, however, it must be stressed that this figure is entirely arbitrary [146].

The identification and tracking of such non-disease causing DNA sequence variants (polymorphic alleles) in a pedigree, can allow the inheritance at these loci to be inferred. The degree of informativity of such alleles depends on the degree of genetic heterogeneity at these loci.

When attempting to deduce mendelian inheritance of alleles in a pedigree at a given locus, if these alleles are the same, they can be referred to as **Identical By State (IBS)**. In classic mendelian inheritance, an individual receives one maternal and one paternal allele. If the parents' alleles are informative enough, it may be possible to deduce from which of the four chromosomes (two maternal and two paternal) each allele

was derived from. Thus if two siblings share alleles that can be identified as coming from specific parental chromosomes they can be referred to as being **Identical By Descent (IBD**).

SNPs

Single-nucleotide polymorphisms (SNPs) are variations in one base pair of DNA sequence at the same locus between paired chromosomes of an individual or within a species, that are not thought to be disease causing. These single base pair changes represent the majority of DNA sequence variation between human individuals and are correspondingly prevalent throughout the human genome. SNPs occur (on average) every 1,000 to 2,000 bases when two human chromosomes are compared [147–149]. The frequency of SNPs has been shown to vary between different human populations [150].

Their frequency throughout the human genome can be used to advantage as SNPs can be used to perform linkage analysis. Genetic polymorphisms such as SNPs can be used to track inheritance of these polymorphisms

Technologies exist which enable genotyping in excess of 900,000 known SNPs throughout the human genome such as the Affymetrix microarray platform (www.affymetrix.com).

If single base pair changes occur within non-coding regions they may not result in any immediately obvious functional change, although they may potentially have an effect in protein transcription or regulatory regions . Non-coding single base pair changes can have a deleterious functional changes if they occur near intron/exon junctions where they may affect mRNA splicing.

If single base pair changes occur the coding regions of genes, they do not always change the amino acid sequence due to the degeneracy of the genetic code. They may however result in the substitution of one amino acid to another. These single amino acid substitutions termed “missense” changes may or may not have a deleterious effect on the protein they encode, depending on various factors such as the relative importance of the amino acid involved and amino acid charge [151].

Deciding whether a sequence variant is pathogenic can be complicated process and can be achieved using a number of different methods such as population studies to determine the prevalence of these changes in control chromosomes (generally, the more common it is, the less likely it is to be pathogenic). Investigation of the entire coding sequence of the gene looking for other putative pathogenic changes can also be informative, especially when used in conjunction with segregation analysis of any putative pathogenic changes within pedigrees. The relative importance (predicted functional significance) of

a particular amino acid change also depends on the likelihood of the amino acid changing the secondary structure of the protein it is part of, which can be inferred using software programs [152], or looking to see whether the amino acid change lies within an important functional domain of the protein by analysing DNA sequence motifs. Additional inferences can also made by assessing the degree of evolutionary conservation within different species and also the change in charge conferred by an amino acid change (conservative vs. non-conservative).

In summary, a single-base pair substitution may simply represent a non-pathogenic population polymorphism (when it is termed an SNP). If they do not cause disease by themselves but influence disease only in tandem with other sequence variants, they are termed genetic modifiers. A single base pair substitution may also be able to cause disease as a splice-site change, missense change or by introducing a stop codon in to the reading frame.

To obtain an estimate of the frequency of a given DNA sequence change (or "allele") in a population, one can assay the frequency of that change in a representative sample of the population. The higher the sample size, the more accurate the resolution will be of detecting the true heterozygosity rates in that population [153].

Thanks to large scale projects such as the Human Genome Project and the HapMap Project over 10 million reported SNPs exist in public database repositories such as the National Center for Biotechnology Institute single nucleotide polymorphism database dbSNP. Approximately two-thirds of these SNPs are found with a minimum allele frequency of 1% or greater, whilst over a third (38%) have a minimum allele frequency of 1% [154][155].

Microsatellite markers

Microsatellites, also termed **S**imple **S**equence **R**epeats (**SSR**s), **S**hort **T**andem **R**epeat **P**olymorphisms (**STRP**s) or **V**ariable **N**umber of **T**andem **R**epeats (**VNTR**s) are polymorphic sequences that consist of repeating units of 1-6 base pairs [156].

These repeated sequences are often simple, consisting of two, three or four nucleotides (di-, tri-, and tetranucleotide repeats respectively) which can be repeated for a number of units. They are found throughout the human genome and are often highly polymorphic. For example, arrays of $(CA)_n$ repeats are very common, accounting for 0.5% of the human genome. When $n \geqslant 12$, the CA repeats are more likely to be polymorphic [146].

To calculate the n value for a polymorphic VNTR, PCR can be used to amplify a DNA sequence containing the VNTR (see Figure 1.12). The length of the PCR product

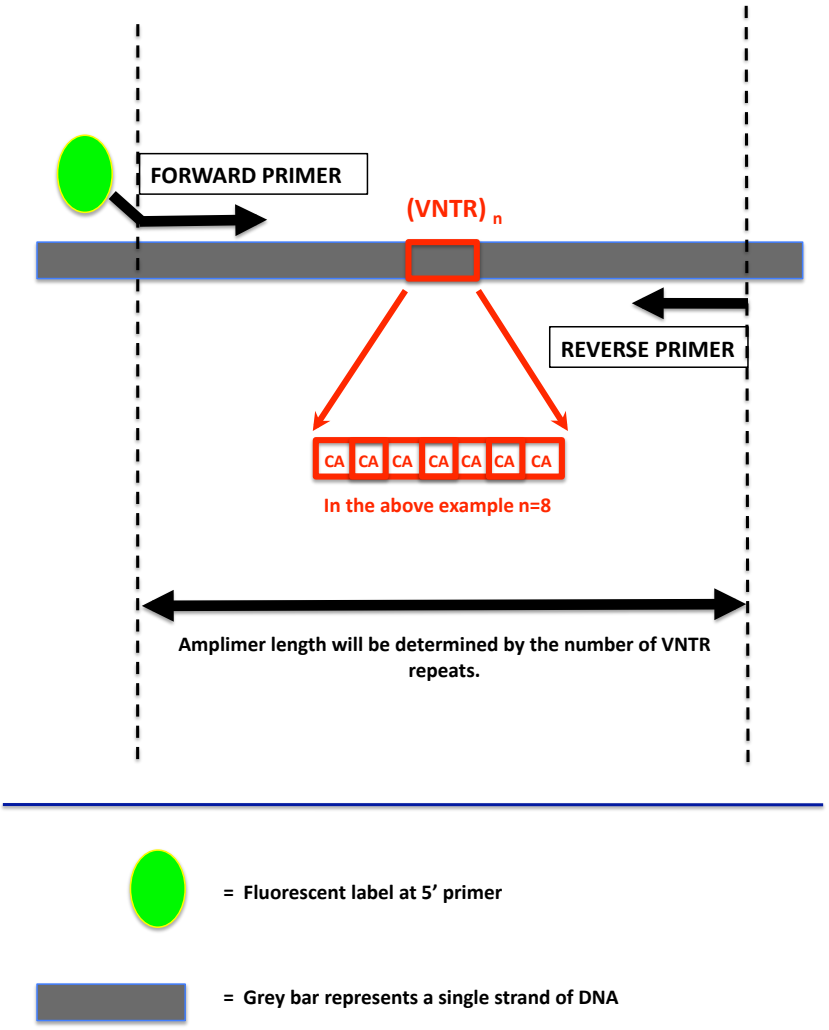

FIGURE 1.12: Schematic representing VNTR markerd for linkage analysis

(termed the **amplimer**) will vary in size depending on the number of VNTRs (n) in the DNA sample amplified.

Practically this can be achieved by designing primers and labelling the 5' end of the forward primer with a fluorescent label. This fluorescent label becomes incorporated in to the PCR product, which is then denatured prior to electrophoresis. The fluorescent label enables sizing of the amplimers. Differences in amplimer sizes thus correspond to differences in the n value for the VNTR which can be regarded as a polymorphic allele at that locus.

These VNTR alleles can then be used as linkage markers to track inheritance of chromosomal loci in the same way as SNPs, but due to their high allelic heterogeneity they are often more informative than SNPs [146].

1.3.3 Regional founder effects

When one particular mutation is the sole or most frequent mutation in a given population as a result of genetic isolation, this phenomenon is referred to as a founder effect.

Regional founder effects in some populations contribute to this wide bandwidth of subtype prevalence.

The high prevalence of the USH3 subtype in Finland can be attributed to two mutations in the *USH3A* gene which are both associated with a common ancestral haplotype. This genetic enrichment from such founder effects is useful information; as the discovery of common alleles within populations can lead to a methodical and efficient approach to molecular diagnosis, carrier screening and genetic counselling as well as opening the door to specific molecular therapies within these groups in the future [34].

To illustrate this point with a practical example: If these two most prevalent USH3A mutations were assayed in a Finnish population with the Usher syndrome USH3 subtype, confirmation of molecular diagnosis would be achieved in approximately 40% of this population. A genetic diagnostic laboratory responsible for molecular diagnosis in this population, would therefore be able to confirm genotype in 40% of cases. This has significant implications as it reduces the time, cost and efficiency of such a service.

Similar examples exist in the Ashkenazi Jewish population, who have been found to segregate their own founder mutations in *USH3A* as well as in *PCDH15* (USH1F) [23][157] and a recent molecular survey reported that four *USH2A* mutations accounted for 64 percent of all pathogenic alleles in Jewish families of non-Ashkenazi descent [158]. Other populations such as the Acadians and Quebecois are now known to also segregate founder mutations in *USH1C* as well as in *USH2A* due to shared ancestry [159, 160]. Nevertheless, despite these founder mutations, and the common c.2299delG mutation in *USH2A* which is found in 16 to 77 % of *USH2A* families (depending on the populations studied) there are a large number of private mutations in most populations [17][161][162][163][164][165][166][59][167][168][167].

1.3.4 MassARRAY®platform and MALDI-TOF®mass spectrometry

Sequenom is a private company who have developed their own MassARRAY®system for DNA analysis. This system is able to yield accurate data from genetic target material that is only available in trace amounts.

The Sequenom genotyping system is based on initial multiplexed PCR reaction, after which the remaining nucleotides are deactivated by enzymatic (shrimp alkaline phosphotase) treatment. A single base primer extension step is then performed, and the primer extension products analyzed using MALDI-TOF mass spectrometry.

Mass spectrometry

Mass spectrometry is an analytical technique employed to determine the elemental composition of a sample. It works by first ionizing chemical compounds generating charged molecules which have their own mass and charge. The mass-to-charge ratio (m/z) of these particles are based on the details of motion of the ions as they transit through electromagnetic fields.

Conventional ionization methods can prove too aggressive in their ionisation of biological molecules such as proteins, peptides and sugars and can cause fragmentation of these more delicate organic molecules. To overcome this, a gentler form of ionization technique termed Matrix-assisted laser desorption/ionization (MALDI) can be used to to ionize intact biomolecules.

The biomolecule being interrogated is mixed with a UV-light absorbing matrix consisting of crystallized molecules mixed with water and an organic solvent such as ethanol. This mixture is then applied on the surface of a MALDI plate and dried, this is sometimes referred to as a MADLIspot. The MALDIspot is then irradiated by a nanosecond laser pulse. Most of the laser energy is absorbed by the matrix, preventing unwanted fragmentation of the biomolecule. The ionizied paticles are then accelerated in an electric field and passed through a flight tube toward a detector. Depending on the mass to charge ratio of the ionized particles, they will be temporally separated, as they reach the detector at different times. This allows each species to yield a distinct signal.

MassEXTEND®reaction

To interrogate an allele located within the genome in a sample of genomic DNA an oligonucleotide primer is designed adjacent to the site in question. A single base pair termination reaction is then carried out to extend the primer by a single nucleotide. This

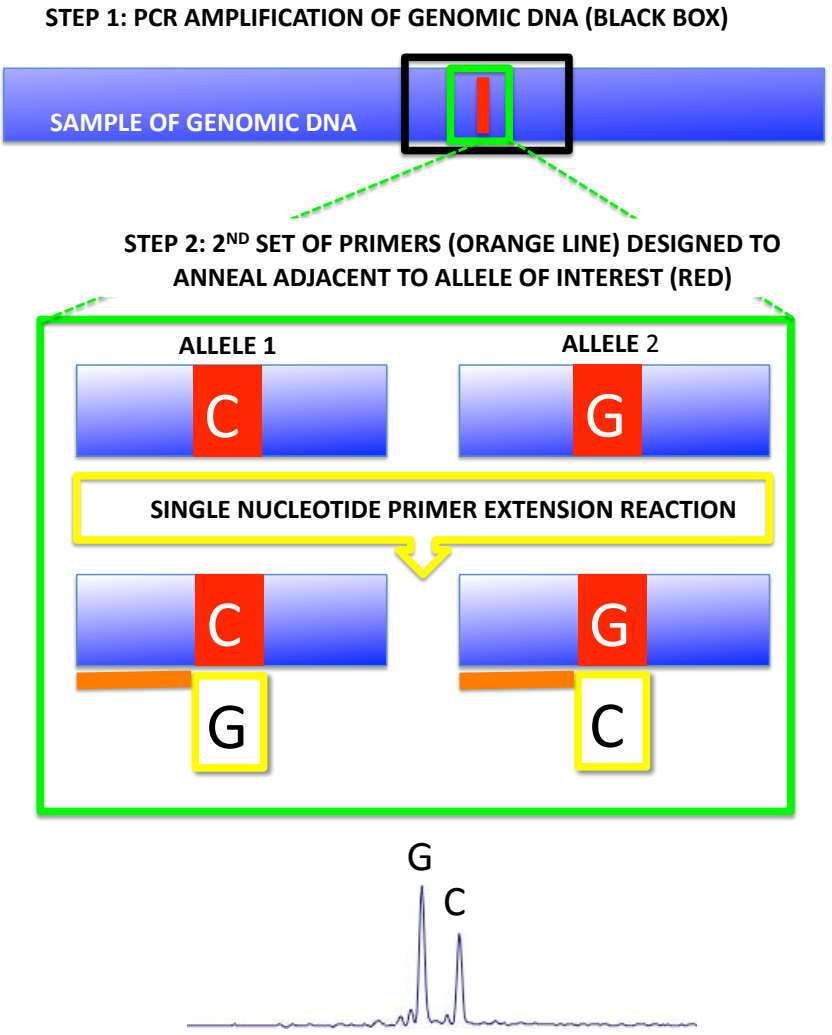

The red boxes represent the nucleotide of interest on two chromosomes from a single individual. In the above example the indivdual has a C/G heterozygous genotype. After PCR amplification of a section of genomic DNA containing the allele, a 2nd set of primers are annealed adjacent to the allele. Subsequently a single base pair extension reaction yields the addition of a G and a C, which are identified by MALDI-TOF spectrometry by two separate peaks corresponding to the mass-to-charge ratio of these two nucleotides.

FIGURE 1.13: Schematic representing the principles of Sequenom's MassARRAY platform for genotyping

nucleotide is then analysed on a MALDIspot and the base pair added can be determined. This process is summarised in Figure 1.13.

Chapter 2

Purpose and Aims

2.1 The National Collaborative Usher Study (NCUS)

The work presented in this thesis derives from The National Collaborative Usher study (NCUS). This section presents an overview of the study prior to stating the aims of the study.

2.1.1 What does the NCUS represent?

The NCUS was a large national study to investigate the clinical and genetic aspects of Usher syndrome. It was set up in 2003 with funding from the Community Fund (National Lottery) and the British Retinitis Pigmentosa Society (BRPS) to employ a family coordinator at the charity Sense, a postdoctoral scientist and an audiologist. The funding also paid for a full-time ophthalmology clinical research fellow (myself).

The main aim of the NCUS was to find out more about the genetic and clinical aspects of Usher syndrome affecting families in the UK.

This was to be achieved by recruiting families with Usher syndrome from the UK, performing detailed phenotyping of their ophthalmic and audiovestibular features and interpret these findings alongside a molecular diagnosis (or *genotype*).

The study represented a unique collaboration between the different disciplines of clinical medicine (ophthalmology and audiovestibular medicine), scientists in the field of molecular genetics and deafblind specialists from the charity Sense.

The clinicians and scientists were based at two academic/clinical institutions from University College London (UCL). The clinical phenotyping was performed in London by

myself and Dr Nell Rangesh (the part-time audiologist on the NCUS). The genetic analysis work was shared between the team of scientists at Institute of Child Health and myself. The NCUS team also collaborated with the Wellcome Trust Sanger Centre, (Cambridge, UK) who were able to provide the facilities and finance to undertake some of the most comprehensive genetic analysis of any cohort of Usher families in the world to date.

Collaboration with Sense, London, UK

The deafblind charity Sense have a long history of providing help to deafblind families and consequently had established links with many of the families with Usher syndrome in the UK. Aside from having a database of Usher families, Sense also maintain active avenues of communication with Usher families by way of Usher groups, meetings, outings and via their website. The operations at Sense were overseen by Mrs Mary Guest Throughout the study newsletters were produced and distributed to the deafblind community via post and their website, keeping families informed of developments as the NCUS progressed and also encouraging other families to participate in the study.

Miss Liz Cook (2003-2007) was employed as the family coordinator, who was based at Sense. The family coordinator's role was to explain the study to family members and encourage participation by visiting as many families as possible either at home, or when they attended London for clinical phenotyping, or through correspondence with families.

Sense were also able to inform clinical collaborators in the NCUS on deafblind culture and offer practical help in meeting the communication needs of the deafblind study population (e.g. lip-reading, sign language, hands-on signing and braille). They were also able to offer their extensive experience to help with the production of all printed or electronic communication material for optimum fonts, colours and contrast for the Usher population.

Collaboration with Institute of Ophthalmology, (University College London) and Moorfields Eye Hospital NHS Foundation Trust, London, UK

The Institute of Ophthalmology is an academic unit specialising in the research and treatment of ocular disorders and was where I was based from 2003-2007 working in Dr Andrew Webster's laboratory, where part of the early genetic analysis was performed. The Institute of Ophthalmology is associated with Moorfields Eye Hospital NHS Foundation Trust, a tertiary referral ophthalmology hospital where many individuals with Usher syndrome have at some point been referred to for assessment. Many of the Usher

patients had at some point been under the care of either Prof Tony Moore and Dr Andrew Webster's clinics and Collaboration with Moorfields Eye Hospital thus provided access to meet many Usher families in the UK and subsequently recruit them in to the NCUS. All ophthalmic clinical examinations and phenotyping was performed by one researcher (myself) at Moorfields Eye Hospital.

Collaboration with Institute of Child Health (University College London) and Great Ormond Street Hospital for Children NHS Trust, London, UK

DNA samples were extracted and stored at the Institute of Child Health. Dr Maria Bitner-Glindzicz was the primary investigator on the NCUS and oversaw part of the molecular work under her team at the Institute of Child Health as well as working as a clinical geneticist in Great Ormond Street Hospital for Children . Over the course of the study two post-doctoral researchers Dr Elene Haralambous (2005-2007) and Dr Polona Le Quesne Stabej (2006-2010) and a research assistant Dr Yasmin Hughes (2005-2007) were employed in Dr Bitner-Glindzicz's laboratory part-time to help out with the molecular aspects of the study.

Prof Linda Luxon headed up the clinical audiovestibular analysis part of the NCUS with Dr Nell Rangesh performing the audiovestibular phenotyping at the National Hospital for Neurology and Neurosurgery Queen Square (UCL) London, UK.

Collaboration with the Wellcome Trust Sanger Institute, Cambridge, UK

For the first two years of the NCUS, the genetic analysis was being performed entirely by myself at Institute of Ophthalmology and the part-time post doctoral scientist and research assistant at the Institute of Child Health.

In 2005 we formed a collaboration with Prof Karen Steel's team at the Wellcome Trust Sanger Institute (Cambridge, UK) which provided the NCUS to obtain a vast amount of genetic data that would have not been possible due to financial and manpower constraints at the start of the study. This collaboration afforded the NCUS the facility to perform direct bidirectional DNA sequencing in nine of the Usher genes (and one candidate gene) in the proband from *each* of the 180+ families recruited in to the study. This generated approximately 264824 base pairs of DNA sequence traces in each of the 180 probands (totalling 47.6 million base pairs for the whole study) which had to be manually analysed.

Outsourcing of second round of molecular analysis to Sequenom®

DNA sequencing at the Wellcome Trust Sanger Institute identified 370 interesting DNA sequence variants in each of the nine Usher genes that warranted further interrogation. For each change, an assay was designed and run by the company Sequenom® (San Diego, USA) on a panel of 1152 DNA samples comprising of DNA 770 affected and unaffected family members recruited in to the NCUS and 600 control DNAs.

2.2 Why perform a study like the NCUS?

2.2.1 Questions a diagnosis of Usher syndrome raises

For a family who are already dealing with the challenges of having a deaf child, the diagnosis of Usher syndrome and the resultant prospect of having to also deal with visual loss can be a devastating blow. Understandably, when an individual or family receive a diagnosis of Usher syndrome this will raise many questions such as:

- What type of Usher syndrome do I have?
- How long will my vision last?
- Will I go blind?
- Are there other related problems e.g. poor balance?
- Will my hearing deteriorate further?
- When I have children will they be affected?
- Are my hearing brothers and sisters carriers?
- Will my child benefit from cochlear implantation to help them develop speech?
- Will I be able to drive to work in 5 years time?
- I communicate using British Sign Language at present, but should I think about learning hands-on signing before my vision deteriorates further?
- Will I be able to carry on my job as an electrician in 10 years time, or do I have to think about another career?

The families will seek the answers to these questions from a number of sources such as their ophthalmologist, their clinical geneticist, teh internet, their audiologist or deaf-blind workers who may have a working knowledge of Usher syndrome. Such prognostic information can guide important decisions families make regarding life plans, accommodation, education and job opportunities.

Due to the wide spectrum of hearing and visual phenotypes seen in Usher syndrome delivering the much needed prognostic information to families is extremely difficult.

The resulting frustration felt by families and clinicians at the lack of reliable prognostic information is one of the reasons behind performing a large study like the NCUS.

For scientists researching Usher syndrome

Outside the clinical setting, the wide clinical variability produced by mutations in the 9 Usher genes (see table 1.1) is a source of great interest for scientists.

Scientists attempting to understand the molecular pathways that underlie retinal function/dysfunction can learn from the clinical effects associated with dysfunction in the Usher genes. This in turn can help contribute to the general understanding of retinal function/dysfunction associated with molecular pathways in the retina. For those scientists attempting to design therapies to prevent or retard the progressive visual loss seen in Usher syndrome, knowing which retinal cells degenerate and different stages of the disease process is a prerequisite. For example, a therapy designed to rescue retinal photoreceptors would need to be initiated at a time before significant photoreceptor death, which (by implication of the variable age of onset and severity of visual loss) probably vary greatly amongst a cohort of individuals with a clinical diagnosis of Usher syndrome. Any human therapy trials will require an idea of the *normal* rate of degeneration in order to ascertain whether or not a treatment is actively influencing the natural course of the disease. Whilst animal models are of some use in this area, there is a paucity of good animal models of Usher syndrome that demonstrate a retinal phenotype (discussed earlier 1.2.6) making *in-vivo* human studies like the NCUS important.

2.2.2 My role in the NCUS

I was employed full time as a clinical research fellow at Institute of Ophthalmology with an honorary contract at Moorfields Eye Hospital from 2003-2007.

My post was funded during this time Community Fund (National Lottery) the British Retinitis Pigmentosa Society (BRPS) with additional help from the Special Trustees of Moorfields Eye Hospital.

- I was solely responsible for performing the ophthalmic clinical phenotyping tests on each of the 220+ affected individuals recruited in to the study.
- I was also responsible for finding and recruiting Usher families in to the study along with the help of a the family coordinator from Sense.
- I took sole responsibility for the DNA sequence analysis of the *USH2A* gene in our 182 probands. This involved manually analysing bidirectional DNA sequence trace data in 100 amplimers per person.
- I designed and created a large multi-user database which was used by different collaborators to input and store the vast amounts of administrative, clinical and genetic data.
- I designed different database user interfaces for the different needs of our collaborators
- I also created strategies to link and query the huge volume of genetic data generated from the study and developed a system to interrogate the pathogenicity of all DNA sequence variants identified from the second round of molecular experiments.

2.3 Aims of the NCUS

1. **Identify a cohort of genotyped individuals with Usher syndrome in the UK**

   Although no treatment exists for Usher syndrome at present, there are a number of research groups around the world working on gene directed therapy of Usher syndrome in animal models. Should these initial trials turn out to be successful, the next stage would be to proceed to Phase 1 testing of these therapies in a subset of human subjects with Usher syndrome and a formal molecular diagnosis would be a mandatory prerequisite for this.

   Most studies on Usher syndrome to date have concentrated on looking retrospectively at clinical data, or genotyping a cohort of individuals with a particular phenotype. This study aims to collect clinical data prospectively (reducing data collection bias) and attempt to identify the causative gene in a cohort of individuals with *different* phenotypes of Usher syndrome in the UK.

2. **Understand natural history of the disorder**

   In order to assess the benefit of any molecular therapies on altering disease course in a progressive disease, one must first have an appreciation of the natural history of the disease. Ideally this requires the collection of prospectively collected clinical data over time (a longitudinal study). Although this study is a cohort study, by performing standardised prospective clinical tests and interpreting these alongside a genetic diagnosis we may begin to explore the similarities and/or differences in disease phenotype that arise due to different mutations in different genes.

3. **Facilitate subsequent longitudinal studies**

   By recording the results of standardised clinical tests in our cohort of affected individuals with a genetic diagnosis, these clinical tests could be repeated in the future. This would generate longitudinal data documenting disease progression giving us a clearer idea of the natural history of disease over time that are associated with a particualr molecular diagnosis.

4. **Help devise a strategy for subsequent molecular analysis in the UK**

   By performing genetic analysis on a representative sample of individuals with Usher syndrome in the UK we will be able to identify which mutations in which genes are responsible for the disease in the UK Usher population. This genetic epidemiological information in tandem with the clinical information will help to determine if genetic testing for USH can be directed by clinical findings, providing a strategy for the subsequent molecular analysis of individuals with Usher syndrome in the UK.

5. **Investigate the possibility of digenic effects and unusual phenotypes**

   Most clinical and genetic studies in Usher syndrome to date have interrogated specific genes in a subset of individuals with a particular clinical subtype of Usher syndrome. This is the first study in the world to comprehensively analyse all nine Usher genes in a population of clinically diagnosed patients with Usher syndrome, regardless of their clinical subtype. This strategy will enable investigation of the possibility of digenic effects and also see if mutations in genes commonly associated with a particular clinical subtype of Usher syndrome may also be associated with other clinical subtypes of Usher syndrome.

6. **Identify which DNA sequence changes are disease causing**

   Many of the DNA sequence variants reported as disease causing in previous studies of Usher syndrome are single nucleotide substitutions resulting in the change of one amino acid to another, which are referred to as *missense* changes. Assaying our putative pathogenic mutations in a large panel of control chromosomes as

well as segregation analysis of these sequence variants will help determine the pathogenicity of DNA sequence variants identified by this study. This molecular genetic data is to be shared with other researchers.

7. **Genetic counselling for individuals and families**

   Achieving a molecular diagnosis in families with a genetic condition can allow for confirmation of the clinical diagnosis and subsequent genetic counselling of individuals, for example, with regard to the risk of transmission to future generations.

8. **Genotype vs. Phenotype: inform clinicians**

   The genotype and phenotype information generated in this study may inform clinicians in making a clinical diagnosis of Usher syndrome ("Can the phenotype predict genotype?"). It may also help clinicians deliver prognostic information to affected individuals and their families ("Does the genotype predict the phenotype?")

Chapter 3

Background to study methods

Devising a workable study methodology required consideration of the multidisciplinary aspects of the NCUS and the challenges faced by working with deafblind study participants.

This chapter provides an overarching view of these challenges and other important considerations relating to this study that influenced methodology. The details of actual molecular and clinical techniques employed can be found in chapters4 and 5.

3.1 Patient recruitment

Recruiting deafblind study participants was one of the most challenging aspects of the study and one which demanded a lot of thought and attention.

There are many difficulties faced when attempting to contact persons with dual sensory impairment. Letters and telephone calls, the standard mode of communication which most hospitals employ to contact patients, can prove unreliable, as visual impairment may preclude letter reading and hearing loss may make telephone conversations difficult or impossible.

By the end of the study, many different methods were used to recruit study participants. This subsection provides an insight in to the communication requirements of the study participants and the factors that needed to be considered during recruiting, consent and phenotyping.

3.1.1 Communication

The challenges presented to a person with dual sensory loss are greater than the sum of the two senses that are lost, as outlined below:

Hearing impairment

Hearing loss in Usher syndrome can vary from moderate to profound. Generally individuals with USH1 communicate via sign language which relies heavily on good visual function [1]. Those with USH2 generally are able to communicate via speech with the help of hearing aids and often relying heavily on lip-reading.

If an USH1 individual who communicates via sign language also has a reduced visual field, this means that the area which they can see their signer (their *visual frame*) is reduced. Thus when using a BSL interpreter to communicate with someone with a reduced visual frame the interpreter must be aware of this and modify their signing accordingly. Additionally if they have deficient colour vision or reduced contrast sensitivity the colour of the signers' clothes relative to their hand colour can be important. If visual function drops precluding adequate use of the visual frame, a technique based upon British Sign Language called **hands-on signing** can be employed. The deafblind person places their hands over those of the signer and interprets them by feeling the signs formed.

For USH1 patients we therefore had to arrange specialist BSL or hands-on interpreters familiar with working with Usher syndome and these professionals had to be booked and arranged for the phenotyping tests.

Some individuals with USH2 have sufficient hearing to manage to communicate via the telephone, however many do not. If an individual who relies heavily on lip-reading looses central visual function, their ability to lip-read can be greatly impaired thus making communication difficult. Due to the high frequency hearing loss in USH2, individuals often find picking out spoken voice in areas with ambient background noise extremely challenging, requiring that all clinical examinations were conducted in a quiet place.

Visual impairment

In all individuals with Usher syndrome, reduction of visual field can make interpreting the non-verbal cues of others difficult. Also many individuals with Usher syndrome are troubled by glare, so optimum lighting conditions e.g. ensuring that bright sunlight is

[1] The exception being those young USH1 individuals who have undergone cochlear implantation allowing them to communicate via speech.

not streaming in through a window and the effects of their nyctalopia (by ensuring the room is well lit, but not too bright) must be accounted for. In order to ensure that someone is able to lip-read, special attention was paid to ensure a clear line of sight and to enunciate words clearly without covering one's mouth.

Each affected individual recruited in to the study was asked to state their preferred mode of communication. This preference was then recorded on the NCUS database so that all researchers were aware of the best method to contact individuals and their families in the future.

TABLE 3.1: Table listing the various modes of communication used to contact individuals with dual sensory impairment

	Requires adequate visual function	Requires adequate hearing
Text phone	Yes	No
SMS messaging	Yes	No
Printed material	Yes	No
Lip-reading	Yes	No
Email	Yes	No
CCTV	Yes	No
BSL	Yes	No
Telephone	No	Yes
Speech	No	Yes
Hands-on signing	No	No
Braille Phones	No	No

3.1.2 Locating Usher families for recruiting in to the NCUS

The task of recruiting up to 200 families with Usher syndrome was shared between the author and the family coordinator based at the charity Sense, with smaller proportions of families recruited from other sources.

Recruitment through Moorfields Eye Hospital (MEH)

The task of identifying and recruiting patients from Moorfields Eye Hospital was the responsibility of the author. Many deaf patients who are suspected of having visual problems or Usher syndrome are referred to MEH for formal ophthalmic examination. Additionally many individuals with a clinical diagnosis of Usher syndrome return to the clinics on an annual basis for routine ophthalmic check up. Moorfields Eye Hospital has a large patient base which was an important source of identifying prospective study participants. Recruitment from Moorfields Eye Hospital was approached in three main ways:

1. The majority of recruits from Moorfields Eye Hospital were identified through the genetics database curated by Dr Andrew Webster. This database has acted as a repository for clinical, administrative and where relevant, molecular data over recent years. This database was queried for affected individuals with a clinical diagnosis of Usher syndrome. Their hospital record number was then recorded and their records accessed via the Hospital Patient Administration System (PAS). The PAS system was then queried for the date and time of their next hospital appointment, which was used as an initial point of contact to meet the affected person and their families and give them information about the study. If they expressed an interest, their preferred method for subsequent communication (e.g. email) was established. This method worked well as in many cases sign language interpreters were already booked for their clinic appointments.

2. The NCUS was publicised amongst clinicians working in the retinal clinics at Moorfields Eye Hospital . Study information packs were also made available to doctors to pass to patients.

3. Doctors working in the retinal clinics at Moorfields Eye Hospital would contact the author to attend clinic to conduct the routine examination and pass on information regarding the study. This helped to lighten the clinical load of each clinic, particularly as many Usher syndrome patients required extra time to communicate their dual sensory impairment.

Recruitment through Sense

A number of families with dual sensory loss are well known to the national deafblind charity Sense, who offer support and advice to individuals and their families. Sense used their records to contact UK Usher families to invite them to participate in the study.

Recruitment through Institute of Child Health Great Ormond Street Children's Hospital

Details of families with Usher syndrome who expressed an interest in the NCUS were sent information packs by the family co-ordinator.

3.1.3 Deliver information and obtain informed consent

In many cases, deaf individuals who were unable to communicate via voicephone, indicated that their preferred mode of contact was via telephone to another family member.

For matters relating to organising dates for phenotyping appointments and other administrative matters this method of proxy communication was employed. For all matters pertaining to consent and clinical examination direct communication was always arranged and if sign-language was required, a professional sign-language interpreter was always employed. Often, family members of deaf individuals volunteered their sign language skills for translation, however this was avoided in order to ensure that the information the affected individual received was entirely impartial and unbiased, allowing them to give their own informed consent to participate in the study.

Ethical approval for the clinical and genetic aspects of the study including the collection of DNA for research purposes, was obtained from the Multi-Centre Research Ethics Committee (MREC) of England and local research ethics committees as appropriate and informed consent was provided according to the Declaration of Helsinki.

Information sheets describing the study aims, purposes and methodology was also approved by MREC. These information sheets were required to be given to participating individuals at least 24 hours prior to obtaining informed consent.

There were separate information sheets and consent forms for children and adults.

All affected individuals participating in the study were required to sign three consent forms for clinical tests, genetic tests and for DNA analysis. All non-affected family members who submitted blood samples for DNA extraction and subsequent analysis were required to sign just one consent form for genetic testing.

The information sheets and consent forms can be found in the Appendix section.

3.1.4 Geographical challenges in performing a national study with deafblind participants

Clinical pheotyping for the ophthalmic and audiovestibular parts of the NCUS were carried out in London. Each phenotyping session required approximately half a day per affected individual. For many families who were based outside of London, these two phenotyping sessions were organised to take place on the same or consecutive days.

Many families from outside London required accommodation to be organised for them to stay overnight.

Some deafblind study participants who travelled to London on their own, required assistance in getting to the phenotyping centres and this was achieved with the help of Sense supplying communicator guides to meet participants at their point of entry in to London and return them to their point of departure from London after phenotyping.

3.2 How to genotype a genetically heterogenous autosomal recessive disease in a population?

The large number of genes associated with Usher syndrome (genetic heterogeneity) and the large genomic size of some of these genes, makes screening these genes for pathogenic changes both costly and time consuming. The *GPR98* gene for example, is associated with an USH2 phenotype (USH2C) and is one of the largest known human genes, comprising of 90 exons encompassing 605 kb (605000 base pairs) of genomic DNA, 19338 base pairs of cDNA which code for 6306 amino acids. In light of the ever present constraints of time and money, what approaches could be employed to achieve a molecular diagnosis in a clinically and genetically heterogeneous condition like Usher syndrome?

3.2.1 Genotyping microarray

One possibility would be to use genotyping microarray platform which holds a finite number of known mutations for all the Usher genes and run that on the proband for each family. Any positive results could then be subsequently analysed on a family by family basis. Such a platform actually exists and in 2006 the NCUS collaborated with researchers in Holland to develop such a platform based on the arrayed primer extension (APEX) method [169]. Whilst the relatively low cost of running a genotyping microarray on the proband of each family is attractive, this method would fail to detect mutations that were not previously known and included on the chip. Due to the difficulties in determining the pathogenicity of alleles, many of the DNA sequence variants included on the microarray are of uncertain pathogenicity. This uncertainty would result in equivocal molecular results and potentially misdirection of subsequent genetic analysis. In a population where there are a high prevalence of known founder mutations were assayed on an array platform, this would be a cost and time effective method of genotyping.

3.2.2 Stratify the molecular analysis

Of the nine known Usher genes, mutations in five are generally associated with an USH1 phenotype, three genes with an USH2 phenotype and one gene with the USH3 phenotype (see table 1.1). Most previous molecular studies in Usher syndrome analysed one or more genes in a selected population of individuals with the clinical subtype of USH *usually* associated with that gene. The advantages of this would be the saving of cost and time in screening other clinical subtypes who were unlikely to have mutations in that gene, but this method would not detect the possibility of atypical phenotypes.

Analyse genes in a logical order

Another possibility would be to order the nine Usher genes in predicted order of decreasing frequency based on previous studies. Each gene could then be sequentially analysed, one gene at a time, in order of decreasing frequency. After analysis on one gene was completed, those families with a confirmed molecular diagnosis for that gene, could be removed from the panel who would all then undergo analysis of the next gene in the remaining subset. The disadvantage with this method is that atypical phenotypes for a given gene would be missed as would the opportunity to interrogate possible digenic effects.

Direct molecular analysis in each family to the subset of genes known to be associated with that families phenotype

This stratified approach could be further expanded by analysing only the subset of genes associated with the clinical subtype of the family in question, further reducing the workload. Both these approaches make the assumption that gene frequency in one population is the same as another, which we know is not the case in Usher syndrome worldwide (see subsection 1.3.3).

Direct molecular analysis in each family based on the result of genetic linkage analysis

Chromosomal linkage markers for each gene or locus could be run in all members of an informative family to exclude or demonstrate linkage to one or more genes/loci and thus reduce subsequent efforts by excluding further analysis of genes that could be confidently excluded.

3.3 Molecular strategy prior to collaboration with Wellcome Trust Sager Institute

At the start of the NCUS in 2003, all genetic analysis was to be performed in-house by two researchers, myself and a part time post-doctoral research fellow based at Institute of Child Health, UCL, London.

The ultimate aim of molecular analysis was to identify the two pathogenic DNA sequence variants in the appropriate gene in each family. Bidirectional DNA sequencing

TABLE 3.2: Table summarising split of molecular analysis for NCUS in 2003

Researcher	Location	Molecular analysis duties
Dr Elene Haralambous	Institute of Child Health	USH1 genes
Dr Zubin Saihan	Institute of Ophthalmology	USH2 and USH3 genes

currently represents the gold standard for identifying disease causing mutations. Performing sequencing on all exonic regions in each of the nine genes associated with Usher syndrome, by two individuals would have been impossible for the following reasons:

1. Time constraints: In-house DNA sequencing is time consuming.
2. Financial constraints: In-house DNA sequencing reagents were expensive
3. Practical resources: DNA sequencing machines were shared with other groups in our respective workplaces and thus only available for limited use per week.
4. Genomic size: There are a large number of genes associated with Usher syndrome (see 1.2) spanning a huge genomic area (see table 3.3)
5. Man hours: In addition to molecular analysis, my time had to be divided between actively recruiting families and performing the ophthalmic phenotyping.

Accepting that we would be limited in our ability to perform bidirectional sequencing, it was important to refine the disease causing loci in each family.

TABLE 3.3: The genomic size of the nine genes associated with Usher sydnrome

Gene	Genomic size (base pairs)
MYO7A	86973
USH1C	50521
CDH23	419008
PCDH15	1825171
USH1G	7175
USH2A	800502
GPR98	605421
WHRN	103376
USH3A	46836
TOTAL	**3944983**

The initial plan was to collect DNA samples from affected individuals and unaffected family members as they were recruited in to the study. Where possible, in-house chromosomal linkage analysis using polymorphic markers would then be performed with the aim of excluding or suggesting linkage to certain genes or loci, reducing the likely number of genes that required subsequent interrogation in each family.

In consanguineous families, it would be anticipated that the affected individuals would be homozygotes for the *same* pathogenic DNA sequence variant. In such consanguineous families, *homozygosity* of linkage markers at a particular locus in *affected* individuals would thus be used to point toward a molecular diagnosis.

In non-consanguineous families with an informative pedigree structure (DNA samples from enough affected and unaffected siblings), providing the markers were informative, we might expect to confidently exclude a number of genes by linkage analysis alone as we would expect all affected siblings to be Identical By Descent for a genotype at a particular locus compared to their unaffected siblings.

It was accepted that running chromosomal markers would be of little practical use on non-informative pedigree structures such as simplex cases (those without siblings) or in families without sufficient parental and/or sibling DNA samples.

After excluding or highlighting loci by linkage analysis, the next stage of refining molecular analysis would be to amplify DNA coding regions by polymerase chain reaction and perform a technique such as Single Strand Conformation Polymorphism (SSCP) or use the WAVE analysis system (heteroduplex analysis) to further reduce the potential number of amplified regions that might need to be sequenced in order to identify the pathogenic sequence variants.

Challenges with this initial approach to molecular analysis

The main challenge with this initial approach was efficient use of laboratory time. Because recruitment in to the study was an ongoing process, DNA samples were collected piecemeal. However linkage analysis for a marker set were only useful after DNA for the whole family had been received and genotyped. In terms of laboratory time and cost, it would have been more efficient to finish recruitment of all individuals and then run sets of markers across the whole panel of DNAs, however due to the time constraints of the study and time pressures resulting from my additional responsibilities of recruiting and ophthalmic phenotyping, this was felt not to be a viable option.

3.4 Collaboration with Wellcome Trust Sanger Institute

In 2006 collaboration with Prof Karen Steel afforded the NCUS to gain access to the high-throughput sequencing pipeline at the Wellcome Trust Sanger Institute.

This new opportunity radically changed the genetic aspect of the study. The previous strategy of piecemeal genetic linkage analysis with markers and in-house sequencing was largely abandoned at this stage.

The high-throughput sequencing pipeline offered to manually re-annotate the nine Usher genes (and one candidate gene) prior to direct bidirectional DNA sequencing on the above ten genes in the proband from each family recruited in to the study.

At this point the entire genetic aspect of the project was re-evaluated and taken in a different direction. The comprehensive genetic data on each of the Usher genes in every family enabled the study to address questions that would not have been possible with the initial approach to molecular diagnosis in addition to providing a broader overview of Usher syndrome.

3.4.1 Why sequence all the Usher genes in each individual?

This strategy was employed for several reasons, outlined below.

- Due to the set up of the high-thoughput sequencing pipeline, DNA samples had to be analysed in batches of exactly 48 (half a plate). At the time of collaboration, less than 48 USH1 probands were recruited in to the study. Thus the initial 48 DNA samples analysed were a mix of USH1, USH2 and USH3 phenotypes.
- This method would give us the unprecedented opportunity to interrogate the possibility of digenic effects in Usher syndrome
- This method would give us the unprecedented opportunity to interrogate the Usher genes for atypical presentations. This would enable us to answer the question, "can mutations in a gene typically associated with one clinical subtype produce phenotypes of a different clinical subtype?"

3.4.2 Summary of the final methods employed for molecular analysis (Figure 3.1)

The genetic analysis aspect of this study was essentially in two stages. The first stage involved bidirectional DNA sequencing of the nine known Usher genes in one affected individual (the index case) from each family. The sequencing experiments were performed at the Wellcome Trust Sanger Institute by collaborators. The raw sequence data was then 'blindly' analysed and interpreted by myself and other collaborators based at the Institute of Child Health, UCL.

DNA sequence variants identified from this stage were then interrogated further in families by means of a series of allele specific assays which was genotyped in a larger panel of DNA samples consisting of index cases, their affected siblings, unaffected family members and a panel of 'control' DNA samples. The experiments were performed by the private company Sequenom and the results validated and analysed by myself and other collaborators based at the Institute of Child Health, UCL.

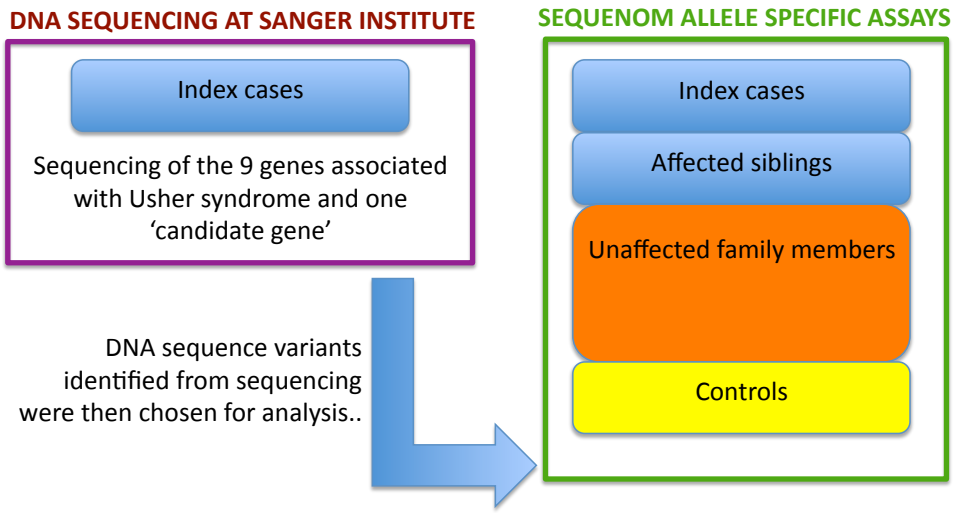

FIGURE 3.1: Simplified schematic illustrating the main methods finally employed for genetic analysis

3.5 Challenges in collecting, storing and analysing clinical and genetic data for a large prospective collaborative study

The NCUS required the secure storage of the vast amounts of clinical, molecular and administrative information collected. I was solely responsible for creating and maintaining a database for this purpose.

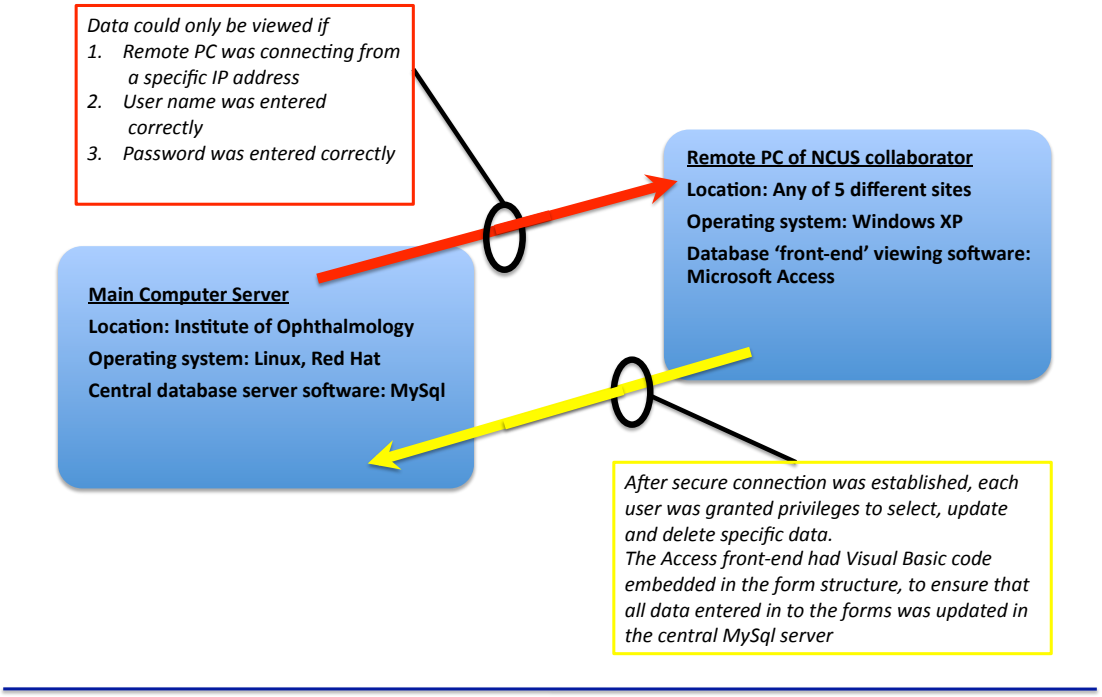

FIGURE 3.2: Overview of NCUS database structure

The NCUS database had to house vast amounts of clinical and genetic data collected from different sites over the course of several years. Access to the data had to be tightly controlled to protect patient identity.

As the study was set to run for several years, the database had to be robust, secure and flexible enough to allow the subsequent addition of different types of data as the study progressed.

Prior to construction of the data storage, consideration was given to how the data was stored bearing in mind that the data would at some point in the future, need to be analysed in order to achieve study aims. Thus the database construction was an important part of study methodology and is discussed in this section.

Database construction was essentially a dynamic process and structured in a hub and spoke model, the hub being a main table called **tblPerson**. Each record in this table corresponded to an individual (either an affected or unaffected family member) that had been recruited in to the study.

Each person had a unique identifier number (termed the **NCUS ID number**) automatically generated and assigned to them.

The database was essentially a relational database which was constructed in a modular fashion to enable the addition of new data tables to be added as required as the study progressed. Each record in the other tables was linked back to the central table, such that a person's identity could be recorded by a simple anonymous number (NCUS ID number).

Each individual was manually ascribed a **Family number**. Unlike the unique identifier NCUS ID number, several individuals from the same family could share a Family number. Data pertaining to the whole family, such as ethnicity and consanguinity were stored under the Family number rather than the NCUS ID number.

Where possible, data entry was forced choice or binary rather than free text, to allow for subsequent electronic filtering of results. Also care was taken to avoid duplication of data in data tables in any form.

When a table was designed for the purposes of recording clinical data, a **date of examination** field was included, such that every clinical entry related exclusively to data collected at a specific date and time. This was done so that if the same clinical data was collected in the future, this could be added to the same table this enabling the collection of longitudinal clinical data from the cohort using the same database.

3.5.1 Multi-user and software problems

Access to the database was required simultaneously by different collaborators at the different sites in the UK listed below:

1. Institute of Ophthalmology, UCL, London
2. Institute of Child Health, UCL, London
3. Sense headquarters, London
4. At the home of the family coordinator (who worked partly from home) outside of London

Because most collaborators ran Microsoft Windows XP operating systems, the database had to be accessible using this operating system. The database also had to comply with UCLs strict policy on data storage, with the confidential patient data encrypted and password protected. Because a collaborator at one of the above five sites might enter data that would need to be viewed collaborators at other sites, the database had to house data that was *live* such that when data was entered it was updated immediately.

In order to maintain tight security to the data, each user could only access the database from the specific known location of their PCs (using a static TCP/IP address) and they were only able to gain access to the data after the correct username and password had been entered. Registration of the database with University College London was mandatory under the data protection act (1998). Following successful registration, permission was granted to house the data (UCL reference number Z6364106, Section 19, Research: Medical Research).

Access to each table in the database had to be granted for each username by the database administrator (myself). For example, scientists working on molecular analysis were not granted privileges to view clinical data, but were granted privileges to view (but not edit) relevant administrative data such as names and date of birth. This was done to comply with data protection regulations and also to safeguard data from inadvertent modification.

As most collaborators were familiar with the Microsoft Office software suite, using the popular database program Microsoft Access seemed a sensible starting point. Initially the web based networking software Citrix was trialled with Microsoft Access but this did not work efficiently and the security levels were not tight enough to comply with UCL's policy for data storage.

To circumvent this, a host MySql server in the UCL computer network was set up. Each researcher had access to the database restricted to a single IP address and access was password protected.

The main problem with using MySql is that whilst the data is stored logically, the user interface is not intuitive and entering data is a cumbersome process involving the use of long strings of command lines.

To get round these problems, a Microsoft Access software "front-end" was created to view the data stored remotely in the MySql database. The forms created were user friendly and easy to navigate due to the incorporation of tabs and pages. Data entry was facilitated by the creation of text boxes. Visual Basic commands were written and embedded in the Microsoft Access front-end such that each time a patient record was navigated to, or updated in any way, this updated the central MySql database and as well as appropriately queried the central MySql database to display the correct live data.

Backup of data

Regular back up of the MySql database tables was performed and stored securely.

Identifier Keys

In addition to the **NCUS ID number** and **Family number** keys which identified individuals and families by a unique integer, similar alphanumeric identifiers were ascribed to aliquots of DNA samples.

When sending aliquots of DNA to collaborators at different research sites, these samples were given unique DNA identifier keys.

3.6 How to determine if a DNA sequence change is pathogenic or not

Identifying whether a DNA sequence change is pathogenic or not is not straightforward.

3.6.1 Rare SNP in a particular population or pathogenic variant?

Although *pathogenic* single base pair changes will be expected to be less prevalent than non-pathogenic population variations like SNPs it does not follow on that all rare single base changes will be therefore be pathogenic. As discussed earlier (1.3.2) one would anticipate that over a third of all SNPs would occur at a frequency of less than 1% depending on the population group studied.

Government figures in the UK suggest approximately 8 percent of the UK population belong to a non-White ethnic group [170]. As our study participants were to be drawn from the ethnically diverse population of the United Kingdom, it was anticipated that many single base changes in our cohort may simply represent rare non-disease causing alleles prevalent in ethnic groups.

One solution to this problem would be to assay the frequency of any rare sequence variants found in a family of ethnic origin, in an ethnically matched control group of chromosomes for that particular family. However, in such an ethnically diverse population as the UK, this solution would be impractical and potentially a whole new study in its own right. The compromise that was reached involved the assembly of a control panel of 433 DNA samples (866 chromosomes) comprising of 376 unrelated UK blood donors from the European Collection of Cell Cultures (ECCAC, UK) and 57 individuals of Pakistani origin (courtesy of Professor Eamonn R Maher, Birmingham, UK). See table 4.2.

3.6.2 Potential methods employed to determine pathogenicity

Deciding whether or not an allele is disease causing is often not straightforward.

The gold standard for deciding whether or not a particular DNA sequence variant is disease causing or not would be to express it in an appropriate cell line and perform functional protein analysis to determine of the suspected mutant allele confers a deleterious effect on protein function compared to the wild type allele.

In a disease such as Usher syndrome where the exact site and biological function of the normal protein is not fully understood, this would present some problems in terms of choosing an appropriate cell line and assay. Furthermore, in addition to their being several different genes that are associated with the disease, many of the mutations reported to date are private (specific to families, rather than populations) creating a huge volume of different potential mutations to analyse.

A fairly robust method is assaying the frequency of the allele in question in a control population. The limitation to this, as discussed above, is that there is the wide variation in polymorphic allele frequency amongst different populations, requiring an ethnically matched control group to the study sample (as discussed above) to interrogate allele frequency.

Interpreting a sequence change in the context of Mendelian inheritance can also be of use in some cases. The assumptions here would be that the disease in question is a monogenic disorder, that is transmitted by Mendelian inheritance. Taking these two prerequistes as given, in the case of an autosomal recessively inherited disease such as Usher syndrome, one would expect an affected individual to inherit two disease alleles in a gene (one from each parent) and this carry these alleles *in trans*. If this can be demonstrated by segregation analysis, this would lend support to the hypothesis that the two alleles in question are disease causing.

Interpreting a sequence change in the context of what we know about the structure of genes can also be useful. For example a DNA sequence change in a coding region of DNA is more likely to affect protein function and thus be disease causing than a non-coding change. Furthermore, changes that cause disruption of the reading frame, will result in all of the codons occurring after the deletion to be read incorrectly during protein translation, which is more likely to affect resultant protein function that a single nucleotide change within the coding region.

For missense changes, determining pathogenicity can prove more tricky. One can perform multiple sequence alignment for DNA or proteins from different species with programs such as **clustalw2** which produces biologically meaningful multiple sequence alignments

of divergent sequences. Clustalw2 determines the best match for selected sequences, and aligns them so that their similarities and differences can be seen. The main hypothesis for this form of analysis is that evolutionary conserved sequences across divergent species are more likely to be important for proper protein function, suggesting that if the change in question is conserved, it is more likely to be disease causing.

Clustalw2 requires that sequences for comparison are selected manually where as the software program **SIFT** (**S**orting **I**ntolerant **F**rom **T**olerant) processes the query sequence by first searching for similar sequences, then chooses closely related sequences that may share similar function, performs alignment of these chosen sequences and then calculates the probability for all possible substitutions from the alignment. If the normalised probability calculation for a nucleotide is <0.05, the change is predicted to be deleterious, whilst if the probability is $0.05\leq$ the change is predicted to be tolerated.

Because many of the DNA sequence variants will have been previously reported by other researchers, some use can be made of the published allele frequency in controls as this is an impartial statistic that can be useful in determining the minimum allele frequency. By the same token, some care must be exercised in designating a particular allele as disease causing simply because it has previously been reported as such.

3.7 Overview of study methods

A detailed schematic of the NCUS can be found in Figure 3.3 which aims to give the reader an overall appreciation of the chronological order of events prior to the more detailed exposition of molecular and clinical methods in the following chapters.

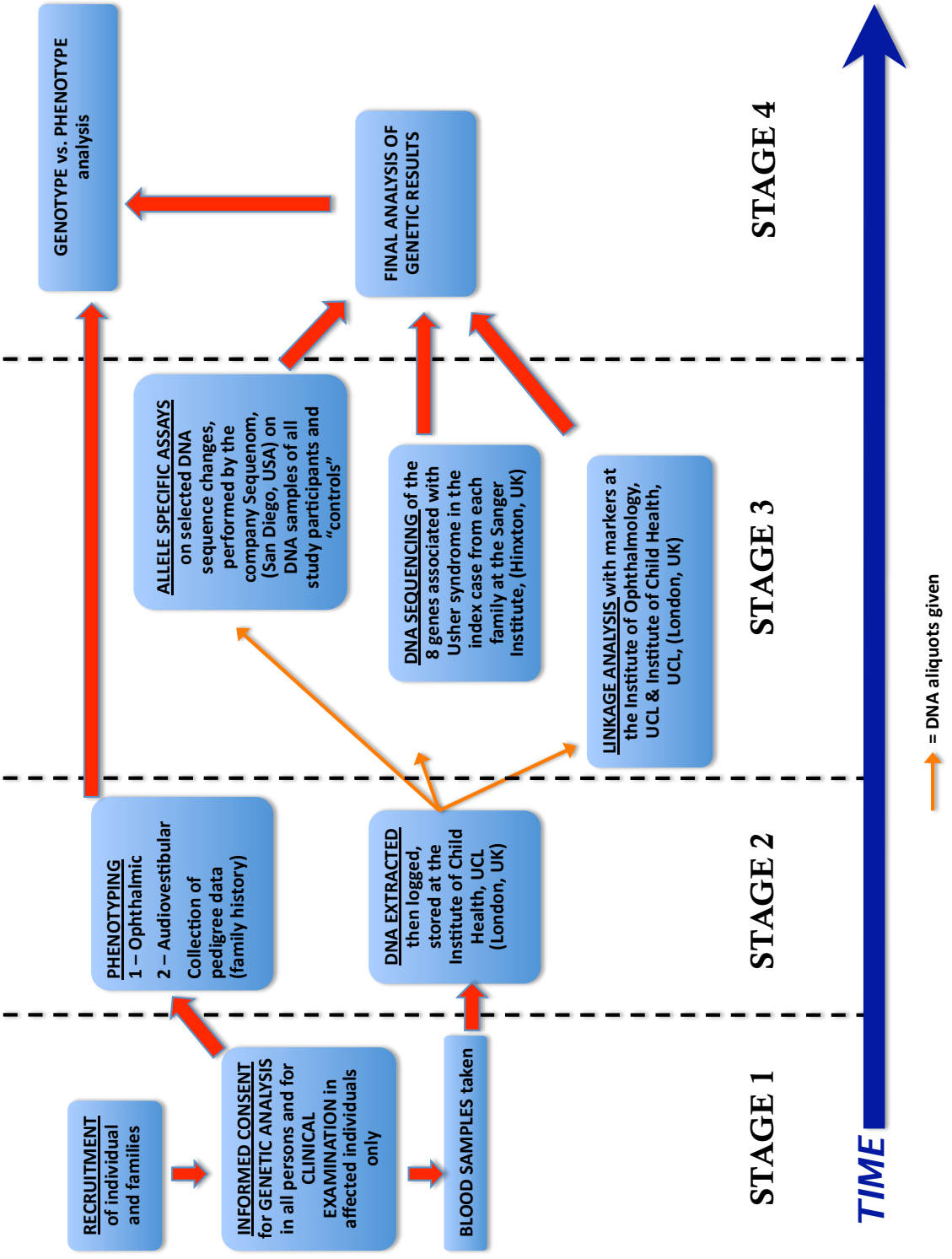

FIGURE 3.3: Detailed schematic giving an overview of study methods

Chapter 4

Molecular Methods

4.1 DNA collection and labelling

4.1.1 From NCUS participants

Blood samples for DNA extraction were collected from all affected individuals and unaffected first degree family members where possible. In some pedigrees, with a consanguineous or unusual family structure, second degree family members also had blood taken for DNA analysis. Blood samples for DNA extraction were obtained in the following ways:

1. during attendance for phenotyping tests in London
2. by the family coordinator during visits to family homes
3. by posting blood packs to study participants which they took to their local GP or Hospital phlebotomy service

Blood packs contained several items listed here 4.1 and were a useful way that individuals could get their blood sample taken locally then posted directly to the Camelia Botnar Laboratory for DNA extraction. The assembly and posting of blood packs was achieved with help from the charity Sense.

4.1.2 Control DNA

Control DNA samples were employed in three areas of the study.

Instruction letter for patient
Instruction letter for General Practitioner's surgery or local Hospital Phlebotomy service
Consent form for DNA analysis to sign and return
x2 EDTA plastic tubes for blood sample and patient details label
Plastic tube to hold EDTA tube
Form with blood sample administrative details to complete and return
Padded envelope with address of DNA extraction laboratory
Biological hazard sticker on envelope

TABLE 4.1: Contents of blood packs used for collection of DNA via post

1. **Optimisation of in-house PCR and in-house linkage analysis**.

   Control DNA samples were drawn from an in-house panel of individuals working at the Institute of Ophthalmology, London, UK.

2. **High throughput sequencing at the Wellcome Trust Sanger Institute, Cambridge, UK**

   A panel of control DNA was used during high throughput sequencing at the Wellcome Trust Sanger Institute. The panel has been used extensively in previous work done at this facility. The panel consisted of 48 individuals from the CEPH families supplied by Coriell Cell Repositories. Full details of this CEPH panel can be found at www.sanger.ac.uk/humgen/exoseq/DNApanel.shtml. The panel of 48 individuals (96 chromosomes) was not used in the final calculations of minimum allele frequency but were used as a quick reference guide to assess whether a DNA sequence change noted on direct sequencing was common or rare.

3. **Allele specific assays performed by Sequenom, San Diego, USA**

   A panel of control chromosomes was assembled to interrogate DNA sequence changes found in the NCUS cohort. This panel of 866 chromosomes was assembled as outlined in table 4.2. A macro was written to generate the minimum allele frequency of each sequence variant assayed.

TABLE 4.2: Control DNA samples used for 2nd round of genetic analysis, the allele specifc assays performed by Sequenom®

Control DNA ethnicity/origin	**DNA samples (n)**	**Chromosomes (n)**
ECCAC controls [1]	381	762
Pakistani controls [2]	59	118
TOTAL	**440**	**880**

1 - from European Collection of Cell Cultures (ECCAC, UK)
2 - from Professor Eamonn R Maher, Birmingham, UK

4.2 DNA extraction of NCUS participants

DNA was extracted from peripheral blood samples at the NHS Camelia Botnar laboratory, located at the Institute of Child Health. Blood samples were centrifuged at 4000 cycles per second for 15 minutes. Cells were suspended in PBS at a concentration of 1 x 106 cells per 100 μL, double the volume of DNA lysis buffer added, mixed and then incubated at 68 degrees centigrade for 5 minutes. The sample was then cooled, mixed with an equal volume of chloroform and centrifuged at 2000rpm for 20 minutes. The upper layer, containing the DNA in solution, was carefully decanted, added to an equal volume of 100 % ethanol and gently mixed until the DNA precipitated. The DNA was transferred to a clean tube and washed twice in 70% ethanol, then dissolved by end-over-end rotation at 4°C in an appropriate volume of ddH20. Samples were stored at 4°C.

The DNA sample was stored in plastic Eppendorf tubes, labelled only with the **NCUS ID number** and stored in labelled boxes. The storage location of a sample (box reference number and location was then logged on to the NCUS database, to enable DNA samples to be located easily.

4.3 In-house molecular methods

For the purposes of clarity, in the exposition of molecular methodology that follows, the prefix "in-house" refers specifically to laboratory work that was performed by the author in Dr Andrew Webster's laboratory at the Institute of Ophthalmology, UCL, London. This is to distinguish molecular work done by myself and that performed by our collaborators from the Institute of Child Health, the Wellcome Trust Sanger Institute and the experiments outsourced to the private company Sequenom® (San Diego, USA).

4.3.1 In-house Polymerase Chain Reaction

PCRs were performed in-house prior to linkage analysis and in-house direct bi-directional sequencing. They were also performed by the Wellcome Trust Sanger Institute prior to high throughput sequencing.

In-house PCRs were designed with the program Primer3 [171]. Desalted primers were synthesised on a 0.05μM scale by the company Sigma Aldrich.

Dry oligonucleotides were briefly spun for around 5 seconds at 1500 rpm and re-constituted with sterile deionised water to a stock concentration of 100μM stock

solution, which was subsequently stored at -20 degrees centigrade. For PCR reactions, this stock solution was diluted down to a concentration of 10μM.

TABLE 4.3: Reagents for in-house PCR

Reagent	**Volume (μ L)**
x10 NH4 buffer (No MgCl2; Bioline UK)	2
MgCl2 [1.5μM] (Bioline, UK)	1
dNTP [2mM]	2
Forward primer [5pM]	2
Reverse primer [5pM]	2
Taq polymerase (Bioline, UK)	0.1
dH2O	9.9
10ng DNA template	1
TOTAL VOLUME	**20**

The PCR conditions were optimised for each set of oligonucleotide primers using a sample of control DNA of known quality and concentration (10ng/μl). To identify the optimum annealing temperature for each set of oligonucleotide primers, reaction mixes were made as outlined in table 4.3 and run with 10ng of the same control DNA using the "gradient" profile on an Eppendorf Mastercycler PCR block (Hamburg, Germany). The settings for the gradient setting were entered as follows: **annealing temperature**=7 °C, **ramp**=3 °C/**sec, gradient**=7 °C on the PCR block. After PCR amplification using the thermoprofile settings listed in Table 4.4, 10μ of each PCR was run on a 1% agarose gel and visualised under ultraviolet light with an appropriate molecular weight ladder. The strongest most discrete band was identified and the annealing temperature corresponding to this sample was used for subsequent PCRs for that particular oligonucleotide primer pair.

TABLE 4.4: Thermoprofile for in-house PCR

Step	Function	Temperature in degrees C	Duration	
1	Hot Start	95	5 minutes	
2	Denature	94	30 seconds	
3	Anneal	50-62∗	30 seconds	35 cycles
4	Extension	72	30 seconds	
5	Final extension	72	10 minutes	

∗ the annealing temparature for each PCR reaction was determined during PCR optimisation

In-house PCRs for in-house linkage analysis

Desalted primers for in-house linkage analysis were synthesised on a 0.05μM scale by the company Sigma Aldrich and labelled with one of the three fluorescent

fluorophores FAM, HEX or TET.

Fluorescently modified oligonucelotides were reconstituted to a stock concentration as described above. They were stored at -20 degrees centigrade in eppendorf tubes wrapped in aluminium foil to reduce exposure to light and prevent dye photobleaching.

4.3.2 In-house Agarose gel electrophoresis

Agarose gels were used for analysing the products of in-house PCR.

A gel tank was prepared with end plates and placed in a freezer at -20 degrees centigrade to cool. During this time, Agarose powder (Bioline, UK) was added to 1.5%TAE buffer in a conical flask to a concentration of 1-2% depending on the degree of resolution required and gently agitated manually for 30 seconds. This suspension was heated gently to for 2-4 minutes in a microwave until all the agarose powder had disolved. Ethidium bromide [50ng/ml] (Sigma, UK) was added to the flask and agitated manually for 30 seconds.

The gel tank was removed from the freezer and a plastic comb was inserted. The contents of the flask were then carefully decanted in to the gel tank and allowed to set at room temperature for 30 minutes. The plastic combs were removed which formed indentation wells in the gel and the end plates of the gel tank were also removed.

The gel was then placed in a gel tank filled with 1.5% TAE buffer. For each row of wells, one well was loaded with DNA ladder to mark out fragments of known molecular size. Either 1μl of phiX174 DNA/HaeIII Markers DNA ladder [0.5 g/10/muL] (Promega, USA) or 0.5μl of HyperLadder ^{TM}IV[0.16g/10μl] (Bioline, UK) was used for this purpose.

PCR products were mixed with bromophenol blue (BPB) loading dye at a ratio of 10:1 and 5-10μl were loaded in to the wells and a current of 200mW passed across the gel tank for approximately 20 minutes or until the BPB dye had progressed sufficiently along the gel. The gel was then imaged using ultraviolet illumination.

4.3.3 In-house genetic linkage analysis using markers

In-house genetic linkage marker construction

A set of markers were assembled for four genes/loci corresponding to the molecular subtypes of Usher syndrome USH2A, USH2B, USH2C and USH3A which were used to interrogate families segregating a non-USH1 phenotype.

These markers consisted of a combination of previously published genetic linkage markers alongside new markers that were created in-house.

Polymorphic markers were chosen a short genetic distance from the gene being interrogated. In some cases, markers were located within the non-coding areas of the gene being interrogated. The main criteria for marker selection was proximity to the gene in question. A secondary criteria was a relatively high heterozygosity score, as these markers were more likely to be informative. In-house markers for a particular gene were created by downloading genomic DNA containing the coding sequence of that gene from the human DNA sequence repository at The National Center for Biotechnology. This section of genomic DNA was limited by 20 kilobases either side (both upstream and downstream) of the coding regions. These sections of genomic DNA were then searched for contiguous repeat sequences of CA/GT dinucleotides using a simple iterative program written in house. Flanking oligonucelotide primers were then designed around the tandem repeat sequence using the software program Primer3 and the primer pair labelled with a fluorescent label as described above (see 4.3.1).

Genotyping markers

The PCR was optimised and then run on ten control DNAs. 1μl of each PCR reaction was then suspended in 9μl of Formamide and run on the ABI 3100 genotyper. The fragment lengths were analysed using ABI Genotyper software ver 3.7 and fragment lengths were measured. If markers amplified reliably and had alleles were of sufficient heterozygosity that could be accurately scored on the ABI PRISM 377 DNA Sequencer in a control panel of 10 DNA samples they were chosen to add to the panel. The fluors used to label markers and the amplimer size of in-house markers were chosen to allow multiplexing of the electrophoresis where possible.

Figure 4.1 shows an example of the traces of one of 6 polymorphic linkage markers that were designed for the *USH2A* gene.

4.3.4 In-house bidirectional DNA sequencing

PCRs were cleaned using Millipore montage PCR clean-up plates (Oxford, UK) as described in table 4.6.

TABLE 4.5: In-house genetic linkage marker information

Gene/Locus	In-house marker name	marker alias	FORWARD Primer	REVERSE Primer	approx amplimer size (bp)	Dye	Annealing Temp
	Ush2aMark2	AFM143XF10	AATTGAGAGGTGGATGAGAATGA	TACCTACAGGATGCCGGGTAA	113	Fam	55
	Ush2aMark3	Ush2a_ca22rpt__118kb_upstm	TAAGCTCTTGGCCAGGGTAT	GGATCACAGAAGGATTGAGAGC	250	Tet	55
	Ush2aMark4	Ush2a_tc24rpt__int13	AAGGACCACTGCAGTCAGGA	TGTTGTGGCTGGTGGTAGAA	201	Fam	55
USH2A	Ush2aMark6	D1S229	GCTTGTTTCCATTTATGGTG	ACTCTAGTTGTGTGTGAATGTATG	200	Hex	55
	D3s1578	AFM268WG9	GCCAACACACATTAATCACATA	GGGGCCAAAATCTGCT	140-166	Fam	50.3
	D3s3647	AFMB320VC1	GGCTCAGAGCAGGCATAC	CCTAACTAATAAAATGTGTTCCCAG	190-228	Fam	58.1
	D3s3658	AFMB330ZE5	AAAAGTTAGCAAACACAATCCTATC	CTGGACTAAATCTAAGTTGGTTATG	104-126	Hex	63.5
USH2B	D3s1619	AFM350TF1	GTCCTGCAAGACTCATTG	TTGCTAGGATGGTTGTTTTC	161-171	Hex	55
	d5s617	AFM190XC11	CCAAAGGCTTGGTGATTTAGTGGAC	CTAGATTGAAGGCCAGAAAACATGC	171-203	Hex	66
	z2c_int7		GGTGTTGGACACAACAATGAA	AAGAAAACAGTGAAGCCATGGTA	162	Fam	66
	z2c_int85		GCAGTGAACCAAGATTGTGC	AGTCCAGGGACTCCTTCTGTT	231	Fam	66
USH2C	d5s495	AFM234VC1	GCATAAGTTTTGCTAGGGGA	CCCATCACAAGTTGAGGAAA	219-241	Hex	51.4-55.5
	D3s1299		ATGTCCGGCATGGAAG	TGACAGTTTGGTTAAGTATCCC	218-228	Tet	60.8-63.5
	ZM Clarin 1kb upstream		AGAGCTCAGGACAATAACATGG	AAACGGTCAAGACCTGGAAA	190	Fam	60.8
	D3s3625		GGCAACCAAGAGTGAAAC	TGAAATTTGGGCAATCAATT	166-194	Tet	55
USH3A	D3s1279 [abi]		CACCATCTGTGTGGTATTGG	GACCTATTTTGGTTAACAATTTAGA	264-282	Fam	51-53

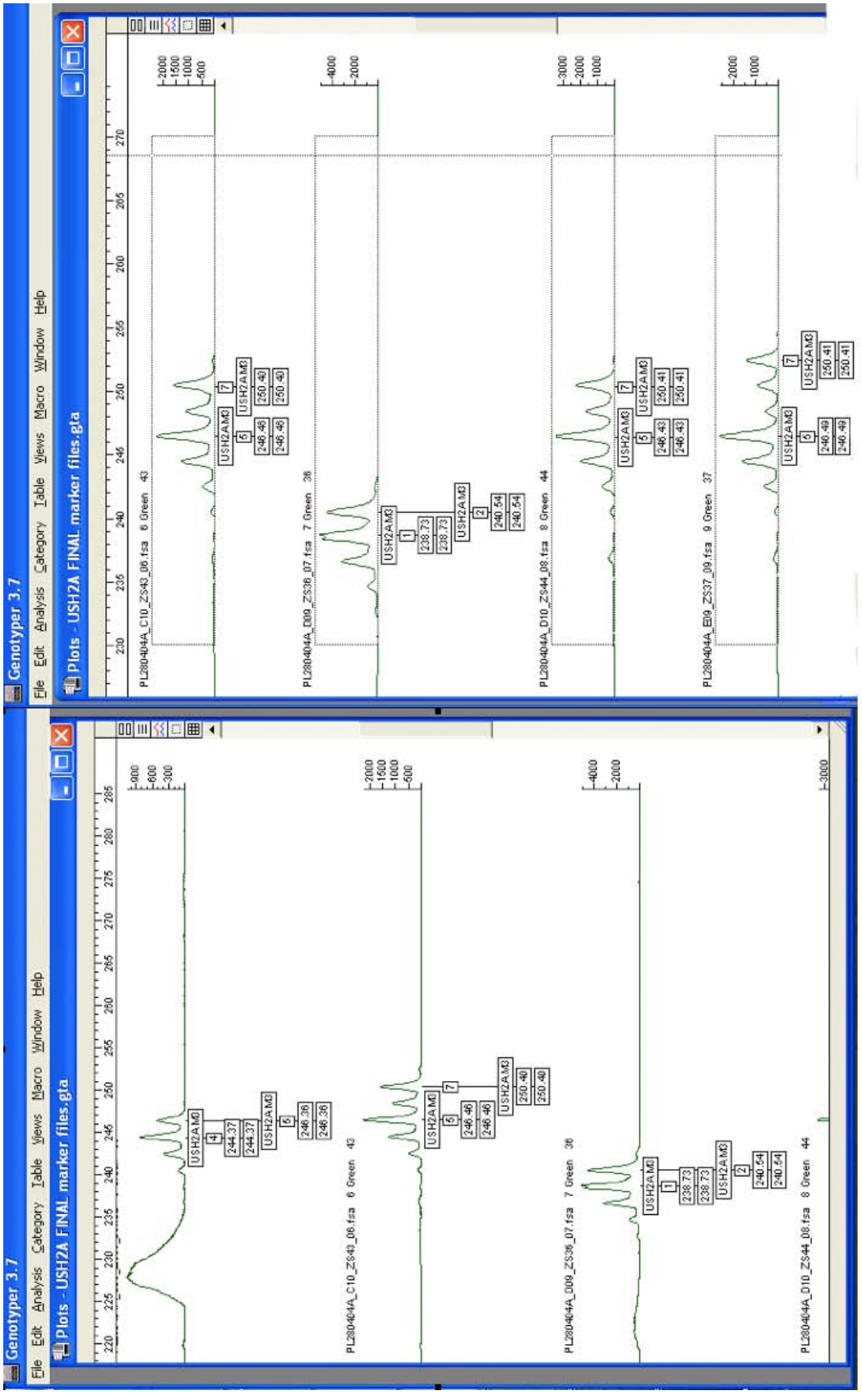

Allele	Size of PCR product (base pairs)
1	238
2	240
3	242
4	244
5	246
6	248
7	250

FIGURE 4.1: Electropherograms of two CA/GT repeat polymorphisms run on the ABI 3100 genotyper on seven control DNA samples from the ECCAC control panels. The alleles (arbitrarily numbered from 1 to 7) scores are shown in the table at the foot of the figure.

TABLE 4.6: Method for in-house PCR clean up prior to in-house sequencing

STEP	
1	Run 5μl of PCR product on an agaorse gel to check PCR success
2	Make up volume of remaining PCR to 100μl with H20
3	Transfer this 100μl to purple plate
4	Vacuum 10 mins
5	Check wells are empty
6	Add 25μl H20 to each well
7	Vacuum 3 mins
8	Wash bevelled plate and leave to dry
9	Add 20μl H20
10	Cover plate & cling-film
11	Vortex at 1000rpm for 10 mins
12	Transfer remaining (approx 15μl) to plate for storage
13	Mark out used wells on purple plate in order to re-use purple plate
14	Use 2 to 2.5μl of this cleaned product for sequencing reaction

Using Millipore PCR clean up montage plates

In-house sequencing reaction

In-house sequencing reaction was performed using cleaned PCR product and the BigDye Terminator v3.1 Cycle Sequencing Kit (Applied Biosystems, UK) as per Table 4.7.

TABLE 4.7: Reagents for in-house DNA Sequencing reaction

Reagent	**Volume (μl)**
BigDye (Applied Bio, UK)	0.5
Sequencing Buffer	2.5
(Forward or Reverse) primer [5pM]	0.5
Clean PCR product	2
dH2O	4.5
TOTAL VOLUME	**10**

In-house sequencing thermoprofile

The sequencing reaction thermoprofile used for in-house sequencing is shown in Table 4.8.

TABLE 4.8: Thermoprofile for in-house sequencing reaction

Step	Temperature in degrees C	Duration	
1	94	30 seconds	
2	96	30 seconds	
3	55	15 seconds	27 cycles
4	60	2 minutes	
5	60	3 minutes	

TABLE 4.9: Method for clean up of in-house sequencing reaction prior to in-house sequencing

STEP	
1	SEQ cleanup (BLUE plates)
2	Add 25μll Injection solution to each well
3	Transfer total volume ~35μl to BLUE plate
4	Vacuum 3 mins
5	Check wells are empty
6	Add 25μlInjection solution to each well
7	Vacuum 4 mins
8	Wash bevelled plate and leave to dry
9	Add 25μl Injection solution to each well & tap it to the bottom of well.
10	Cover plate & cling-film
11	Vortex at 1000rpm 10 mins
12	Transfer remaining vol (11μl) to sequencing plate
13	Mark out used wells on blue plate in order to re-use purple plate

Using Millipore sequencing clean up montage plates

4.4 Wellcome Trust Sanger Institute

4.4.1 Sequencing work performed

The index case ("proband") from each family underwent bidirectional DNA sequencing of the nine Usher genes and one candidate gene at the Wellcome Trust Sanger Institute.

This group of individuals will subsequently be referred to as the **Sanger cohort**.

The annotation of each of the nine Usher genes and the one candidate gene, primer design and sequencing reactions were performed entirely by collaborators at the automated high-throughput pipeline at the Sanger Institute.

The raw sequence traces generated from these sequencing reactions were automatically stored in an electronic repository.

Although the reactions were performed entirely by collaborators, the analysis of the sequence trace data was performed manually using computational software aids described in a later subsection 4.4.4. Due to the large volume of sequence

trace data generated from ten genes in 186 families, this analysis work was divided up between a group of six individuals (including the author) based at the Institute of Child Health, Institute of Ophthalmology and at the Sanger Institute.

In addition to the panel of DNA samples from this study, each amplimer was also sequenced in a panel of 30 control DNA samples from CEPH families (see 4.1.2 for details). This panel of DNAs served as a screening panel to enable the detection of common polymorphic changes. Prior to undertaking sequencing analysis for an amplimer, the CEPH control panel was first analysed. Any sequence variants that looked polymorphic (e.g. present in a significant proportion of control DNA samples) were marked by their position in the amplimer such that when the amplimer was subsequently analysed in the USH index case panel, this information would be available to indicate common polymorphic changes.

Any sequence changes identified were recorded by the amplimer name, the base pair change, and the location of the sequence variant within the amplimer. All sequence traces were aligned to a reference sequence that was defined and numbered in relation to the forward and reverse primers. This is illustrated in Figure 4.2. Thus if a sequence change was located at number 154 in a contig, the position of this nucleotide could be subsequently by locating the forward primer and counting 154 base pairs downstream. This transformation of data was achieved by assembling a contig of genomic DNA for the gene, which was aligned with sequence files for the primers used as well as sequences for all coding regions. this was performed using the software tools in DNASTAR v.8.0.2 (Lasergene Madison, USA).

A decision was made based on the position and frequency of a sequence variant identified as to whether it was recorded. Any sequence change that was in or around a coding region was considered worthy of subsequent analysis and recorded on a database. Only polymorphic changes (that were present in significant proportions in he control DNA panel) were not scored in each individual.

The results from this initial round of sequencing was thus recorded in a largely abstract format. Subsequently this 'raw' data was transformed in to meaningful genomic and coding sequence data and recorded alongside the raw data on the same database.

The sequencing analysis was a significant undertaking that took several years to complete as it generated 278475 base pairs of sequence per individual, which totals just under 53 million base pairs for the Sanger cohort.

The author was solely responsible for the analysis of the *USH2A* gene in each of the index cases and 30 control DNAs that were also sequenced at the Sanger Institute,

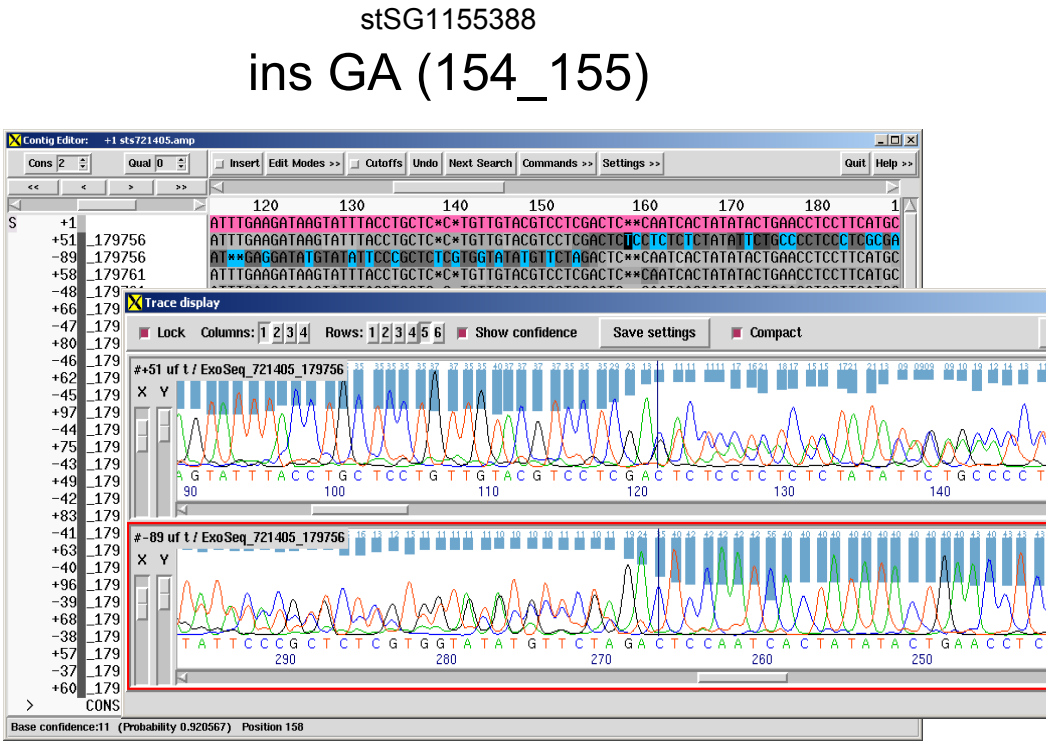

FIGURE 4.2: Screengrab of a GA insertion between nucleotide numbers 154 and 155. The pink bars in the reference sequence indicate that these nucleotides are coding in the reference sequence. The amplimer reference is stSG1155388. This data would then be used at a later stage to locate the position of nucleotides 154 and 155 on an alignment of genomic DNA and revealed that this change represents the novel frame-shift sequence variant p.Arg1946LeufsX22 (Family 173)

whilst the sequence trace analysis in the other genes was shared amongst the rest of the team.

Following the conclusion of the second round of molecular experiments all individuals with an USH2 phenotype and no putative pathogenic changes in addition to index cases in whom only one putative pathogenic sequence change was identified were reanalysed by another member of the team Dr Polona Le Quesne Stabej, who rechecked the sequence trace files analysing raw electropherogram traces to double check for missed sequence variants in this subset of individuals in whom another disease causing allele in this gene were suspected.

Anonymity of DNA samples

DNA samples were submitted to the Sanger Centre labelled only with their (anonymised) NCUS ID number. The Sanger Centre generated a new alphanumeric key to refer to each sample. All DNA sequence trace analysis was undertaken using these alphanumeric keys rather than patient names. This was done in order to comply

with departmental policy as well as removing the potential bias of analysing DNA from an individual in whom the phenotype was already known; i.e. the DNA samples were analysed "blindly".

Two probands had duplicate DNA samples sent and despite the clinical diagnosis of some of the families with suspected non-USH were known soon after recruitment, these DNA samples were left in the Sanger cohort and still underwent sequencing.

4.4.2 Vega gene re-annotation

Prior to sequencing each gene was re-annotated using the VEGA annotation algorithms for predicting exon structure. These were compared against published findings. The re-annotated genes can be found online in the VEGA genome browser

4.4.3 High-throughput sequencing pipeline

Primer Design

This was carried out using the program Primer3. Primers for all genes were designed to cover all exonic regions and intron/exon boundaries as well as 3 prime and 5 prime untranslated regions (UTRs) using the Primer3 to amplify the exon and at least 125 base pairs either side of the exon to capture the splice sites and regions and sequences that may be of other functional importance. The target amplimer size was between 450 and 550 base pairs.

Primers with 1 base pair mismatches (or SNPs) in their sequence were excluded and re-designed. Larger exons required several overlapping primer pairs to obtain complete coverage of the exonic area.

Any exons that failed automatic primer design at this size range were re-designed with an increased permitted product size of up to 700 base pairs. If primers failed at this target amplimer size they were then designed manually.

Primers were checked for uniqueness in the human genome using the In-silico PCR experiment simulation system (ipcress) software program.

Primers were screened for optimum amplification conditions . A full list of primers can be obtained by searching using gene name at this location.

Primers with exact or 1 bp mismatches (or SNPs) in their sequence were excluded and re-designed. For large exons a series of overlapping primer pairs were designed to enable adequate coverage on sequencing.

PCRs and sequencing reactions were tested initially in a panel of 48 CEPH DNAs (2). Those primers that failed to amplify successfully were redesigned.

High throughput PCR

The Standard ExoSeq PCR reaction conditions and thermoprofiles used for PCR are available online from the Wellcome Trust Sanger Institute at www.sanger.ac.uk/resources/downloads/human/exoseq.html

Over 700 primer pairs were designed to cover the nine genes associated with Usher syndrome and another candidate gene *SLCA4*. Each primer pair was given a unique alphanumeric identifier code termed an **STS number**. Each panel of DNAs sequenced for a particular STS number were given a unique numeric identifier code termed **GROUP ID**. Both these identifiers were generated from the high sequencing department at the Wellcome Trust Sanger Institute.

Sequencing reaction conditions

PCR products were sequenced with specific primers bidirectionally to produce double-stranded sequence. Protocols are available at www.sanger.ac.uk/humgen/exoseq/protocol-sequencing.shtml.

4.4.4 DNA sequence analysis using the Staden Package

DNA sequence traces were analysed using the open source software the Staden Package.

Raw trace files from bidirectional sequencing at the Wellcome Trust Sanger Institute were initially processed with the **pregap4** program, prior to analysis with the **gap4** program in search of DNA sequence changes. I was responsible for the analysis of sequence data for the 100 amplimers of sequence data for the *USH2A* gene in all 180 probands, whilst several other researchers based at the Institute of Child Health and Wellcome Trust Sanger Institute performed sequence analysis of the other genes sequenced.

pregap4

pregap4 is a software program which is part of the Staden Package which provides a graphical user interface (GUI) to the processing of raw trace sequence files. As it's name suggests it is used prior to analysing the sequences in the gap4 software program. pregap4 has the facility to perform several functions that can be realised in gap4 and it also assembles files in to a contig. pregap4 can also be used to convert file format, screen for contaminant sequences and perform repeat searching. A useful feature of pregap4 is the integration of an algorithm which is

used to assign a numerical value to sequence files to quantify base read confidence. An overview for the stages of pregap4 processing are outlined in figure 4.3.

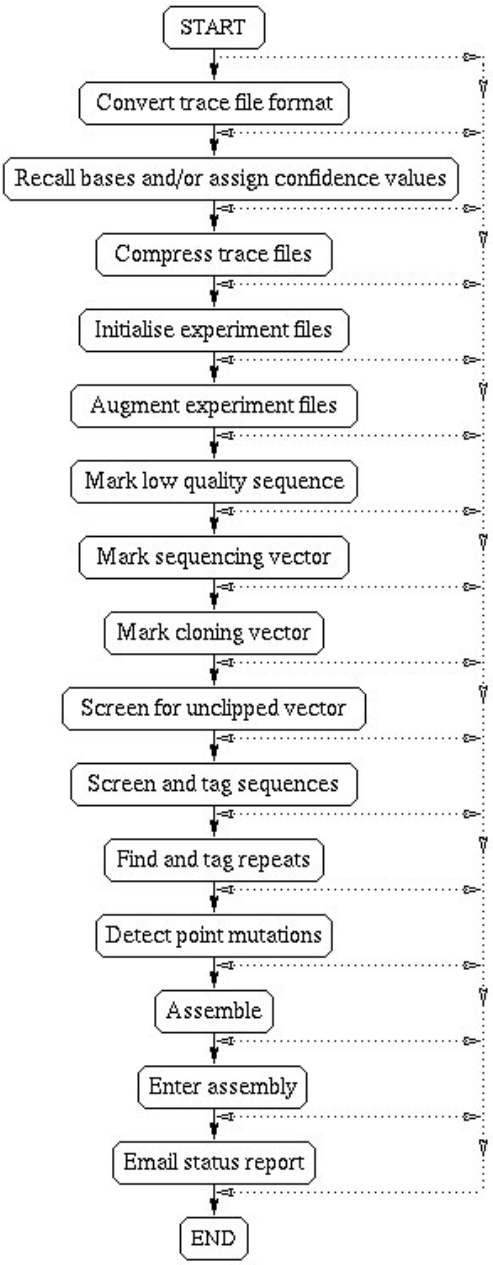

FIGURE 4.3: Overview of pre-GAP4 trace file processing

The configuration settings for pregap4 were set as indicated in figure 4.4. These settings were important prerequisites in order to process the sequence data appropriately to allow automated estimation of base accuracies and the highlighting possible mutations when subsequently analysing the traces in gap4.

Importing sequence files in to pregap4 is achieved by selecting the **files to process** tab. In addition to the sequence files for a group of individuals, reference sequence

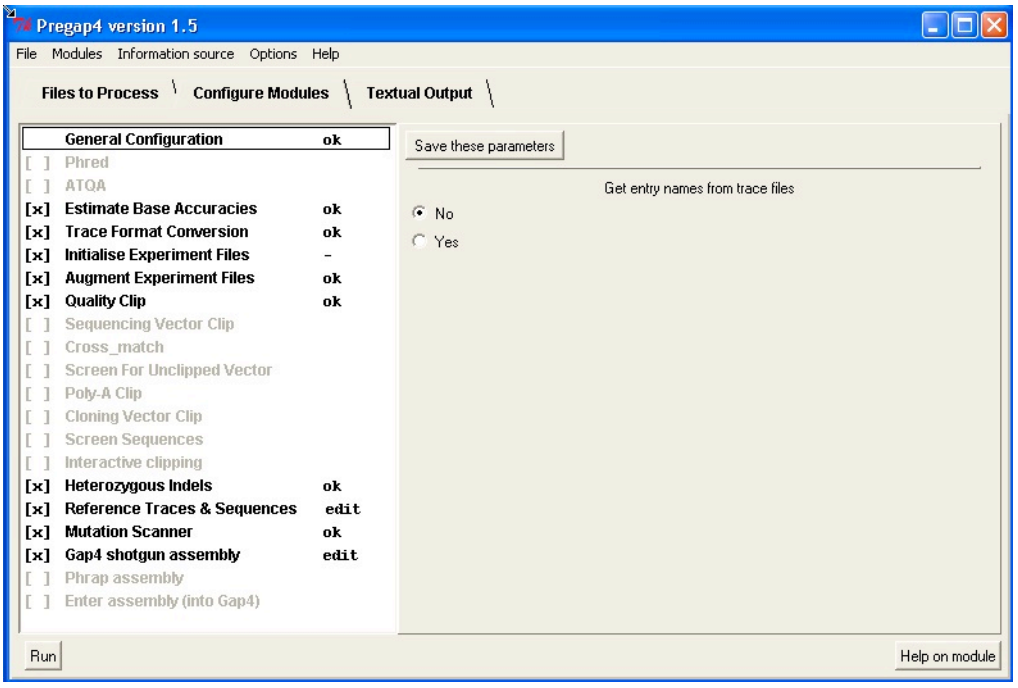

FIGURE 4.4: Screengrab of the pregap4 settings used for processing sequence trace files

traces (both forward and reverse) were added and in some cases a sequence file containing the exonic sequence contained in the amplimer was also imported. This was done so that when analysing the contig in gap4 one could easily view the position of a particular sequence variant within a contig was exonic or intronic. Sequence files that were of very poor quality or absent were excluded in the contig selection.

Each time a set of samples was processed using pregap4, a new gap4 database was generated, the name of which had to be chosen and manually entered as indicated in Figure 4.5.

When a group of samples was successfully processed by pregap4 an experiment file (extension .aux) was created with the same name as the database.

4.4.5 Analysis of DNA sequence files using gap4

Due to the vast number of electropherograms generated from the bidirectional sequencing process, analysing millions of electropherograms by eye would be unlikely to give a high pick up rate of subtle base pair changes such as substitutions or indels, which is why gap4's Graphical User Interface (GUI) was employed.

gap4 is a Genome Assembly Program. Its utility lies in the power of its GUI and additional tools that can be used to interrogate DNA sequence trace files. gap4 can analyse each sequence trace individually and within the broader context of

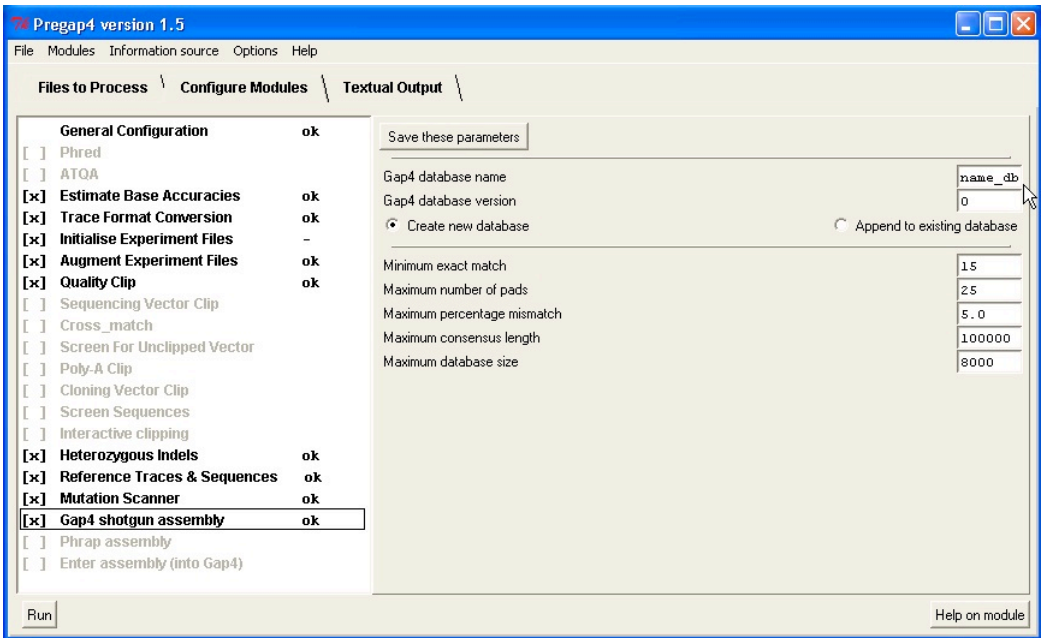

FIGURE 4.5: Screengrab of the pregap4 settings used for creating a new gap4 database

an assembled contig and highlight areas in the display window that warranted closer inspection, which was then achieved by opening up a small proportion of the electropherogams.

Because the purpose of sequence analysis in this study was to identify mutations (i.e. differences to "normal" sequences) in each amplimer, we were only interested in sequences that were different to the reference sequence for that section of DNA.

The Contig Editor window

Figure 4.6 shows the alignment of a group of DNA traces for the STS number stSG1157243.

The display of base characters in the Contig Editor is generated from analysing the sequence trace and ascribing them to the letters A, T, C or G. The traces are aligned in rows, sandwiched between the reference sequence traces, located at the top and bottom rows.

Electropherograms can be opened up for a particular trace by double clicking over the appropriate letter or alternatively every trace can be

In order to interrogate this highlighted DNA sequence change the forward and reverse traces were opened (see Figure 4.7) along with the un-highlighted trace corresponding to the individual from the row above (individual USH0124). This shows that the highlighted sequence change actually represents a heterozygous C>A base pair change.

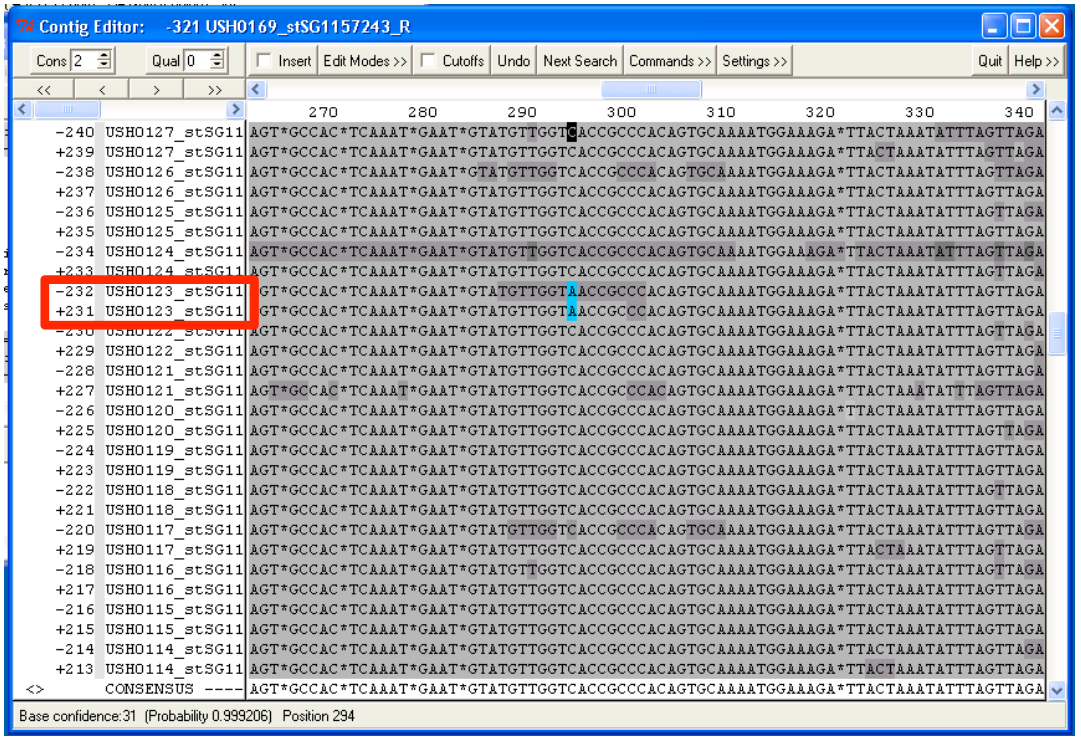

FIGURE 4.6: he traces have been aligned *by template*, such that forward and reverse traces (indicated by + and - signs respectively) for an individual are on adjacent rows. The consensus (reference) sequence is displayed at the bottom of the screen. Asterisks have been inserted to compensate for differences in one or more of the sequences in the contig compared to that of the reference sequence.A red box has been superimposed on the screengrab to highlight that trace on the 9th and 10th rows belongs to an individual identified by the code USH0123. Following processing with pregap4, two base pairs have been identified as differing from the reference sequence in individual USH0123 and these have been highlighted in blue. The cursor has been positioned at the position of position 294 in the contig

Opening a gap4 experiment file

On opening an experiment (.aux) file in gap4 a Contig Selector window (see Figure 4.8) appears in addition to an output window, the latter of which contains information about the number of sequences, average sequence read length and number of contigs created (which should be equal to one).

Missing sequences

A record was kept of how many and which sequence files were missing from a contig. If a sequence was missing this could potentially be due to lack of amplification.

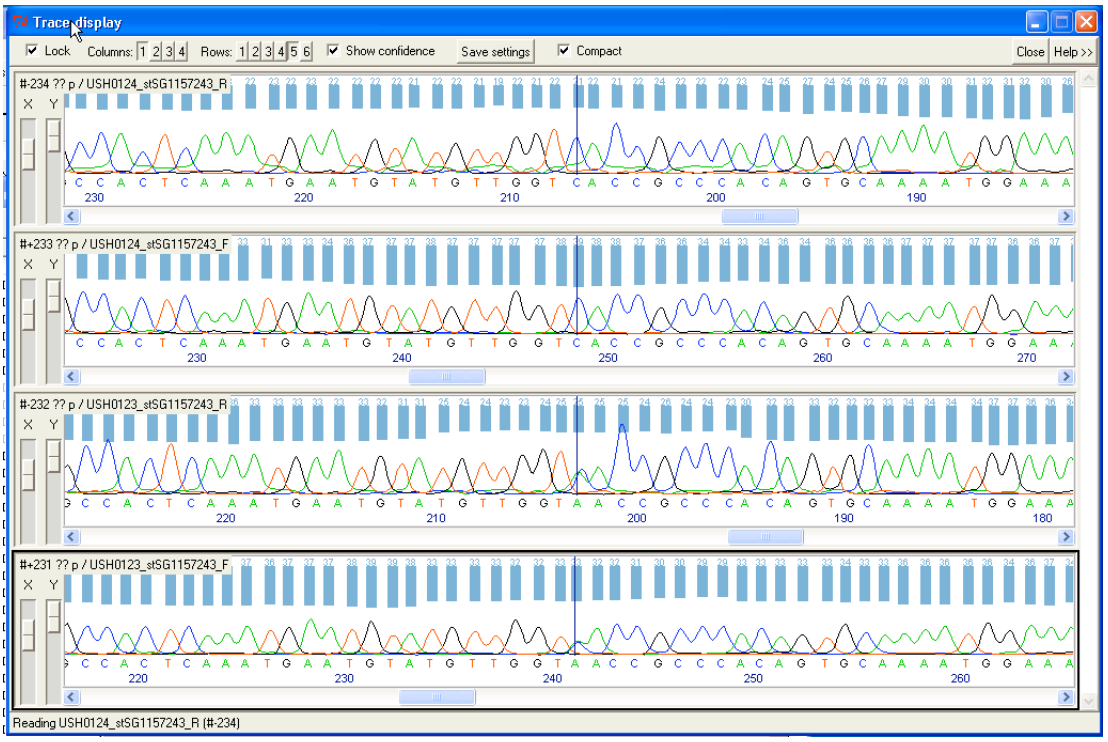

FIGURE 4.7: Screengrab of an electropherogram trace showing an example of a heterozygous base pair change

The lower two traces show a heterozygous C>A base pair change on both forward and reverse strands from individual USH0123, whilst the upper two traces show the wild type C nucleotide at this position on both forward and reverse strands of individual USH0124

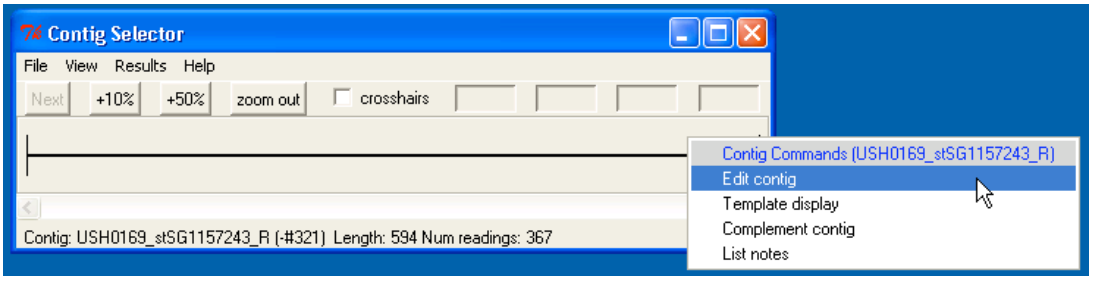

FIGURE 4.8: Screengrab of gap4 Contig Selector window

Right clicking on the Contig Selector (see Figure 4.8) opens up the the Contig Editor window which is the main window used for sequence analysis. If bidirectional sequences from an individual were missing (or present from only one strand) their absence was recorded, as this may represent evidence of a homozygous deletion within that amplimer for that individual.

Estimation of read quality

The "read quality" setting is a very useful feature that graphically displays the quality of the trace data by the grey-scale shading of the surrounding area to a

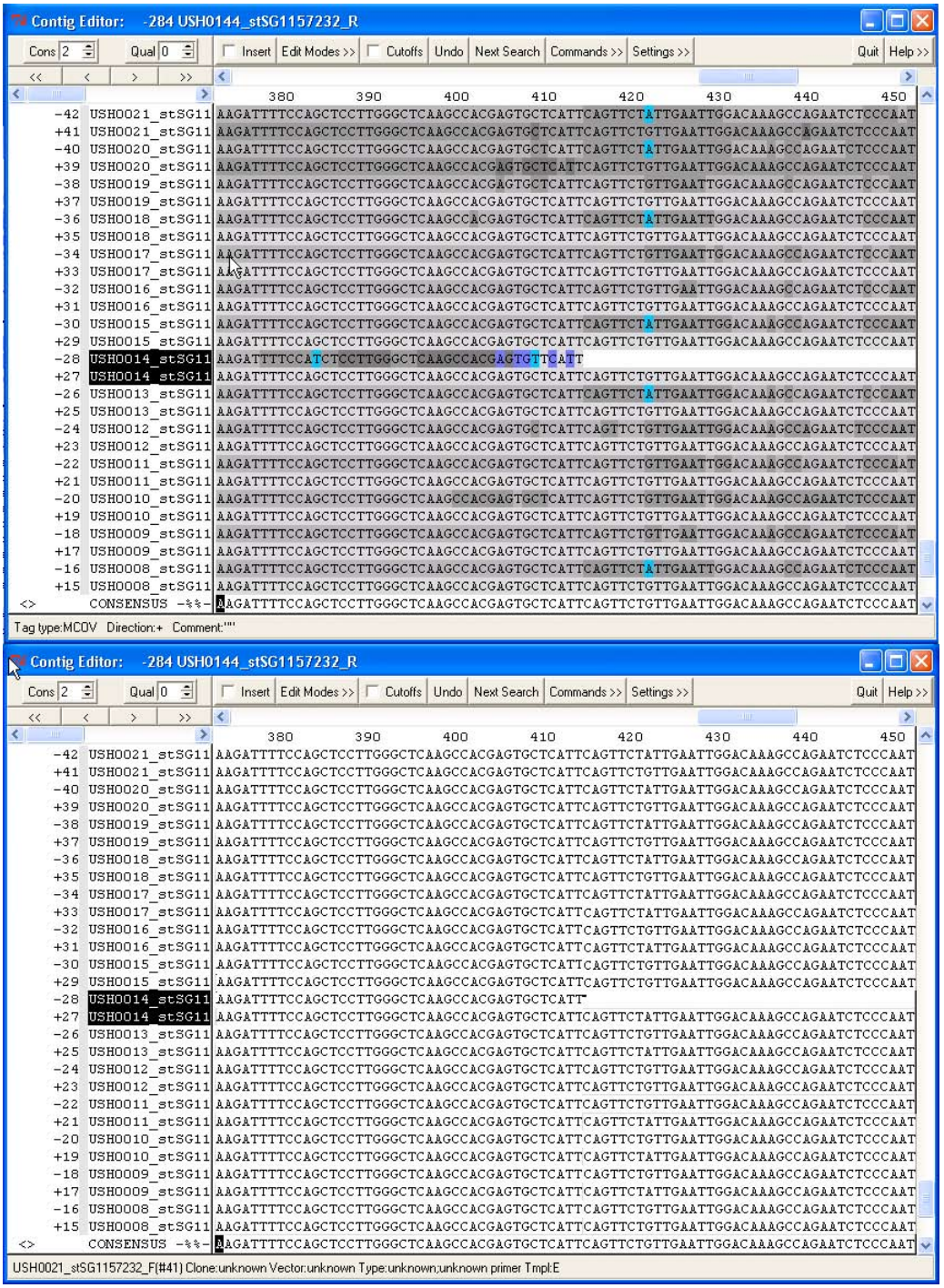

FIGURE 4.9: Screengrab of the Contig Editor in gap4 demonstrating the use of the read quality and base error calling

The graphical interface of gap4 makes spotting the missing sequence in individual USH0014 more obvious and also highlights the G >A heterozygous base pair substitution at position 421. The darker grey background colour corresponds to a poor read quality.

base letter such that lighter the background the better the data and the darker the background the poorer the sequence trace data is. This can be a useful tool in analysing batches of sequences as illustrated in Figure 4.9.

In some cases where the read quality of a seqment of a sequence trace is very poor, that part of the sequence might be ommitted altogether. For heterozygous deletions this produces a characteristic pattern This is illustrated if Figure 4.10.

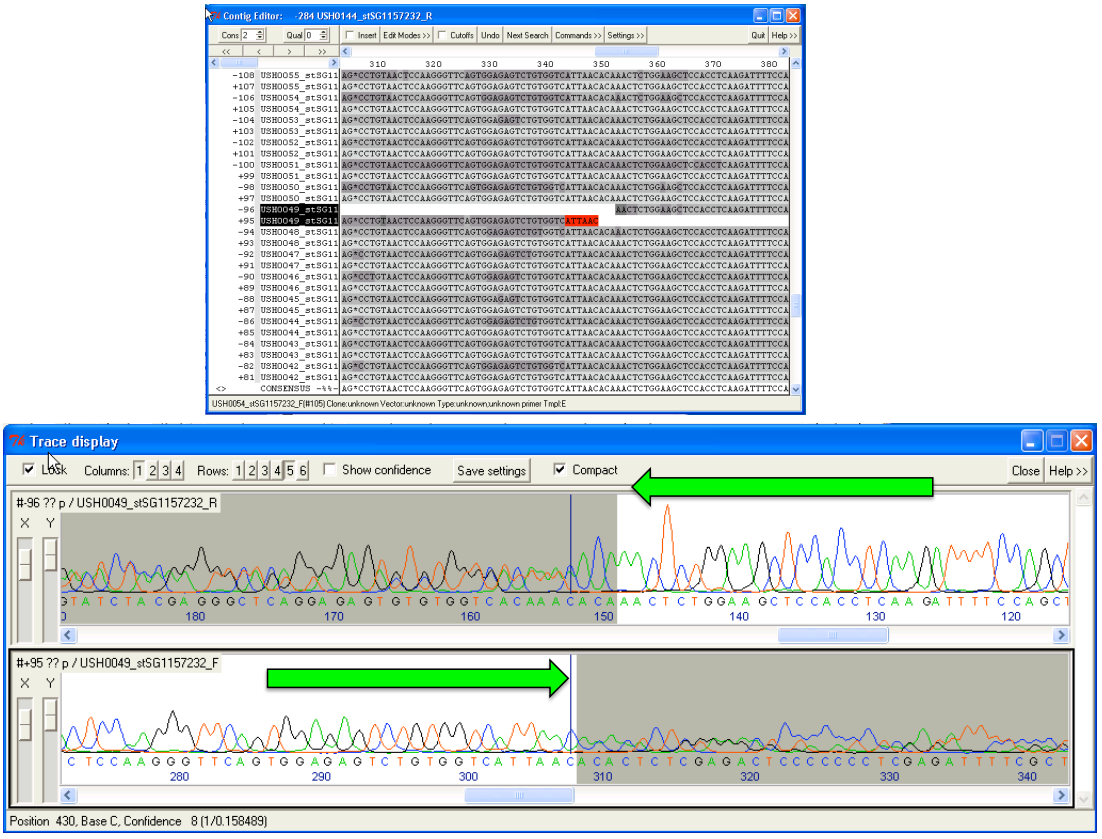

When the electropherogams for the individual (USH0049) with the deletion pattern are opened it can be seen that in both directions, the sequence traces are clean up until the point where the deletion is reached, after which the traces are superimposed from the normal strand and the deleted strand. This example is the c.11875delC in *USH2A* causing p.Gln3959LysfsX25

FIGURE 4.10: Screengrab showing the characteristic pattern of a heterozygous deletion

Highlighting sequence conflicts

gap4 is able to highlight differences in bases when compared to the reference sequence by modifying the background colour in the Contig editor display window (see 4.6). When surveying a contig, attention could thus be directed to opening the relevant electropherograms.

4.4.6 System of analysing a contig with gap4

As mentioned earlier each "contig" was created in pregap4 and consisted of a reference sequence aligned with the forward and reverse strands from a group of individuals (usually 48 individuals).

This main goal of surveying contigs was to identify any DNA sequence in an individual when compared to the reference sequence.

When analysing the contigs in the Contig Eritor window, due to the large number of traces and the size of the contigs (around 600 base pairs) the viewing window would have to be scrolled to enable a survey of the full contig.

(a) The traces were grouped by template (DNA sample)

(b) The contig was checked for missing sequences and those that were absent were recorded

(c) The contig was checked for unidirectional sequences and recorded

(d) The traces were grouped by strand (forward strands together and reverse strands together)

(e) Both extremes of the contig were inspected for sequence changes.

Chapter 5

Clinical Methods

5.1 Family history

Detailed pedigrees were taken following consultation with the index cases and where possible other members of their family.

In all families

Specific enquiry was made with regard to family history of visual or hearing loss in other family members. Specific enquiry was also made as to whether there was a history of consanguinity. Ethnicity was also ascertained by asking the country of origin of grandparents

In some families

In families with a history of consanguinity, specific details with regard to the nature of any consanguinity was made. This was done so that subsequent molecular analysis could be interpreted accordingly.

5.2 Past medical history

A full past medical history was taken based around a loose structure:

5.2.1 Audiovestibular history

- Age that hearing loss was first suspected/noticed
- Age that hearing loss was diagnosed
- Did the patient feel their hearing loss was progressive?
- Was their any objective evidence for progressive hearing loss?
- Hearing aid/Cochlear implant history (where appropriate)

5.2.2 Ophthalmic history

One important question we wanted to answer was if the age of onset of retinal symptoms was different amongst the different clinical and molecular subtypes of Usher syndrome.

Determining the age of onset of retinal symptoms *objectively* would be an impossible task in a cohort study like the NCUS, because the time of onset of retinal symptoms would be expected to have been in the past (this event having precipitated the actual diagnosis of Usher syndrome)

Accepting that determining ago of onset would therefore have to be a *subjective* assessment, care was taken to standardize the questions asked in order not to introduce further bias.

The questions were initially as open ended as possible and if the appropriate information could not be gleaned from this initial response as series of further questions were asked until a response was given.

i. Age that visual problems were first noticed
ii. The nature of the initial visual problems
iii. Age that nyctalopia was first suspected/noticed
iv. Age that visual field loss was first suspected/noticed
v. Age that a formal diagnosis of Retinitis Pigmntosa was first made
vi. Any history of previous ophthalmic problems, diagnoses or surgery

If an affected individual denied having problems seeing in the dark, further clarification was sought by asking the following questions:

> "Are you able to see the stars in the sky at night?"
>
> "Have you ever had trouble finding you seat in a cinema when the lights go down?"

If the answer was still negative, then this was recorded.

If an affected individual denied having problems with their visual field, further clarification was sought by asking the following questions:

> "Have you noticed that you have been bumping in to people or tripping over things?"

If the answer was still negative, then this was recorded.

In the results chapters the term **disease duration** was used as a variable for correlation analysis. Disease duration was an integer computed as a logical function and only calculated in individuals in whom a value for 'age of 1st visual symptom' was recorded as illustrated below.

Disease duration = (age at time of examination)−(age of 1st visual symptom) (5.1)

5.2.3 Medical History

A formal medical history including past or present medical diagnoses.

5.2.4 Surgical History

Enquiry was made with regard to any previous ophthalmic, audiovestibular or general surgery

5.2.5 Drug History

Current medications were recorded.

Family History of dual sensory loss

Specific enquiry was made with regard to hearing loss, visual loss or any other disorders in parents, grandparents and extended family members.

5.3 Visual acuity

Visual acuity (VA) was determined using a retro-illuminated ETDRS chart using LogMAR optotypes at 4 metres. VA was checked with the patient's own distance refractive correction if appropriate first and then through a pinhole in order to reduce the artefact of uncorrected refractive error or media opacity. The best corrected visual acuity was the best VA recorded by either method.

If no letters on the chart were read at 4 metres, the test distance was reduced to 1 metre and the appropriate correction (adding 0.6) made to calculate the correct LogMAR VA.

For those individuals with severely impaired visual acuity, the LogMAR approximation of 2.6 was used to represent counting fingers vision and extrapolated values of 2.7, 2.8, and 2.9 LogMAR to represent hand movement, light perception, and no light perception, respectively.

As a benchmark standard for "good" central vision, the minimum level of visual acuity used by the DVLA was taken. Whilst this represents an arbitrary criterion, it is a level of vision that is understandable as it is in layman's terms and such is a meaningful criterion that can be imparted to patients.

The DVLA standards compatible with 'driving vision' is taken to approximate to 6/10 Snellen (equivalent to logMAR $\leqslant 0.22$) [172]. Survival analysis was performed using log-rank (Mantel-Cox) test.

5.4 Colour vision

Colour vision of the red-green and blue-yellow axes, were assessed using the 4th edition Harvey-Rand-Rittler (HRR) colour pseudoisochromatic colour plates from Richmond products. These were used in preference to the more commonly used Ishihara plates which only assess colour vision in the red-green axis. The original HRR color vision test was developed 60 years ago by LeGrand Hardy, M.D., Gertrude Rand, Ph.D. and M.Catherine Rittler, B.A. at Columbia University USA with help from their colleagues Judd, Farnsworth and Nickerson. The test was designed to screen for, diagnose and quantify colour vision defects along the protan or deutan, tritan or tetartan axes. Following modification of the test's diagnostic accuracy and printing accuracy the 4th edition is now most widely used.

Colour vision tests were performed directly after testing visual acuity to ensure that study subjects had not dark adapted in any way prior to testing. They were thus performed in photopic conditions, after appropriate correction of any refractive error.

Clear instructions were given prior to the start of the test and responses were recorded on a proforma score-sheet see Figure 5.1 that is included with the test book.

The HRR plates are a book of 24 pages, each page representing a plate (see Figure 5.2).

The test is divided in to three parts.

1. Demonstration plates: (plates 1-4)

The first four plates of the test are demonstration plates and were not scored. All subjects apart from those with poor visual acuity, total color deficient vision or malingerers will be able to see the shapes on the first three plates (the fourth is blank).

2. Screening plates (plates 5-10)

Plates five to ten inclusive are screening plates and if correct responses were

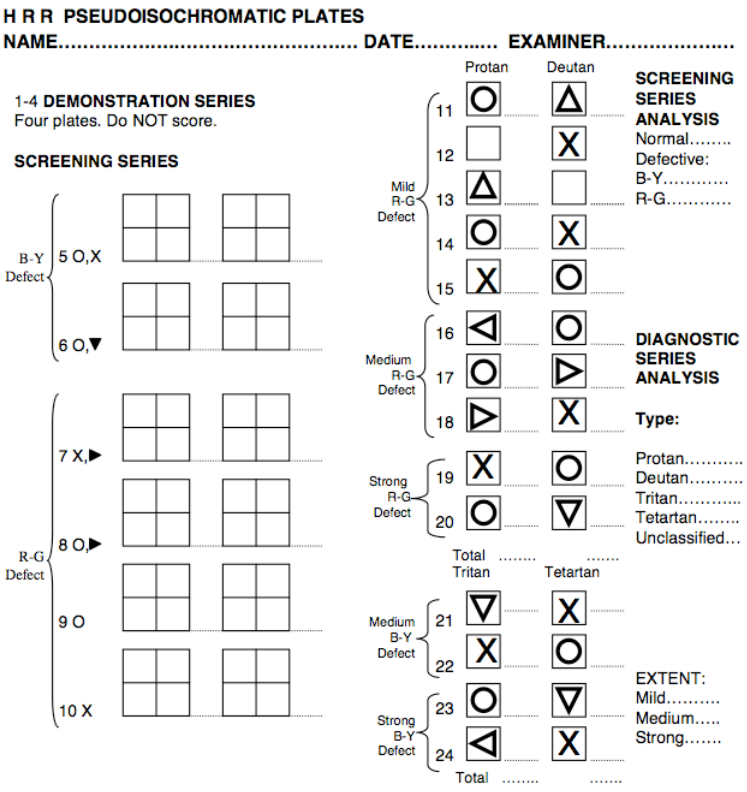

FIGURE 5.1: Scorecard for the Hardy-Rand-Rittler (HRR) psudoisochromatic colour vision test

supplied for these plates, the subject was deemed to have normal color vision and no further testing need be done.

3. Diagnostic plates (plates 11-24)

If there were any incorrect responses from plates 1-10, or if there appearred to be some difficulty in providing responses for the screening plates, the remainder of the test using the diagnostic plates was undertaken.

5.4.1 HRR Test instructions

The study subject was given a clean brush to hold and instructed with the following:

INSTRUCTION 1 : "I am going to show you some coloured symbols. Without touching them, how many do you see?"

INSTRUCTION 2 : "What are they?"

After naming the symbol the subject was asked the question..

INSTRUCTION 3 : ''Where are they?"

and asked to trace out any shapes seen using the hand-held brush used as a pointer. The test subject was requested not to touch the plates directly

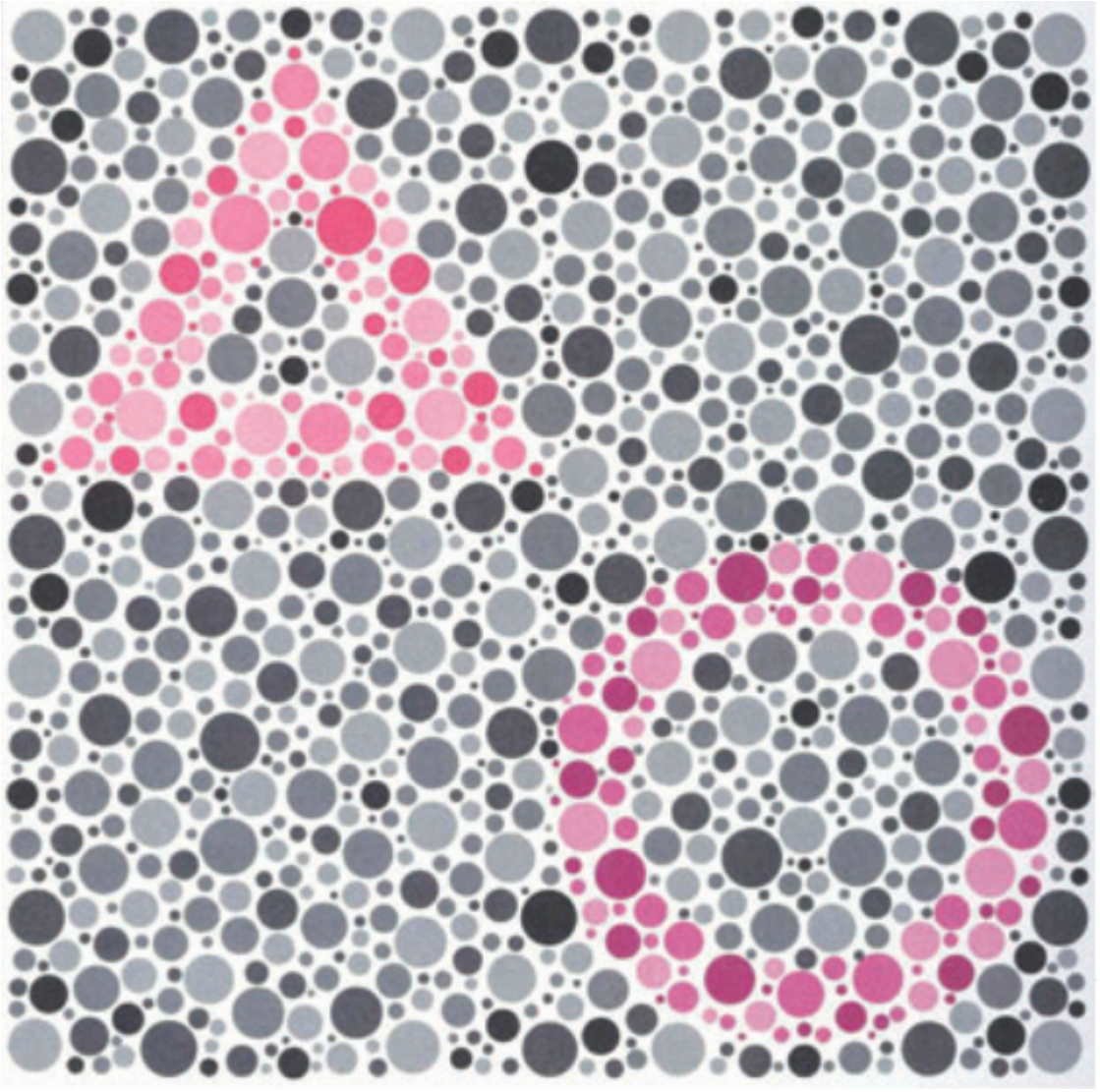

FIGURE 5.2: A HRR diagnostic plate showing symbols made from coloured dots on a grey background testing for deficiencies on the protan/deutan axis

with their finger to avoid marking the test plates and adversely affecting the validity of their subsequent use. Finally the remainder of the test was explained to the test subject:

> INSTRUCTION 4 : "The test itself is made up of just these three symbols with either two, one, or none on each page. Some of them will be harder for you to see as they may be less strong in color. Draw round the outline of any shape you see on each page"

In cases where study subjects communicated by sign language the instructions were modified so as to communicate the test requirements appropriately using a sign language interpreter.

5.4.2 HRR Test scoring

If the subject gave the correct response to questions 1, 2 and 3 for each plate they were scored as correct with a $\surd$ placed in the appropriate box on the score-sheet (see Figure 5.1). If they gave an incorrect response to any of the three questions, the box was left blank.

The diagnostic plates (plates 11-24) are split in to those that test for colour defects on the protan/deutan (red/green) axis (plates 11-20) and those that test the tritan/tetartan (blue/yellow) diagnostic plates (plates 21-24).

The diagnostic plates from each axis are further subdivided in to three subsections indicating mild, medium and severe defects for the red/green axis and in to two subsections testing for medium and severe defects for the blue/yellow axis.

At the conclusion of the test, the binary responses to each box were then analysed to determine the nature and severity of colour vision defect. Figure 5.3 is a schematic representing the method of scoring.

Plate number	Axis tested		Example A	Example B	Example C
11	RED / GREEN	MILD	✔	✔	
12			✔		
13			✔	✔	
14			✔	✔	
15			✔	✔	
16		MEDIUM	✔	✔	
17			✔	✔	
18			✔	✔	✔
19		STRONG	✔	✔	
20			✔	✔	✔
21	BLUE / YELLOW	MEDIUM	✔		
22			✔	✔	✔
23		STRONG	✔	✔	✔
24			✔	✔	✔

FIGURE 5.3: Schematic representing the scoring system for responses of the HRR colour vision plates

Examples of three individuals are given to illustrate the scoring system in Figure 5.3. In Example A, all responses were correct and it is likely that the responses to the screening plates (5-10) were also correct. In Example A the test subject has normal colour vision for the red/green and blue/yellow axes.

In Example B the subject makes an error in the mild red/green subset (plates11-15) and provides correct responses for the medium red/green (16-18) and strong red/green (19-20) subsets. They thus have a mild defect on the red/green axis. In Example B the subject also makes an error in the medium blue/yellow subset (plates 21-22) and provides correct responses for the strong blue/yellow (23-24) subsets. They thus have a medium defect on the blue/yellow axis.

Example 3 demonstrates a strong blue/yellow defect and medium blue/yellow defect.

Although not indicated on the schematic in Figure 5.3, it is actually possible to further categorise the nature of a colour visual defect by counting which of the two columns present on the score-sheet (see Figure 5.1) have the most correct responses . For example if more $\surd$ responses were entered in the "Protan" rather than "Deutan" column then the subject had a ProtanDeutan defect.

Although this detail was available, for the purposes of clarity colour vision responses were simply recorded in terms of the overall deficiency on red/green and blue/yellow axes.

5.5 Visual fields

Visual Fields were obtained using kinetic Goldmann perimetry. This method of visual field testing was used in preference to other more standard and arguably easier methods of visual field testing such as the automated Humphrey visual field 30-2. The benefits of the using Goldmann kinetic perimetry were essentially threefold. Firstly the Goldmann perimeter was able to test a significantly larger area of visual field than other methods. Secondly, the interactive nature of the test, allowing mid-peripheral scotomas (often present in RP) to be delineated more accurately and thirdly, the ability to map out isotpers of visual field sensitivity at standardised levels of luminance afforded the opportunity to compare standardised visual field areas between individuals better than using data from static perimetry which is much harder to compare between individuals.

The Goldmann perimeter was calibrated prior to use, initially calibrating the target to 1000 asb followed by calibration of the background to 31.5 asb.

5.5.1 Calibration of Goldmann perimeter

This was performed daily prior to performing testing in order to standardise test conditions. This was done in a darkened room with the door nearly fully closed with the ambient room lights off (i.e. same conditions for testing).

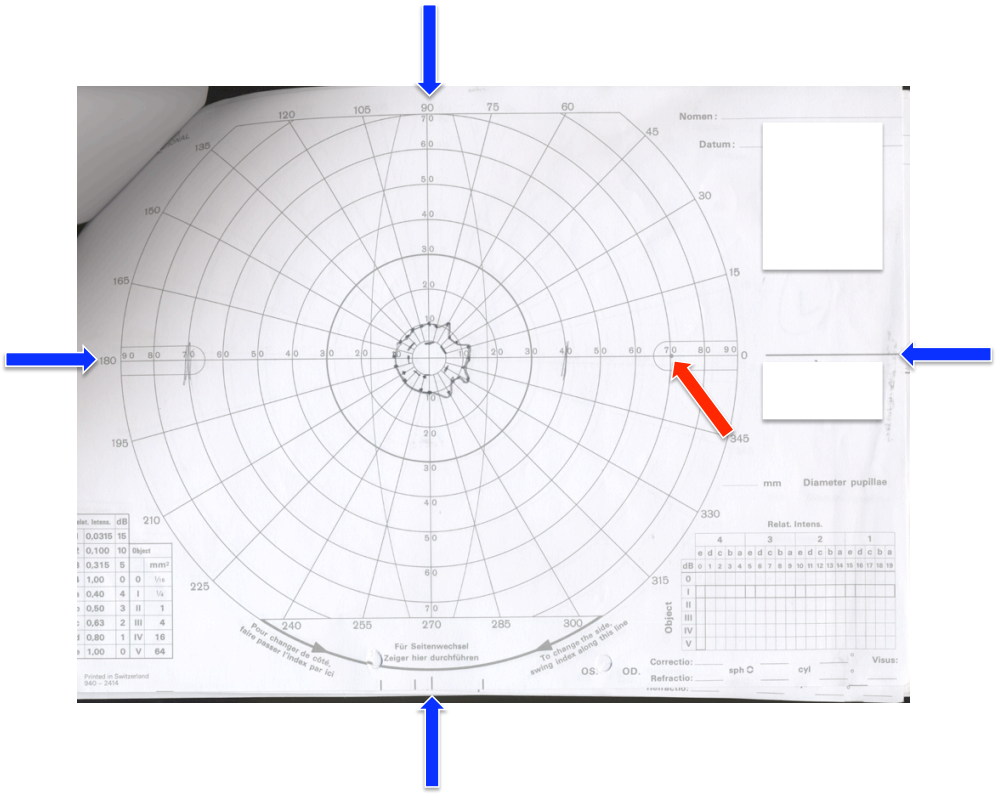

FIGURE 5.4: Orientation lines (blue arrows) and target locking position (red arrow) for calibration of Goldmann perimeter

Below is the process followed to calibrate the machine:

i. Turn the machine on.

ii. Paper inserted in to the machine and aligned in horizontal and vertical meridians (see blue arrows in Figure 5.4).

iii. The pantograph arm (sometimes called the target light projector arm) of the machine was placed in the locking position (see red arrow in Figure 5.4) and pressed forwards to lock the pantograph handle in position. This causes the pantograph to direct the target light toward the slot on the left side of the machine.

iv. All filter handles were turned to their far right producing the largest brightest target V4e.

v. The light meter was inserted into slot on the left side of machine.

vi. The small bulb on left side of bowl was turned on to illuminate the light meter screen.

vii. The photometer screen was opened by pushing the white flag up and out the way of the light path allowing it to measure the brightness of the target.

viii. Luminosity was adjusted such that the target light was 1000 apostilbs.

ix. If unable to obtain maximum luminosity, the main bulb could be removed and rotated or replaced.

x. Light meter screen was switched off.

xi. The handle of photometer screen (the white flag) was pulled down.

xii. The target light will now be directed on to white flag.

xiii. The light filters at the operator side of the machine were adjusted to the V1e setting.

xiv. Walking round to the test subject's side of the machine and looking through the aperture obliquely, the brightness of the target light was equated to that of the photometer screen by sliding the rheostat at the top of the machine until brightness was judged to be the same as that on the white flag.

xv. This should be equivalent to a background luminance of the perimeter of 31.5 apostilbs.

xvi. After calibration the pantograph arm was unlocked and placed in a safe position prior to bringing the patient to the machine.

5.5.2 Instructions to study subjects prior to Goldmann visual field testing

Due to the deafblind population being studied, prior to seating the study subject at the machine, the test procedure and purpose of the test was fully explained verbally or via a sign language interpreter as appropriate. Another important consideration at this stage in the clinical examination testing was that subjects would be changing from the photopic conditions used to test visual acuity and colour vision, in to a dark environment. Due to the nature of their RP, this often adversely affected their vision subsequently for an indefinite time dependant on their retinal disease. Thus prior to measurement

of visual fields, time was taken to summarise the following battery of tests that would be performed in the session for the benefit of study subjects.

The following points were clearly explained to the patient:

i. The purpose of this test is to determine the area in each eye in which you are able to see different sized targets of light
ii. You should be seated comfortably at the machine, so that you can keep your head still for the duration of the test.
iii. If you get tired during the test or want a break, that is fine, but they should indicate this to the tester (myself) by means of a prearranged signal
iv. One eye would be tested at a time, whilst the other is covered with a patch
v. You should *only* look directly at the target in the centre of the bowl and keep your gaze fixed here for the duration of the test
vi. If you are unable to clearly see the target in the centre of the bowl then the test would be abandoned.
vii. You will be given a hand held device with a button (connected to a buzzer), which you should press down *only* when they can see a light
viii. Lights will appear and disappear throughout the test
ix. If you see a light during the test, press and hold the button
x. The button should be held down for the entire duration of time that they were able to see the light
xi. When the light disappears, they should immediately let go of the button
xii. The lights will be of different sizes and brightness
xiii. Not to worry too much about the test as they would not be expected to see lights all of the time
xiv. No matter where the lights appear/disappear their gaze should remain fixed firmly on the target in the centre of the bowl
xv. I (as the examiner) will be viewing your eye (the test subject) from behind the target to ensure that their gaze was fixed firmly on the target in the centre of the bowl

The patient was seated at the machine and the table height and chin rest was adjusted to optimise the subjects comfort and body habitus. The eye not being tested was occluded up with an eye patch.

Each eye was tested separately starting with the eye with better visual acuity. Gaze fixation was constantly monitored through the viewing telescope on the device. The largest isopter (V4e) was tested initially moving from the

periphery of the visual field toward the centre. Scotomatous areas identified within the visual field were interrogated more closely by moving the light target from a non-seeing (scotomatous) to a seeing area, to delineate the borders of the scotoma.

If the visual field was able to be measured for the V4e isopter, the middle sized target (II4e) was then tested in the same fashion, followed by the smallest sized isopter (I4e) where possible.

In most cases the visual field was taken with an individuals appropriate refractive correction. In some cases the central 30 degrees was re-checked using the appropriate lens correction as calculated by using Goldmann's near add table

TABLE 5.1: Goldmann's near add table

Age in years	**Dioptres of near add**
40-45	**+1.5**
45-50	**+2.0**
50-55	**+2.5**
55-60	**+3.0**
60+ or pseudophakes	**+3.25**

5.5.3 Calculation of visual field area

The paper for each Goldmann visual field for each eye, was scanned as a digital image (.tif file) which was subsequently analysed with the planimetry software 'Retinal Area Analysis Tool', a package designed by Fred Fitzke and Anthony Halfyard (2002) to calculate the two-dimensional area from the visual field plot and convert this in to degrees squared units. Calibration of the two-dimensional image file was performed by using the central point of fixation and the centre of the blind spot as the eqivalent scaling factor between fovea and optic nerve head. In eyes where deliniation of the blind spot was not performed or not possible (see Figure 5.5) the approximate location of the centre of the blind spot was 15 degrees temporal to the point of central fixation.

When calculating the area of visual field for each of the three isopters V4e, II4e and I4e, the area of central contiguous islands of visual field was recorded in addition the the area of any peripheral islands of visual field, the total area of visual field size for each isopter being the sum of central and peripheral islands. This meant that for each isopter, three variables were recorded (central, perihperal and total area in degrees squared). This was done for both eyes resulting in a maximum of 18 data variables per individual. For brevity

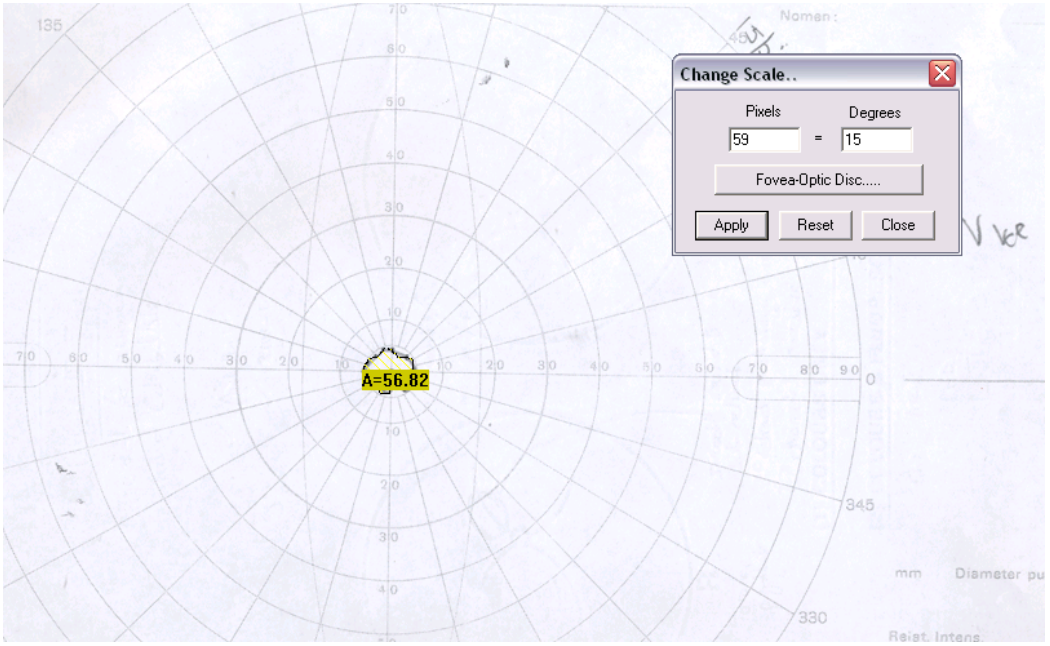

The blind spot for this individual (with a severely constricted visual field) lay outside the area of their visual field and was impossible to map. The fovea-optic disc calibration required for calibration of the software was therefore performed by using the central target (fovea) and a point 15 degrees temporal to this point (estimated location of blind spot) as an approximation

FIGURE 5.5: Screengrab of the planimetry software retinal analysis tool developed by Fitzke and Halfyard, used to calculate the area of Goldmann visual fields

these variables were ascribed a categorical label, prefixed by **R** (right) or **L** (left) to indicate laterality. These labels are summarised in Table 5.2.

TABLE 5.2: Table illustrating the system of naming categories of visual field area. Each value label was prefixed by R or L to indicate laterality

ISOPTER	central island	peripheral island	TOTAL area within the isopter
V4e	cV4e	pV4e	V4eTotal
II4e	cII4e	pII4e	II4eTotal
I4e	cI4e	pI4e	I4eTotal

5.6 Refractive error

Refractive error was assessed either from the individual's most recent glasses prescription or by focimetry of their distance glasses.

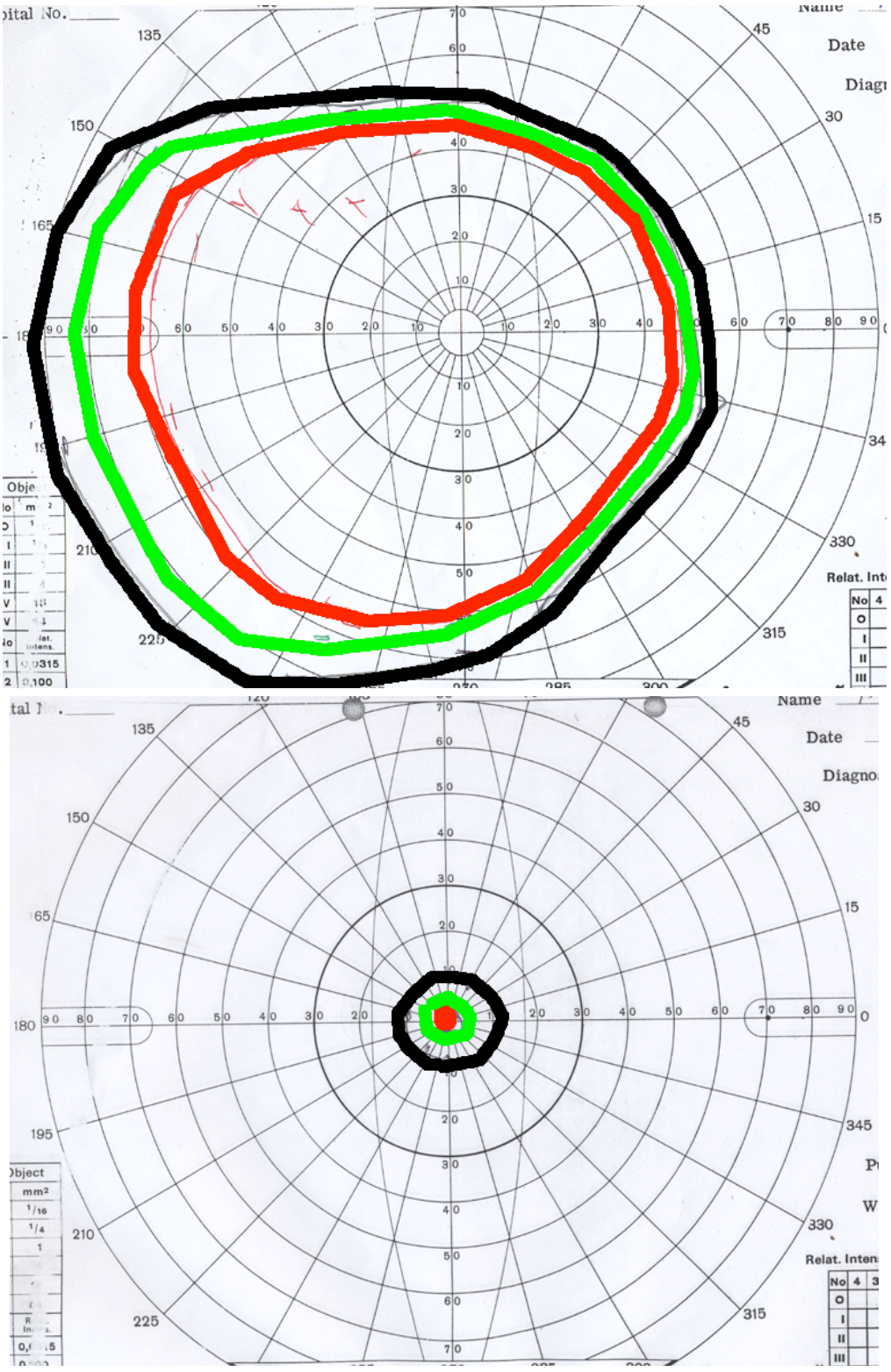

FIGURE 5.6: Visual fields taken in the right eye of two individuals with (above) a normal visual field; (below) an individual with USH2 due to disease in *USH2A* restricted to a central 10 degrees. The isopters represented are for the different target sizes used to map visual fields. Largest (V4e) - black, Intermediate (II4e) - green, Smallest (I4e) - red

5.7 Colour fundus photography

Colour photographs of the retina were obtained after pupil dilatation with tropicamide 1 %. Where possible the fundus was surveyed in all nine positions of gaze. The images were taken with the Topcon TRC-501X digital camera using the IMAGEnet 2000 software used to collect and store the images.

Images were cropped and assembled as a montage using Adobe Photoshop CS2 and the open source program GIMP (The GNU Image Manipulation Program, for X Windows systems software).

5.8 Fundus autofluorescence

Fundus autofluorescence imaging was performed using the Heidelberg confocal scanning laser ophthalmoscope (SLO) system (Heidelberg Retina Angiograph, Heidelberg Engineering, Dossenheim, Germany). Images of fundus autofluorescence were recorded after pupillary dilation with a 30 degree field-of-view mode. The ametropic corrector was employed to correct for refractive error. An argon blue laser (wavelength of 488 nm) was used for excitation and the emitted light of greater than 495 nm was detected with a barrier filter. To amplify the autofluorescence signal, a flash mode was used (i.e. laser power was increased 2-fold for 32 milliseconds). At least 24 single autofluorescence images of 512 x 512 pixels were acquired in series mode with a frequency of 12 images per second. The best 10 images were selected for automatic alignment, and the creation of a single mean image for each eye.

5.9 Optical coherence tomography

Optical coherence tomography images were taken using the Zeiss OCT3 machine (Stratus OCT3; Carl Zeiss Meditec, Dublin, CA). 6mm scans centred on the fovea were obtained employing firstly the 'fast macular' preset followed by a horizontal cross hair scan.

High resolution optical coherence tomography images were also available on some individuals and were taken with the Spectralis HRA+OCT (Heidelberg Engineering, Germany), Camera version 1.6.0.0 and OCT camera version 1.45.0.0, acquisition software version 4.0.2.0.

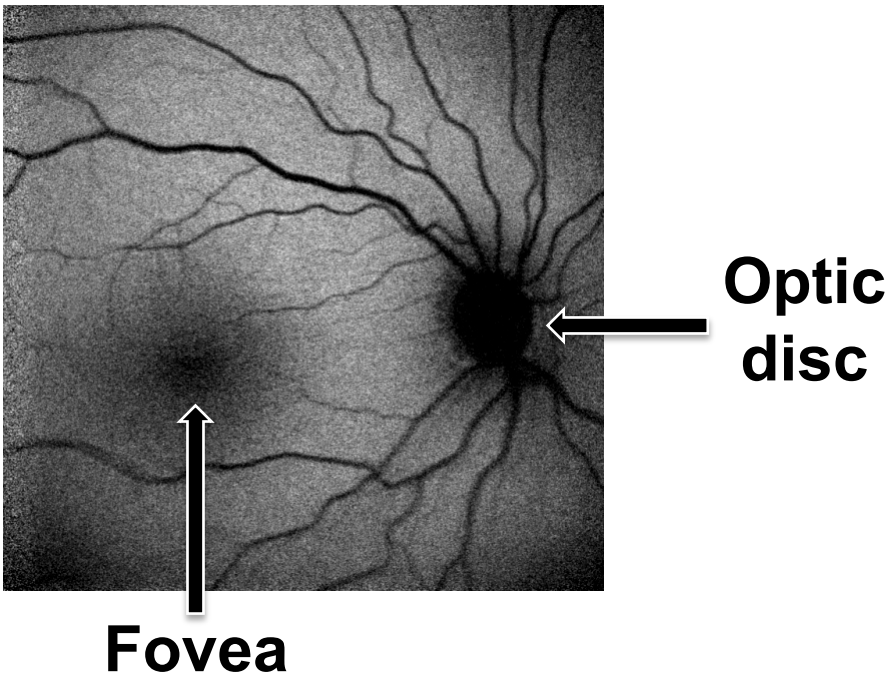

FIGURE 5.7: Fundus autofluorescence imaging in a normal right eye. The area of hypofluorescence corresponding to the fovea can be seen. There is no autofluorescence produced at the optic disc and there is total masking of autofluorescence by the retinal vessels, which are seen as branching curvilinear lines from the optic disc

5.10 Statistical Analysis

Statistical analysis was performed with SPSS for Windows, Rel. 16.0.2 2008, SPSS Inc. (Chicago, USA) and GraphPad Prism version 4.00 for Windows, GraphPad Software, (San Diego California USA) www.graphpad.com.

If variables were not normally distributed, bivariate correlation analysis was performed using Spearman's rank coefficient. For all statistical tests significance was assumed at levels of $P < 0.05$.

5.11 Terms used to describe study subsets

In subsequent chapters, the term **affected NCUS cohort** will be used to refer to all affected individuals from USH families. These individuals have a diagnosis of USH1, USH2, USH3 or ARRP [1]

Chapter 6

Results - Molecular Results

6.1 Demographics

This chapter describes the breakdown of the demographic of the NCUS study cohort. Individuals with a clinical diagnosis consistent with Usher syndrome type 1, type 2 or type 3 are referred to as **USH1**, **USH2** and **USH3** respectively. Each family had received a diagnosis of Usher syndrome at some point prior to recruitment in to the study. However, during the course of the study it became clear that a small subset of families had clinical phenotypes or pedigree structures that were not consistent with a diagnosis of either USH1, USH2 or USH3. These **non-USH** families are discussed in a later section. Where the causative gene was identified in a family, this was referred to as their **"molecular diagnosis"**.

6.1.1 Total numbers recruited

This study recruited affected individuals with a diagnosis of Usher syndrome and their unaffected family members in to the study. A total of 734 individuals from 190 families were recruited in to the study. Of the 734 individuals, 242 were affected.

Not all individuals consented for all aspects of the study. Some unaffected family members did not want to, or were unable to give a blood sample for DNA analysis. Some affected individuals were happy to submit a DNA sample, but did not wish to carry out the clinical phenotyping tests either in their entirety or at all.

At the conclusion of the study, 673 DNA samples (236 of these were from affected individuals) from this NCUS cohort were collected for analysis and ophthalmic data was available on 209 affected individuals.

TABLE 6.1: Clinical diagnosis of all 190 families recruited in to the NCUS

Segregation pattern	Clinical diagnosis	Families (n)	Families (n) with USH	Families (n) with non-USH
visual loss and hearing loss apparently segregating as the same disorder	Usher_Type1	46	178	
	Usher_Type2	130		
	Usher_Type3	2		
	Sector RP and SNLHL	1		12
	atypical AV phenotype	3		
	SNHL (no retinal disease)	2		
	atypical retinal phenotype (no AV data available)	1		
	Alstrom syndrome	1		
	unknown_syndromic_cause	1		
visual loss and hearing loss segregating as two separate disorders	Late onset SNHL + ARRP	1		
	Acquired SNHL (? post meningitis) +RP	1		
	SNHL+ ADRP segregating as separate disorders	1		
	TOTAL	190		

Av *Audiovestibular*
RP *Retinitis Pigmentosa*
SNHL *Sensorineural Hearing Loss*
ARRP *Autosomal Recessive Retinitis Pigmentosa*
ADRP *Autosomal Dominant Retinitis Pigmentosa*

6.1.2 Total numbers analysed

As per study protocol, individuals and families reserved the right to withdraw from the study at any point.

Of the initial 190 families recruited, three families Family 156 (USH1); Family 186 (USH2); and Family 167 (non-USH) withdrew from the study altogether and did not undergo clinical or molecular analysis. The affected individual NCUS 276 (Family 84) consented to undergo clinical phenotyping, but withdrew consent for genetic analysis.

This resulted in clinical and genetic cohorts of slightly different sizes. For the purposes of clarity, the total number of families that were recruited, underwent ophthalmic examination and those that underwent molecular analysis are shown in Table 6.2.

219 individuals from 188 families underwent ophthalmic phenotyping. Each of the 219 individuals did not perform every ophthalmic test modality. In the following chapters when reporting ophthalmic test results, the distinction between individuals who *did not* perform a particular test, and those that were *unable* to perform the test due to severe visual dysfunction is made. If

TABLE 6.2: Number of families that were recruited into the study and the subsets of these families that underwent clinical and molecular analysis

		Families (n)		
	Clinical diagnosis	TOTAL RECRUITED	AVAILABLE FOR CLINICAL ANALYSIS	AVAILABLE FOR MOLECULAR ANALYSIS
	Usher_Type1	46	45	45
	Usher_Type2	130	129	128
	Usher_Type3	2	2	2
SUBTOTAL	**USH**	**178**	**176**	**175**
SUBTOTAL	**Non-USH ***	**12**	**11**	**11**
TOTAL	**ALL**	**190**	**187**	**186**

$*$ = families with visual and hearing dysfunction attributable to causes other than Usher syndrome

an individual lacked the visual function to perform a test (e.g. central vision too poor to test colour vision) the numbers of these indivduals are stated as they represent an important clinical finding. When stating the outcomes or relative proportions of test performance for different subgroups, the number of individuals performing the test are stated.

Individuals from 186 families were submitted for bidirectional DNA sequencing analysis and their clinical diagnoses are outlined in table 6.2.

A total of 175 families had a clinical diagnosis of USH1, USH2 or USH3. 11 families were subsequently identified as having their hearing and visual loss attributable to other causes. Only one of these eleven 'non-USH' families were found to have disease causing mutations in any of the Usher genes sequenced, reaffirming the clinical findings. This family (Family 142) had an atypical phenotype due to mutations in the *USH1C* gene, representing a novel phenotype for *USH1C*.This sibling pair along with the other non-USH families are discussed in greater detail in a separate section 10.1.1.

Of the 178 families with a diagnosis of Usher syndrome, just under a quarter were USH1, and 70% were USH2, with only two USH3 families identified (Figure 6.3).

Paucity of USH3 families

Of the 188 families available for clinical analysis, 176 families were identified with a clinical diagnosis consistent with either USH1, USH2 or USH3. During recruitment it became apparent that many individuals reported progressive hearing loss, raising the possibility that they had USH3. During the early stages of the study, other researchers published findings documenting progression of hearing loss (greater than could be explained by simply presbyacusis

TABLE 6.3: Piechart representing the proportion of families available for ophthalmic clinical examination

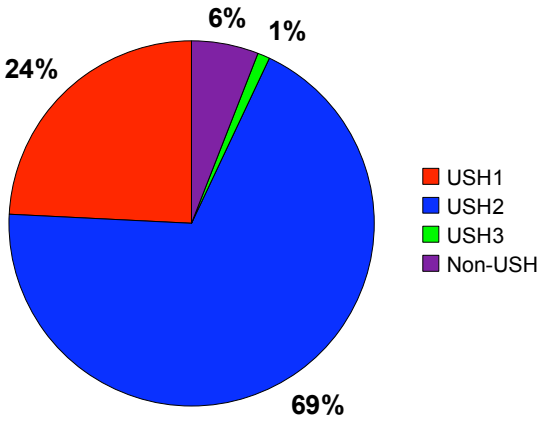

alone) in individuals with a clinical diagnosis of USH2, a subset of which also had a molecular diagnosis of *USH2A* [173].

This important finding suggested that the clinical distinction between USH2 and USH3 was less clear-cut than reported previously. A number of individuals recruited into this study reported a history of subjective and in some cases objective progression of hearing loss. Of this subset of 'non-USH1' individuals, most were subsequently found to have disease due to USH2A, one individual was subsequently identified as not having Usher syndrome, leaving only three individuals from two families with a molecular diagnosis of USH3A. Due to the small numbers of USH3 families identified in this study, they have been omitted in some sections of subsequent chapters, as the small sample size precluded useful statistical analysis when comparing this small group against the larger USH1 and USH2 groups.

6.1.3 Gender (Figure 6.1)

The gender spread was similar in the USH1 and USH2 groups, resulting in an equal mix of males and females in each clinical group . The three individuals with USH3 were all male

Statistically, there was no significant difference between males and females in the USH1, USH2, USH3 and non-USH groups (chi-squared test, alpha <0.05).

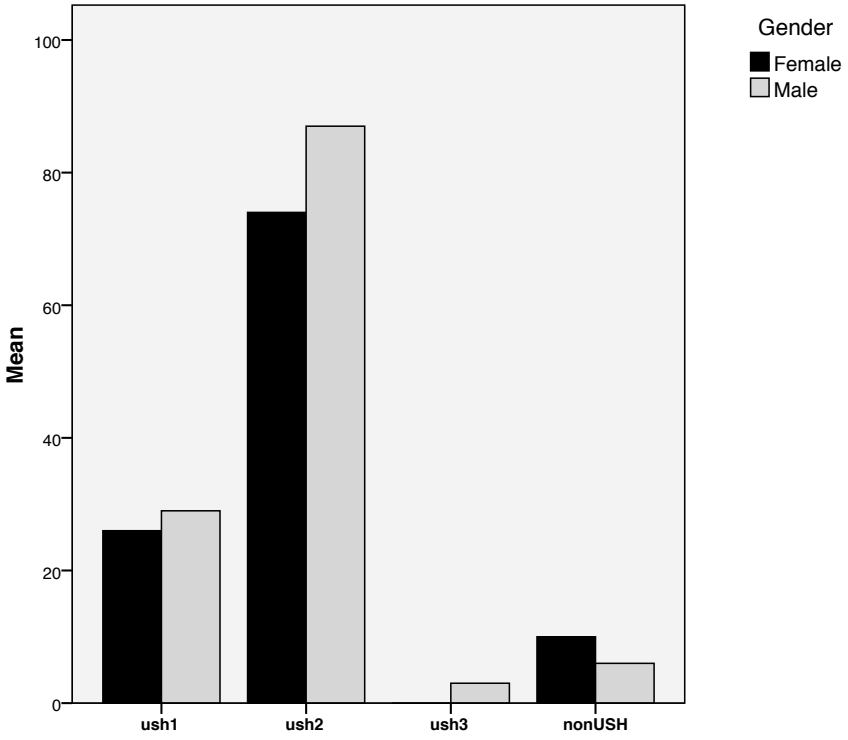

FIGURE 6.1: Barchart displaying gender per clinical group

6.1.4 Age (Figure 6.1.4)

Unlike gender, the ages of affected individuals amongst the clinical groups varied significantly, with the USH1 cohort having a younger median age than the USH2 cohort.

The significant difference in ages between USH1, USH2 and USH3 (Kruskal-Wallis test, P<0.0001) most likely represents a recruitment bias.

The median age of affected individuals was **28yrs for the USH1** and **41yrs for USH2**.

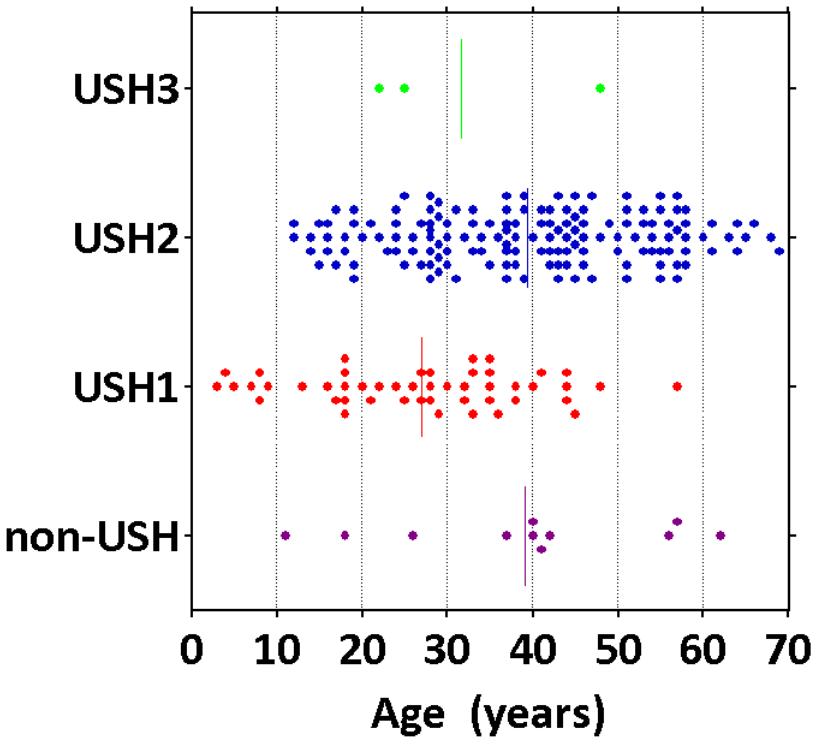

(a) Scattergraph

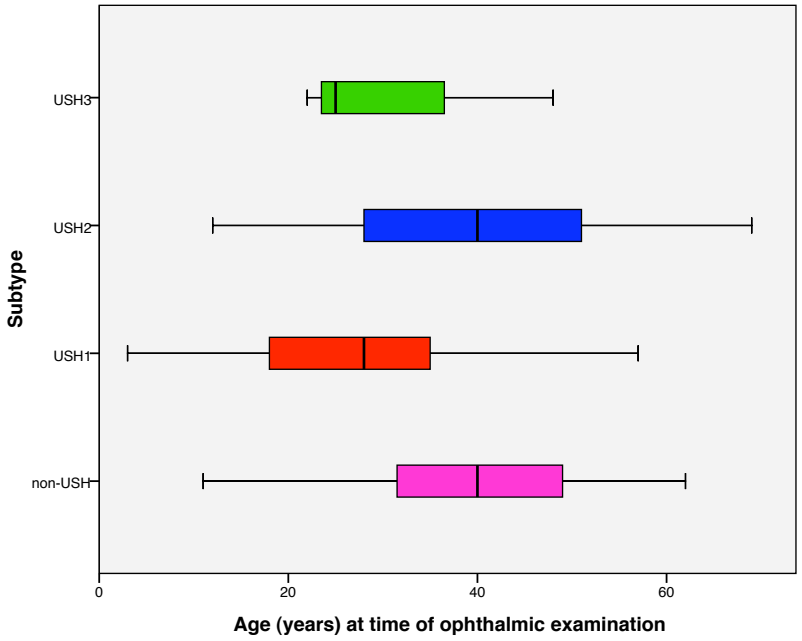

(b) Box and whisker plot

FIGURE 6.2: Scattergraph (above) showing the age in years at the time of ophthalmic examination and Box and whisker plot (below) showing the range, interquartile range and median ages per clinical subtype

6.1.5 Recruitment

Time course of families recruited

The progress of recruitment of families to the study is displayed graphically in Figure 6.3.

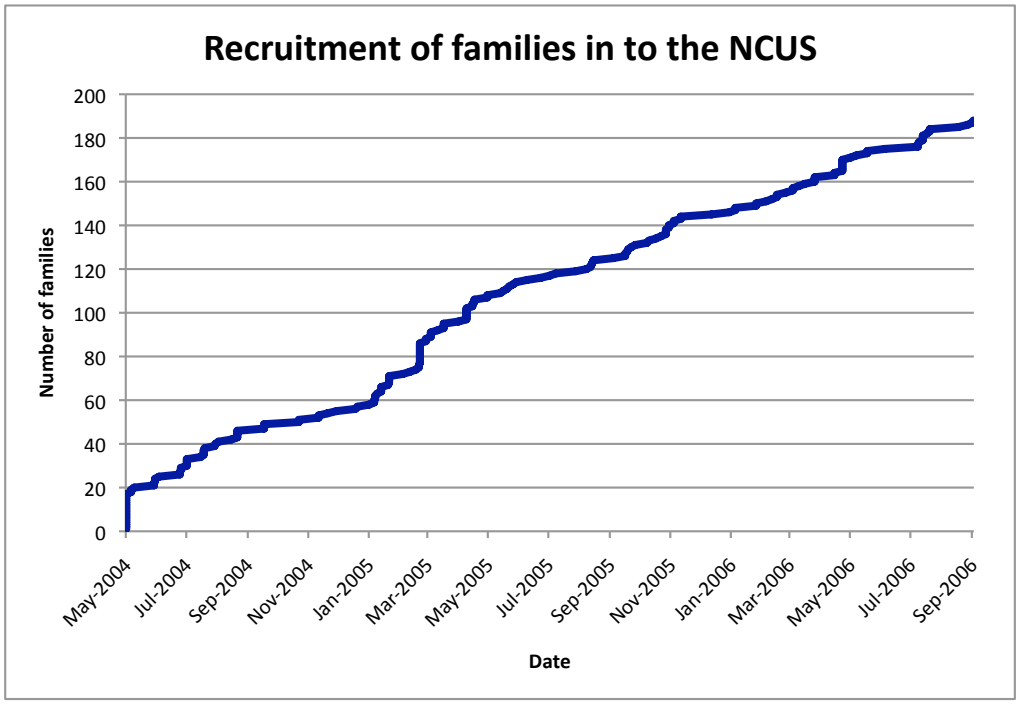

FIGURE 6.3: Graph showing the number of families recruited in to the NCUS over the course of the study

Sources of recruitment (Figure 6.4)

The NCUS had ethical approval for recruitment on a nationwide basis and families were recruited from throughout the UK.

The majority of participants were recruited through three main channels. Moorfields Eye Hospital (MEH), the charity Sense and self-referral. A smaller but important contribution from the amalgamated London paediatric centres Great Ormond Street Hospital (GOSH) and the Institute of Child Health (ICH) who referred the majority of younger index cases

Approximately a quarter of families with Usher syndrome self-referred after hearing about the study through friends, family, the deaf-blind community and/or the Sense website illustrating the importance of awareness of the study in the deafblind community in helping recruiting numbers.

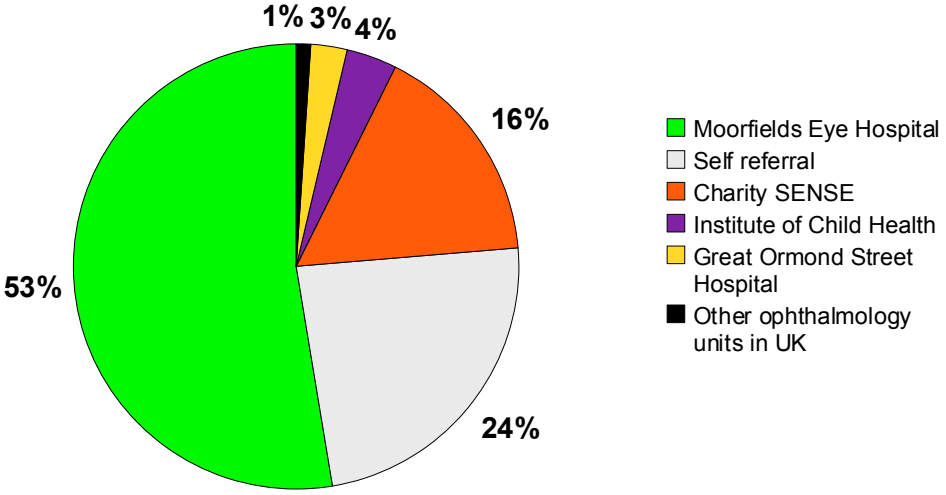

FIGURE 6.4: Piechart showing sources of recruitment of families with Usher syndrome

Preferred contact mode

Following initial contact with families, each affected individual was asked to state their preferred mode of contact. Whilst this may seem a trivial point to detail in the results section of this study, it is included here because these data may be useful for similar studies conducted within the UK Usher population in the future. Due to the dual sensory impairment in individuals with Usher syndrome face, establishing a reliable mode of communication is extremely important. Figure 6.5 illustrates the differences in the preferred modes of communication such as the reliance of non-verbal modes such as email, via a relative or SMS in the USH1 cohort and by voicephone in the USH2 cohort. Whilst this data is from a UK population with Usher syndrome recruited from c.2003-2006, such data may also be of use for other researchers around the world.

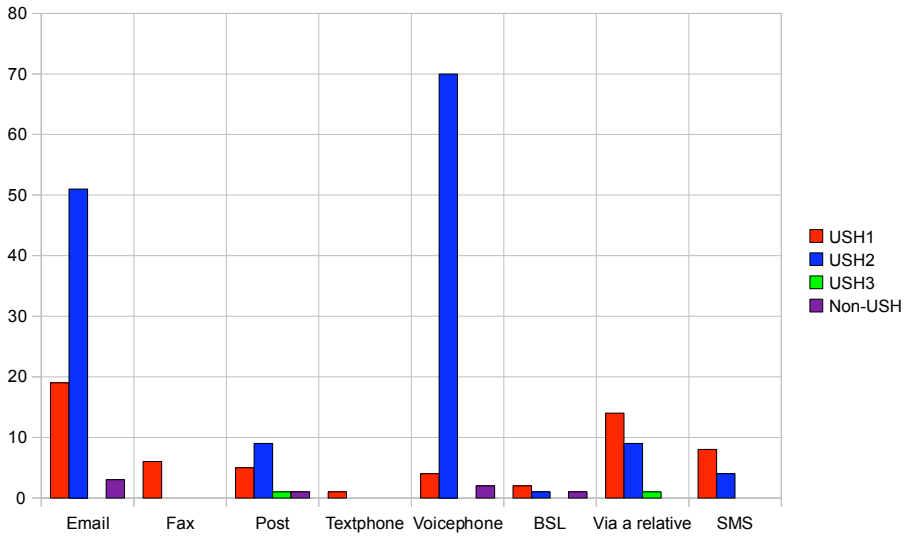

FIGURE 6.5: Bar chart showing the number of families requesting different types of communication as their preferred mode of contact. The categories are not mutually exclusive

6.1.6 Ethnicity

The majority of families recruited in to the study had index case grandparents who originated from the United Kingdom or Europe.

The ethnicity of index case grandparents is displayed graphically in Figure ref{fig:clusterbar$_e$*tnicity*$_u$*sh*123*whichshowsnumbersforbroadethnicgroups*.

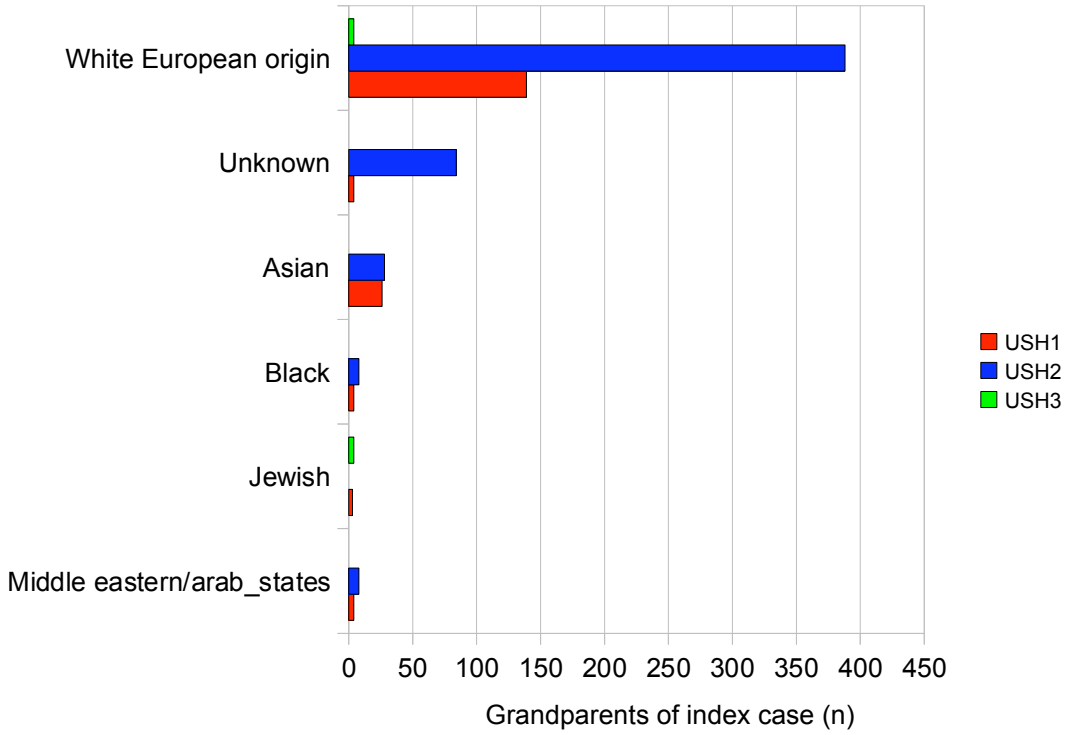

FIGURE 6.6: Cluster bar chart showing ethnicity of the grandparents of each index case

6.2 DNA sequencing analysis of the nine USH genes

The direct bidirectional sequencing of the nine known Usher genes and one candidate gene generated a vast amount of raw electropherogram data to analyse. The volume of sequence data generated is summarised in Table 6.4.

TABLE 6.4: Breakdown of the bidirectional DNA sequencing performed on each DNA sample submitted to the Wellcome Trust Sanger Centre

GENE	Number of Amplimers	Total number of base pairs
MYO7A	60	28106
USH1C	34	14739
CDH23	97	45328
PCDH15	54	25494
USH1G	13	6702
USH2A	105	51819
GPR98	123	61392
WHRN	27	13209
USH3A	13	6195
SLC4A7	52	25491
TOTAL	**578**	**278475**

6.2.1 Data collection from sequence analysis

The data presented pertains to the sequencing data of one of the above genes, *USH2A* for which the author was solely responsible for screening.

Each amplimer was analysed and entered in to a database consisting of 22169 records. Each record pertained to a result of sequencing in each index case for each amplimer. Of the 22169 records, no sequence trace was produced in 670 cases (3%). Unidirectional traces were noted in 372 cases (1.7%). 936 instances of sequence variants of interest were identified (4%) across the panel of DNAs analysed. From these 936 individual sequence changes, a total of 142 sequence variants were identified for subsequent analysis with a second round of molecular experiments in the form of an Sequenom allele specific assays for that particular variant in a larger panel of DNAs. In the remainder (>90%) of the records, the sequenced amplimer was no different to the reference sequence. Within this last group, many records were noted to have common polymorphisms noted from prior analysis of that amplimer in the CEPH panel of control DNAs. Because all these sequence variants were by definition prevalent and polymorphic, most were not recorded.

6.2.2 Results of Sequenom allele specific assay data

The return rate for successful genotypes was >95% in successful assays. A summary of assays passing validation are summarised in Table 6.5

TABLE 6.5: Summary of allele specific assays after validation

Gene	PASSED	FAILED	TOTAL
MYO7A	54	8	62
USH1C	12	0	12
CDH23	40	5	45
PCDH15	19	2	21
USH1G	3	3	6
USH2A	121	21	142
GPR98	56	3	59
WHRN	7	0	7
USH3A	5	0	5
SLC4A7	6	0	6
TOTAL	**323**	**42**	**365**

Of the 323 assays that passed assay validation, a third had a MAF of greater than 0.246% and were thus considered polymorphic. The genotype calls pertaining to these assays were mainly used for segregation analysis in families to determine phase as well as to exclude or confirm possible linkage of loci amongst informative families.

6.2.3 Assays of rare sequence variants

The remaining two-thirds of assays (n=212) had an MAF <0.246%. Table 6.6 lists the predicted effect of each of these changes.

TABLE 6.6: Rare sequence variants with an MAF <0.246%

SEQUENCE VARIANT PREDICTED EFFECT	Number of successful assays
frameshift/indels	10
isocoding/silent	39
missense	109
invariant splice site (coding sequence +/-1 or +/-2)	10
stop codon	26
uncertain	17
uncertain splice? (coding sequence +/-3)	1
TOTAL	**212**

Analysis of the predicted effect of each of these changes in some cases was instructive in ascribing a pathogenicity score. Sequence variants that were predicted to result in stop

codons, affecting invariant acceptor/donor splice sites, insertions, deletions, duplications or any similar classes of sequence variant that were predicted to cause frameshifts were designated as pathogenic alleles and ascribed a pathogenicity score of 4. However this was only possible for around a fifth of assays (n=46) the remaining assays were to interrogate sequence variants of equivocal pathology.

This was the case for the majority of assays within this subset of rare sequence variants (n=166), the majority of which were missense changes (n=109).

Table 6.7 presents the breakdown of the predicted effect of the sequence variants that were analysed by assays and found to have an MAF of <0.246%. This illustrates the high proportion of missense changes in *USH2A*, *MYO7A* and *GPR98*.

TABLE 6.7: Predicted effect of the sequence variants that were analysed by assays and found to have an MAF of <0.246%

GENE	Class of sequence variant identified	Number of assays
CDH23	missense	15
CDH23	silent	10
CDH23	splicesite	1
CDH23	stop codon	1
GPR98	missense	23
GPR98	silent	9
GPR98	stop codon	4
GPR98	splicesite	1
MYO7A	missense	27
MYO7A	silent	8
MYO7A	splicesite	5
MYO7A	stop codon	5
PCDH15	inframe deletion	1
PCDH15	missense	1
PCDH15	silent	1
PCDH15	splicesite	1
SLC4A7	silent	1
SLC4A7	missense	1
USH1C	missense	4
USH1C	silent	2
USH1C	frameshift	1
USH1C	splicesite	1
USH1G	missense	2
USH1G	Silent	2
USH2A	missense	35
USH2A	uncertain	17
USH2A	stop codon	16
USH2A	frameshift	8
USH2A	isocoding	3
USH2A	silent	2
USH2A	splicesite	1
USH2A	uncertain - ?splice	1
USH3A	silent	1
USH3A	missense	1
TOTAL		**212**

Each missense change was analysed using segregation data generated from the assays. Rather than present the mass of data relating to this work, some examples of the types

of results analysis could yield are illustrated using three representative cases of rare missense changes identified by direct sequencing and further interrogated by allele specific assays in the gene *USH2A*.

Rare missense changes - straightforward example of disease causing change

The c.1036 A>C (**p.Asn346His**) sequence variant in *USH2A* was one of the rare missense changes initially identified by sequencing analysis and subsequently assayed.

The assay returned a positive result of wild type (AA) in 437 control DNA samples (874 chromosomes) and thus had a MAF of 0%.

TABLE 6.8: Genotypes and family structure for p.Asn346His specific assay. Segregation analysis of this variant in each family reveal that although only families 74 and 95 are fully informative, segregation of the rare variant (C) would be consistent with disease in families 162 and 181. The other significant sequence variants identified in the index cases from each family are shown in ***bold italics*** on the top left of each family structure. The number in brackets following the sequence variant represent represents the ascribed pathogenicity score

p.Asn346His (3)

ASSAY genotype	Status	Diagnosis	Family	Case	NCUS ID
CA	Unaffected		74	Index Father	227
AA	Unaffected		74	Index Mother	226
CA	**Affected**	**Usher Type2**	**74**	**Index case**	**225**

p.Asn346His (3) ***p.Thr4439Ile (3)***

CA	Unaffected		95	Index Mother	330
CA	Unaffected		95	Index Sib Unaffected	363
AA	Unaffected		95	Index Sib Unaffected	364
AA	Unaffected		95	Index Father	329
CA	**Affected**	**Usher Type2**	**95**	**Index case**	**321**

p.Asn346His (3) ***p.Arg669X (4)***

CA	**Affected**	**Usher Type2**	**111**	**Index case**	**385**

p.Asn346His (3) ***p.Trp3521Arg (3)***

CA	Unaffected		162	Index Sib Unaffected	594
CA	Unaffected		162	Index Sib Unaffected	593
CA	Unaffected		162	Index Father	592
CA	Affected	Usher Type2	162	Index Sib Affected	590
CA	**Affected**	**Usher Type2**	**162**	**Index case**	**591**

p.Asn346His (3) ***p.Cys419Phe (3)***

CA	Unaffected		181	Index Sib Unaffected	682
CA	Unaffected		181	Index Mother	681
CA	**Affected**	**Usher Type2**	**181**	**Index case**	**680**

Direct sequence analysis of the Usher genes in all index cases had identified this change heterozygously in four index cases (NCUS 225, 385, 591, 680). The allele specific assay returned positive results for all the above four individuals who were positive controls. In addition to the above index cases, the assay *also* returned a heterozygous result for another index case, NCUS 321). In order to validate this assay, the direct sequence traces

were revisited for NCUS 321 and revealed that they did indeed carry the change heterozygously, but this had been missed because the sequence trace was unidirectional (one strand failed to amplify around the region) and as the change had not been highlighted by the GAP4 software it had been missed by visual inspection.

Table 6.8 lists the relevant genotype calls for the assay in the relevant five families. In each family the index case had an USH2 phenotype. In four of the families, another putative pathogenic allele had been identified.

This illustrates some of the benefits of performing the allele specific assays across the large panel of DNAs used as it afforded the opportunity to validate the results of sequencing, highlight potential errors in sequence trace analysis, confirm segregation of the allele in four of five families who carried the variant is consistent with disease and determine that the allele is rare in the control population.

This allele has also previously been reported by other research groups [161, 168, 174, 175], who all independantly determined the allele was disease causing, lending further support to the conclusion that p.Asn346His was pathogenic. This variant was ascribed a pathogenicity score of 3.

Rare missense changes - not disease causing

The c.2844 C>G (**p.Cys948Trp**) sequence variant in *USH2A* was one of the rare missense changes initially identified by sequencing analysis and subsequently assayed.

TABLE 6.9: Genotypes and family structure for the p.Cys948Trp specific assay. Putative pathogenic sequence variants identified in the index cases from each family are shown in ***bold italics*** on the top left box of each family structure. The number in brackets following the sequence variant represent represents the ascribed pathogenicity score

ASSAY genotype	Status	Diagnosis	Family	Relationship To Index Case	NCUS ID
p.Glu767fsSerfsX21 (4)		***p.His308GlnfsX16 (4)***			
GC	Unaffected		4	Index_Father	34
CC	Unaffected		4	Index_Mother	33
GC	**Affected**	**Usher Type2**	**4**	**Index_case**	**32**
GC	Unaffected		4	Index_Sib_Unaffected	60
p.Glu767fsSerfsX21 (4)		***p.Lys4816X (4)***			
CC	Unaffected		55	Index_Mother	172
GC	**Affected**	**Usher Type2**	**55**	**Index_case**	**171**
p.Glu767fsSerfsX21 (4)		***p.Glu767fsSerfsX21 (4)***			
GC	Unaffected		13	Index_Father	13
CC	Unaffected		13	Index_Mother	48
GC	**Affected**	**Usher Type2**	**13**	**Index_case**	**14**
GC	Affected	Usher Type2	13	Index_Sib_Affected	15
CC	Unaffected		13	Index_Sib_Unaffected	16

Direct sequence analysis of the Usher genes in all index cases had identified this change heterozygously in three index cases (NCUS 14, 32, 171). All three index cases had an USH2 phenotpe and their grandparents were of all of white European origin. The allele specific assay for p.Asn346His confirmed each index case (acting as the positive control for the assay) carried the change heterozygously and did not identify it in any other index case. The assay also returned 434 genotypes in the control group all of which were wild type (CC) yielding an MAF of 0%.

Table 6.9 presents the genotype data relating to this assay as well as the interesting finding that all three individuals also carry the common frameshift change p.Glu767fsSerfsX21 in the same gene.

Moreover, in addition to the common frameshift change, each index case also had another truncating (and likely pathogenic) sequence variant in the same gene. In light of this finding it would be reasonable to assume that the missense change p.Cys948Trp is not the cause of the disease in these three families. The more parsimonious explanation to account for this finding would be that p.Cys948Trp is in linkage disequilibrium with the common p.Glu767fsSerfsX21 in these families.

Rare missense changes - rare population 'polymorphism'

The c.13984 C>G (**p.Gln4662Glu**) sequence variant in *USH2A*

TABLE 6.10: Genotypes and family structure for the p.Gln4662Glu specific assay. Putative pathogenic sequence variants identified in the index cases from each family are shown in ***bold italics*** on the top left box of each family structure. The number in brackets following the sequence variant represent represents the ascribed pathogenicity score

ASSAY genotype	Status	Diagnosis	Family	Relationship To Index Case	NCUS ID
?PCDH15 deletion					
CG	Unaffected		35	Index_Mother	120
CC	Unaffected		35	Index_Father	121
CC	Affected	Usher_Type1	35	Index_case	119
CC	Affected	Usher_Type1	35	Index_Sib_Affected	195
p.Pro2124LeufsX5 (4)		***p.Arg1240Trp (3) in MYO7A***			
CG	Affected	Usher_Type1	49	Index_case	182
CC	Affected	Usher_Type1	49	Index_Sib_Affected	156

was one of the rare missense changes initially identified by sequencing analysis and subsequently assayed.

Direct sequence analysis of the Usher genes in all index cases had identified this change heterozygously in two index cases NCUS 182. Although initial sequence analysis was

performed 'blind' (masked to the identity of the index case) subsequent review of the data revealed that the index case had an USH1 phenotype and was of African origin.

The results from the p.Gln4662Glu assay are presented in Table 6.10.

The USH1 index case NCUS 182 was found to already carry two pathogenic mutations in the *MYO7A* gene accounting for her disease. The p.Gln4662Glu assay genotype for her affected sibling was wild type. In summary the two affected siblings had an USH1 phenotype, did not both carry the allele and ad two two putative pathogenic mutations in another USH1 gene.

The assay also identified the p.Gln4662Glu change heterozygously in the mother of an index case in Family 35. The mother did not pass the variant to either of her affected siblings which provides evidence to suggest that the variant is not responsible for disease in this family. Such examples of non-transmission of alleles suggest that they are unlikely to be disease causing. Although no pathogenic changes were identified in the two USH1 sibs from Family 35, they are suspected of having disease due to PCDH15 gene for which they may be homo/hemizygous (see Figure 6.7). They are scheduled to undergo Multiplex Ligation-dependent Probe Amplification (MLPA) analysis to investigate this further.

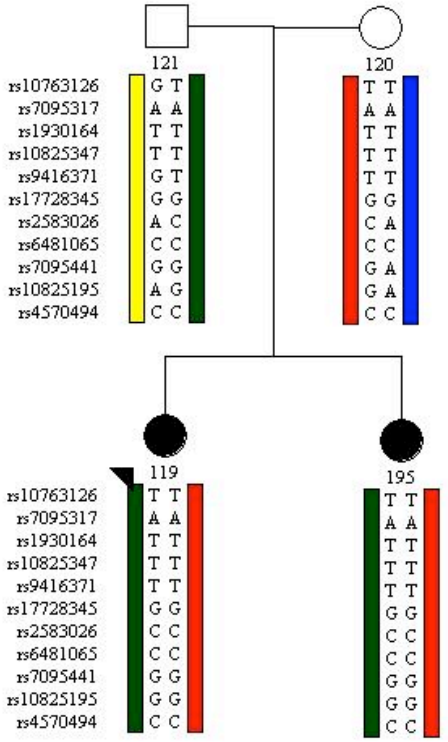

FIGURE 6.7: Haplotype analysis for the *PCDH15* gene in Family 35

6.3 Molecular diagnoses for USH families

TABLE 6.11: Molecular diagnoses for the entire study cohort (a total of 175 families) that underwent genetic analysis. The percentage contribution of each gene is detailed in the table and the corresponding number of families is annotated on the piechart. The segment of USH2A labelled E767fs, pertains to the proportion of families (n=52) who carry at least one allele of the common pathogenic allele p.Glu767SerfsX21

Gene	Families (%) with USH
USH2A	56.0%
unknown	18.3%
MYO7A	12.0%
GPR98	4.6%
USH1C	3.4%
CDH23	2.9%
PCDH15	1.7%
USH3A	1.1%
USH1G	0.0%
WHRN	0.0%

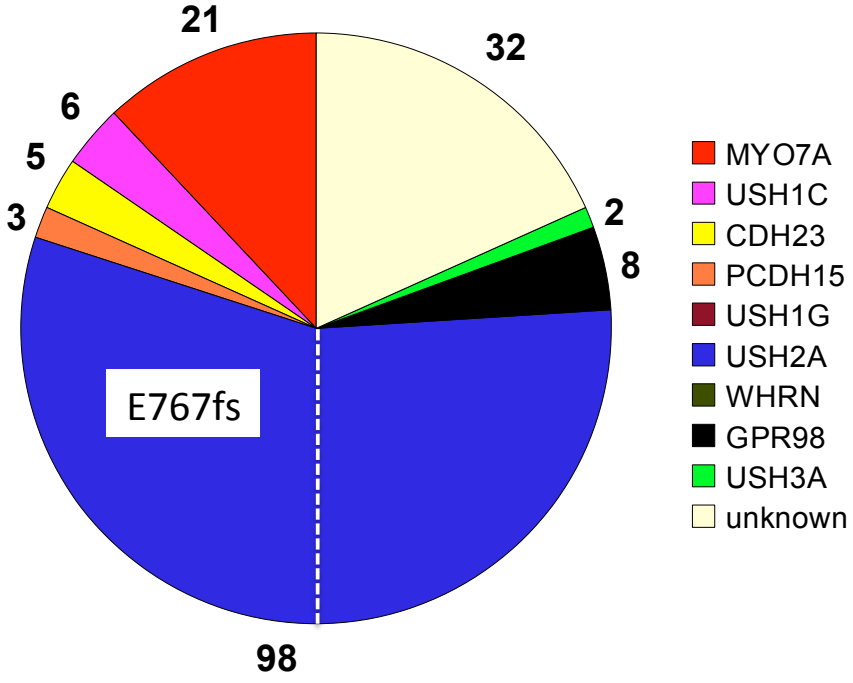

175 families with a clinical diagnosis consistent with USH1, USH2 or USH3 were available molecular analysis. A molecular diagnosis was achieved when at least one putative pathogenic sequence variant (pathogenicity score of 3 or 4) was confirmed.

The molecular diagnosis achieved per family is represented in table and piechart 6.11. This illustrates that over half of all cases of USH in our UK cohort are due to disease

in the *USH2A* gene. This represented the largest molecular group identified (n=98). The majority of this group (53%, n=52) carried the common pathogenic sequence variant p.Glu767SerfsX21 on at least one allele, six of these families carrying the variant homozygously.

In 18% of families no molecular diagnosis was achieved. This empty molecular group was the second largest category when subdividing the study cohort on the basis of genotype.

Disease due to the *MYO7A* gene (12%) was the third largest molecular group. Of the six families with an USH1 phenotype due to *USH1C*, the previously reported invariant splice site change c.496+1 G>A [160] was identified in five families and present homozygously in four.

In the entire cohort we were unable to identify disease due to the two genes *USH1G* and *WHRN*. No putative pathogenic changes were identified in the candidate gene *SLCA4* in any family.

Across the cohort no convincing evidence of digenic effects were identified, in that no affected individual had sequence variants of pathogenicity score 3 or 4 in two different genes.

6.4 Molecular diagnosis per subtype

Just under half of USH1 families have disease due to the *MYO7A* gene (47%), with 13% of families due to USH1C and relatively smaller contributions made by the two cadhedrin family USH1 genes, *CDH23* and *PCDH15*. No family had disease due to the *USH1G* gene.

Over three-quarters of USH2 families (76%) had disease due to *USH2A* with much smaller contribution from the *GPR98* gene (6%). No disease causing mutations were identified in *WHRN*, the other gene known to cause an USH2 phenotype.

No molecular diagnosis was achieved in 22% of USH1 and 18% of USH2 families.

Figure 6.4 illustrates that this 20% is equally split between the USH1 and USH2 groups.

Gene	USH1		Gene	USH2		Gene	USH3
unknown	20.00%		unknown	17.97%		unknown	0.00%
MYO7A	46.67%		*USH2A*	75.78%		*USH3A*	100.00%
USH1C	15.56%		*WHRN*	0.00%			
CDH23	11.11%		*GPR98*	6.25%			
PCDH15	6.67%						
USH1G	0.00%						
Index cases with genetic diagnosis	80.00%			82.03%			100.00%
Index cases without a genetic diagnosis	20.00%			17.97%			0.00%

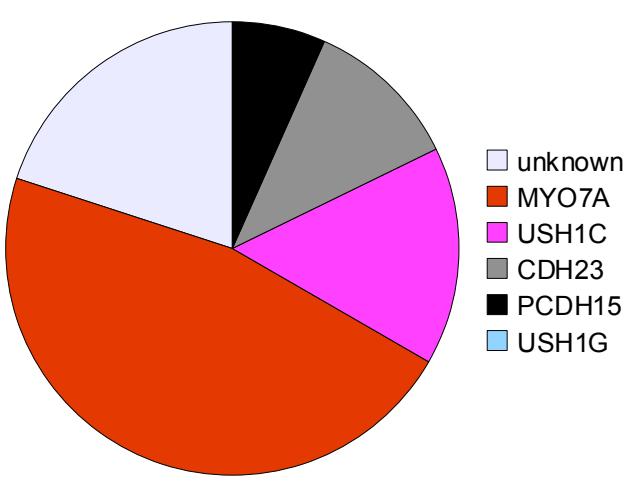

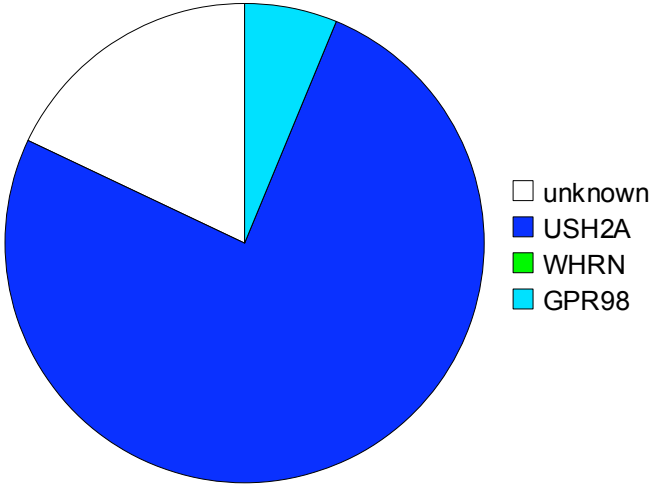

Table and piechart showing families with a molecular diagnoses separated by clinical subtypes USH1, USH2 and USH3

6.5 Number of alleles identified per subtype

For this section, only alleles that were were considered disease causing were included in the summary figures. These were alleles with a pathogenicity score of 3 or 4. Although there were alleles identified achieving a pathogenicity score of 2.5 and may well be disease causing, as the pathogenicity of these variants has not yet been verified they were omitted. The figures below therefore represent conservative estimates.

In an autosomal recessive disease such as Usher syndrome two disease-causing alleles are thought to be required to cause disease. The proportion of families with two, one and zero alleles identified is displayed in Table 6.12.

FIGURE 6.8:

TABLE 6.12: Number of two, one and zero alleles identified per family subdivided by clinical subtype

	USH1		USH2		USH3	
alleles found	**Families (n) with USH**	**Families (%) with USH**	**Families (n) with USH**	**Families (%) with USH**	**Families (n) with USH**	**Families (%) with USH**
2	26	57.78%	74	57.81%	2	100.00%
1	9	20.00%	31	24.22%	0	0.00%
0	10	22.22%	23	17.97%	0	0.00%
TOTAL	**45**	**100.00%**	**128**	**100.00%**	**2**	**100.00%**

6.6 Number of alleles identified per gene

Figure 6.9 displays the number and percentage of families within each molecular category in whom one or two disease causing alleles were identified.

Of those with a molecular diagnosis of *USH1C, PCDH15* and *USH3A* both disease causing alleles were identified in each family. in the remaining genes, a significant proportion (30-60%) of second alleles remained unidentified.

	Percentage of families per GENE						
alleles found	**MYO7A**	**USH1C**	**CDH23**	**PCDH15**	**USH2A**	**GPR98**	**USH3A**
2	71%	100%	40%	100%	71%	63%	100%
1	29%	0%	60%	0%	29%	38%	0%
TOTAL	**100%**	**100%**	**100%**	**100%**	**100%**	**100%**	**100%**

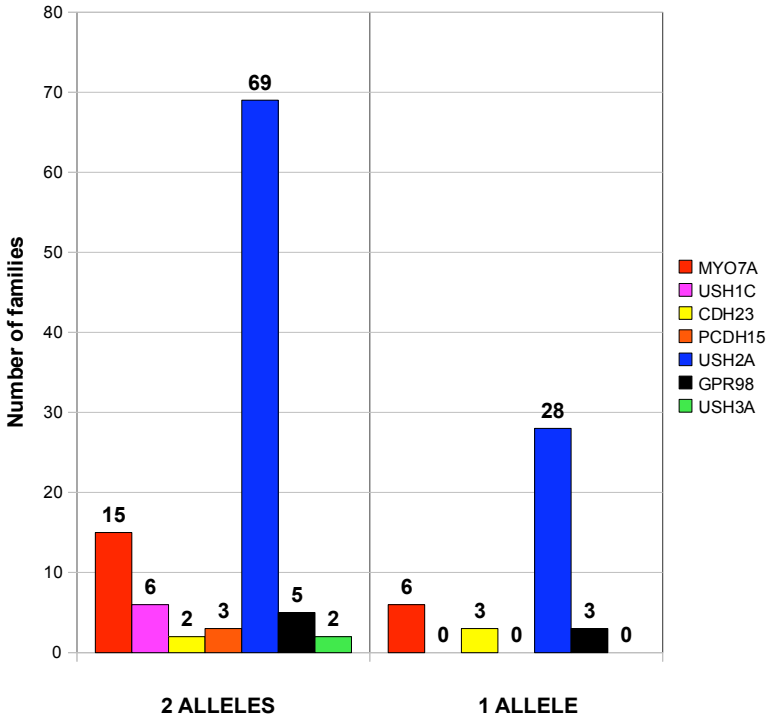

FIGURE 6.9: The number of pathogenic alleles (pathogenicity grade 3 or 4) identified per gene. The percentage of one or two alleles from the total pathogenic alleles identified in each gene is detailed in the table. The corresponding number of families is annotated on the bar chart.

6.7 Molecular results per clinical subtype

6.7.1 USH1

Genotypes of Usher syndrome type I probands (novel variants are in bold).

NCUS ID	Gene	Allele 1[a]	Allele 2[a]	Pathogenicity Allele_1	Pathogenicity Allele_2	Ethnicity[b]
30	*MYO7A*	p.Lys1255ArgfsX8	p.Ala26Glu[e]	Pathogenic	Pathogenic	Caucasian
35	*MYO7A*	p.Arg2024X	**p.Asp75His**	Pathogenic	UV4	Caucasian
42	*MYO7A*	p.Arg1701X	Unknown	Pathogenic		Caucasian
68	*MYO7A*	p.Gly214Arg	p.Arg212His	Pathogenic	Pathogenic	Caucasian
69	*MYO7A*	**p.Arg241Pro**	c.5944G>A[f1]	UV4	Pathogenic	Caucasian
79	*MYO7A*	p.Arg1240Gln	**p.Leu2193Phe**	Pathogenic	UV4	Caucasian
87	*USH1C*	p.Arg80ProfsX69	c.496+1G>A	Pathogenic	Pathogenic	Caucasian
93	*MYO7A*	c.3504-1G>C[e]	p.Leu1858Pro	Pathogenic	Pathogenic	Caucasian
100	*MYO7A*	**c.3108+1G>A**	**c.3108+1G>A**	Pathogenic	Pathogenic	Indian
111	*MYO7A*	p.Arg669X	c.5944G>A[f1]	Pathogenic	Pathogenic	Caucasian
119	*PCDH15*	Exon 10 deleted[j]	Exon 10 deleted[j]	Pathogenic	Pathogenic	Caucasian
132	*MYO7A*	p.Arg972X	p.Arg972X	Pathogenic	Pathogenic	Iranian
146	*MYO7A*	p.Lys1255ArgfsX8	p.Asp521GlufsX8	Pathogenic	Pathogenic	Caucasian
163	*CDH23*	p.Arg2107X	**p.Leu2436ThrfsX3**	Pathogenic	Pathogenic	Caucasian
182	*MYO7A*	**p.Pro2126LeufsX5**	p.Arg1240Trp	Pathogenic	UV3	Black African (Ghana)
257	*MYO7A*	p.Cys31X	p.Arg1883Gln	Pathogenic	UV4	Caucasian
262	*MYO7A*	p.Asp1613ValfsX32	**p.Lys420X**	Pathogenic	Pathogenic	Caucasian
287	*MYO7A*	**p.Gly1942X**	p.Gly25Arg	Pathogenic	Pathogenic	Caucasian
313	*PCDH15*	c.3717+1G>A	**Exons 9-15 deleted**[i]	Pathogenic	Pathogenic	South Pacific
407	*CDH23*	**c.2177-2A>G**	**p.Leu3041Pro**	Pathogenic	UV4	Caucasian
435	*MYO7A*	p.Arg1240Gln	c.133-2A>G	Pathogenic	Pathogenic	Caucasian
444	*MYO7A*	p.Lys1255ArgfsX8	p.Lys542GlnfsX5	Pathogenic	Pathogenic	Caucasian
461	*USH1C*	p.Arg80ProfsX69	p.Arg80ProfsX69	Pathogenic	Pathogenic	Jewish
500	*MYO7A*	**p.Trp1431X**	p.Ala826Thr[g]	Pathogenic	UV4	Caucasian
516	*MYO7A*	**p.Gly1378TrpfsX6**	**p.Glu968Asp**	Pathogenic	UV4	Caucasian
555	*CDH23*	**c.7362G>A**[f]	**c.6254_6254-3delCAGGinsT**	UV3	Pathogenic	Caucasian
578	*MYO7A*	p.Arg669X	p.Lys542GlnfsX5	Pathogenic	Pathogenic	Caucasian
676	*MYO7A*	**p.Arg241Pro**	**p.Glu380Lys**	UV4	UV2	Caucasian
692	*MYO7A*	p.Arg212His	**c.1798-3C>G**	Pathogenic	UV2	Caucasian
705	*MYO7A*	**c.1798-3C>G**	Unknown	UV2		Caucasian
731	*MYO7A*	p.Ala2009ProfsX32	**c.-48A>G**[h]	Pathogenic	Pathogenic	Caucasian
129,340	Unknown					Caucasian
104[c]	*MYO7A*[d]	Unknown[d]	Unknown[d]			Turkish Cypriot
140[c]	*CDH23*	p.Arg2107X	p.Arg2107X	Pathogenic	Pathogenic	Pakistani (Sindi)
168[c]	*CDH23*[d1]	Unknown[d1]	Unknown[d1]			Turkish Cypriot
206[c]	*MYO7A*[d]	p.Tyr2015His	p.Tyr2015His	UV2	UV2	Caucasian
291[c]	*PCDH15*	**p.Gly942ValfsX22**	**p.Gly942ValfsX22**	Pathogenic	Pathogenic	Greek Cypriot
399[c]	*PCDH15*	**c.3501+2T>C**	**c.3501+2T>C**	Pathogenic	Pathogenic	Caucasian
4 families	*USH1C*	c.496+1G>A	c.496+1G>A	Pathogenic	Pathogenic	Caucasian
530[c]	*USH1C*	**p.Glu149del**	**p.Glu149del**	Pathogenic	Pathogenic	Indian
706[c]	*MYO7A*	p.Phe1963del	p.Phe1963del	UV4	UV4	Asian

[a]Unless stated otherwise, the alleles were not observed in control chromosomes

[b]Caucasian: UK and European

[c]Consanguineous family

[b] IVS1-2A>G

[d]Consanguineous family demonstrating linkage to Usher type1 genes. The causative mutations were either not found of were of uncertain pathogenicity (UV2).[d1]See Figure 1

[e]Found in 1/872 (0.11%) control chromosommes

[f]Last nucleotide of exon (possibly affects splicing); [f1]Last nucleotide of exon; causes MYO7A:p.Val1953GlufsX12 (Le Guédard-Méreuze et al. 2010)

[g]Found in 2/826 (0.23%) control chromosomes (both heterozygotes are Pakistani controls)

[h]IVS1-2A>G

[i]See Figure 2. Deletion of *PCDH15* exons 9-15 was confirmed by MLPA

[j]A homozygous deletion of *PCDH15* exon 10 was confirmed by MLPA. The family is not knowingly consanguineous.

6.7.2 USH2 and USH3

Genotypes of Usher syndrome type II and III probands (novel variants are in bold).

NCUS ID	Diagnosis	Gene	Allele 1[a]	Allele 2[a]	Pathogenicity Allele_1	Pathogenicity Allele_2	Ethnicity[b]
3	Type_2	*USH2A*	p.Glu767SerfsX21	**p.Arg4971X**	Pathogenic	Pathogenic	Caucasian
5	Type_2	Unknown					Indian
21	Type_2	*USH2A*	p.Glu767SerfsX21	p.Arg626X	Pathogenic	Pathogenic	Caucasian
29	Type_2	*USH2A*	p.Arg4192His[d]	p.Arg4192His[d]	UV2	UV2	Caucasian (Italy)
32	Type_2	*USH2A*	p.Glu767SerfsX21	p.His308SerfsX16	Pathogenic	Pathogenic	Caucasian
38	Type_2	*USH2A*	p.Glu767SerfsX21	p.Arg34X	Pathogenic	Pathogenic	Caucasian
45	Type_2	*USH2A*	p.Glu767SerfsX21	**p.Ser1173X**	Pathogenic	Pathogenic	Caucasian
57	Type_2	*USH2A*	p.Glu767SerfsX21	p.Cys536Arg	Pathogenic	Pathogenic	Caucasian
61	Type_2	*USH2A*	p.Pro560LeufsX31	p.Glu2265_Tyr2266delinsAsp	Pathogenic	Pathogenic	Caucasian
64	Type_2	*USH2A*	**p.Trp1607X**[e]	**p.Cys620Phe**	Pathogenic	Pathogenic	Caucasian
82	Type_2	*USH2A*	**c.11047+1G>A**	**p.Cys3575Tyr**	Pathogenic	UV4	Caucasian
110	Type_2	*MYO7A*	p.Gly1942X	Unknown	Pathogenic		Caucasian
113	Type_2	*USH2A*	**p.Cys982LeufsX2**	p.Trp3955X[f]	Pathogenic	Pathogenic	Arab
147	Type_2	*USH2A*	p.Gln3959AsnfsX53	**p.Asn4762Ser**	Pathogenic	UV3	Caucasian
151	Type_2	*USH2A*	p.Gln1063SerfsX15	Unknown	Pathogenic		Caucasian
155	Type_2	*USH2A*	p.Glu767SerfsX21	p.Arg1946X	Pathogenic	Pathogenic	Caucasian
165	Type_2	*USH2A*	p.Glu767SerfsX21	p.Trp2945X	Pathogenic	Pathogenic	Caucasian
170	Type_2	*GPR98*	**p.Arg2286X**	**p.Ser3339Asn**	Pathogenic	UV3	Caucasian
171	Type_2	*USH2A*	p.Glu767SerfsX21	**p.Lys4816X**	Pathogenic	Pathogenic	Caucasian
179	Type_2	*USH2A*	p.Arg1504LysfsX26	**p.Trp2744X**	Pathogenic	Pathogenic	Caucasian
187	Type_2	*USH2A*	p.Glu767SerfsX21	p.Gln1063SerfsX15	Pathogenic	Pathogenic	Caucasian
192	Type_2	*USH2A*	**p.Pro746Ala**	c.7595-3C>G[j]	UV4	Pathogenic	Caucasian
193	Type_2	*USH2A*	p.His308SerfsX16	**c.9371+1G>C**[e]	Pathogenic	Pathogenic	Caucasian
194	Type_2	*USH2A*	p.Thr4439Ile	p.Cys3267Arg	Pathogenic	UV4	Caucasian
200	Type_2	*USH2A*	p.Glu767SerfsX21	**c.11390-1G>C**	Pathogenic	Pathogenic	Caucasian
207	Type_2	Unknown					
215	Type_2	*USH2A*	p.Glu767SerfsX21	**p.Ala4153Thr**[e]	Pathogenic	UV4	Caucasian
220	Type_2	*USH2A*	**p.Arg3689X**	p.Trp3521Arg	Pathogenic	Pathogenic	Caucasian
221	Type_2	*USH2A*	**Exon 47 deleted**[g]	**Exon 47 deleted**[g]	Pathogenic	Pathogenic	Greek
222	Type_2	*GPR98*[c1]	Unknown	Unknown			Indian
225	Type_2	*USH2A*	p.Asn346His	Unknown	Pathogenic		Caucasian
239	Type_2	*USH2A*	p.Thr4809Ile	Unknown	Pathogenic		Caucasian
247	Type_2	*USH2A*	p.Glu767SerfsX21	**p.Gln3959AsnfsX53**	Pathogenic	Pathogenic	Caucasian
271	Type_2	*GPR98*	**p.Arg4802X**	**p.Ile3325Thr**	Pathogenic	UV2	Caucasian
275	Type_2	*GPR98*	**p.Asp1375His**	Unknown	UV2		Caucasian
296	Type_2	*USH2A*	p.Glu767SerfsX21	p.Gln675X	Pathogenic	Pathogenic	Caucasian
312	Type_2	Unknown					Somali
321	Type_2	*USH2A*	p.Thr4439Ile	p.Asn346His	Pathogenic	Pathogenic	Caucasian
332	Type_2	*USH2A*	p.Glu767SerfsX21	**p.Cys620Phe**	Pathogenic	Pathogenic	Caucasian
345	Type_2	*USH2A*	p.Glu1492X	**c.11047+1G>A**	Pathogenic	Pathogenic	Caucasian
347	Type_2	*USH2A*	p.Glu2288X	**p.Gly268Arg**	Pathogenic	UV3	Unknown
355	Type_2	*USH2A*	p.Glu767SerfsX21	p.Glu4458AspfsX3	Pathogenic	Pathogenic	Caucasian
357	Type_2	*GPR98*	**p.Arg800X**	**c.13433G>T**[h]	Pathogenic	UV3	Caucasian
359	Type_2	*USH2A*	p.Cys5153X	p.Trp3521Arg	Pathogenic	Pathogenic	Caucasian
369	Type_2	*USH2A*	p.Arg1504LysfsX26	p.Glu767SerfsX21	Pathogenic	Pathogenic	Caucasian
374	Type_2	*USH2A*	p.Pro560LeufsX31	**p.His340Leu**	Pathogenic	UV3	Caucasian
377	Type_2	*USH2A*	**p.Arg1777Trp**	**p.Asn2285Ser**	UV3	UV2	Indian
385	Type_2	*USH2A*	**p.Glu3305ArgfsX41**	p.Asn346His	Pathogenic	Pathogenic	Caucasian
387	Type_2	*USH2A*	p.Glu767SerfsX21	**p.Ile2754AsnfsX15**	Pathogenic	Pathogenic	Caucasian
389	Type_2	*USH2A*	p.Glu767SerfsX21	**p.Tyr4801X**	Pathogenic	Pathogenic	Caucasian
394	Type_2	*USH2A*	p.Glu767SerfsX21	p.Glu284AspfsX38	Pathogenic	Pathogenic	Caucasian
398	Type_2	*USH2A*	p.Gln675X	**p.Gln4541X**	Pathogenic	Pathogenic	Caucasian
401	Type_2	*USH2A*	p.Glu767SerfsX21	p.Glu2288X	Pathogenic	Pathogenic	Caucasian
417	Type_2	*USH2A*	p.Glu767SerfsX21	p.Thr4439Ile	Pathogenic	Pathogenic	Caucasian
418	Type_2	*USH2A*	p.Arg63X	p.Arg1549X	Pathogenic	Pathogenic	Caucasian
427	Type_2	*USH2A*	p.Cys1452LeufsX25	Unknown	Pathogenic		Afro-Caribbean
429	Type_2	Unknown					
432	Type_2	*USH2A*	p.Glu767SerfsX21	**c.12295-3T>A**	Pathogenic	UV2	Indian
440	Type_2	*USH2A*	**p.Cys620Phe**	Unknown	Pathogenic		Caucasian
455	Type_2	*USH2A*	**p.Ser4377X**	p.Cys419Phe	Pathogenic	Pathogenic	Caucasian

465	Type_2	*USH2A*	p.Glu767SerfsX21	c.10585G>A[h]	Pathogenic	UV3	Caucasian
481	Type_2	*GPR98*	**p.Ser5048ArgfsX29**	**p.Val2321AlafsX4**	Pathogenic	Pathogenic	Caucasian
490	Type_2	*USH2A*	p.Arg1281X	p.Met1280Ile	Pathogenic	UV4	Caucasian
509	Type_2	*USH2A*	p.Glu767SerfsX21	**p.Trp4713X**	Pathogenic	Pathogenic	Caucasian
520	Type_2	*MYO7A*	p.Leu326Gln	Unknown	UV2		Indian
531	Type_2	*USH2A*	p.Glu767SerfsX21	**p.Gly257Arg**	Pathogenic	UV2	Unknown
542	Type_2	*USH2A*	p.Cys759Phe	p.Cys3358Tyr	Pathogenic	UV3	Caucasian
545	Type_2	*USH2A*	p.Glu767SerfsX21	**p.Leu1378Pro**	Pathogenic	UV4	Caucasian
546	Type_2	*USH2A*	**p.Cys3281Phe**	Unknown	UV2		Caucasian
549	Type_2	*USH2A*	p.Gly4403ProfsX15	**p.Ser1588HisfsX5**	Pathogenic	Pathogenic	Caucasian/Philippinian
568	Type_2	*USH2A*	p.Gly4403ProfsX15	Unknown	Pathogenic		Caucasian
591	Type_2	*USH2A*	p.Asn346His	p.Trp3521Arg	Pathogenic	Pathogenic	Caucasian
595	Type_2	*USH2A*	p.Glu767SerfsX21	p.Trp3521Arg	Pathogenic	Pathogenic	Caucasian
601	Type_2	*USH2A*	p.Glu767SerfsX21	**p.Ser1136Asn**	Pathogenic	UV4	Caucasian
611	Type_2	*USH2A*	p.Glu767SerfsX21	**c.651+1G>A**	Pathogenic	Pathogenic	Caucasian
620	Type_2	*USH2A*	p.Glu767SerfsX21	**p.Cys999LeufsX9**	Pathogenic	Pathogenic	Caucasian
644	Type_2	*USH2A*	**p.Asn1967TrpfsX5**	**p.Arg1578Cys**	Pathogenic	UV4	Caucasian
648	Type_2	*USH2A*	p.Arg1504LysfsX26	p.Cys419Phe	Pathogenic	Pathogenic	Caucasian
651	Type_2	*USH2A*	**p.Arg1946LeufsX22**	Unknown	Pathogenic		Caucasian
657	Type_2	*USH2A*	p.Arg63X	Unknown	Pathogenic		Caucasian
665	Type_2	*GPR98*	**p.Ala3579ValfsX6**	p.Val3363AspfsX11	Pathogenic	Pathogenic	Caucasian
669	Type_2	*USH2A*	p.Glu767SerfsX21	**p.Phe1868Cys**	Pathogenic	UV2	Unknown
670	Type_2	*USH2A*	**p.Gly1751Val**	Unknown	UV2		Unknown
680	Type_2	*USH2A*	p.Asn346His	p.Cys419Phe	Pathogenic	Pathogenic	Caucasian
697	Type_2	*GPR98*	**c.9623+1G>A**	Unknown	Pathogenic		Caucasian
212,702	Type_2	*USH2A*	p.Glu767SerfsX21	p.Cys419Phe	Pathogenic	Pathogenic	Caucasian
219,672	Type_2	*USH2A*	p.Glu767SerfsX21	**p.Ala1872LeufsX58**	Pathogenic	Pathogenic	Caucasian
334,386	Type_2	*USH2A*	p.Glu4458AspfsX3	c.7595-3C>G[j]	Pathogenic	Pathogenic	Caucasian
11 families (223,236,304 ,72,207,340, 368,480,537, 631,712)	Type_2	Unknown					Caucasian
136[c]	Type_2	*GPR98*	**Exon 83 deleted[i]**	**Exon 83 deleted[i]**	Pathogenic	Pathogenic	Arab (Palestinian)
203[c]	Type_2	*USH2A*	**p.Cys870X**	**p.Cys870X**	Pathogenic	Pathogenic	Turkish Cypriot
205[c]	Type_2	*USH2A*	Unknown	Unknown			Indian
26,46	Type_2	*USH2A*	p.Glu2288X	Unknown	Pathogenic		Caucasian
300[c]	Type_2	*GPR98*	**p.Glu2103X**	p.Gln2301X	Pathogenic	Pathogenic	Caucasian
314[c]	Type_2	*USH2A*	c.1841-2A>G	c.1841-2A>G	Pathogenic	Pathogenic	Caucasian
367,17	Type_2	*USH2A*	p.Glu767SerfsX21	**p.Gln4541X**	Pathogenic	Pathogenic	Caucasian
408[c]	Type_2	*USH2A*	p.Cys419Phe	p.Cys419Phe	Pathogenic	Pathogenic	Caucasian
5 families	Type_2	*USH2A*	p.Glu767SerfsX21	p.Glu767SerfsX21	Pathogenic	Pathogenic	Caucasian
53[c]	Type_2	*USH2A*	p.Cys1452LeufsX25	p.Cys1452LeufsX25	Pathogenic	Pathogenic	Indian
558[c]	Type_2	*USH2A*[d]	**p.Thr281Lys**	**p.Thr281Lys**	UV2	UV2	Turkish Cypriot
683[c]	Type_2	*USH2A*	**Exons 50-55 deleted[g]**	**Exons 50-55 deleted[g]**	Pathogenic	Pathogenic	Pakistani (Kashmir)
9 families	Type_2	*USH2A*	p.Glu767SerfsX21	Unknown	Pathogenic		Caucasian
49	Type_3	*USH3A*	p.Ser50LeufsX12	p.Ser50LeufsX12	Pathogenic	Pathogenic	Caucasian
82	Type_3	*USH3A*	p.Asn48Lys	p.Asn48Lys	Pathogenic	Pathogenic	Jewish (Ashkenazi)

[a]Unless stated otherwise, the alleles were not observed in control chromosomes

[b]Caucasian: UK and European

[c]Consanguineous family; [c1]Not reported as a consanguineous family.

Usher is linked to *GPR98* (affected sibs are homozygous for a GPR98 haplotype) ; USH2A is excluded by haplotype analysis

[d]Parental origin could not be determined. Patient and affected sib are homozygous for the mutation. However, USH2A haplotypes are not homozygous. It is possible they are p.Arg4192His hemizygous and have a deletion on the other allele.

[e]Found in 1/872 (0.11%) control chromosomes

[f]Found in 2/860 (0.23%) control chromosomes

[g]Large deletion speculated based on patient's homozygosity of *USH2A* haplotypes and failure to amplify exon

[h]Last nucleotide of the exon

[i]Deletion strongly suspected based on linkage to *GPR98* (*USH2A* excluded based on haplotype analysis), apparent non-inheritance of GPR98 SNPs in the family and PCR non-amplification of patient's as well as affected sib's DNAs (Figure 3).

[j] Last nucleotide of exon; causes USH2A:p.Pro2533Asnfs*5 (Le Guédard-Méreuze et al. 2010)

6.8 Novel sequence variants

6.8.1 Novel pathogenic sequence variants identified

6.8.2 Novel changes of uncertain pathogenicity with in-silico analysis

Novel Pathogenic variants

Novel Pathogenic sequence variants				
Gene name	**DNA change**	**Protein change**	**MAF in controls[a]**	**Pathogenicity**
CDH23	c.2177-2A>G	p.?	0 [0/96 CEPH]	Pathogenic
CDH23	c.6254_6254-3delCAGGinsT	p.?	0 [0/96 CEPH]	Pathogenic
CDH23	c.6712+1G>A	p.?	0	Pathogenic
CDH23	c.7305dup	p.Leu2436ThrfsX3	0 [0/96 CEPH]	Pathogenic
GPR98	c.10736_37delCC	p.Ala3579ValfsX6	0 [0/96 CEPH]	Pathogenic
GPR98	c.14404C>T	p.Arg4802X	0	Pathogenic
GPR98	c.15144delC	p.Ser5048ArgfsX29	0 [0/96 CEPH]	Pathogenic
GPR98	c.2398C>T	p.Arg800X	0.11	Pathogenic
GPR98	c.6307G>T	p.Glu2103X	0	Pathogenic
GPR98	c.6856C>T	p.Arg2286X	NA	Pathogenic
GPR98	c.6962_63delTG	p.Val2321AlafsX4	NA	Pathogenic
GPR98	c.9623+1G>A	p.?	0	Pathogenic
GPR98	Large deletion: Exon 83	p.?	0 [0/96 CEPHs]	Pathogenic
MYO7A	c.1258A>T	p.Lys420X	0 [0/96 CEPHs]	Pathogenic
MYO7A	c.3108+1G>A	p.?	0	Pathogenic
MYO7A	c.338_348dup	p.Glu117SerfsX33	0 [0/96 CEPH]	Pathogenic
MYO7A	c.4131dup	p.Gly1378TrpfsX6	0 [0/96 CEPH]	Pathogenic
MYO7A	c.4293G>A	p.Trp1431X	0	Pathogenic
MYO7A	c.4838delA	p.Asp1613ValfsX32	0 [0/96 CEPH]	Pathogenic
MYO7A	c.-48A>G (IVS1-2A>G)	p.?	0	Pathogenic
MYO7A	c.5824G>T	p.Gly1942X	0	Pathogenic
MYO7A	c.6070C>T	p.Arg2024X	0 [0/96 CEPH]	Pathogenic
MYO7A	c.6377delC	p.Pro2126LeufsX5	0 [0/96 CEPH]	Pathogenic
PCDH15	c.2823delG	p.Gly942ValfsX22	0 [0/96 CEPH]	Pathogenic
PCDH15	c.3501+2T>C	p.?	0	Pathogenic
PCDH15	Large deletion: Ex 12-15	p.?	0 [0/96 CEPH]	Pathogenic
USH1C	c.2227-1G>T[c]	p.?	0	Pathogenic
USH1C	c.446_448delAGG	p.Glu149del	NA	Pathogenic
USH2A	c.10561T>C	p.Trp3521Arg	0	Pathogenic
USH2A	c.11047+1G>A	p.?	0 [0/96 CEPH]	Pathogenic
USH2A	c.11065C>T	p.Arg3689X	0 [0/96 CEPH]	Pathogenic
USH2A	c.11390-1G>C	p.?	0 [0/96 CEPH]	Pathogenic
USH2A	c.11872_11873delAC	p.Gln3959AsnfsX53	0	Pathogenic
USH2A	c.13130C>A	p.Ser4377X	0	Pathogenic
USH2A	c.13621C>T	p.Gln4541X	0	Pathogenic
USH2A	c.14139G>A	p.Trp4713X	0	Pathogenic
USH2A	c.14403C>G	p.Tyr4801X	0	Pathogenic
USH2A	c.14446A>T	p.Lys4816X	0	Pathogenic
USH2A	c.14911C>T	p.Arg4971X	0 [0/96 CEPH]	Pathogenic
USH2A	c.1859G>T	p.Cys620Phe	0	Pathogenic
USH2A	c.2610C>A	p.Cys870X	0 [0/96 CEPH]	Pathogenic
USH2A	c.2942_2943insT	p.Cys982LeufsX2	0	Pathogenic
USH2A	c.2994_3007del	p.Cys999LeufsX9	0 [0/96 CEPH]	Pathogenic
USH2A	c.3518C>A	p.Ser1173X	0	Pathogenic
USH2A	c.4354dup	p.Cys1452LeufsX25	0 [0/96 CEPH]	Pathogenic
USH2A	c.4761delG	p.Ser1588HisfsX5	0 [0/96 CEPH]	Pathogenic
USH2A	c.4821G>A	p.Trp1607X	0.12	Pathogenic
USH2A	c.5614_5620delGCTGTCG	p.Ala1872LeufsX58	0 [0/96 CEPH]	Pathogenic
USH2A	c.5834_5835insTC	p.Arg1946LeufsX22	0	Pathogenic
USH2A	c.5898_5899delAA	p.Asn1967TrpfsX5	0 [0/96 CEPH]	Pathogenic
USH2A	c.651+1G>A	p.?	0 [0/96 CEPH]	Pathogenic
USH2A	c.8231G>A	p.Trp2744X	0 [0/96 CEPH]	Pathogenic
USH2A	c.8261delT	p.Ile2754AsnfsX15	0 [0/96 CEPH]	Pathogenic
USH2A	c.9371+1G>C	p.?	0.12	Pathogenic
USH2A	c.9459C>A	p.Cys3153X	NA	Pathogenic
USH2A	c.9912dup	p.Glu3305ArgfsX41	0	Pathogenic
USH2A	Large deletion: Exon 47	p.?	0 [0/96 CEPH]	Pathogenic
USH2A	Large deletion: Ex 50-55	p.?	0 [0/96 CEPH]	Pathogenic

*Last nucleotide of an exon

a_Minimum Allele Frequecy in 876 control chromosomes unless stated otherwise

b_Identified in NCUS proband with RP atypical for the Usher syndrome

c_Identified in NCUS proband who was diagnosed with sector RP and hearing loss (Saihan et al., 2011)

Novel UV2-UV4 and pathogenic variances					ORTHOLOG CONSERVATION									3D ANALYSIS		
Gene name	**DNA change**	**Protein change**	**MAF in controls[a]**	**Pathogenicity**	**Number of sequences**	**AAPI**	**AAPI R**	**Number of divergencies**	**Number of mutant**	**Number of gaps**	**Conserv of aa position**	**Conserv – gap ^**	**Domain conservation**	**Secondary structure analysis**	**Affect hydrogen bond network?**	**Introduce steric clashes?**	**other predicted effects**
CDH23	c.9122T>C	p.Leu3041Pro	0	UV4	18	80.21 %	92.16 %	1	0	0	16 / 18 (88.89%)	16 / 17 (94.12%)	The residue does not belong to a defined domain	Residu L3041 is predicted to belong to an α helice. Probability is 0.914			
MYO7A	c.223G>C	p.Asp75His	0	UV4	24	76.99 %	94.20 %	0	0	0	24 / 24 (100.00%)	24 / 24 (100.00%)	The residue belongs to the domain Motor domain.	Residu D75 is predicted to belong to a loop. Probability is 0.607.	+	-	
MYO7A	c.6577C>T	p.Leu2193Phe	0	UV4	24	76.99 %	94.69 %	0	0	1	23 / 24 (95.83%)	23 / 23 (100.00%)	The domain FERM 2 of myosin VIIa is very likely to interact with: harmonin - PDZ 1 and sans - central	Residu L2193 is predicted to belong to an α helice. Probability is 0.984.			
MYO7A	c.722G>C	p.Arg241Pro	0	UV4	24	76.99 %	84.23 %	0	0	1	23 / 24 (95.83%)	23 / 23 (100.00%)	The residue belongs to the domain Motor domain.	Residu R241 is predicted to belong to a loop. Probability is 0.649.	+	-	
USH2A	c.10724G>A	p.Cys3575Tyr	0	UV4	17	55.91 %	67.58 %	0	0	0	17 / 17 (100.00%)	17 / 17 (100.00%)	The residue belongs to the domain Fibronectin type-III 20.	Residu C3575 is predicted to belong to a loop. Probability is 0.829.	+		loss of disulphide bridge
USH2A	c.12457G>A	p.Ala4153Thr	0.12	UV4	17	55.91 %	53.22 %	4	2	0	13 / 17 (76.47%)	13 / 17 (76.47%)	The residue does not belong to a defined domain	Residu A4153 is predicted to belong to a loop. Probability is 0.608.	-	-	
USH2A	c.2236C>G	p.Pro746Ala	0	UV4	17	55.91 %	61.48 %	1	0	0	16 / 17 (94.12%)	16 / 17 (94.12%)	The residue belongs to the domain Laminin EGF-like 4.	Residu P746 is predicted to belong to a loop. Probability is 0.672.	-	-	
USH2A	c.3407G>A	p.Ser1136Asn	0	UV4	17	55.91 %	46.18 %	0	0	0	17 / 17 (100.00%)	17 / 17 (100.00%)	The residue belongs to the domain Fibronectin type-III 1.	Residu S1136 is predicted to belong to a loop. Probability is 0.494.	+	-	
USH2A	c.4133T>C	p.Leu1378Pro	0	UV4	17	55.91 %	55.81 %	2	0	0	15 / 17 (88.24%)	15 / 17 (88.24%)	The residue belongs to the domain Fibronectin type-III 4.	Residu L1378 is predicted to belong to a β strand. Probability is 0.979.			
USH2A	c.4732C>T	p.Arg1578Cys	0	UV4	17	55.91 %	72.48 %	2	0	0	15 / 17 (88.24%)	15 / 17 (88.24%)	Laminin G-like 1 of usherin domain alignment including p.R1578 residue.	Residu R1578 is predicted to belong to a β strand. Probability is 0.751.			
CDH23	c.7362G>A*	p.Thr2454Thr	0	UV3													
USH2A	c.1019A>T	p.His340Leu	0	UV3	17	55.91 %	64.46 %	0	0	0	17 / 17 (100.00%)	17 / 17 (100.00%)	The residue belongs to the domain Laminin N-terminal.	Residu H340 is predicted to belong to a loop. Probability is 0.778.			

USH2A	c.14285A>G	p.Asn4762Ser	0	UV3	17	55.91 %	55.60 %	0	0	0	17 / 17 (100.00%)	17 / 17 (100.00%)	The residue belongs to the domain Fibronectin type-III 33.	Residu N4762 is predicted to belong to a loop. Probability is 0.901.	-	-	
USH2A	c.5329 C>T	p.Arg1777Trp	0	UV3	17	55.91 %	41.18 %	11	0	0	6 / 17 (35.29%)	6 / 17 (35.29%)	The residue belongs to the domain Laminin G-like 2.	Residu R1777 is predicted to belong to a β strand. Probability is 0.994.	-		The two residues have different polarity and different charges, which can interfere with ionic bonds or potential inter- or intra-molecular interactions.
GPR98	c.10016G>A	p.Ser3339Asn	0	UV3	20	65.35 %	40.39 %	2	0	1	17 / 20 (85.00%)	17 / 19 (89.47%)	The residue belongs to the domain EAR 2.	Residu S3339 is predicted to belong to a β strand. Probability is 0.930.			
GPR98	c.13433G>T *	p.Ser4478Ile	0	UV3	20	65.35 %	62.34 %	1	0	0	19 / 20 (95.00%)	19 / 20 (95.00%)	The residue belongs to the domain Calx-beta 30.	Residu S4478 is predicted to belong to a loop. Probability is 0.629.	+	-	
MYO7A	c.1138G>A	p.Glu380Lys	0 [0/93 CEPH]	UV2	24	76.99 %	76.65 %	2	0	1	21 / 24 (87.50%)	21 / 23 (91.30%)	The residue belongs to the domain Motor domain.	Residu E380 is predicted to belong to a loop. Probability is 0.622.	-	-	
MYO7A	c.1798-3C>G	p.?	0 [0/96 CEPH]	UV2													
USH1C	c.1016G>A	p.Arg339Gln[b]	0	UV2	21	80.16 %	84.29 %	4	0	0	17 / 21 (80.95%)	17 / 21 (80.95%)	The residue belongs to the domain Coiled coil.	Residu R339 is predicted to belong to an α helice. Probability is 0.467.			
USH2A	c.12295-3T>A	p.?	0 [0/96 CEPH]	UV2													
USH2A	c.5252 G>T	p.Gly1751Val	0	UV2	17	55.91 %	64.18 %	3	0	0	14 / 17 (82.35%)	14 / 17 (82.35%)	The residue belongs to the domain Laminin G-like 2.	Residu G1751 is predicted to belong to a loop. Probability is 0.543.	-	-	The mutant residue is predicted to modify the hydrophobic interaction network.
USH2A	c.5603T>G	p.Phe1868Cys	0 [0/96 CEPH]	UV2	17	55.91 %	54.46 %	6	0	0	11 / 17 (64.71%)	11 / 17 (64.71%)	The residue belongs to the domain Laminin G-like 2.	Residu F1868 is predicted to belong to a β strand. Probability is 0.678.	-	-	The mutant residue is predicted to modify the hydrophobic interaction network.
USH2A	c.6854A>G	p.Asn2285Ser	0 [0/96 CEPH]	UV2	17	55.91 %	52.06 %	1	1	0	16 / 17 (94.12%)	16 / 17 (94.12%)	The residue belongs to the domain Fibronectin type-III 9.	Residu N2285 is predicted to belong to a loop. Probability is 0.621.	-	-	
USH2A	c.6928A>C	p.Thr2310Pro	0 [0/96 CEPH]	UV2	17	55.91 %	76.16 %	0	0	0	17 / 17 (100.00%)	17 / 17 (100.00%)	The residue belongs to the domain Fibronectin type-III 9.	Residu T2310 is predicted to belong to a β strand. Probability is 0.736.	+	-	Introduction of a proline is likely to rigidify the region.

USH2A	c.769G>A	p.Gly257Arg	0 [0/96 CEPH]	UV2	17	55.91 %	48.00 %	1	0	0	16 / 17 (94.12%)	16 / 17 (94.12%)	The residue does not belong to a defined domain	Residu G257 is predicted to belong to a loop. Probability is 0.681.			
USH2A	c.842C>A	p.Thr281Lys	0 [0/93 CEPH]	UV2	17	55.91 %	72.23 %	2	0	0	15 / 17 (88.24%)	15 / 17 (88.24%)	The residue belongs to the domain Laminin N-terminal.	Residu T281 is predicted to belong to a loop. Probability is 0.925.			
USH2A	c.9842G>T	p.Cys3281Phe	0 [0/96 CEPHs]	UV2	17	55.91 %	63.17 %	0	0	0	17 / 17 (100.00%)	17 / 17 (100.00%)	The residue belongs to the domain Cysteine rich.	Residu C3281 is predicted to belong to a loop. Probability is 0.666.			
GPR98	c.4123G>C	p.Asp1375His	0	UV2	20	65.35 %	65.36 %	6	0	0	14 / 20 (70.00%)	14 / 20 (70.00%)	The residue does not belong to a defined domain	Residu D1375 is predicted to belong to a loop. Probability is 0.644.			
GPR98	c.9974T>C	p.Ile3325Thr	0 [0/96 CEPHs]	UV2	20	65.35 %	49.47 %	2	0	1	17 / 20 (85.00%)	17 / 19 (89.47%)	The residue belongs to the domain EAR 2.	Residu I3325 is predicted to belong to a β strand. Probability is 0.988.			

AAPI Alignment Average Percentage Identity
AAPIR Alignment Average Percentage Identity of the Region (10aa downstream and 10 aa upstream)
Conservation focuses on the wild-type residue
^ Conservation - gap is the same figure as for Conserv of aa position but where gaps in the orthologous sequences are not taken into account

In silico analysis was performed on variants of uncertain pathogenicity (UV2-UV4) as presented earlier in 6.8.2. The results of the analysis clearly demonstrate the trend that UV4 variants were more highly conserved, predicted to be involved in secondary conformational structures and on 3D analysis, were more likely to be predicted to interfere with hydrogen bonding or steric effects than UV3 or UV2 variants, lending support to our classification.

Of note, the two variants USH2A:p.Leu1378Pro and USH2A:p.Arg1578Cys were found to less highly conserved and neither predicted to affect secondary or tertiary structure, however they still fitted our criteria to be classified as UV4.

USH2A:p.Leu1378Pro was identified in trans in proband NCUS 545 (Family 154) along with the common frameshift mutation USH2A:p.Glu767SerfsX21. The missense change was not observed in 876 control chromosomes.

USH2A:p.Arg1578Cys was identified in proband NCUS 644 (Family 171) in trans with the novel frameshift USHA:p.Asn1967TrpfsX5 . This missense change was not identified in 878 control chromosomes.

Conversely many of the UV2 changes were found to be less highly conserved than the UV4 changes, supporting the hypothesis that these changes are less likely to be disease causing.

6.8.3 Novel polymorphic changes (UV1) identified

Novel UV1 and Neutral variances.

Gene name	DNA change	Protein change	MAF in controls[a]	Pathogenicity
CDH23	c.10036G>C	p.Glu3346Gln	0.11	UV1
CDH23	c.129C>T	p.Ser43Ser	NA	UV1
CDH23	c.1307G>A	p.Ser436Asn	0.34	Neutral
CDH23	c.1369C>T	p.Arg457Trp	0.23	UV1
CDH23	c.1595C>T	p.Thr532Met	0	UV1
CDH23	c.173A>G	p.Gln58Arg	NA	UV1
CDH23	c.1752+6G>A	p.?	NA	UV1
CDH23	c.1919C>T	p.Thr640Met	0	UV1
CDH23	c.198G>A	p.Val66Val	NA	UV1
CDH23	c.204C>T	p.Gly68Gly	NA	UV1
CDH23	c.2235C>T	p.Ile745Ile	0	UV1
CDH23	c.2289+20G>C	p.?	NA	UV1
CDH23	c.2970C>T	p.Asp990Asp	0.69	Neutral
CDH23	c.3337G>C	p.Glu1113Gln	0	UV1
CDH23	c.3664G>A	p.Ala1222Thr	NA	UV1
CDH23	c.3801C>T	p.Thr1267Thr	0.11	UV1
CDH23	c.3845A>G	p.Asn1282Ser	0.93	Neutral
CDH23	c.3895G>A	p.Val1299Ile	0	UV1
CDH23	c.4231G>A	p.Glu1411Lys	0	UV1
CDH23	c.4287C>T	p.Pro1429Pro	0	UV1
CDH23	c.442G>A [ENST00000224721]	p.Gly148Arg [ENST00000224721]	NA	UV1
CDH23	c.444+3T>C [ENST00000224721]	p.?	NA	UV1
CDH23	c.4786C>T	p.Arg1596Cys	0	UV1
CDH23	c.4846-19G>A	p.?	NA	UV1
CDH23	c.4890C>T	p.Asn1630Asn	0	UV1
CDH23	c.4947G>A	p.Thr1649Thr	0	UV1
CDH23	c.5067+15G>A	p.?	NA	UV1
CDH23	c.551G>A	p.Arg184His	0	UV1
CDH23	c.5541C>T	p.Asn1847Asn	0.12	UV1
CDH23	c.5660C>T	p.Thr1887Ile	0.34	Neutral
CDH23	c.6197G>A	p.Arg2066Gln	0.36	Neutral
CDH23	c.6648C>T	p.Ala2216Ala	0	UV1
CDH23	c.67+19G>A	p.?	NA	UV1
CDH23	c.7722C>T	p.Tyr2574Tyr	0.34	Neutral
CDH23	c.8722G>A*	p.Gly2908Arg	0	UV1
CDH23	c.9014C>T	Ala3005Val	0	UV1
CDH23	c.9015G>A	Ala3005Ala	0.11	UV1
CDH23	c.9238G>A	Ala3080Thr	0.23	UV1
CDH23	c.9319+11G>A	p.?	NA	UV1
CDH23	c.9973C>G	Arg3325Gly	0	UV1
MYO7A	c.1081-10G>C	p.?	NA	UV1
MYO7A	c.1407G>A	Val469Val	NA	UV1
MYO7A	c.144-7C>T	p.?	NA	UV1
MYO7A	c.1543A>C	Lys515Gln	0.12	UV1

MYO7A	c.1554+8G>A	p.?	NA	UV1
MYO7A	c.1817G>A	p.Arg606His	0	UV1
MYO7A	c.1969C>T	p.Arg657Trp	0	UV1
MYO7A	c.2057G>A	p.Arg686His	0.11	UV1
MYO7A	c.2120G>A	p.Arg707His	0	UV1
MYO7A	c.2617C>T	p.Arg873Trp	0.11	UV1
MYO7A	c.2886G>C	p.Gln962His	0	UV1
MYO7A	c.3283G>A	p.Glu1095Lys	NA	UV1
MYO7A	c.3453G>A	p.Leu1151Leu	NA	UV1
MYO7A	c.359 G>A	p.Arg120His	0	UV1
MYO7A	c.4023C>T	p.Pro1341Pro	0	UV1
MYO7A	c.4074C>T	p.Ser1358Ser	0.47	Neutral
MYO7A	c.4161C>A	p.Asp1387Glu	0	UV1
MYO7A	c.4461C>T	p.Asn1487Asn	0.23	UV1
MYO7A	c.4505 A>G	p.Asp1502Gly	0	UV1
MYO7A	c.4619 C>T	p.Ala1540Val	0	UV1
MYO7A	c.4845C>A	p.Pro1615Pro	NA	UV1
MYO7A	c.4950C>T	p.Asn1650Asn	0	UV1
MYO7A	c.495G>A	p.Thr165Thr	0.12	UV1
MYO7A	c.5122C>A	p.Arg1708Ser	0	UV1
MYO7A	c.5216G>A	p.Arg1739Gln	NA	UV1
MYO7A	c.5245C>T	p.Arg1749Trp	0.12	UV1
MYO7A	c.54G>C	p.Gln18His	0.12	UV1
MYO7A	c.5619G>A	p.Arg1873Arg	NA	UV1
MYO7A	c.569T>G	p.Leu190Trp	0 [0/96 CEPH]	UV1
MYO7A	c.5866G>A	p.Val1956Ile	0.24	UV1
MYO7A	c.6051+16C>G	p.?	NA	UV1
MYO7A	c.6509C>T	p.Thr2170Ile	NA	UV1
MYO7A	c.6626G>A	p.Arg2209Gln	0	UV1
MYO7A	c.6640G>A	p.Gly2214Ser	0.11	UV1
MYO7A	c.973A>T	p.Ile325Phe	0	UV1
MYO7A	c.974T>G	p.Ile325Ser	0	UV1
MYO7A	c.5598C>A	p.Leu1866Leu	0.23	UV1
PCDH15	c.2625G>C	p.Ser875Ser	NA	UV1
PCDH15	c.319-20A>T	p.?	NA	UV1
PCDH15	c.3502-8C>T	p.?	NA	UV1
PCDH15	c.3795A>G	p.Glu1265Asp	0	UV1
PCDH15	c.3983+12T>C	p.?	NA	UV1
PCDH15	c.4974A>C	p.Ser1658Ser	0.11	UV1
PCDH15	c.5247_5249delTCC	p.Pro1752del	0.57	Neutral
PCDH15	c.5263C>T	p.Pro1755Ser	NA	UV1
PCDH15	c.5358_5359insCCTCTT	p.Ile1786_Pro1787insProLeu	NA	UV1
PCDH15	c.5359C>T	p.Pro1787Ser	NA	UV1
PCDH15	c.5398G>A	p.Val1800Ile	NA	UV1
PCDH15	c.5550C>A	p.Thr1850Thr	NA	UV1
PCDH15	c.5707A>G	p.Ile1903Val	NA	UV1
USH1C	c.1086-13G>T	p.?	NA	UV1
USH1C	c.1430G>A	p.Arg477Gln	0	UV1

USH1C	c.2340C>T	p.Val780Val	NA	UV1
USH1C	c.324T>C	p.Phe108Phe	0	UV1
USH1C	c.421T>C	p.Ser141Pro	NA	UV1
USH1C	c.461T>C	p.Ile154Thr	NA	UV1
USH1G	c.1152C>T	p.Asp384Asp	0	UV1
USH1G	c.388A>G	p.Lys130Glu	0	UV1
USH1G	c.501C>G	p.Arg167Arg	0.12	UV1
USH1G	c.566G>A	p.Arg189Gln	0.12	UV1
USH1G	c.678C>A	p.Gly226Gly	0	UV1
USH1G	c.705G>A	p.Glu235Glu	0.12	UV1
USH1G	c.83C>T	p.Pro28Leu	NA	UV1
GPR98	c.10260C>T	p.Phe3420Phe	0	UV1
GPR98	c.10796+9A>G	p.?	NA	UV1
GPR98	c.10873C>G	p.Leu3625Val	NA	UV1
GPR98	c.10927A>G	p.Thr3643Ala	0.11	UV1
GPR98	c.11599G>A	p.Glu3867Lys	NA	UV1
GPR98	c.12121-16A>G	p.?	NA	UV1
GPR98	c.12175A>G	p.Thr4059Ala	NA	UV1
GPR98	c.12269C>A	p.Thr4090Asn	NA	UV1
GPR98	c.13232-7A>G	p.?	NA	UV1
GPR98	c.13358A>G	p.His4453Arg	0	UV1
GPR98	c.13919G>A	p.Gly4640Glu	0	UV1
GPR98	c.14309G>A	p.Arg4770His	0.92	Neutral
GPR98	c.14856C>T	p.His4952His	0	UV1
GPR98	c.15105C>T	p.Ser5035Ser	NA	UV1
GPR98	c.15301G>A	p.Gly5101Arg	0.36	Neutral
GPR98	c.15343C>T	p.Leu5115Leu	0	UV1
GPR98	c.16164A>G	p.Arg5388Arg	1.54	Neutral
GPR98	c.16312A>G	p.Thr5438Ala	0.48	Neutral
GPR98	c.18026G>A	p.Arg6009Gln	0	UV1
GPR98	c.18040T>C	p.Phe6014Leu	0	UV1
GPR98	c.18273A>G	p.Ala6091Ala	0.23	UV1
GPR98	c.18311-8_12delTTTT	p.?	NA	UV1
GPR98	c.1849G>A	p.Val617Met	NA	UV1
GPR98	c.18746T>G	p.Leu6249Arg	0	UV1
GPR98	c.18753C>T	p.Ala6251Ala	0	UV1
GPR98	c.18782T>C	p.Leu6261Ser	0	UV1
GPR98	c.18802+9G>A	p.?	NA	UV1
GPR98	c.18803-13A>G	p.?	NA	UV1
GPR98	c.2185A>G	p.Ile729Val	0	UV1
GPR98	c.2284C>T	p.Arg762Cys	0	UV1
GPR98	c.2516T>C	p.Val839Ala	0.12	UV1
GPR98	c.2553+11T>A	p.?	NA	UV1
GPR98	c.2735-10C>A	p.?	NA	UV1
GPR98	c.2834G>A	p.Gly945Glu	NA	UV1
GPR98	c.3022+8T>C	p.?	NA	UV1
GPR98	c.3255T>C	p.Asp1085Asp	0.12	UV1
GPR98	c.327C>T	p.Asp109Asp	0.24	UV1
GPR98	c.3289G>A*	p.Gly1097Ser	0.11	UV1

GPR98	c.3635-10C>A	p.?	NA	UV1
GPR98	c.3805T>C	p.Phe1269Leu	0	UV1
GPR98	c.380T>G	p.Leu127Arg	2.22% [2/90 CEPH]	UV1
GPR98	c.3975G>A	p.Thr1325Thr	0	UV1
GPR98	c.4214C>T	p.Ser1405Ser	NA	UV1
GPR98	c.4260A>G	p.Glu1420Glu	0.84	Neutral
GPR98	c.5104C>T	p.Pro1702Ser	0	UV1
GPR98	c.5221T>C	p.Leu1741Leu	0	UV1
GPR98	c.5525-7C>T	p.?		UV1
GPR98	c.5785G>T	p.Ala1929Ser	0.24	UV1
GPR98	c.6012G>T	p.Leu2004Phe	NA	UV1
GPR98	c.6289C>T	p.Arg2097Cys	1.19	Neutral
GPR98	c.6317C>T	p.Ala2106Val	0.69	Neutral
GPR98	c.6318G>A	p.Ala2106Ala	0.68	Neutral
GPR98	c.6608 T>C	p.Val2203Ala	0.34	Neutral
GPR98	c.6695A>G	p.Tyr2232Cys	NA	UV1
GPR98	c.6938C>T	p.Pro2313Leu	0	UV1
GPR98	c.6994A>T	p.Ile2332Phe	0	UV1
GPR98	c.7176C>T	p.Ser2392Ser	0.24	UV1
GPR98	c.7179C>T	p.Asp2393Asp	1.48	Neutral
GPR98	c.7229A>G	p.Tyr2410Cys	0.11	UV1
GPR98	c.7293C>T	p.Ala2431Ala	0	UV1
GPR98	c.7576 A>G	p.Ile2526Val	0	UV1
GPR98	c.7821G>A	p.Glu2607Glu	0.36	Neutral
GPR98	c.7874G>A	p.Arg2625His	NA	UV1
GPR98	c.9280G>A	p.Val3094Ile	NA	UV1
GPR98	c.9650C>T	p.Ala3217Val	0.8	Neutral
GPR98	c.9743G>A	p.Gly3248Asp	NA	UV1
USH2A	c.10062G>C	p.Val3354Val	0.11	UV1
USH2A	c.10510 C>G	p.Pro3504Ala	0.12	UV1
USH2A	c.11597C>T	p.Ala3866Val	0	UV1
USH2A	c.1174C>T	p.Pro392Ser	0	UV1
USH2A	c.11928G>A	p.Thr3976Thr	NA	UV1
USH2A	c.12505A>G	p.Thr4169Ala	0	UV1
USH2A	c.12823T>A	p.Ser4275Thr	0.11	UV1
USH2A	c.12910G>A	p.Glu4304Lys	0	UV1
USH2A	c.13631G>T	p.Gly4544Val	0	UV1
USH2A	c.1453A>G	p.Ile485Val	0	UV1
USH2A	c.1731C>T	p.Cys577Cys	0.24	UV1
USH2A	c.2844 C>G	p.Cys948Trp	0	UV1
USH2A	c.2844C>G	p.Cys948Trp	0	UV1
USH2A	c.3261 C>T	p.Ile1207Ile	0	UV1
USH2A	c.3945T>C	p.Asn1315Asn	1.12	Neutral
USH2A	c.4115C>A	p.Pro1372His	0.12	UV1
USH2A	c.4560C>T	p.Ile1520Ile	0.46	Neutral
USH2A	c.5142 T>C	p.Asn1714Asn	0	UV1
USH2A	c.550A>C	p.Thr184Pro	0 [0/96 CEPH]	UV1

Novel UV1_Neutral

USH2A	c.6049G>T*	p.Gly2017Cys	NA	UV1
USH2A	c.7130A>G	p.Asn2377Ser	0.81	Neutral
USH2A	c.7584C>T	p.Thr2528Thr	0.11	UV1
USH2A	c.785-17_-14delAT	p.?	0	UV1
USH2A	c.8681+18A>G	p.?	4.35 [4/92 CEPH]	UV1
USH2A	c.9228C>A	p.Asp3076Glu	0	UV1
USH3A	c.126G>A	p.Thr42Thr	0	UV1
USH3A	c.6A>C	p.Pro2Pro	0.46	Neutral
WHRN	c.1166+18 G>A	p.?	NA	UV1
WHRN	c.1365T>C	p.Ser455Ser	NA	UV1
WHRN	c.1653 C>T	p.Gly551Gly	NA	UV1
WHRN	c.2118A>G	p.Pro706Pro	NA	UV1
WHRN	c.2485 G>A	p.Ala829Thr	NA	UV1
WHRN	c.409 G>C	p.Glu137Gln	0 [0/134 ECCAC]	UV1
WHRN	c.755A>G	p.Gln252Arg	0 [0/98 ECCAC; 0/84 Pakistani]	UV1
SLC4A7	c.1740-3T>C	p.?	NA	UV1
SLC4A7	c.2314C>T	p.Pro772Ser	1.72	Neutral
SLC4A7	c.3624G>A	p.Val1208Val	0	UV1
SLC4A7	c.402-7C>T	p.?	NA	UV1
SLC4A7	c.459T>C	p.Tyr53Tyr	NA	UV1
SLC4A7	c.756A>T	p.Glu252Asp	0.12	UV1

*Last nucleotide of an exon

[a]Minimum Allele Frequecy in 878 control chromosomes unless stated otherwise; NA-not assesed

6.9 System for determining pathogenicity

An overview of the methods used to determine the pathogenicity of alleles were discussed earlier in subsection **??**.

6.9.1 minimum allele frequency for most prevalent pathogenic allele

After reviewing the results for the allele specific assays, one previously reported mutation in the *USH2A* gene stood out as being the most prevalent allele returned in *all* families regardless of clinical subtype. This change, c.2299delG (p.Glu767SerfsX21) has been well reported as disease causing and is a common disease causing allele prevalent in other populations studied across Europe [66, 164, 168, 175] [167] the prevalence of this allele in the control population served as a benchmark.

The inherent limitations of assembling a control group for an ethnically diverse population such as the NCUS cohort were discussed earlier in subsection 3.6.1.

Accepting these limitations and assuming that our control population is representative of the NCUS cohort, being the most prevalent allele in out NCUS cohort, one would also expect its prevalence in the control population (carrier frequency) would be the greatest of all USH alleles in all USH genes.

The allele specific assay for the c.2299delG allele in our control population of 440 DNA samples failed to return a genotype in 17 samples, 421 samples were returned as wild type and 2 samples were returned as heterozygous (carriers). Using the formula for calculation of minimum allele frequency described earlier (**??**) and excluding the samples that failed the assay, the MAF was calculated as below:

$$\frac{2}{(421+2)\times 2} = \frac{2}{846} = 0.00236 = 0.236\% \tag{6.1}$$

French investigators reported the prevalence of the same allele as 1 in 1080 control chromosomes (of unknown ethnic origin) which is equivalent to a minimum allele frequency of 0.046%. This figure is significantly less than our figure (approx 20% of our value of 0.236%.

Even if we assume that our control population is enriched for the c.2299delG allele and that our estimation of allele frequency is an overestimation, it would be fair to assume that it would be very unlikely for another pathogenic allele in any of the Usher genes to be present in the control population at a greater frequency than 0.236%.

This assumption was incorporated in the final algorithm devised for assaying the pathogenicity of alleles identified.

NCUS Pathogenicity grade	4	3	2.5		2	1
Pathogenicity grade for LOVD USHbase	Pathogenic	UV4	UV3	UV2	UV1	Neutral
Frequency in ethnically matching controls ≤ 0.236	yes	yes	yes	yes*	unknown	no
In trans with a 'Pathogenic' or 'UV4' mutation	yes	yes	unknown	unknown	unknown	no
Segregates with disease in >2 NCUS families or previously published as 'Pathogenic' or 'UV4'	yes	no	no	no	no	no
Novel, segregates with disease in only one NCUS family	no	yes	yes	yes	no	no
Indentified in proband with one or two other mutations with a higher pathogenicity grade	no	no	no	no	yes or unknown	yes or unknown

*Genotyped only on 96 CEPH control chromosomes

FIGURE 6.11: Algorithmic approach to determining the pathogenicity of DNA sequence changes identified. The pathogenicity grades used in this study are shown in yellow, and the corresponding nomenclature used to upload the variants to the USHbases database is shown on the second row

6.9.2 Grading systems to determine pathogenicity of alleles

NCUS pathogenicity grading system; numerical grades from 1 - 4

An algorithm was created to rank the estimated pathogenicity of all DNA sequence changes identified. This algorithm was based around the benchmark frequency of the most prevalent disease causing allele in the entire study population (0.236%) as the upper cut-off frequency for what was considered to be likely to be a pathogenic allele.

The algorithm also employed segregation data obtained from the allele specific alleles where possible. Other important factors that were considered in the algorithm were the predicted effect of the sequence change and segregation with disease as outlined in table **??**.

Each allele was given a numerical score for its predicted pathogenicity ranging from 1 to 4. A pathogenicity score of 1 indicates a polymorphic non-disease causing allele. Conversely an allele with a pathogenicity score of 4 indicates an allele that was confidently predicted to be disease causing. For the purposes of clarity, this simple grading system has been used in the clinical results chapters 7, 8 and 9.

Pathogenicity grading system; USHbases

In order to conform with other researchers and submit our DNA sequence variants to the USHbases database, the above pathogenicity grading system was reclassified as follows.

Sequence variants were graded using two definite pathogenicity grades, i.e. pathogenic (equivalent to NCUS pathogenicity grade 4) and neutral (equivalent to NCUS pathogenicity grade 1). Variants which could not be confidently classified as either pathogenic or neutral were called unclassified variants (UV1-UV4), with UV4 being probably pathogenic and UV1 being probably neutral. A full description of the grading system is outlined in table **??**

Frame-shift mutations, nonsense mutations and mutations of the first two nucleotides of canonical intron splice acceptor or donor sites have been classified as pathogenic. A missense or intronic change was described as pathogenic if it fulfilled all of the following criteria: it occurred in controls with a frequency <0.236%, was identified in trans to a pathogenic or probably pathogenic mutation and it was either novel and segregated with USH in more than two families, or was previously published as pathogenic/likely pathogenic.

The benchmark frequency of 0.236% was determined based on the minimum allele frequency of the most common USH mutation USH2A:p.Glu767SerfsX21 in 846 control chromosomes assayed in this study (see 6.9).

If a novel variant fulfilled the above criteria, but segregated with USH in only one family, it was deemed to be probably pathogenic and was classified as UV4. Missense variants were classed as UV3 (likely pathogenic) if the frequency in control chromosomes was <0.236%, but phase of the variant could not be ascertained due to missing family data. Missense and silent changes of the last nucleotide of the exon that are likely to affect splicing were also described as UV3 if they were found in the same gene as another Pathogenic or UV4 variant. Our determination of a variant as pathogenic, is therefore stringent.

Variants with uncertain pathogenicity were described as UV2. UV2 variants fulfilled the criteria described for UV3, but were only genotyped in 96 CEPH control chromosomes. A missense variant was also classified as UV2 if it was the only possibly pathogenic variant in the gene. Furthermore, novel intronic variants residing three nucleotides from the start/end of the exon and not found in 846 control chromosomes were also classified as UV2. UV1 (probably neutral variants) variants were found in patients who already had two other pathogenic/probably pathogenic mutations or did not segregate with disease. The MAF of UV1 in control chromosomes was either <0.236% or was not assessed. We cannot exclude the possibility that such variants may modify disease phenotype. Neutral variants did not segregate with disease, were either previously published as neutral or were found in controls with a frequency 0.236%<.

Definition of "molecular diagnosis"

Using the grading system to determine pathogenicity of alleles described earlier, alleles with a pathogenicity score of 3 or 4 were taken as disease causing. Although alleles with a pathogenicity score of 2.5 might well be disease causing, for the purposes of defining a confirmed molecular diagnosis these alleles were ignored. This conservative approach was also employed to ensure that the subsets of individuals analysed when performing phenotype vs. genotype correlations between individuals with disease due to different genes, did not include individuals who might subsequently be identified as not having disease due to that particular gene.

6.10 Challenges encountered

6.10.1 Limitations of sequencing

Whilst the strategy of DNA sequencing the nine Usher genes in each family is an extremely comprehensive method of molecular analysis, it has its limitations.

Conceptual errors

The DNA sequencing performed in this study was restricted to the exonic and intron/exon boundaries of all the Usher genes (see 6.4 for a breakdown of this). It was expected that screening these regions would pick up the majority of disease causing changes in these genes. Determining whether DNA sequence changes in exonic sequences is not always straightforward, but the role that DNA sequence changes play in non-coding areas is even less clear.

Thus, by omitting sequencing these large non-coding areas of the Usher genes we would not detect any intronic sequence changes which may well be disease causing.

Employing direct sequencing might make heterozygous deletions difficult to detect.

Inaccurate annotation of genes

Gene prediction and manual annotation was performed initially by computational analysis an subsequently checked manually by collaborators at the Sanger centre.

6.10.2 Human error

When undertaking a large study such as the NCUS, there is always a possibility of human error leading to DNA sample mix up or contamination. This could occur at any stage such as blood sample labelling, DNA extraction, DNA storage, a mix up in the alphanumeric identifier codes used to identify DNA samples, error in labelling the

DNA aliquots that were sent to the different collaborator sites or practical errors at the experiment stage of sequencing or the allele specific assays.

6.10.3 Software error

Software used to screen sequence data for base calling missed

Missing heterozygous missense changes Ignoring poor sequencing read quality

6.10.4 Sequencing errors and artefacts

Sanger sequencing has inherent errors which mainly occur as a result of errors in DNA amplification (PCR). Repetitive sequences, SNPs under primer sites and the possibility of missed pseudogenes interfering with sequence reads are all potential pitfalls in DNA sequencing.

6.11 Haplotype analysis on families with no pathogenic sequence variants identified

Polymorphic marker data from SNPs genotyped during the Sequenom allele specific assays part of this study were available on all study subjects and used in many families to help establish linkage to a gene or in some cases to establish phase. Identification of one or two putative pathogenic alleles to some extent makes much of this data redundant. The polymorphic marker data however is useful when looking at those index cases in whom were were unable to identify even one putative pathogenic DNA sequence change. In some of these families, linkage analysis was not helpful due to family structure, specifically the lack of other genotyped family members. The following section presents data pertaining to some of the families in whom no putative pathogenic DNA sequence variants were identified.

FAMILY 38
USH1
Index case NCUS ID 29

FAMILY 38 Index case NCUS ID 29, USH1

23/09/2009

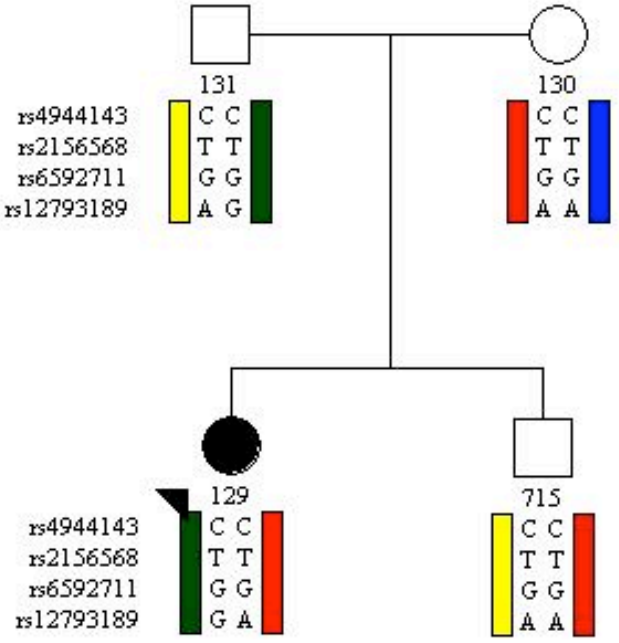

MYO7A possible

FAMILY 38 Index case NCUS ID 29, USH1

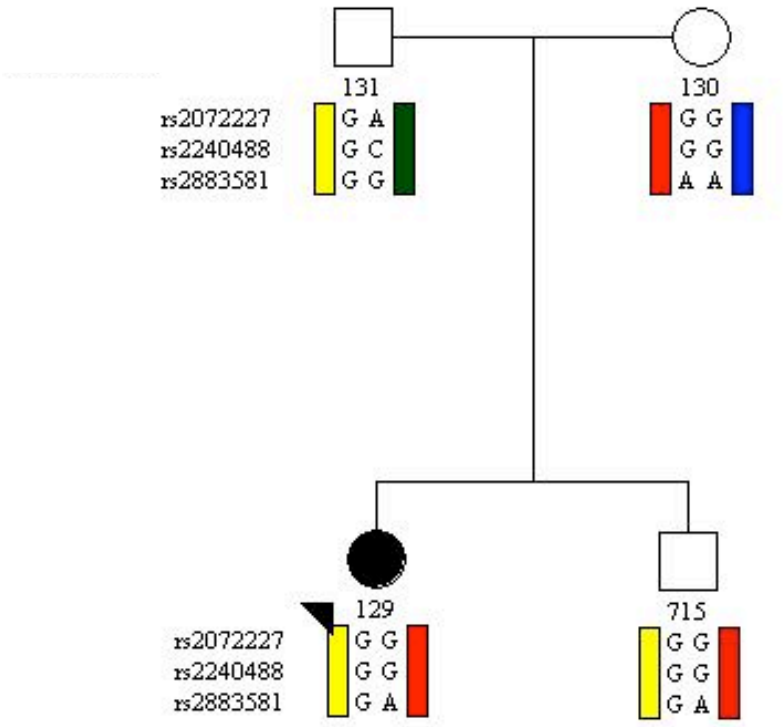

USH1C excluded

FAMILY 38 Index case NCUS ID 29, USH1

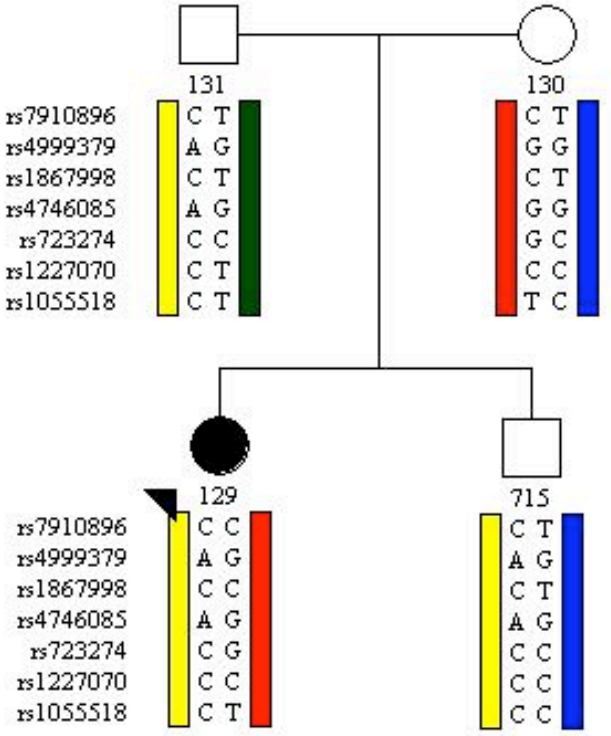

CDH23 possible

Status = Affected Proband status = 1

FAMILY 38 Index case NCUS ID 29, USH1

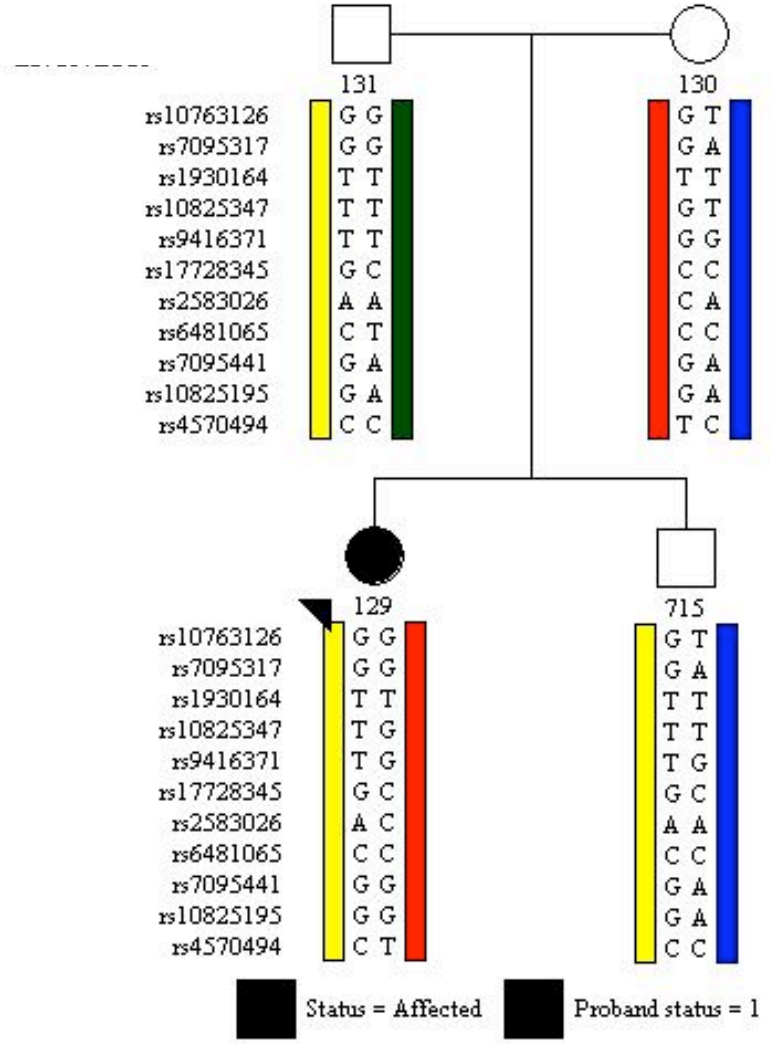

PCDH15 possible

FAMILY 38 Index case NCUS ID 29, USH1

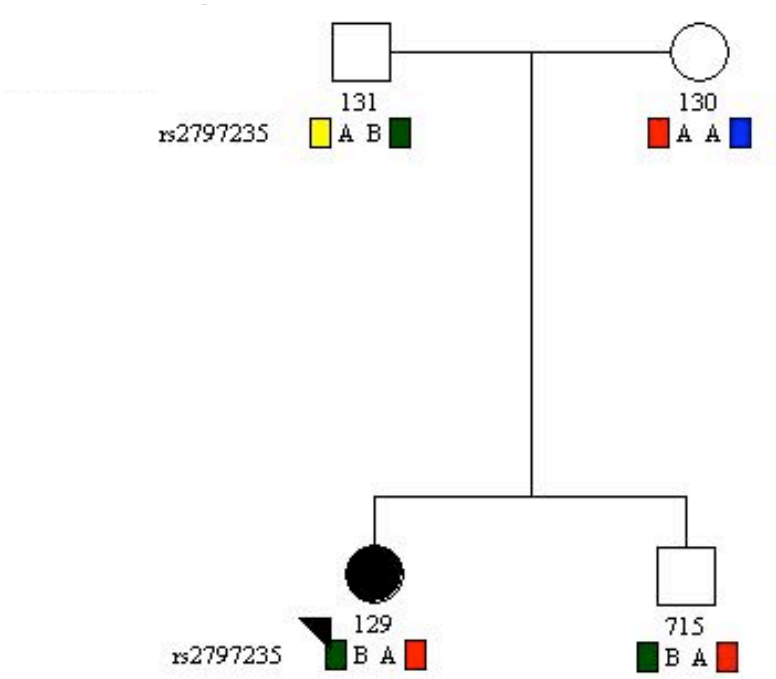

USH2A inconclusive

FAMILY 38 Index case NCUS ID 29, USH1

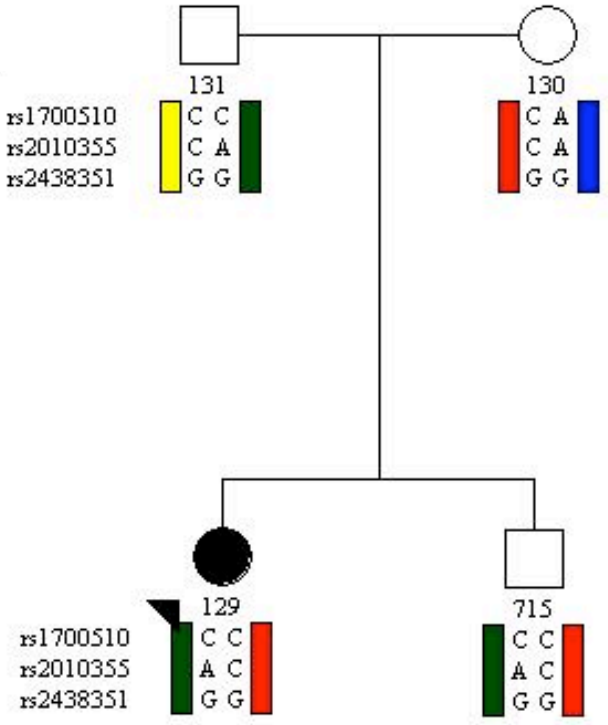

GPR98 EXCLUDED

FAMILY 38 Index case NCUS ID 29, USH1

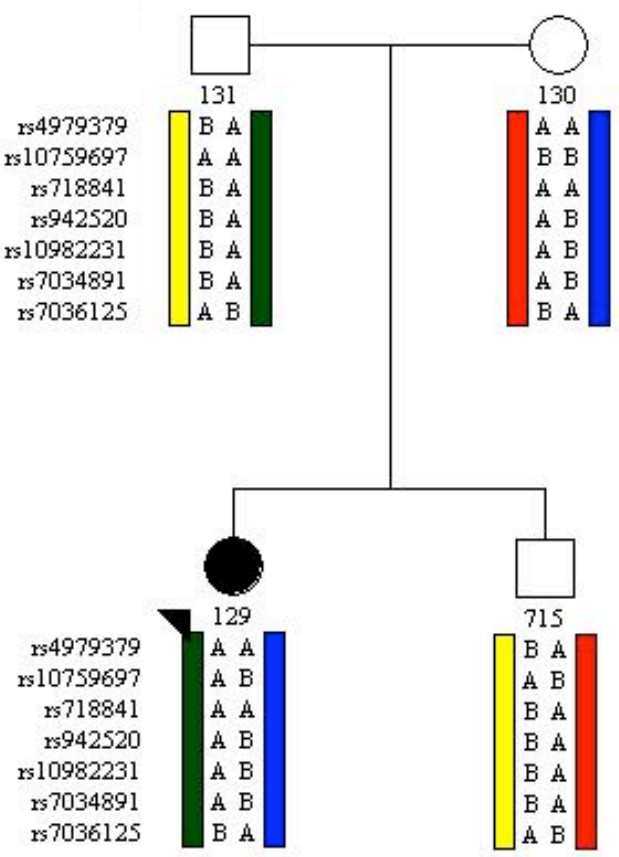

WHRN possible

FAMILY 38 Index case NCUS ID 29, USH1

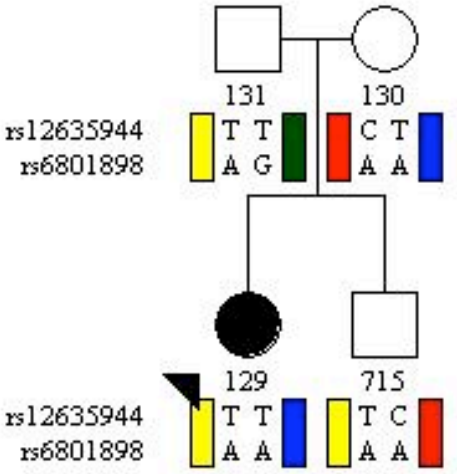

USH3A possible

FAMILY 100
USH1
Index case NCUS ID 340

FAMILY 100 Index case NCUS ID 340 USH1

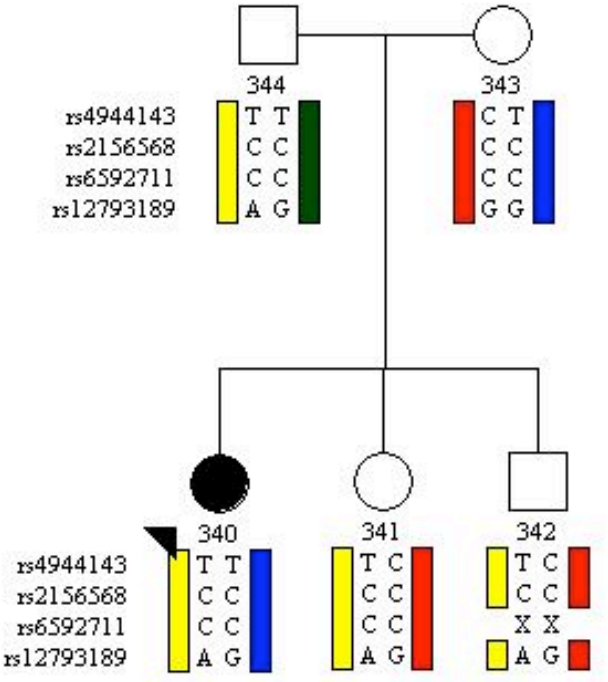

Prob

MYO7A possible

FAMILY 100 Index case NCUS ID 340 USH1

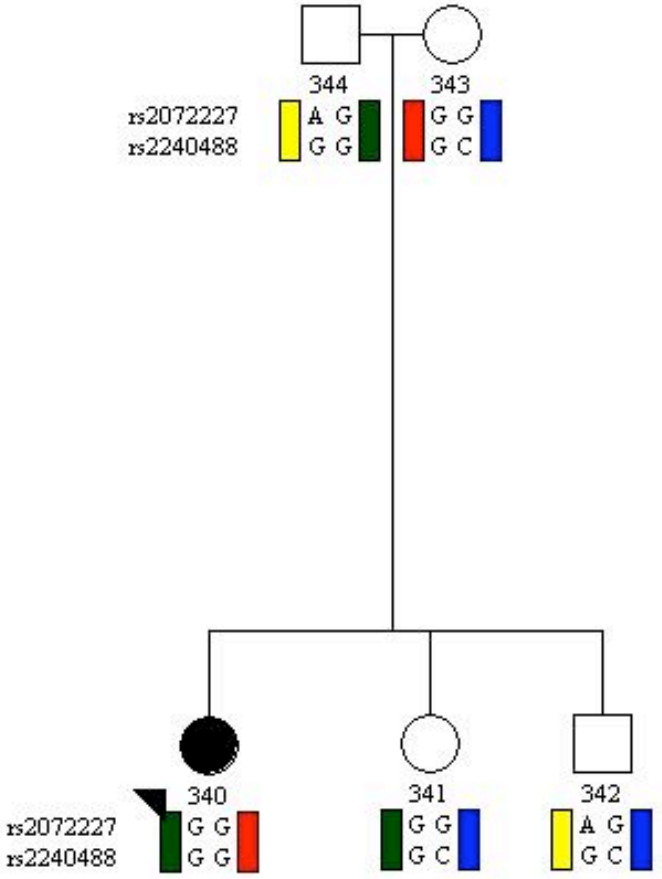

USH1C possible

FAMILY 100 Index case NCUS ID 340 USH1

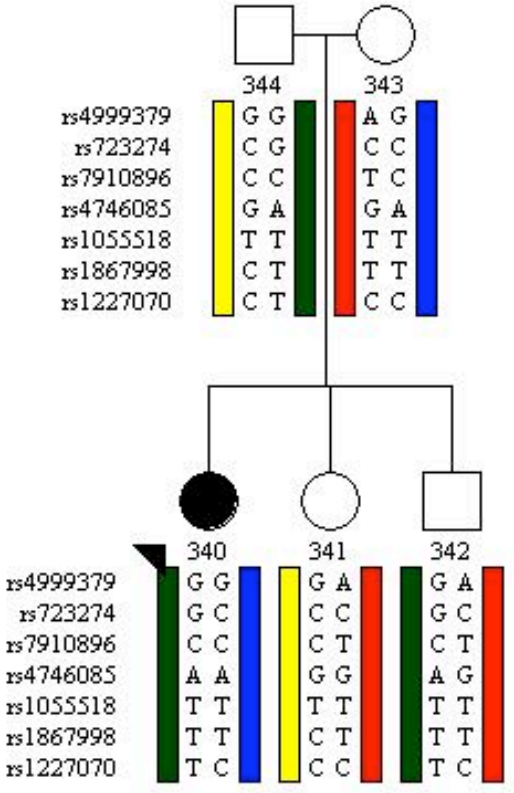

CDH23 possible

FAMILY 100 Index case NCUS ID 340 USH1

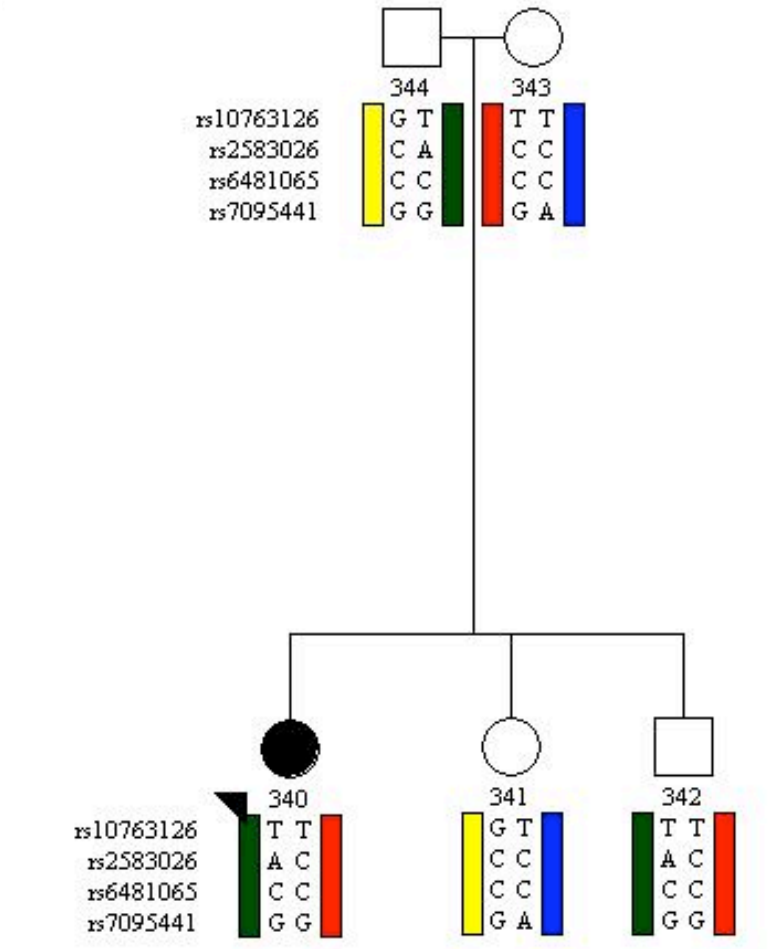

PCDH15excluded

FAMILY 100 Index case NCUS ID 340 USH1

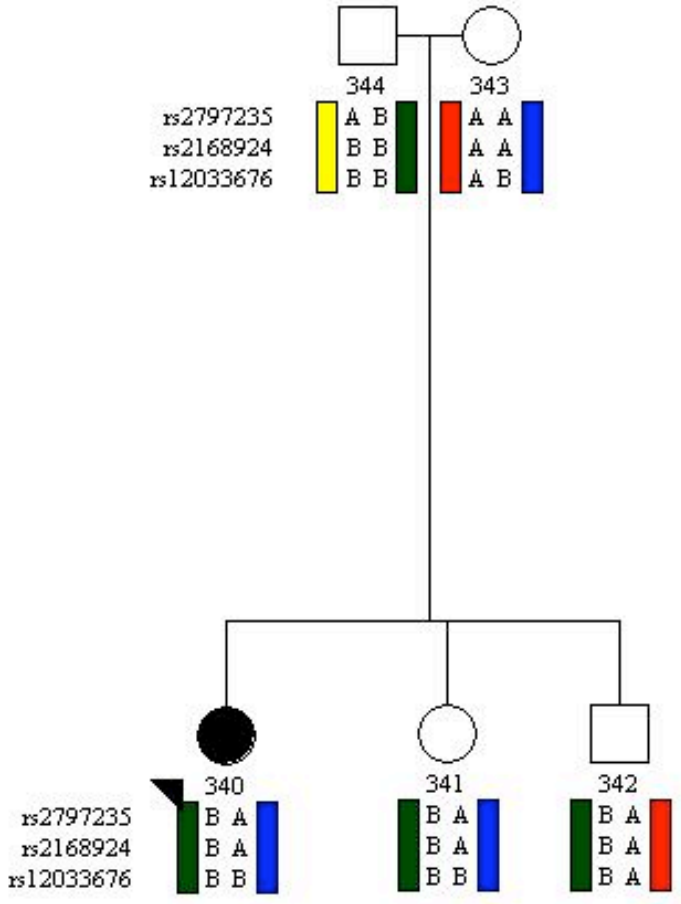

USH2A excluded

FAMILY 100 Index case NCUS ID 340 USH1

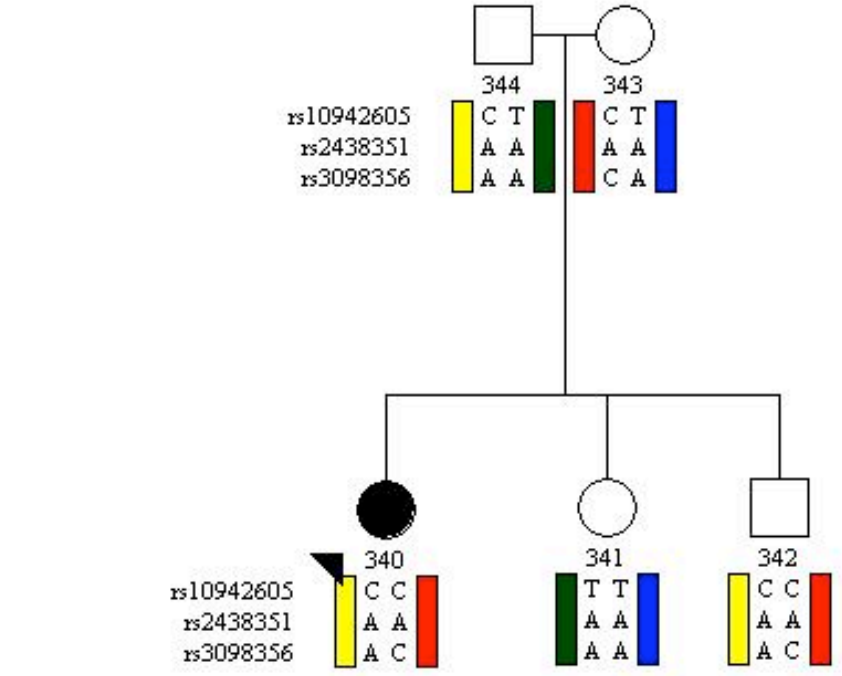

GPR98 excluded

Proband status = 1

FAMILY 100 Index case NCUS ID 340 USH1

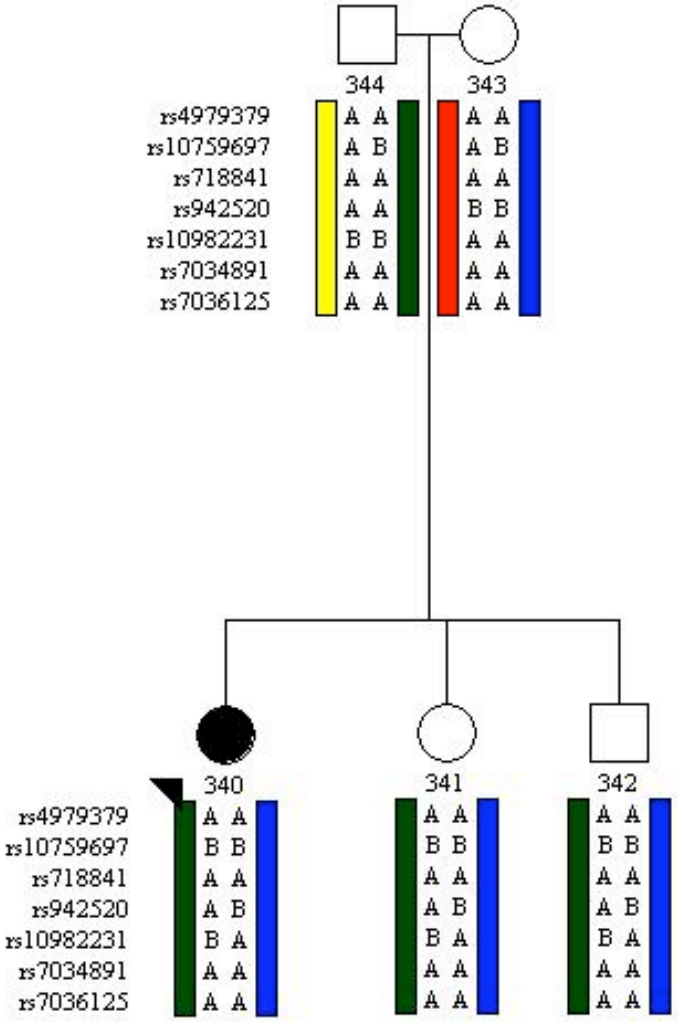

WHRN excluded

Proband status = 1

FAMILY 100 Index case NCUS ID 340 USH1

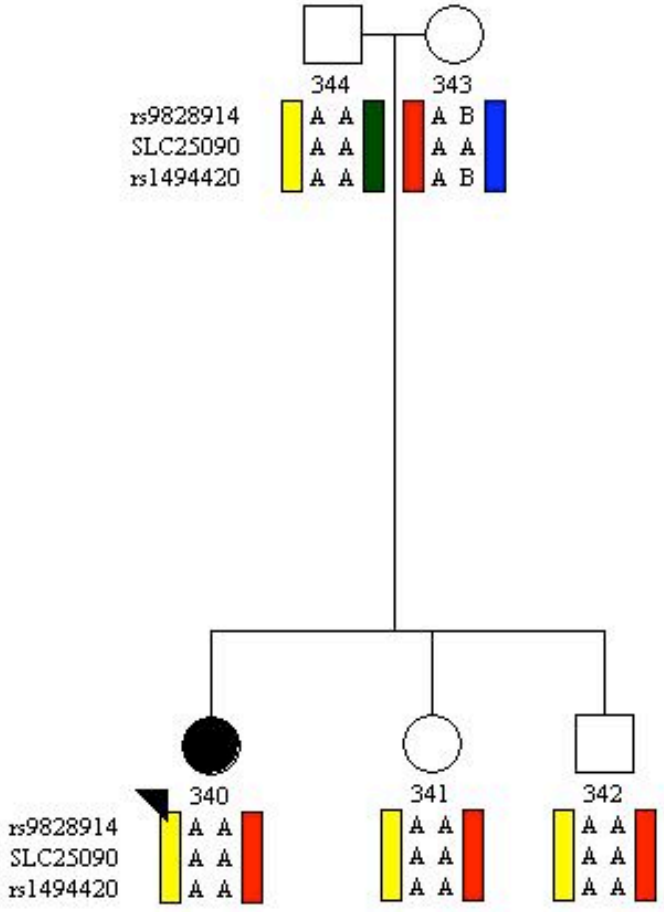

SLC4A7 excluded

FAMILY 100 Index case NCUS ID 340 USH1

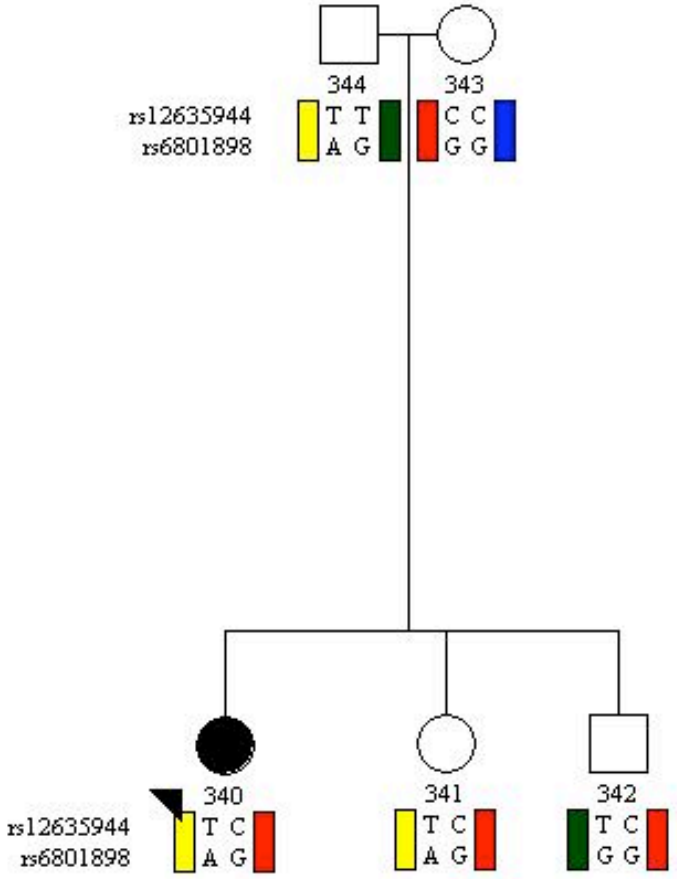

USH3A excluded

FAMILY 53
[consanguineous]
USH1
Index case
NCUS ID 168

FAMILY 53 Index case NCUS ID 168 [*consanguineous]*

Ercan_53

23/09/2009

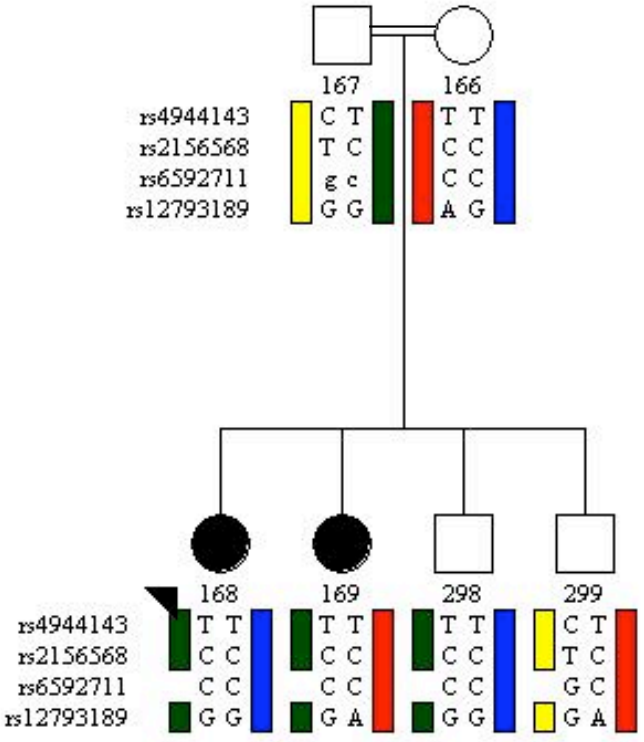

FAMILY 53 Index case NCUS ID 168
[*consanguineous]*
USH1

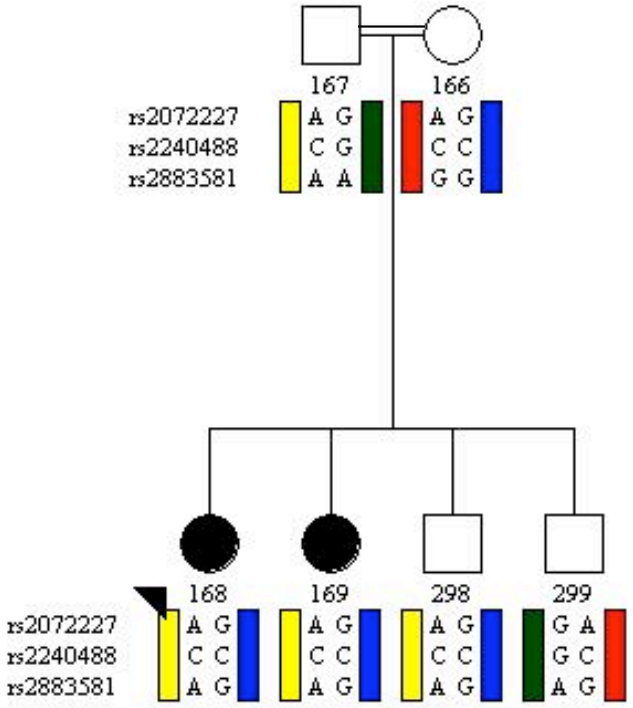

USH1C unlikely

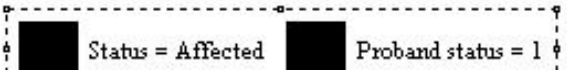

FAMILY 53 Index case NCUS ID 168
[*consanguineous]*
USH1

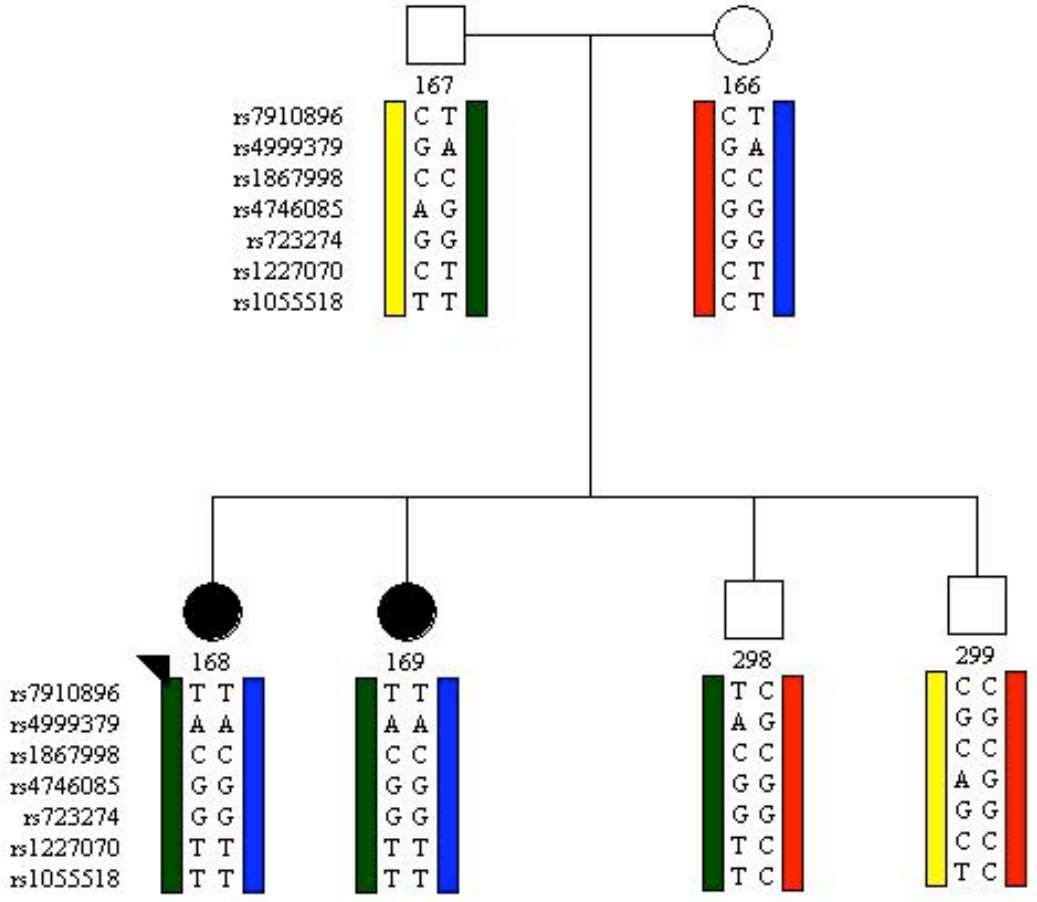

CDH23 linked to

FAMILY 53 Index case NCUS ID 168
[*consanguineous]*
USH1

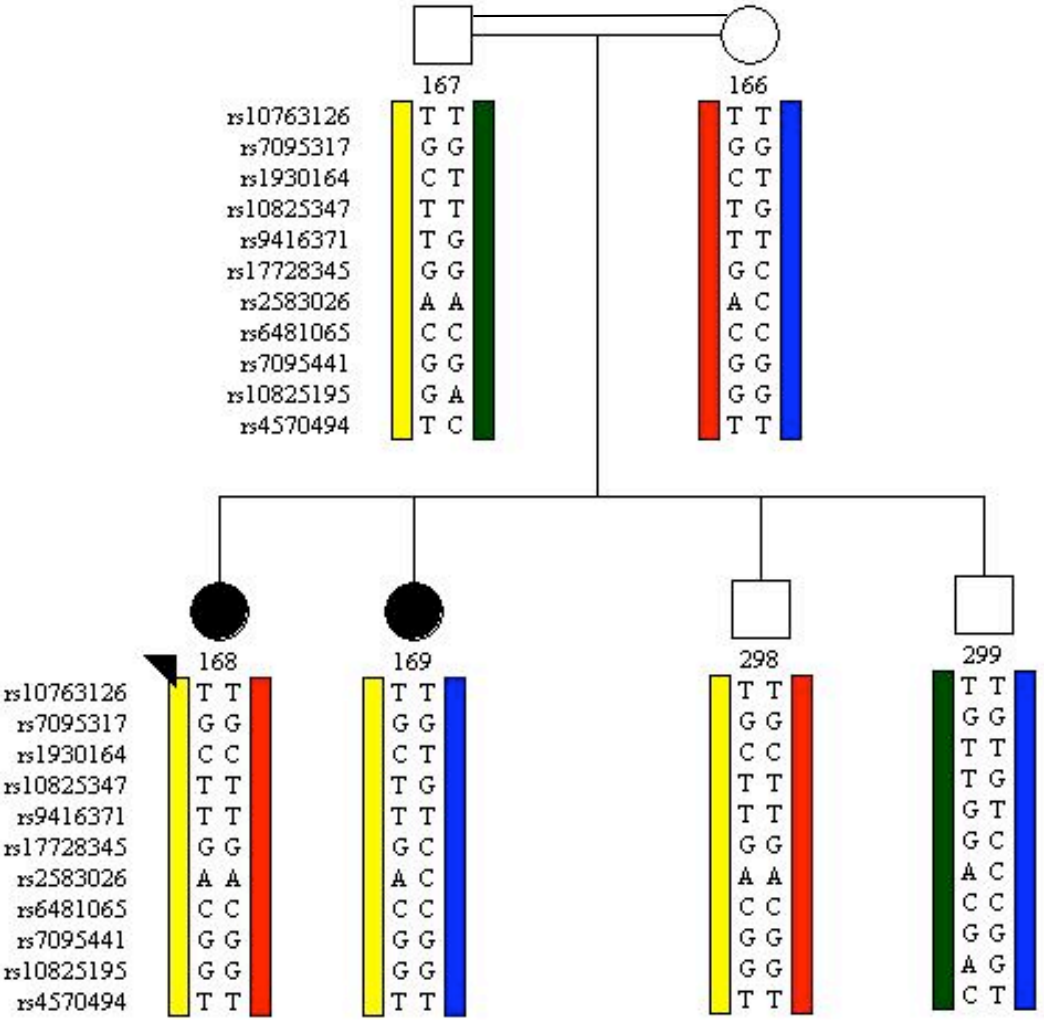

PCDH15 unlikely

Status = Affected Proband status = 1

FAMILY 53 Index case NCUS ID 168
[*consanguineous]*
USH1

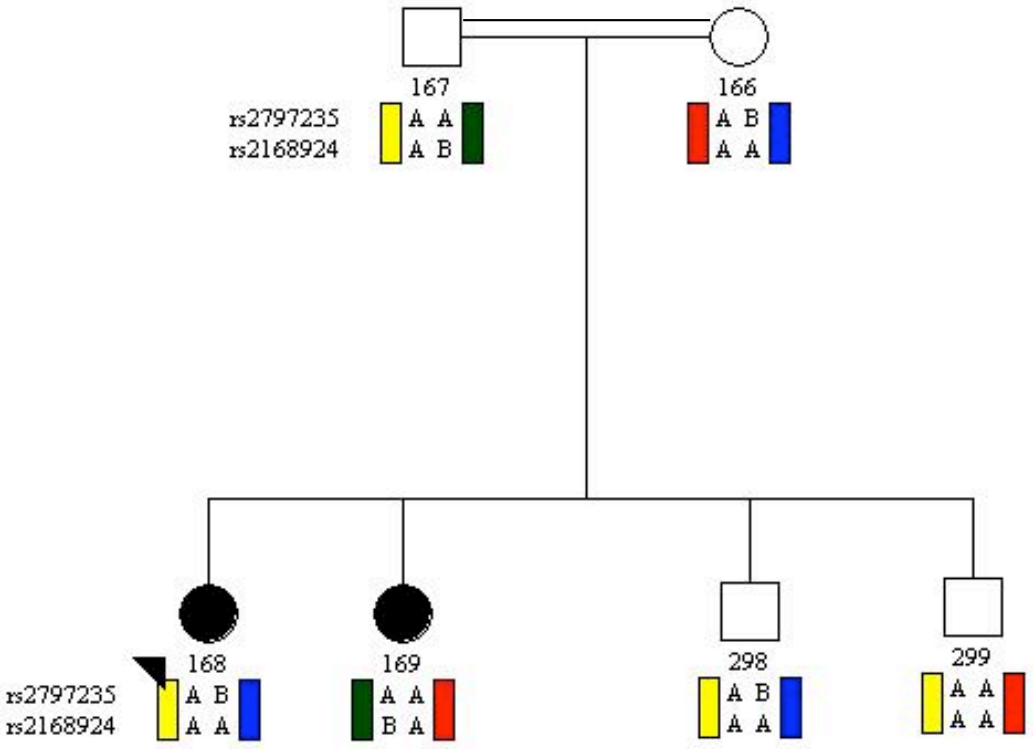

USH2A unlikely

FAMILY 53 Index case NCUS ID 168
[*consanguineous]*
USH1

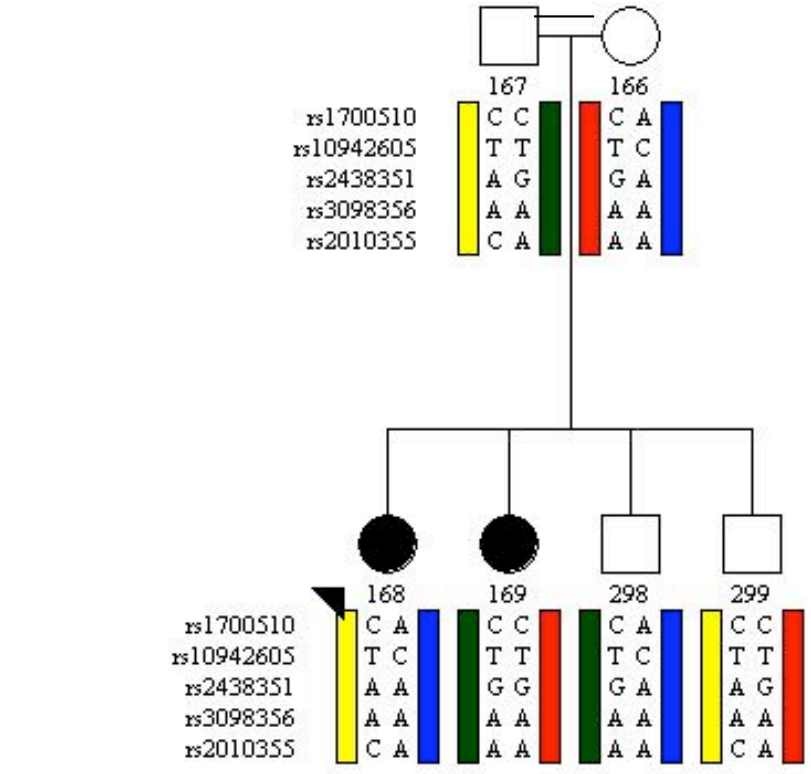

GPR98 excluded

Status = Affected Proband status = 1

FAMILY 53 Index case NCUS ID 168
[*consanguineous]*
USH1

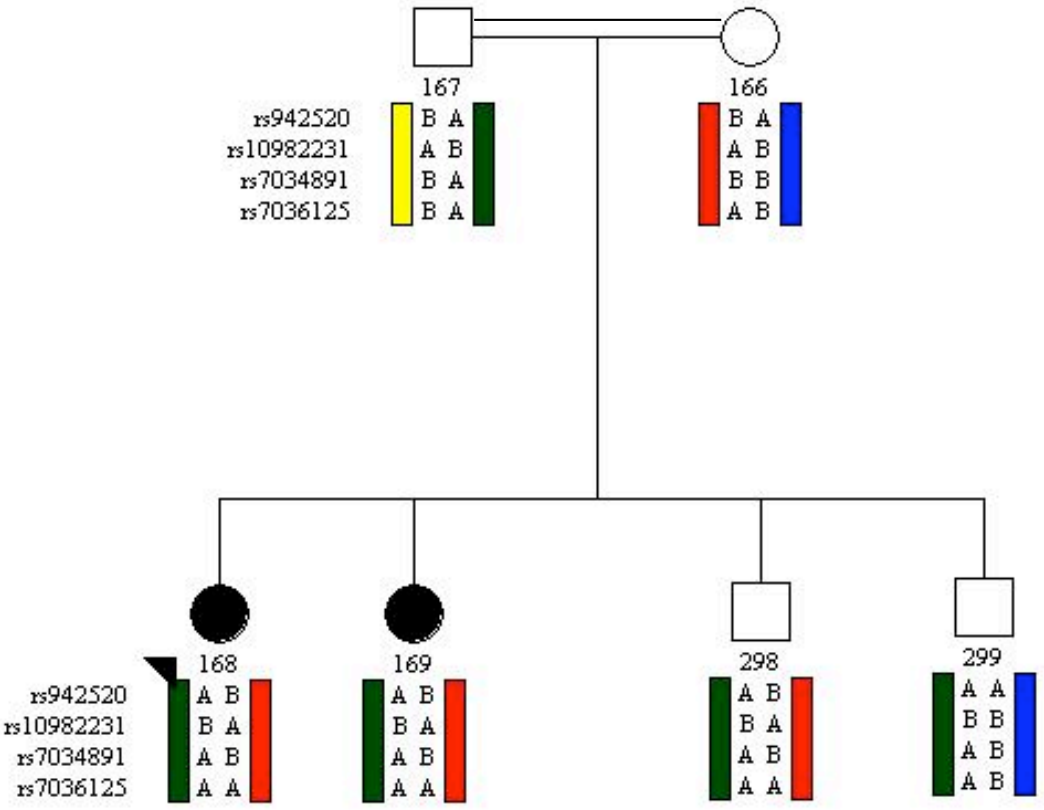

WHRN unlikely

FAMILY 53 Index case NCUS ID 168
[*consanguineous]*
USH1

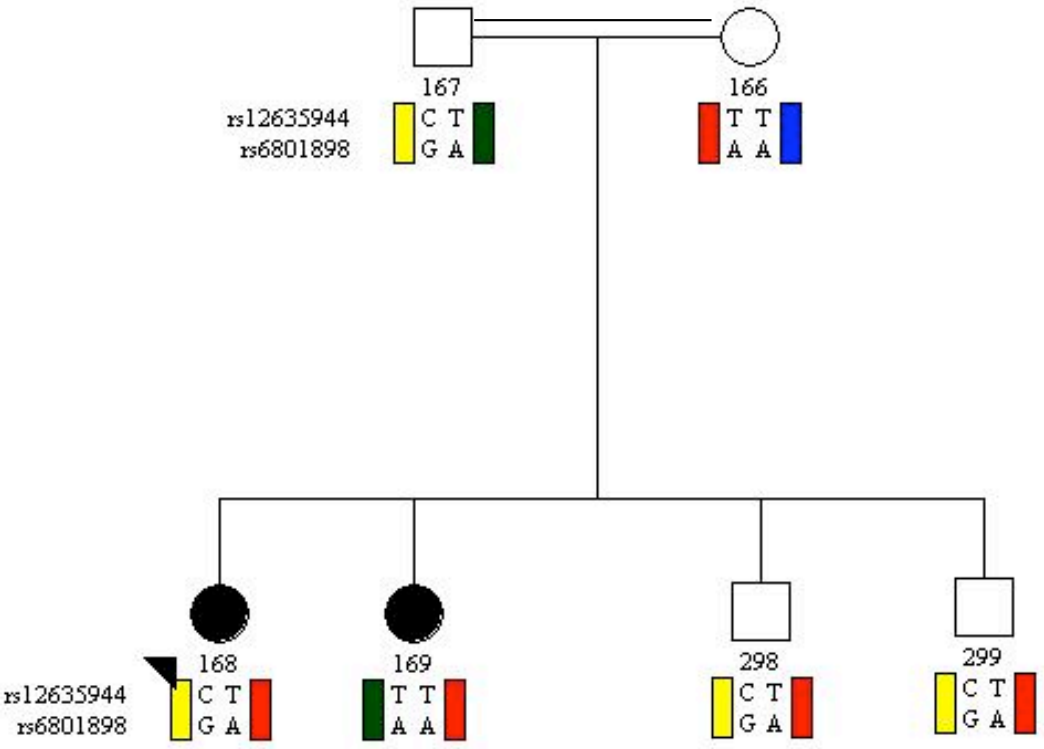

USH3A excluded

FAMILY 72
USH2
Index case NCUS ID 222

FAMILY 72 Index case NCUS ID 222

USH2

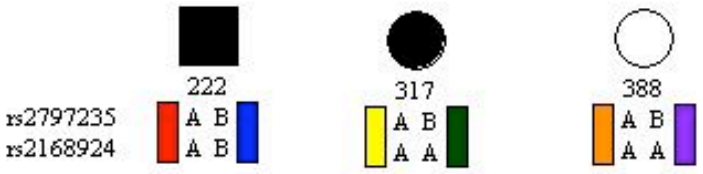

USH2A excluded

Both affected individuals have learning difficulties. Deletion in GPR98 suspected due to haplotype analysis, apparent non-inheritance of GPR98 SNPs in the family and PCR non-amplification of both affected sib's DNAs

FAMILY 72 Index case NCUS ID 222

USH2

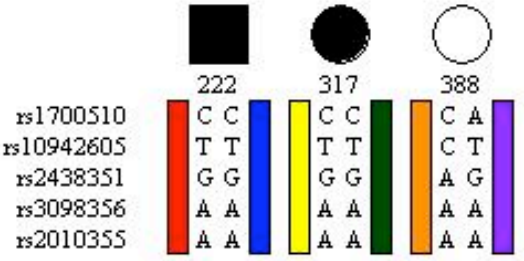

GPR98 linkage to

Both affected individuals have learning difficulties. Deletion in GPR98 suspected due to haplotype analysis, apparent non-inheritance of GPR98 SNPs in the family and PCR non-amplification of both affected sib's DNAs

FAMILY 23
USH2
Index case NCUS ID 72

FAMILY 23 Index case NCUS ID 72

USH2

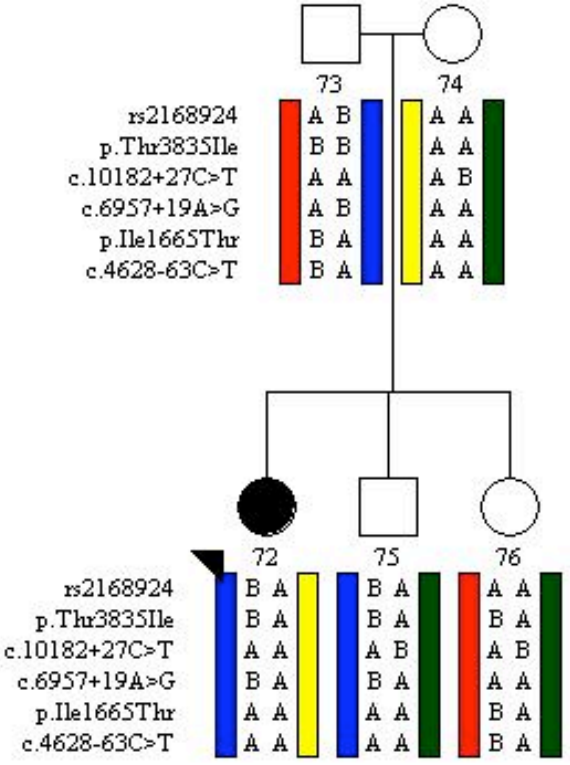

USH2A possible

FAMILY 23 Index case NCUS ID 72

USH2

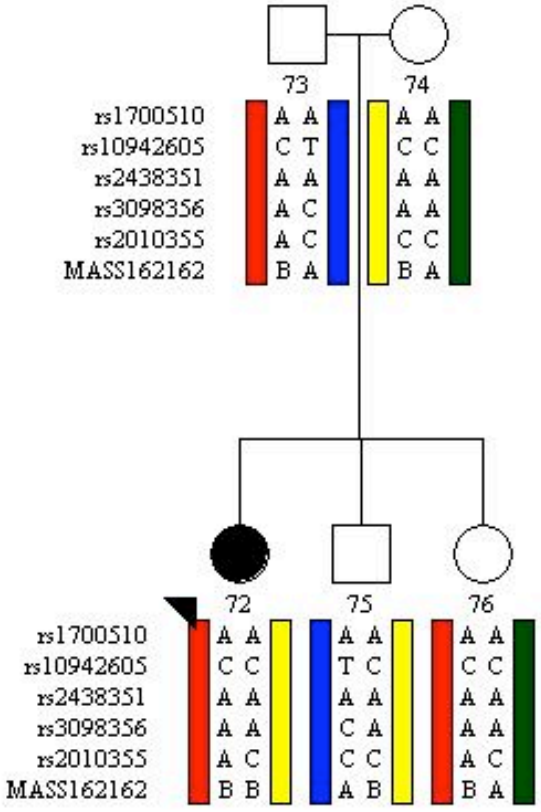

GPR98 unlikely

FAMILY 23 Index case NCUS ID 72

USH2

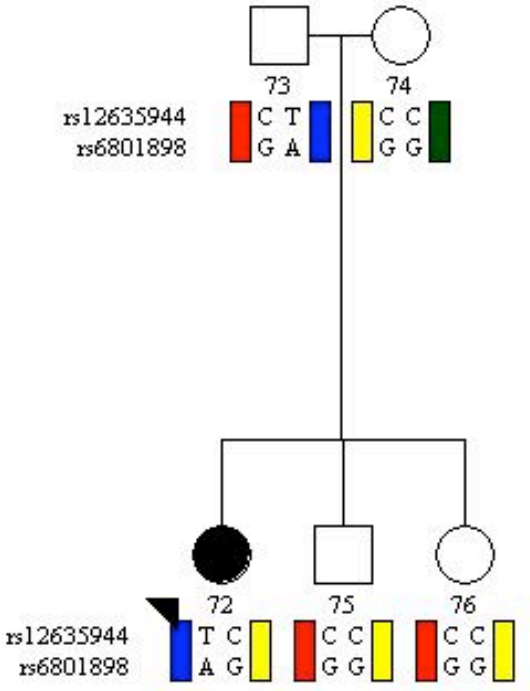

USH3A possible

FAMILY 152
USH2
Index case NCUS ID 537

index case has learning difficulties. Previous CT head scan = cerebral atrophy only.

FAMILY 152 Index case NCUS ID 537

USH2

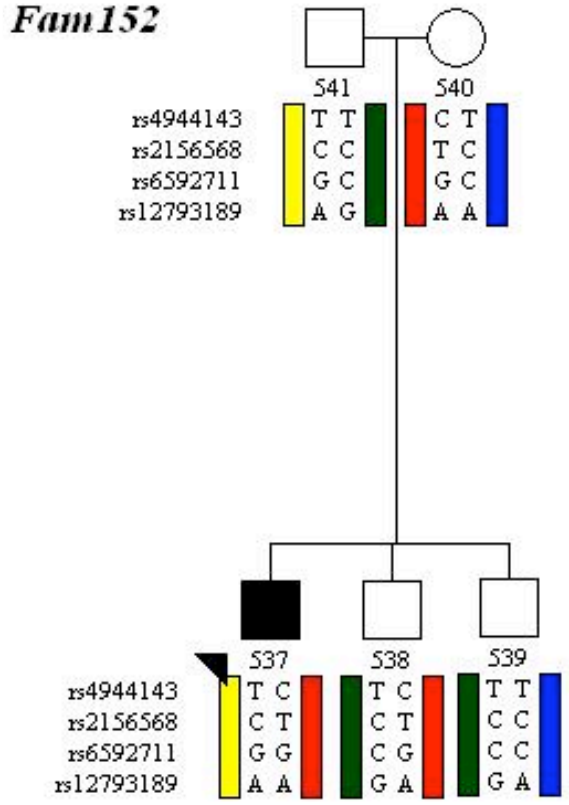

MYO7A possible

FAMILY 152 Index case NCUS ID 537

USH2

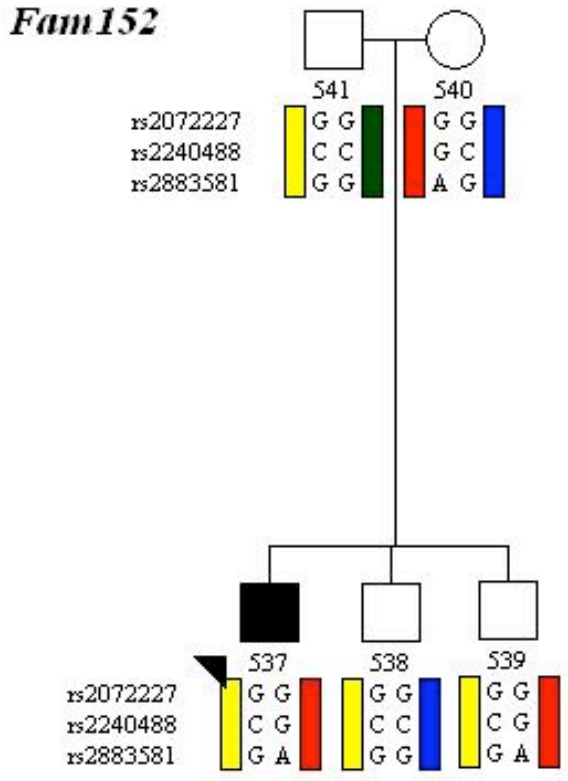

USH1C unlikely

FAMILY 152 Index case NCUS ID 537

USH2

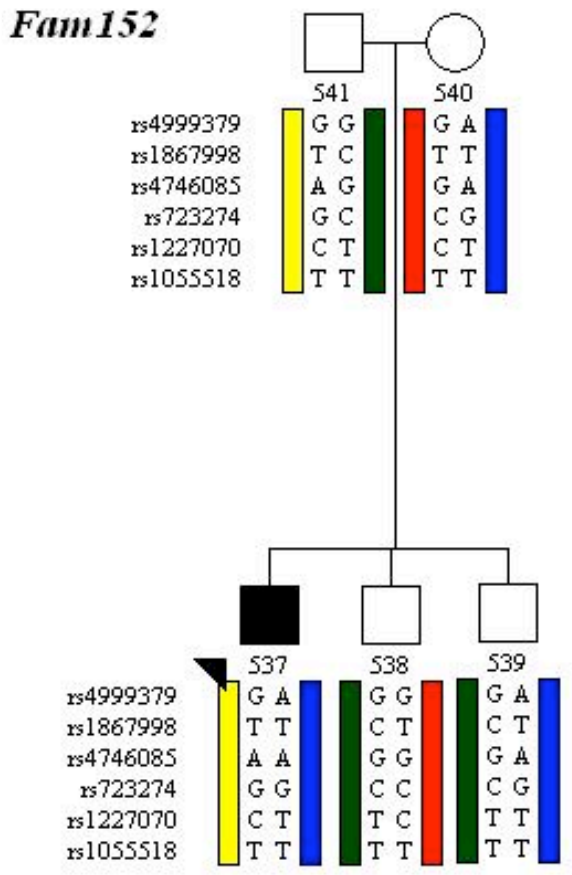

CDH23 possible

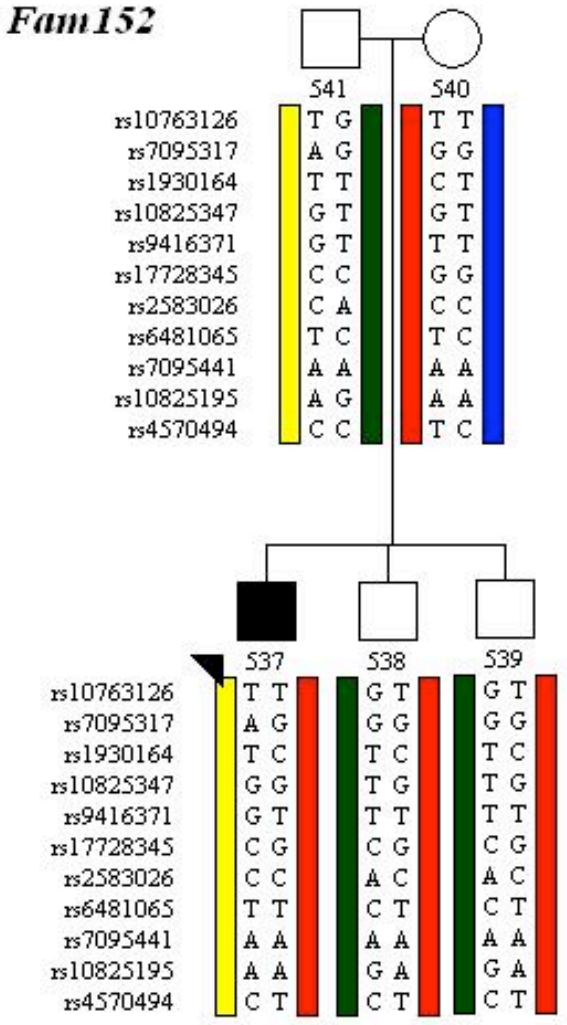

PCDH15 possible

FAMILY 152 Index case NCUS ID 537

USH2

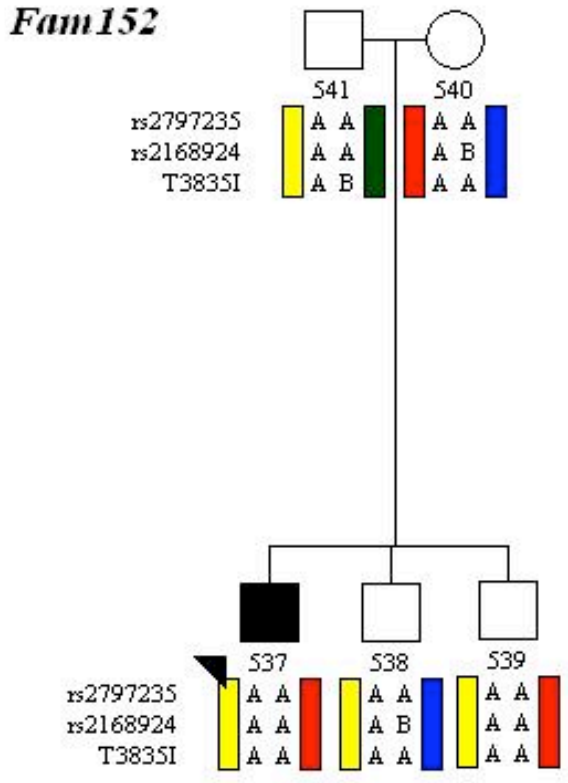

USH2A unlikely

FAMILY 152 Index case NCUS ID 537

USH2

Fam152

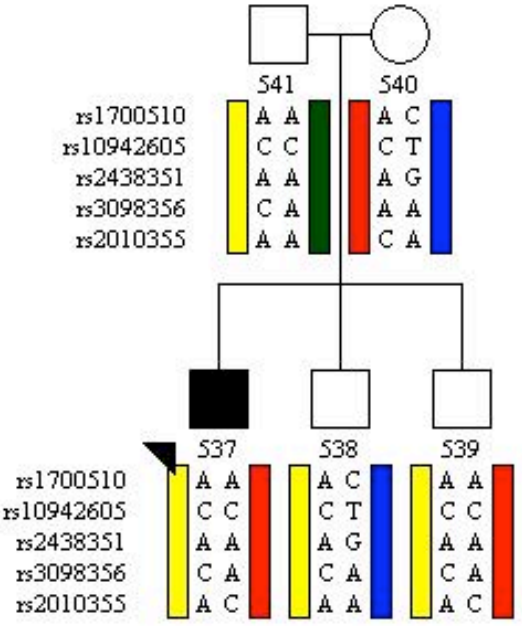

GPR98 excluded

FAMILY 152 Index case NCUS ID 537

USH2

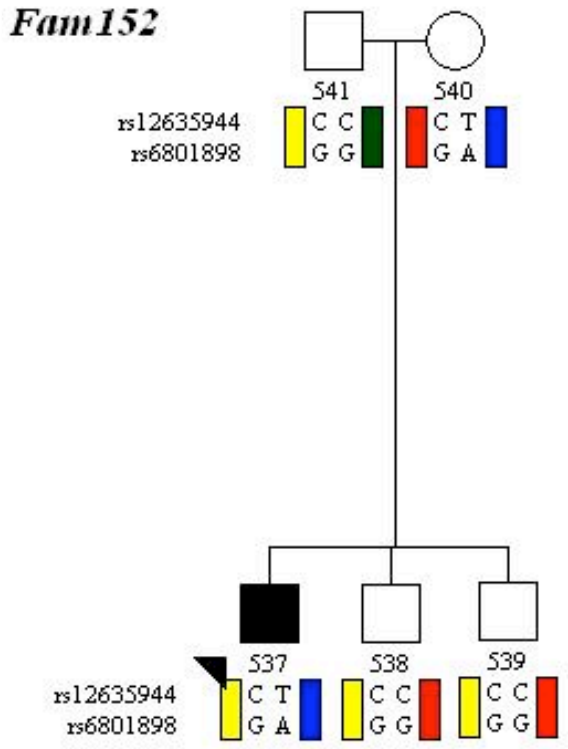

USH3A possible

FAMILY 64

[consanguineous]

USH2

Index case NCUS ID 205

FAMILY 63 Index case NCUS ID 205 [*consanguineous]*

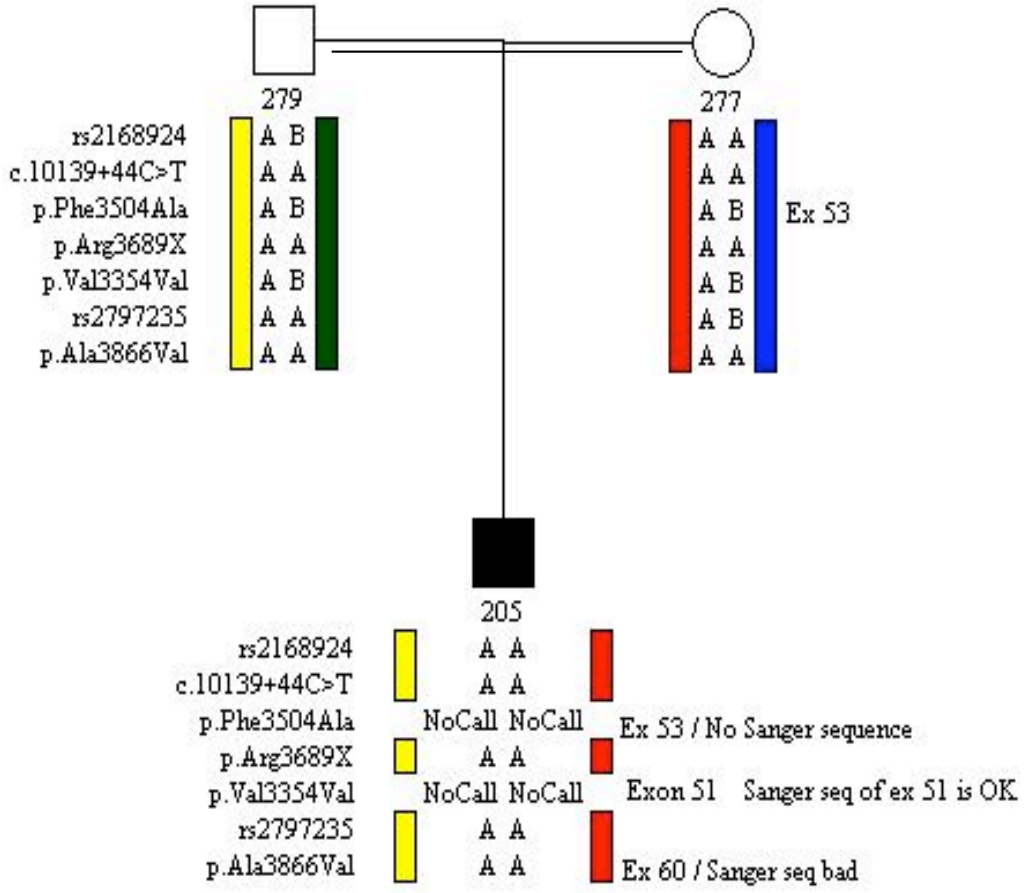

USH2A likely, as homozygous IBD with consanguineous family – but no disease causing mutations identified on DNA sequencing

FAMILY 63 Index case NCUS ID 205
[*consanguineous]*
USH2

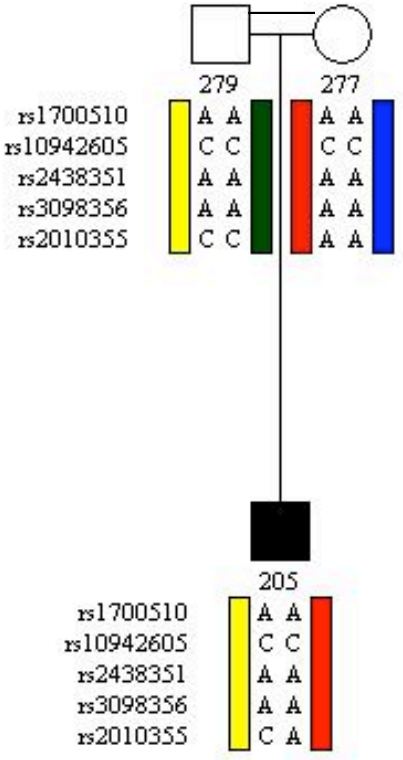

GPR98 excluded [presuming disease is due to homozygosity]

6.12 Summary of molecular data per family

This data is a summary of the molecular data as it pertains to each family recruited in to the study and **can be found on the electronic appendix attached to this thesis**. Each page represents data from one family. The top section titled **Family structure and ethnicity** lists the family number and the ethnicity of the four index case grandparents as well as if the family was consanguineous. The uppermost table lists all family members that were recruited in to the study and indicates whether a DNA sample was available for analysis.

The lower half of each page titled **Index case genotype data**, summarises the clinical diagnosis of the index case, the causative gene, the two disease causing alleles identified in the index case following the bidirectional DNA sequencing of the nine Usher genes.

In some cases, the genotypes of other family members that were determined by allele specific assays are also included.

6.13 Discussion - Genetic Epidemiology

This study represents an original contribution to the knowledge of Usher syndrome, as it is the first prospective clinical study to sequence the coding regions of each of the nine genes associated with this disorder in families with Usher syndrome regardless of clinical subtype. This comprehensive strategy of molecular analysis has afforded the unique opportunity to interrogate the possibility of digenic effects, for which no supporting evidence was found. This approach has also lead to the discovery of hypomorphic mutations in the *USH1C* gene associated with sector RP and milder hearing loss representing a novel phenotype for this gene.

USH2A was the most common molecular diagnosis of the study cohort, accounting for 76% of USH2 families and more than half of all families with Usher syndrome in this study.

Of those families with disease due to the *USH2A* gene (n=98) over half carried the common p.Glu767SerfsX21 (n=52) mutation on at least one allele. Aside from the missense change p.Cys419Phe identified in 6 families and the three sequence variants p.Asn346His, p.Trp3521Arg and p.Glu2288X each identified in four families, all other mutations in *USH2A* were private.

After *USH2A*, the *USH1C* gene was the only other gene in which a pathogenic sequence variant was common to more than three families. *USH1C* mutations have been reported in the UK [95] and from other populations [54, 94]. In this study the c.496+1G>A sequence variant *USH1C* was found in five families, four of whom were homozygous, making it the most common pathogenic sequence variant resulting in an USH1 phenotype

from our UK study. The second most prevalent change resulting in the USH1 phenotype was p.Lys1255fs in the *MYO7A* gene which was identified in three families.

Due to the nationwide recruitment for this study, it is likely to be representative of the clinical and genetic mix of Usher syndrome in the UK. Some degree of ascertainment bias against recruitment of USH1 families is possible due to the extra communication obstacles to overcome when recruiting this group due to their severe dual sensory impairment. In this study USH1 represented around a third of all cases of Usher syndrome which is comparable to previous reports of the relative prevalence of this clinical subtype as a proportion of all Usher syndrome [7, 24, 176].

Ascertainment bias in this study was evident and resulted in the recruitment of a significantly younger aged cohort of USH1 index cases, the reasons for this were unclear.

No putative pathogenic changes were identified in the *USH1G* or *WHRN* gene and only two families with mutations in *USH3A* were identified suggesting these are rare in the UK population.

The relatively high proportion of single alleles identified in families with disease due to the most prevalent genes *USH2A* and *MYO7A*, suggest that sequencing methods alone failed to identify the second allele. The reasons for this are unclear but might be due to factors such as unidentified or missed heterozygous deletions, non-coding variants or other potentially digenic effects with as yet unknown genes. The large number of families with no molecular diagnosis (n=30) despite this comprehensive molecular analysis strategy, suggest that more disease-causing genes are yet to be identified for this disorder.

The challenges of determining the pathogenicity of the large number of rare DNA sequence variants assayed in a control population were illustrated. Many of these sequence variants were missense changes that remain of uncertain pathogenicity and will be subject to further analysis. The in silico analysis of missense changes showed that most variants classified as UV4 were highly conserved at their amino acid position and many were also predicted to effect secondary and tertiary structure. Conversely the UV2 variants were less well conserved and were generally not predicted to effect secondary or tertiary structure. These findings highlight the utility of in silico analysis as another method of gathering evidence to support hypothesis regarding the pathogenicity of alleles, but their robustness is not as yet sufficient to be confidently integrated in to an algorithm to assess the pathogenicity of alleles. This also highlights the fact that simple tests to measure allele frequency in a population are still important when deciding whether a DNA sequence change is pathogenic or not.

A molecular algorithmic system was devised and implemented to help the grading of putative pathogenic alleles for this study. This system is transferable to other genetic studies of autosomal recessive disease.

Chapter 7

Results - Onset of retinal disease

This chapter presents an overview of the subjective responses given by affected individuals regarding their initial visual symptoms. The results are presented when dividing the NCUS cohort of the basis of clinical subtype for 57 individuals from 45 USH1 families, 163 individuals from 129 USH2 families and three individuals from two USH3 families. Results are also presented for the subsets of individuals with a confirmed molecular diagnosis, which was taken as at least one putative pathogenic allele (pathogenicity score 3 or 4) identified in one of the Usher genes.

7.1 Age of reported first visual symptom

When an individual with hearing loss notices visual problems this may prompt an ophthalmic referral and examination. If their visual symptoms are due to previously undiagnosed retinitis pigmentosa their diagnosis will change from simply 'hearing loss' to 'Usher syndrome'.

The age at which individuals with Usher syndrome report their visual symptoms is thus relevant to clinicians and families with deaf children.

The results will be presented by analysing the different subsets of the study cohort, both clinical and molecular.

7.1.1 Clinical subtypes of Usher syndrome

The reported age of onset of the first visual symptom was significantly different between the three clinical subtypes USH1, USH2 and USH3 (Kruskal-Wallis test, $P<0.0001$)

Individuals with a clinical diagnosis of USH1 experienced onset of their first visual symptom at a younger age than those with USH2 (Mann Whitney test, $P<0.0001$)

By 14 years of age, ***all*** USH1 individuals in this study had experienced visual symptoms suggestive of RP. By the same age, less than half of the USH2 individuals had experienced any visual symptoms.

The median age of reported first visual symptom was 9yrs for the USH1 cohort, and 17yrs for USH2 cohort .

Due to the small number of individuals with USH3 in the UK, achieving statistically significant conclusions was not possible.

37% (n=63/170) of individuals with all subtypes of Usher syndrome and half of all USH2 (n=61/123) reported adult onset (aged 18 years of age or older), of their retinal symptoms.

The range of reported age of onset of visual symptoms was much narrower for the USH1 cohort compared to the USH2 cohort.

TABLE 7.1: Table showing median and mean age of onset of visual symptoms across the clinical subtypes of Usher syndrome

	USH1	**USH2**	**USH3**
Number of values	41	124	3
Minimum	3	2	10
25% Percentile	6	13	
Median	**9**	**17**	**11**
75% Percentile	11	22	
Maximum	14	45	12

7.1.2 Age of first visual symptom vs. molecular subtype (Figure 7.2)

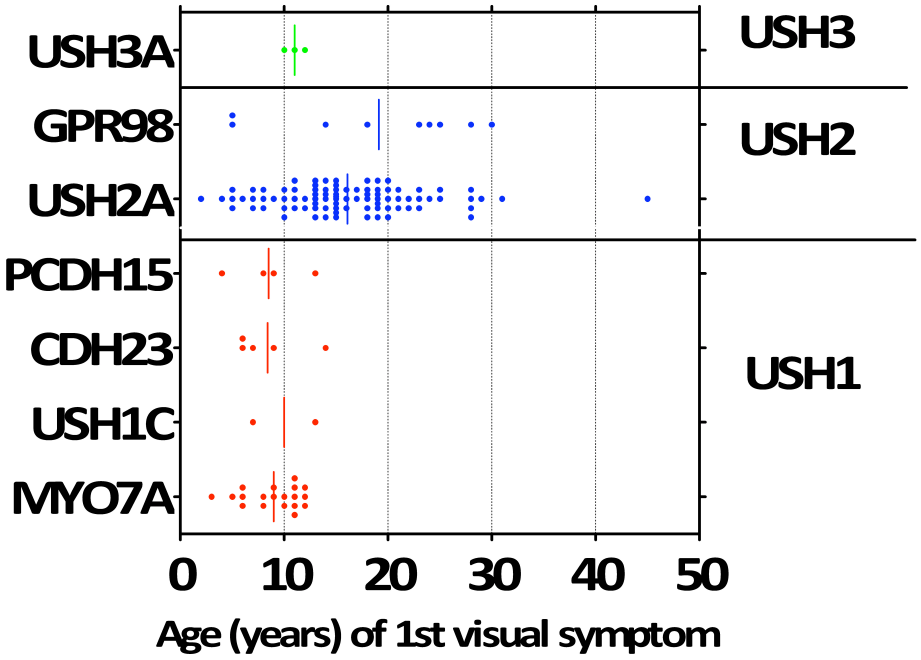

FIGURE 7.2: Scatter graph showing the age of the 1st visual symptom of individuals with Usher syndrome grouped by molecular diagnosis
The clinical subtype pertaining to each gene is shown on the right

USH1 genes - *MYO7A*, *USH1C*, *CDH23* and *PCDH15*

The median age of the first reported visual symptom did not differ significantly between individuals with a molecular diagnosis of *MYO7A*, *USH1C*, *CDH23* or *PCDH15* (Kruskal-Wallis test, $P<0.05$).

USH2 genes - *USH2A* and *GPR98*

The median age of first reported visual symptom did not differ significantly between individuals with a molecular diagnosis of *USH2A* and *GPR98* (Mann Whitney test, $P<0.05$)

USH1 genes vs. USH2 genes

There was however a highly significant difference between those with a moleulcar diagnosis in the USH1 genes (*MYO7A*, *USH1C*, *CDH23* and *PCDH15*) and the two USH2 genes *USH2A* and *GPR98* (Mann Whitney test, $P<0.0001$).

Does the pathogenicity grade of mutations in the USH1 genes influence age of onset of visual symptoms?

There was no difference between the median age of reported first visual symptom for those with two identified "severe" alleles (pathogenicity score=4) compared to the those with one or less severe alleles (Mann Whitney test, $P<0.05$).

Does the pathogenicity grade of mutations in the USH2 genes influence age of onset of visual symptoms?

When subdividing all individuals with a molecular diagnosis associated with an USH2 phenotype,individuals with two "null" alleles (where the pathogenicity score for both alleles was 4) reported their first visual symptom at a younger age when compared to others with one or less null alleles (Mann Whitney test, $P=0.0345$).

USH2A subgroup analysis: p.Glu767SerfsX21 vs. all other USH2A alleles

Amongst the USH2A molecular group, there was a highly significant difference between reported median age of onset of visual symptoms, which were reported earlier in those that carried the common allele p.Glu767SerfsX21 compared to those who did not.

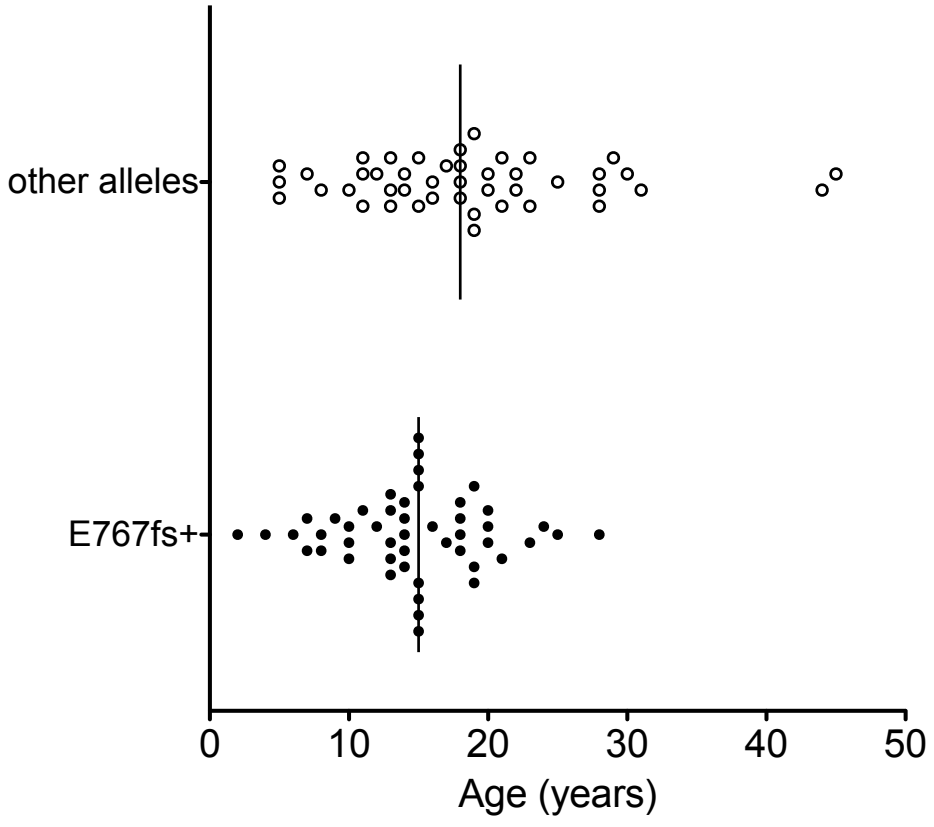

FIGURE 7.3: Scattergraph and median (vertical line) of age of first reported visual symptom comparing individuals with the common p.Glu767SerfsX21 allele (E767fs+) in *USH2A* vs. all other *USH2A* alleles

7.2 Nature of first visual symptom

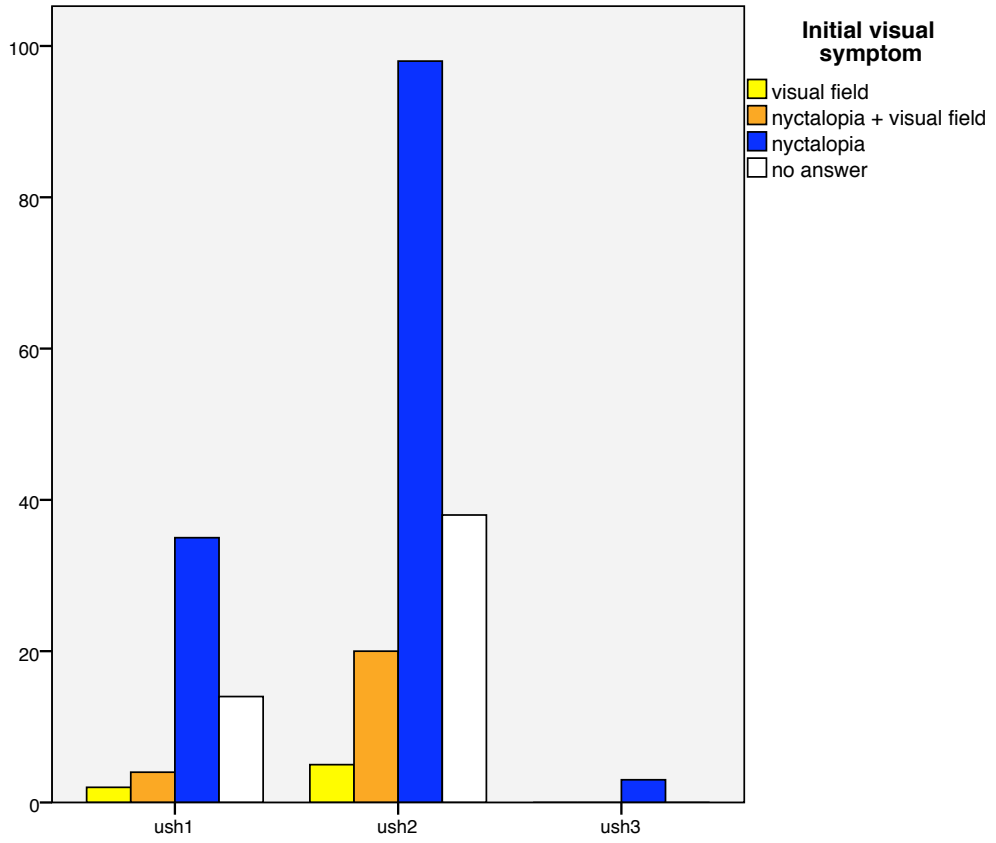

FIGURE 7.5: Cluster barchart showing the nature of the first reported visual symptom in each clinical subtype

Nyctalopia was the most common initial visual symptom reported by the whole cohort across all clinical subtypes of USH (Figure 7.5) and when dividing affected individuals in to molecularly diagnosed cohorts (Figure 7.6).

The second most frequent response recorded across all groups was that no clear visual symptom was recalled or recorded. These "no answer" responses consisted of some missing data sets (the question was not asked/the answer not recorded) in addition to cases where affected individuals were unable to provide an answer due to inability to recall a specific initial visual symptom.

There was no statistically significant difference in the relative proportions of the four responses (nyctalopia, no answer, nyctalopia and visual field loss and visual field loss

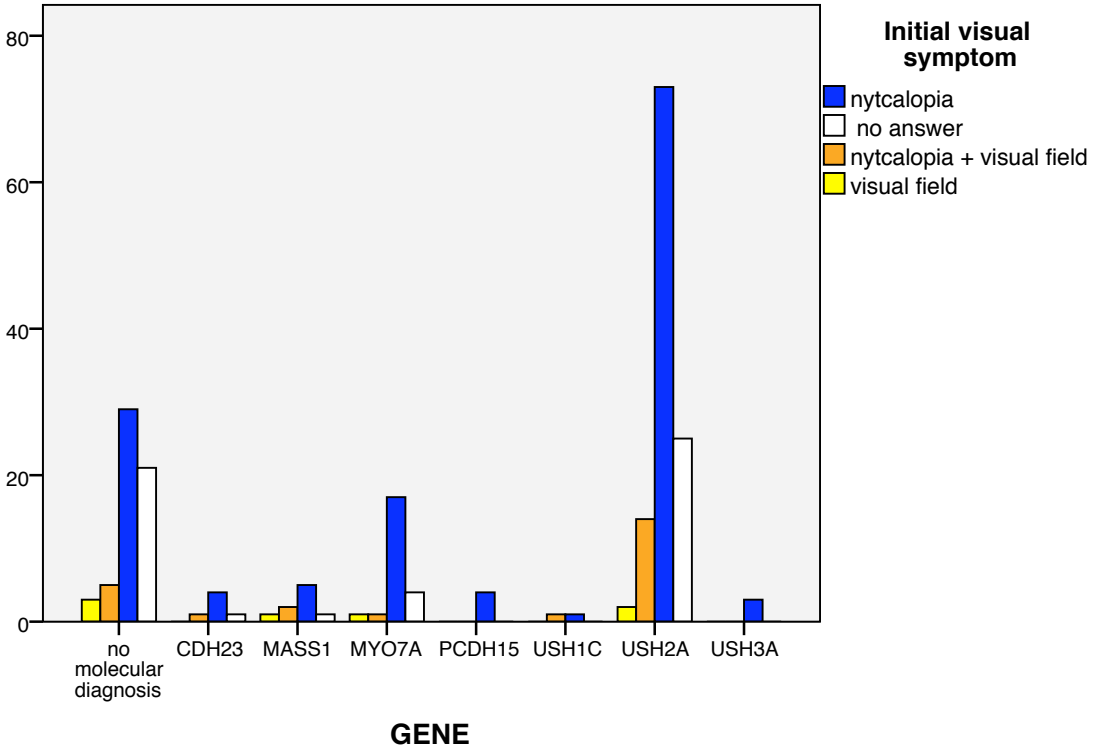

FIGURE 7.6: Cluster barchart showing the nature of the first reported visual symptom per molecular diagnosis

alone) between the clinical subtypes of USH or the different molecular cohorts (chi-squared test, alpha <0.05)

7.3 Summary - Onset of retinal disease

The prospective data collected in this study shows that the subjective report of onset of visual symptoms occurs at a significantly younger age amongst the USH1 group compared to USH2.

A more interesting finding is that when dividing the cohort in to molecular groups, the reported age of initial visual symptom is statistically similar amongst the four USH1 genes and amongst the two USH2 genes, but quite different between these two groups.

This suggests that there is some phenotypic similarity amongst the USH1 genes and the USH2 genes respectively with regard to the subjective onset of visual symptoms.

It is interesting to note that despite the statistically significant earlier age of onset of USH1 individuals, there was some overlap between the USH1 and USH2 groups with both groups containing individuals with childhood onset of visual symptoms. All USH1 individuals reported onset of their first visual symptom by the age of 14 years, along with approximately 40 % of USH2 individuals.

As none of the USH1 individuals reported age of onset of first visual symptom later than 14 years of age, from these data, it seems unlikely that if a child with profound hearing loss does not develop any visual symptoms by their mid-teens they would be unlikely to go on to develop RP (i.e have USH1). This represents an important finding for clinicians.

Conversely, half of all USH2 individuals did not report visual symptoms until the age of 18 or older with many reporting onset of their visual symptoms in to their thirties or even forties. This is a significant and unexpected finding which ophthalmic clinicians might consider when assessing adults with moderate hearing loss.

Unlike USH1, adults with USH2 are able to communicate with spoken language and with the use of hearing aids their significant hearing impairment may not be obvious to others. This flags the importance of specific enquiry with regard to the presence of hearing impairment in adults who present with symptoms or signs suggestive of RP.

Confounding factors in reporting onset of disease

An important consideration for any scientific methodology is to attempt to reduce bias and confounding factors as much as possible. In clinical medicine one way of reducing bias is to use objective rather than subjective measures wherever possible. Determining the age of onset of retinal symptoms in a cohort study such as this, requires the use of

such subjective data, as many study participants' visual dysfunction actually precipitated their diagnosis of Usher syndrome. Steps were taken to reduce the response bias such as prospectively asking the same questions to all individuals and questions were kept clear, precise and short which would be subject to less bias than a retrospective review of medical case notes as has been the source of previous studies regarding the onset of visual symptoms in this disorder.

Despite these steps, the main limitation to the data presented in this chapter is that it is derived from the subjective responses given by affected individuals, in some cases with help from their parents, regarding the onset of visual symptoms.

Considerations in difference in symptom reporting of USH1 and USH2

Due to the profound hearing loss in USH1 affected individuals rely heavily on their vision for communication, navigation and social interaction more than USH2 individuals who use their residual hearing for these tasks. This heavy reliance on visual function in the profoundly hearing impaired might prompt an earlier recognition of visual pathology than in the hearing USH2 group. The increased contact with healthcare professionals that USH1 individuals encounter due to their severe audiological dysfunction may also prompt an earlier discovery of visual symptoms by others.

Chapter 8

Results - Central retinal function

8.1 Visual Acuity (VA)

For the purposes of clarity, the term NCUS cohort refers to the affected individuals (n=224) from the 178 families with Usher syndrome. The clinical subtypes are USH1, USH2, USH3 and one case of ARRP who is the sister of an index case with USH2 (Family 141). The results for this section are presented in three subsections. Firstly the whole NCUS cohort of affected individuals with Usher syndrome, secondly the cohort after subdivision in to clinical subtypes and finally after subdivision in to molecular subtypes.

8.1.1 VA - Entire NCUS cohort

8.1.1.1 VA between left and right eyes

There was a high degree of correlation between the logMAR visual acuity between the right and left eyes per individual (Spearman's rank coefficient 0.799, P <0.01) across the whole study population as illustrated in Figure 8.1. The outliers on the plot were all individuals with advanced disease associated with either small islands of remaining central retina or an atrophic macular appearance.

The remainder of this section on VA results will present data relating to the logMAR VA in the *better seeing* eye per individual.

8.1.1.2 VA correlations with age and disease duration

When analysing all affected individuals from families with Usher syndrome, there was a statistically significant correlation between visual acuity in the better seeing eye and **age**

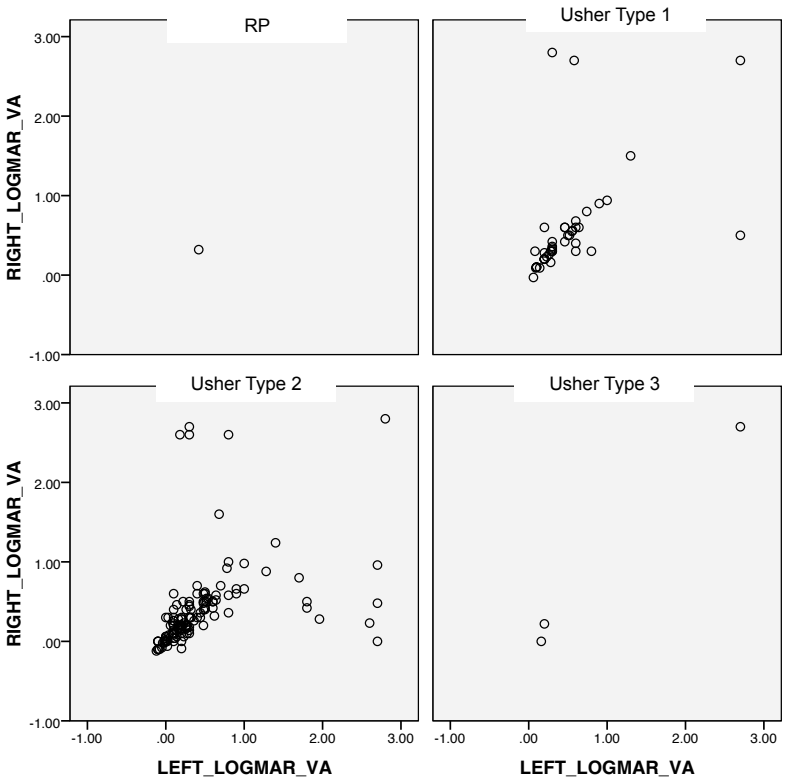

FIGURE 8.1: Scatterplot of visual acuity in left right eyes of all NCUS affecteds

TABLE 8.1: Correlation matrix for visual acuity across all NCUS affecteds. The highly significant correlations between age and disease duration are highlighted in red text

Correlations					
NCUS affected individuals			AgeAtExam	disease_duration	GENE
Spearman's rho	LogMAR VA in better eye	Correlation Coefficient	.400**	.485**	-.122
		Sig. (2-tailed)	.000	.000	.087
		N	197	168	197
**. Correlation is significant at the 0.01 level (2-tailed).					

(Spearman's rank coefficient 0.400, P <0.001) as well as **disease duration** (Spearman's rank coefficient 0.485, P <0.001).

The *degree* of correlation between VA and either age or disease duration was not significantly different (Z-test value=0.81).

8.1.1.3 VA regression analysis with age and disease duration

Age vs. VA regression analysis

A Linear regression model for age vs. VA for all NCUS affected individuals was highly significant in predicting VA as a function of age . The regression model was y=0.01x

+c (r2=0.117, 195 d.f., P <0.001). Age as a variable accounted for 12% (r2=0.117) of the decline in VA. The rate of decline in VA was 0.01 logMAR units per year of age (P <0.001). The regression calculation was unable to predict the baseline logMAR VA when age=0 (P=0.565).

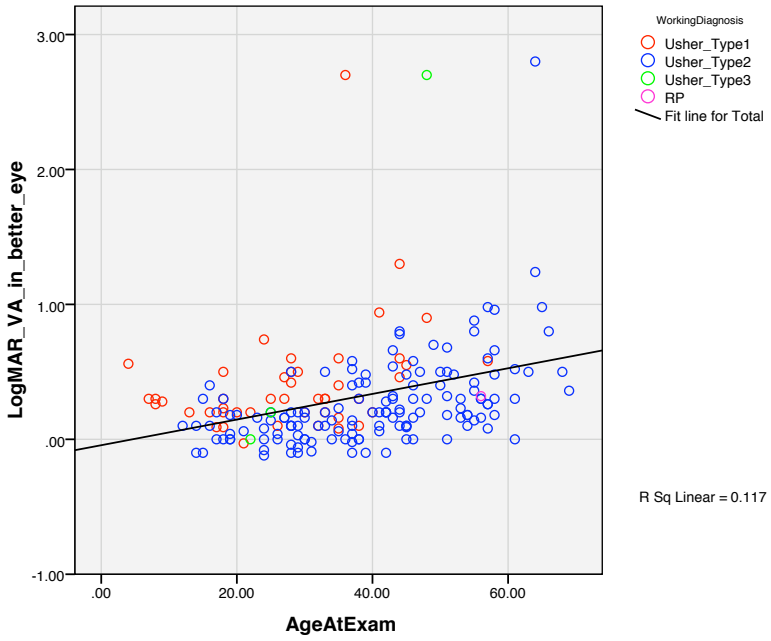

FIGURE 8.2: Scattergraph and linear regression line showing the relationship between age and visual acuity for the entire cohort of NCUS affected individuals. For comparison with the cohort, the different clinical subtypes are highlighted on the scattergraph to demonstrate their relationship to the overall regression line

Disease duration vs. VA regression analysis

A Linear regression model for disease duration vs. VA for all NCUS affected individuals was highly significant in predicting VA as a function of disease duration . The regression model was y=0.013x +c (r2=0.177, 166 d.f., P <0.001). Disease duration could explain 18% (r2=0.177) of the decline in VA. The decline in VA per year of disease duration was 0.013 logMAR units per year. The regression calculation was unable to predict the baseline logMAR VA with significance (P =0.623) when disease duration=0.

Although the degree of correlation was greater and the linear regression model a better fit for disease duration compared to age, the difference between these two variables as a predictor of VA was not statistically significant (P <0.05).

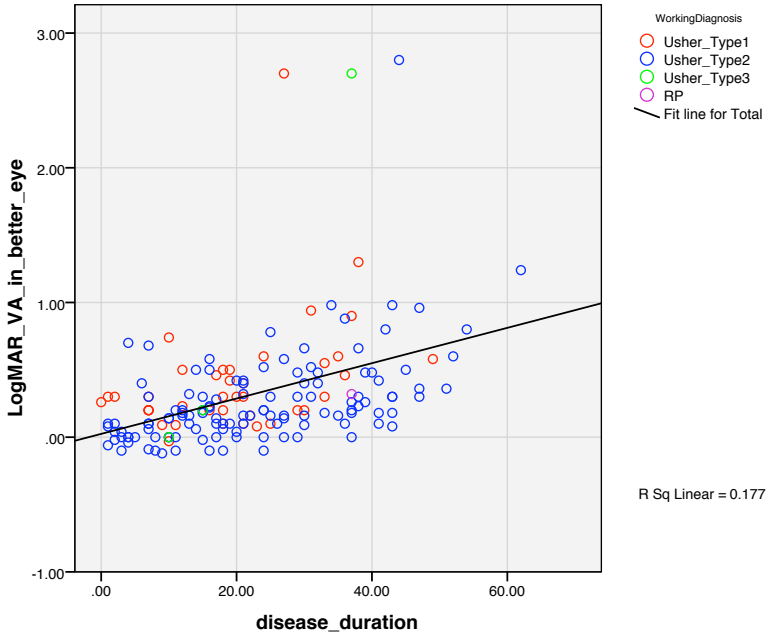

FIGURE 8.3: Scattergraph and linear regression line showing the relationship between disease duration and visual acuity for the entire cohort of NCUS affected individuals. For comparison with the cohort, the different clinical subtypes are highlighted on the scattergraph to demonstrate their relationship to the overall regression line

8.1.2 VA - Clinical subtypes

8.1.2.1 Ranges of VA seen per clinical subtype

There was a statistically significant difference between the median visual acuity in the better seeing eye between the three clinical subtypes USH1, USH2 and USH3 (Kruskal-Wallis test, P <0.05).

There was a highly significant difference between USH1 and USH2, with the USH2 group having the better median visual acuity of 0.18 logMAR whilst the USH1 group median was 0.3 logMAR (Mann Whitney test, P <0.001).

The spread of VA for all NCUS affecteds is shown in Figure 8.4. It is important to appreciate that this figure does not take age into consideration. This highlights that despite the USH1 group having a significantly *younger* age than the USH2 group (see Figure 6.1.4), they still had *worse* visual acuity. The effect of age as a predictor of visual acuity is considered later with regression analysis.

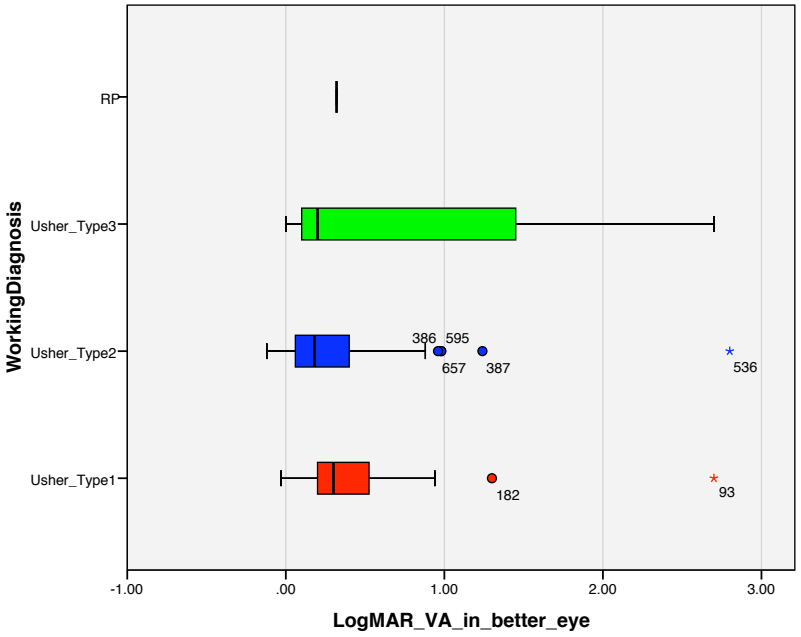

FIGURE 8.4: Boxplot (median and interquartile range) and whisker (data range) figure demonstrating the distribution of visual acuity in the better eye for all NCUS affecteds. The results are shown per clinical subtype. Outliers are annotated with their NCUS ID number

8.1.2.2 Survival curves for USH1 vs USH2

Survival plots (Figure 8.5) were generated to determine the percentage of each clinical group who retained 'driving vision' as per DVLA standards, taken to approximate to

6/10 Snellen or better (equivalent to logMAR $\leqslant$ 0.22).

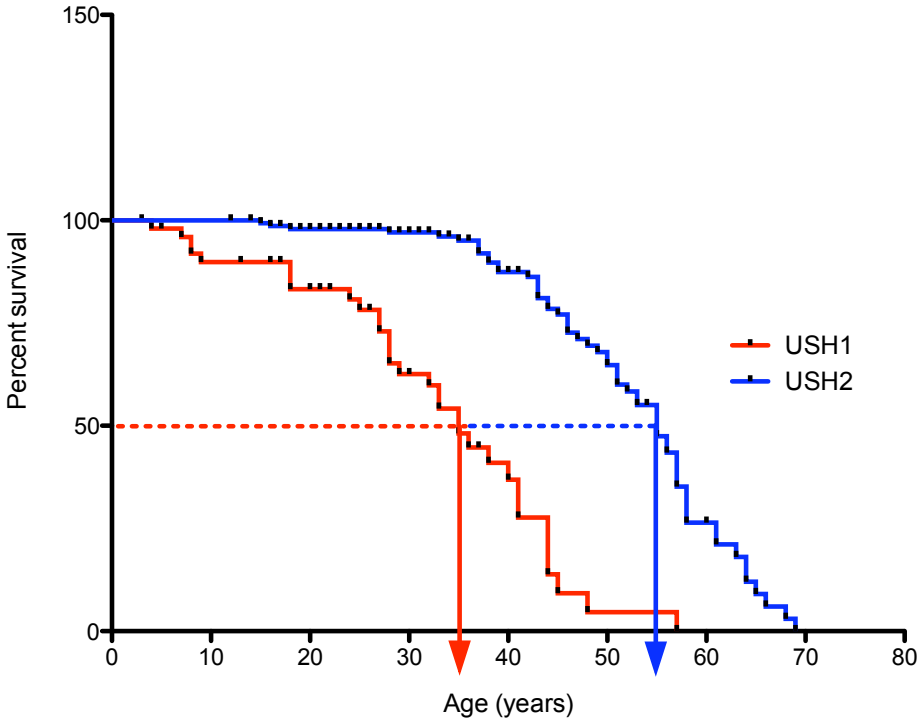

FIGURE 8.5: Survival curve for visual acuity USH1 and USH2 clinical groups. The end point for this was taken as a VA not compatible with driving standards (logMAR VA of 0.22<)

The difference between the two curves was highly significant (Mantel-Cox Test P <0.0001) with half of USH1 individuals maintaining driving vision' until the age of 35 years and half of USH2 maintaining a similar level of visual acuity until the much later age of 55 years.

8.1.2.3 VA relationships with age and disease duration per clinical subtype

When splitting the affected individuals of the entire NCUS cohort in to subgroups based on clinical subtype, similar levels of correlation were identified between age and disease duration. Correlation coefficients for VA and age and disease duration were not statistically different between the USH1 and USH2 groups, suggesting the relationship between VA and these two variables is similar. The RP and USH3 groups were too small in size to permit useful conclusions to be drawn.

8.1.2.4 VA regression analysis with age and disease duration

Age vs. VA regression analysis

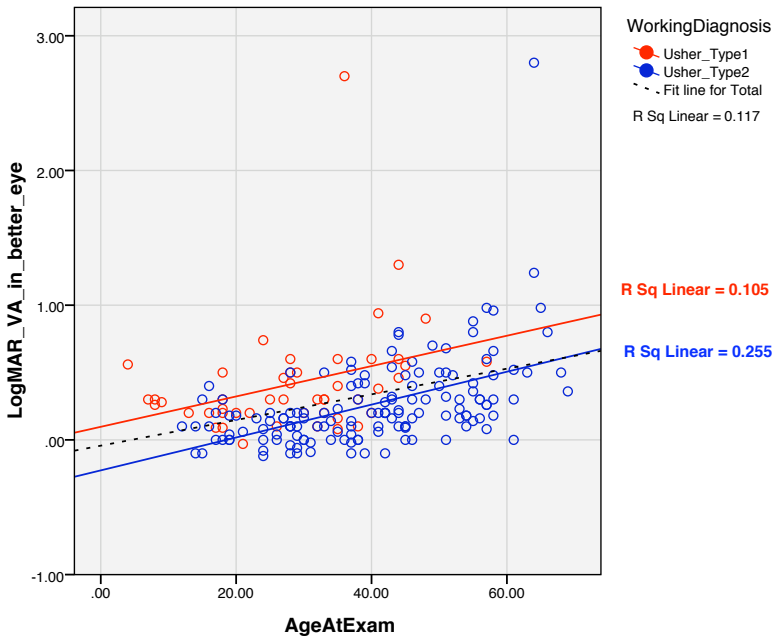

FIGURE 8.6: Scattergraph and regression lines for age vs. VA for USH1 and USH2. The regression line (dotted) for the entire NCUS cohort is also shown for comparison

After splitting the NCUS affecteds cohort in to groups based on clinical subtype, regression analyses was repeated.

When analysing age as a predictor of VA, age was able to account for 11% (r2=0.105) of the decline in VA observed in USH1, which was comparable to the regression model for the entire NCUS cohort. For USH2, age was able to account for 26% (r2=0.255) of the decline in VA observed, however the difference between these figures for r2 ('goodness of fit') for USH1 and USH2 groups were not significantly different.

Linear regression analysis for age vs. VA for USH1, USH2 and USH3 groups all yielded statistically significant models using age as a predictor for VA. Regression analysis yielded significant results for the USH3 group, despite the extremely small sample size (n=3) however these data are not discussed further due to the limited conclusions that can be drawn from this small sample size.

The USH2 model was able to confidently predict baseline logMAR VA of -0.226 (95% confidence intervals -0.372 to -0.081), P =0.03) when age=0, but a similar statistically significant prediction was not possible in the USH1 group.

The regression models for age vs VA were:
USH1: y=0.011x + c (r2=0.011, 46 d.f., P <0.03)
USH2: y=0.012x - 0.226 (r2=0.012, 143 d.f., P <0.01)

The **slope** of the regression lines **was not** significantly different between the USH1 and USH2. The **elevations** of USH1 and USH2 regression lines ***were*** significantly different from each other (P <0.01) This suggests that the overall elevations were identical, there is a less than 0.01% chance of randomly choosing data points with elevations as different as those observed.

Both models predicted a decline of 0.01 logMAR units per year of age (P <0.05). The significance of this is discussed at the end of this section.

Disease duration vs. VA regression analysis

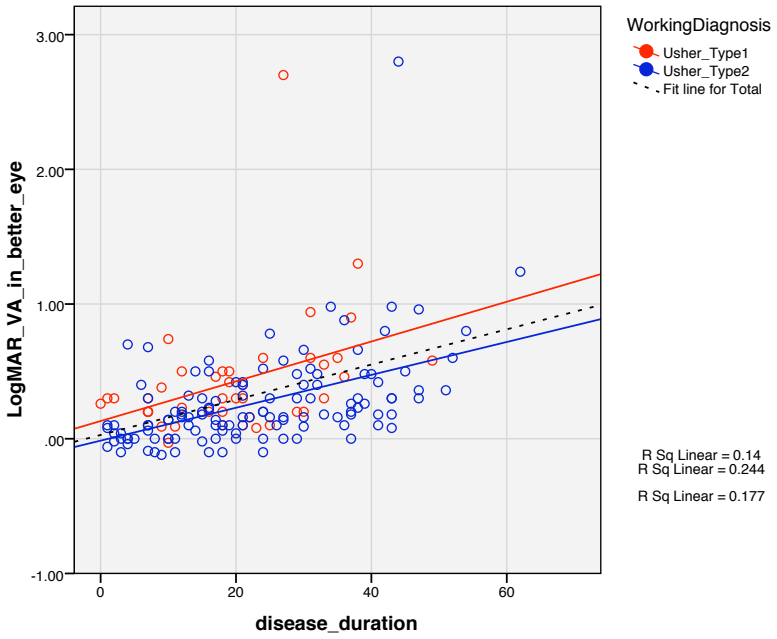

FIGURE 8.7: Scattergraph and regression lines for disease duration vs. VA for USH1 and USH2 groups. The regression line (dotted) for the entire NCUS cohort is also shown for comparison

After splitting the NCUS affecteds cohort in to groups based on clinical subtype, regression analyses was repeated for disease duration vs. VA.

The regression models were:
USH1: y=0.015x + c (r2=0.140, 40 d.f., P=0.014)
USH2: y=0.012x - 0.014 (r2=0.244, 120 d.f., P <0.0001)

The linear regression models for disease duration for USH1 and USH2 groups both provided a statistically significant predictors of VA. The **slope** of the regression lines **was not** significantly different between USH1 and USH2 (P=0.62).

The elevations of USH1 and USH2 regression lines **were** significantly different from each other (P <0.0014). This suggests that if the elevations were identical for the two lines, there is a less than 0.001% chance of randomly choosing data points with elevations this different.

When analysing disease duration as a predictor of VA, disease duration (years) was able to account for 14% (r2=0.140) of the decline in VA for USH1 which was comparable to the linear regression model for the entire cohort. For USH2, age was able to account for 24% (r2=0.244) of the decline in VA in this group, however the difference between

these figures for r2 ('goodness of fit') for USH1 and USH2 groups were not significantly different. The model coefficients predicted a decline in VA of 0.015 logMAR in USH1 and 0.012 logMAR per year of disease.

The USH2 model was able to confidently predict a logMAR VA of -0.014 (95% confidence interval -0.119 to +0.091) when disease duration=0 in the USH2 group, but a similar statistically significant prediction was not possible in the USH1 group.

8.1.3 VA - Molecular subtypes

8.1.3.1 Ranges of VA seen per molecular subtype

The ranges of VA per molecular group are shown in figure 8.8. There was a statistically significant difference between the four USH1 genes and the two USH2 genes (Mann Whitney test, P<0.001), however as there was also a significantly significant difference between the median ages (Mann Whitney test, P<0.0001) this demonstrates that these two subgroups were drawn from different age ranges.

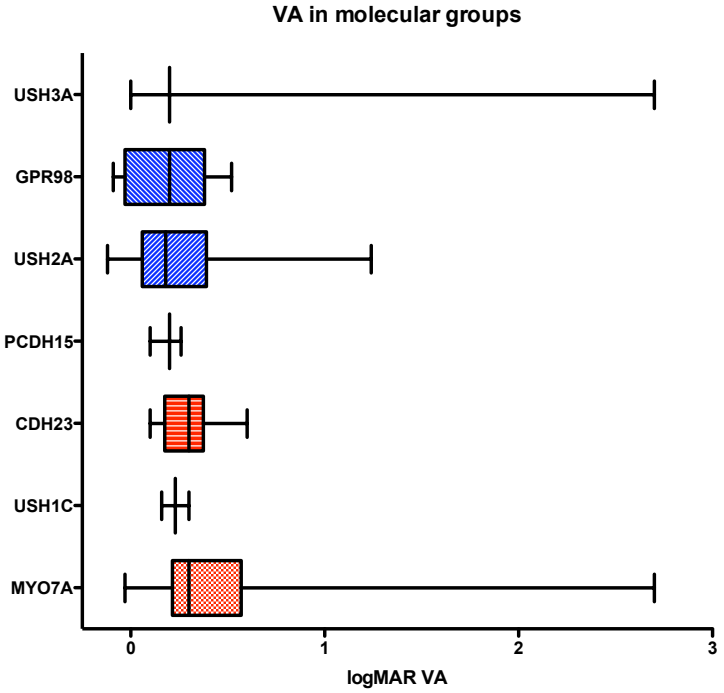

FIGURE 8.8: Boxplot and whisker showing the median, interquartile range and data range for VA amongst all molecular groups identified

The USH1 genes - *MYO7A, USH1C, CDH23* and *PCDH15*

There was no significant difference between the ages of individuals with a molecular diagnosis of each of four USH1 genes (Kruskal-Wallis test, P=0.52).

There was no significant difference between the visual acuity in the better seeing eye amongst the four USH1 genes (Kruskal-Wallis test, P<0.05).

The USH2 genes - *USH2A* and *GPR98*

There was no significant difference between the ages of individuals with a molecular diagnosis of each of the two USH2 genes (Mann Whitney test, P=0.51).

There was no significant difference between the visual acuity in the better seeing eye between the two USH2 genes (Mann Whitney test, P<0.05).

The USH3 gene *USH3A* Only three individuals with USH3 were identified in the study. A sibling pair in their twenties had good central visual acuity and one 48 year old individual who had hand movements vision in both eyes.

8.1.3.2 Survival curves for *MYO7A* vs *USH2A*

Survival plots were generated to determine the percentage of each of the two largest molecular groups *MYO7A* vs *USH2A* who retained 'driving vision' as per DVLA standards, taken to approximate to 6/10 or better Snellen (equivalent to logMAR $\leqslant$ 0.22).

The difference between the two curves was highly significant (Mantel-Cox Test P <0.0001) with half of the *MYO7A* individuals maintaining driving vision' until the age of 36 years and half of *USH2A* group maintaining a similar level of visual acuity until the much later age of 55 years.

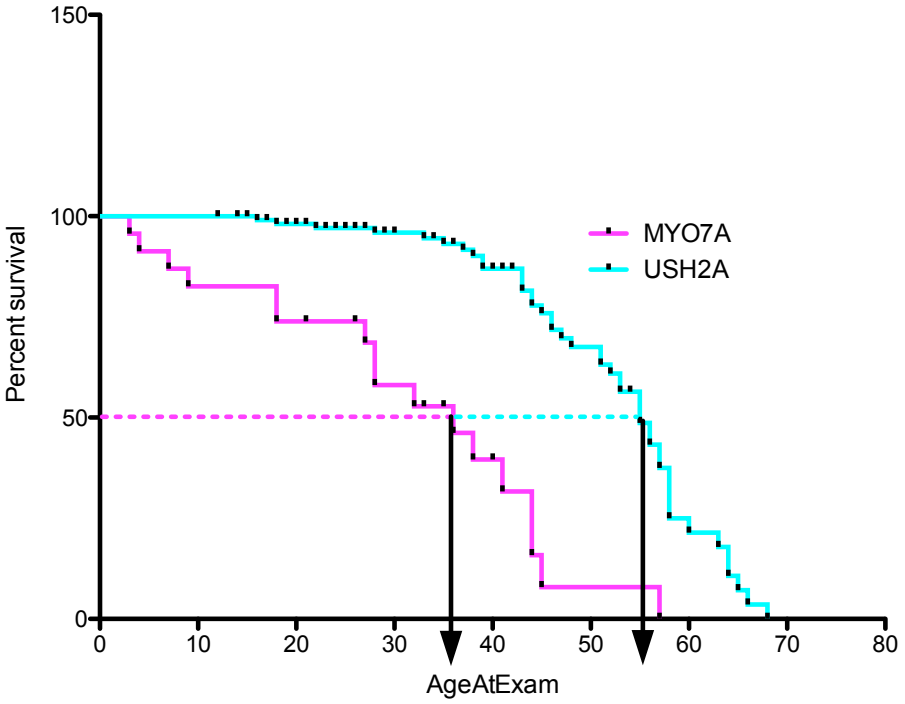

FIGURE 8.9: Survival curve for visual acuity in *MYO7A* vs *USH2A* molecular groups. The end point for this was taken as a VA incompatible with driving standards (logMAR VA of 0.22<)

8.1.3.3 VA regression analysis with age and disease duration

Age vs VA regression analysis

After splitting the NCUS affecteds cohort in to groups based on molecular diagnosis, regression analyses was repeated. The raw data is presented in Figure 8.10. Individuals from the NCUS cohort who did not have a confirmed molecular diagnosis were placed in a category and included with the analysis.

Linear regression models only provided a significant result for two molecular groups, USH2A and USH3A. Due to the small sample size of the USH3A group these data are not discussed further due to the limited conclusions that can be drawn from this small sample size (n=3).

For the USH2A molecular group, age was able to account for 30% (r2=0.297) of the decline in of the decline in VA observed in this group. The USH2A model was able to confidently predict baseline logMAR VA of -0.273 (95% confidence intervals -0.446 to -0.1), P =0.02) when age=0.

The regression model for age vs VA was:
USH2A: y=0.012x - 0273 (r2=0.297, 106 d.f., P <0.001)

Comparing the linear regression models for USH2A and the entire NCUS cohort, the slope and elevation of the regression lines are not significantly different.

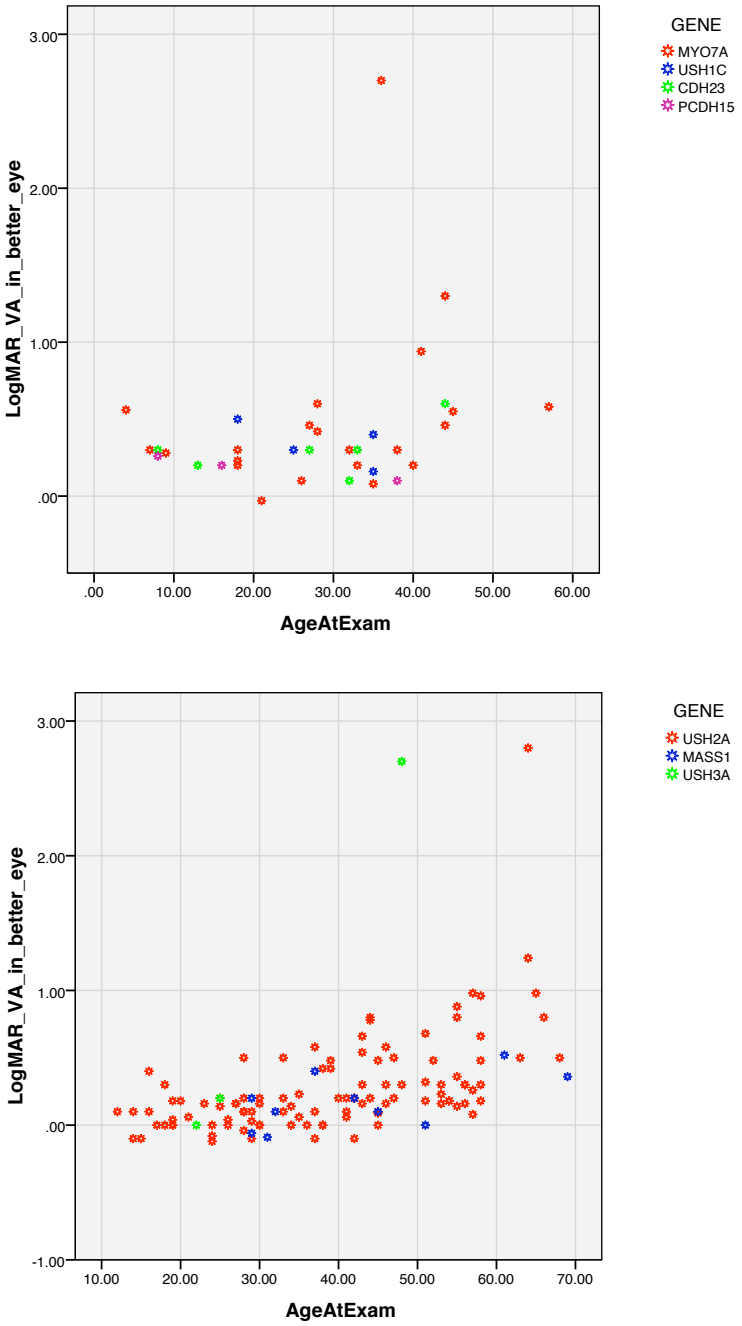

FIGURE 8.10: Scattergraph of age vs. VA in the USH1 genes (above) and the USH2 and USH3 genes (below). Linear regression models to fit this data were only significant for the *USH2A* molecular group (*USH2A* regression line not shown)

Disease duration vs. age regression analysis

After splitting the NCUS cohort in to groups based on molecular diagnosis, regression analyses was repeated. Individuals from the NCUS cohort who did not have a confirmed molecular diagnosis were placed in a category and included with the analysis.

Linear regression models only provided a significant result for the USH2A molecular group.

For the *USH2A* molecular group, disease duration was able to account for 26% (r2=0.264) of the decline in of the decline in VA observed in this group. The USH2A model was not able to confidently predict baseline logMAR VA when age=0 (P=0.567).

The regression model for age vs VA was:
USH2A: y=0.014x + c (r2=0.26, 90 d.f., P <0.001)

Comparing the linear regression models for *USH2A* and the entire NCUS cohort, the slope and elevation of the regression lines are not significantly different.

8.1.4 USH2A subgroup analysis: p.Glu767SerfsX21 vs. all other *USH2A* alleles

Due to the large numbers in the USH2A group and the significant proportion who carried the common allele p.Glu767SerfsX21, subgroup analysis was performed after dividing up all individuals with a diagnosis of *USH2A* in to two groups; the p.Glu767SerfsX21 group (who carried the change heterozygously or homozygously) and those that did not. There was no significant difference between the regression models for both groups when models were constructed for age vs. VA (shown in Figure 8.11) and disease duration vs. VA.

The regression model for the p.Glu767SerfsX21 sub-group was slightly (but not significantly) a better fit for the data for age (r2=0.33, 53 d.f., P <0.0001) compared to the non-p.Glu767SerfsX21 group (r2=0.30, 51 d.f., P <0.0001).

Similarly, the regression model for the p.Glu767SerfsX21 sub-group was slightly (but not significantly) a better fit for the data for disease duration (r2=0.32, 45 d.f., P <0.0001) compared to the non-p.Glu767SerfsX21 group (r2=0.29, 42 d.f., P <0.0001).

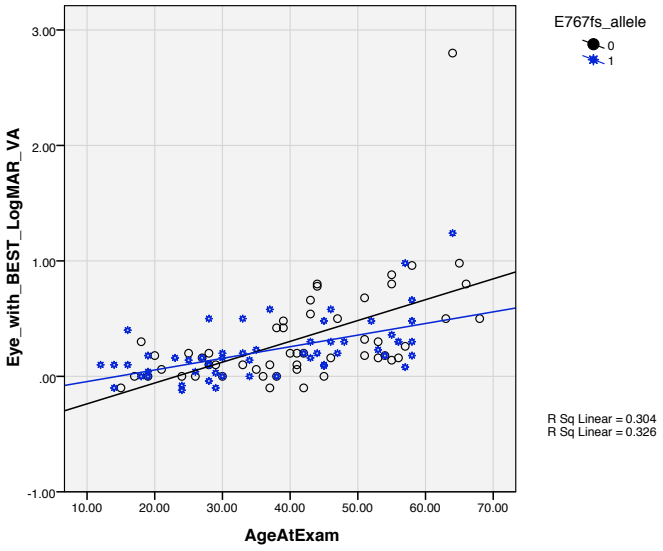

FIGURE 8.11: Scattergraph and regression lines for visual acuity in the USH2A molecular group after subdivision in to the group carrying the common allele **p.Glu767SerfsX21** (**labelled "1"**) and those that did not (labelled "0")

8.2 HRR Colour vision

8.2.1 Colour vision per clinical subtype

There was a significant difference between the proportion of normal vs. abnormal (errors in the test or unable to perform the test) between the USH1 and USH2 groups, with USH2 having more abnormal responses (Mann Whitney test, $P<0.001$).

This result should be interpreted with consideration to the older age of the USH2 group in the study population. The median ages of those with a recorded result for HRR testing were 27.5 years old for USH1 and 40 years old for USH2. From this data alone it is not clear if the greater proportion of 'abnormal' responses seen in the USH2 group was a function of their diagnosis or the older median age of the USH2 group.

To answer this question, the data on HRR testing was filtered to a smaller data set which excluded analysis of individuals in whom HRR testing was not performed or disease duration was not determined. This was done to remove missing cases that would prevent logistic regression. The results of analysis in this smaller subset of individuals is reported in subsections 8.2.1.1 and 8.2.1.2.

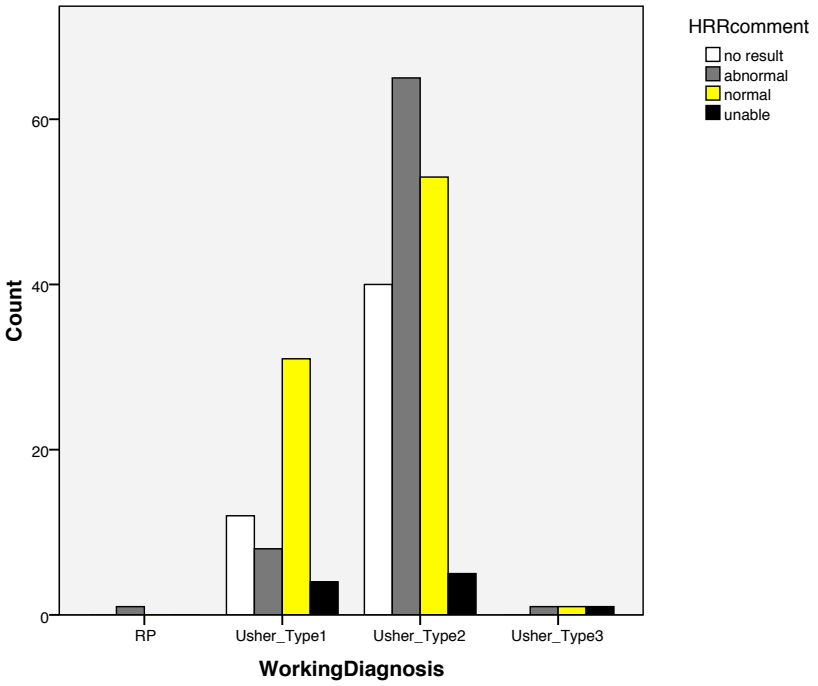

FIGURE 8.12: Cluster barchart showing results of HRR colour vision testing per clinical subtype

Note the greater proportion of abnormal vs. normal colour vision tests in the USH2 group and the opposite for the USH1 group. Note this barchart does not consider age

8.2.1.1 Colour vision vs. age

HRR test results were correlated negatively with age (r=-0.296, P<0.0001) and disease duration (r=-0.192, P<0.0001). Initial analysis performed in subset of individuals with complete dataset for HRR result, age and disease duration (n=144) is presented below. It was important to remove these individuals from analysis in order to construct a logistic regression model. An 'abnormal' HRR test result was scored for those individuals who were unable to score a result due to poor visual acuity.

To determine whether the greater proportion of abnormal colour vision test results seen in USH2 were due to the *diagnosis* of USH2 or the older *age of this sample* population, the data was split in to two groups, those with normal colour vision and those with abnormal colour vision. The median ages of USH1 and USH2 subsets within each group were then compared.

In both the abnormal and normal groups, the median age of USH1 and USH2 were significantly different. (Mann Whitney test, P<0.01), as well as in those with a normal result. This confirmed that the USH2 group was older than the USH1 group regardless of HRR test performance.

8.2.1.2 Colour vision vs. disease duration

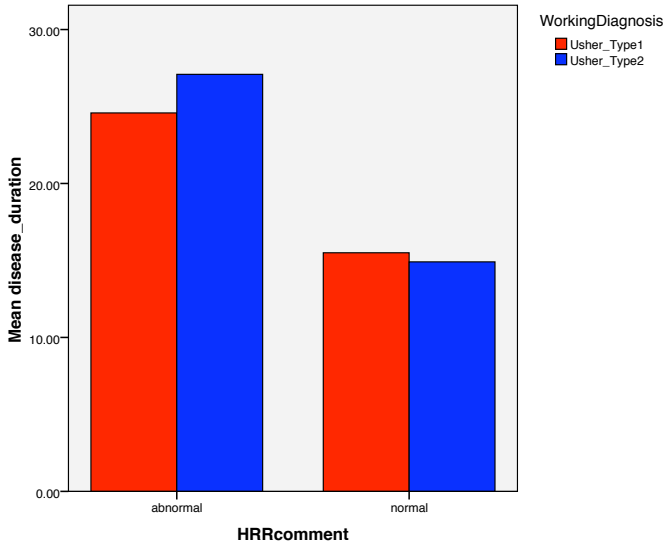

FIGURE 8.13: Bar chart displaying the mean disease duration of groups divided on the basis of HRR colour vision testing and clinical .diagnosis

The USH2 group were significantly older in the normal and abnormal colour vision test result groups as as shown above. It is noteworthy that it in chapter 7 it was shown

that the onset of retinal disease occurs later for USH2 compared to USH1. To attempt to reduce the influence of the later disease onset on the results for HRR testing, the subgroup analysis was repeated comparing the median value of *disease duration* between the USH1 and USH2 groups in those with a normal colour and those with an abnormal colour vision HRR test result. Disease duration was calculated by (age at exam - age at reported first visual symptom). Figure 8.13 shows the relative proportions in each group.

The medan disease duration was not significantly different between the USH1 and USH2 subsets in those with an abnormal HRR colour vision test result (Mann Whitney test, P>0.667), as well as in those with a normal result (Mann Whitney test, P>0.554).

This strongly suggests that when accounting for the earlier age of onset of visual symptoms reported in the USH1 group, there was no difference in HRR test performance.

8.2.2 Colour vision logistic regression

To test this hypothesis further, binary logistric regression models were constructed using the primary outcome variable as HRR test result and the covariables age and working diagnosis.

Formulating the null hypothesis that all HRR test results were abnormal (the majority of test results in the entire study population were abnormal) and the reference group as USH1, the observed data would be predicted 54% of the time.

Of the covariables; age and diagnosis, only age was statistically significant at predicting the outcome of the test result. The Exp(B) effect of age was 0.933 (95% confidence interval 0.904 - 0.962) which suggests that for every advancing year of age, the odds ratio of attaining a normal HRR test result is 0.933; i.e. there is a 6.7% chance per year of age of getting an abnormal HRR test result. This model had a non-significant Hosmer Lemeshow test (P >0.6) and thus provided a good fit for the observed data. This model increased correct prediction of the outcome from 54% (the null hypothesis) to 71%.

Adding the interaction of working diagnosis (USH1 or USH2) to the model did not provide a statistically significant improvement in prediction of outcome.

These data suggest that age alone was likely responsible for the increased proportion of abnormal HRR test results observed in the USH2 vs. USH1 subset.

8.2.3 Colour vision survival curve

The difference between the survival curves plotted for the proportion of USH1 and USH2 maintaining a normal colour vision test with age was equivocal, achieving statistical significance using the log-rank (Mantel-Cox) Test but not the Gehan-Breslow-Wilcoxon Test. Figure 8.14 demonstrates how close the curves mirror each other until the paucity of data points for USH1 for older individuals skews the data. The 95% confidence intervals for both curves are overlap for their entirety of the curves. This data supports the findings from logistic regression, that age is more of a predictor of colour vision test performance than clinical subtype.

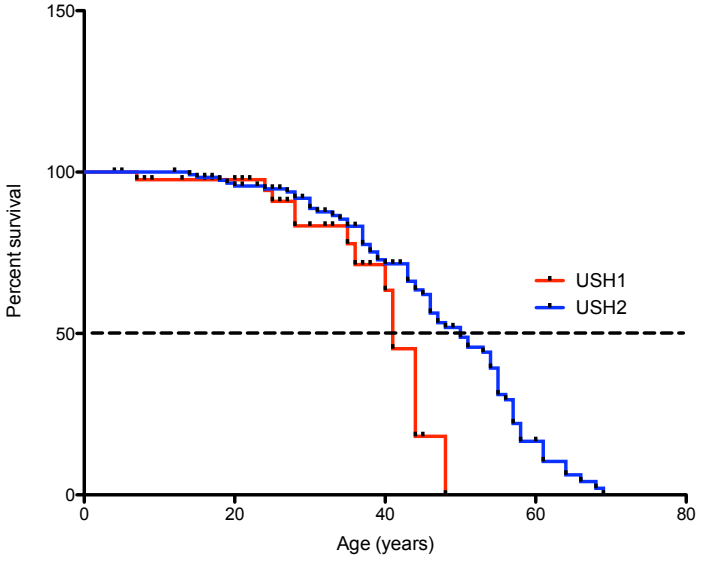

FIGURE 8.14: Survival curve representing the percentage of individuals who achieve a normal result on HRR colour vision testing. The curves for USH1 and USH2 are similar. The median survival point indicated by the broken black line intercepts the survival curves at a point where there 95% confidence intervals (lines not shown) overlap

8.2.4 Abnormal HRR test results

Whole NCUS cohort

Of the individuals with abnormal HRR colour test results, defects on the blue-yellow axis were significantly more common than defects on the red-green axis (Mann Whitney test, $P<0.05$) This is illustrated in Figure 8.15. This suggests that blue-yellow colour vision is affected earlier in the disease, with red-green colour vision defects occurring later.

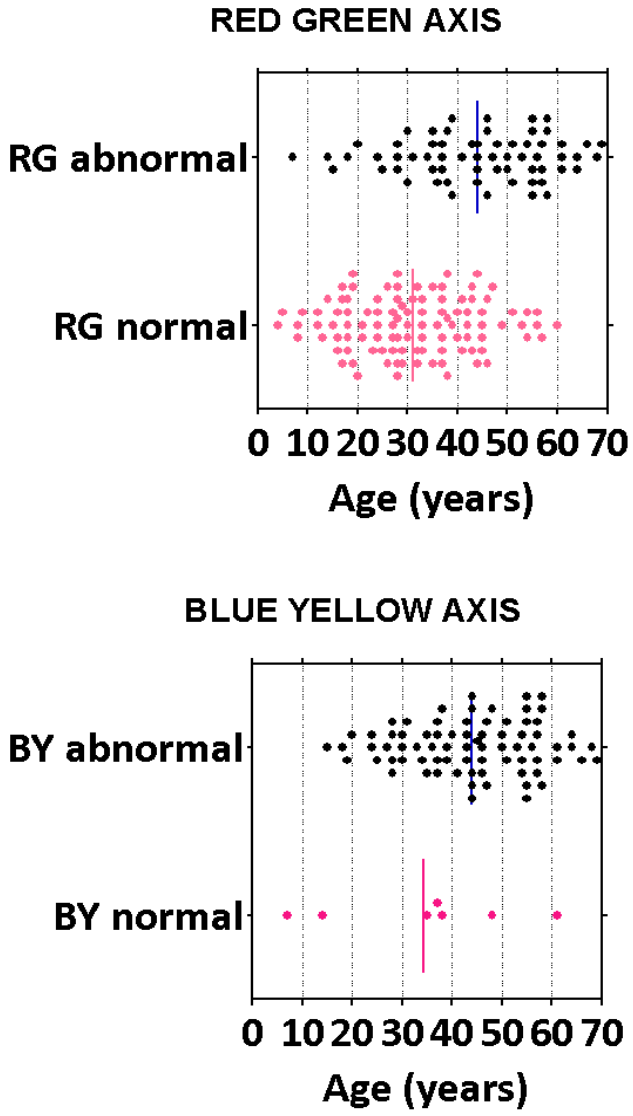

FIGURE 8.15: Data spread of the ages of individuals who had an abnormal test result on HRR testing

8.3 Cystoid Macular Oedema (CMO)

8.3.1 CMO prevalence all NCUS affected individuals

OCT data was available for 75% (n=167) of the entire cohort of NCUS affected individuals (n=222).

Of the 167 affected individuals with an OCT scan available for review 75% (n=125) had no evidence of CMO. 38% (n=15/40) of USH1 and 22% (n=28/125) of USH2 affected individuals had CMO in one or more eyes, this difference was close to statistical significance with two-tailed Chi Squared Test P=0.04 and with Fisher's exact test P=0.07.

8.3.2 Age vs. CMO prevalence

Age vs. CMO prevalence in all NCUS affected individuals

CMO occurrence was independent of age There was no significant difference between the median age of all NCUS individuals with CMO in one or more eyes, than those without CMO (Mann Whitney test, P>0.05).

8.3.3 CMO prevalence vs. Clinical subtype

TABLE 8.2: Proportion of individuals with cystoid macular oedema in one or both eyes per clinical subtype

	Usher_Type1		Usher_Type2		Usher_Type3	
	number	%	number	%	number	%
Cystoid Macular Oedema	15	37.5%	28	22.4%	0	.0%
NO Cystoid Macular Oedema	25	62.5%	97	77.6%	3	100.0%

Of the 25% of individuals from the NCUS cohort (all subtypes) with CMO, it was found unilaterally in a third of cases and bilaterally in two-thirds of cases, irrespective of clinical subtype.

8.3.4 Visual significance of CMO

The median VA of individuals for USH1 with CMO was logMAR 0.38 (n=13) and in the absence of CMO was logMAR 0.33 (n=26). This difference was not significantly different (Mann Whitney test, P=0.69). This lack of a significant difference in median VA was maintained when repeating analysis after the removal of outliers with poor VA (logMAR VA >1.0) (Mann Whitney test, P=0.39).

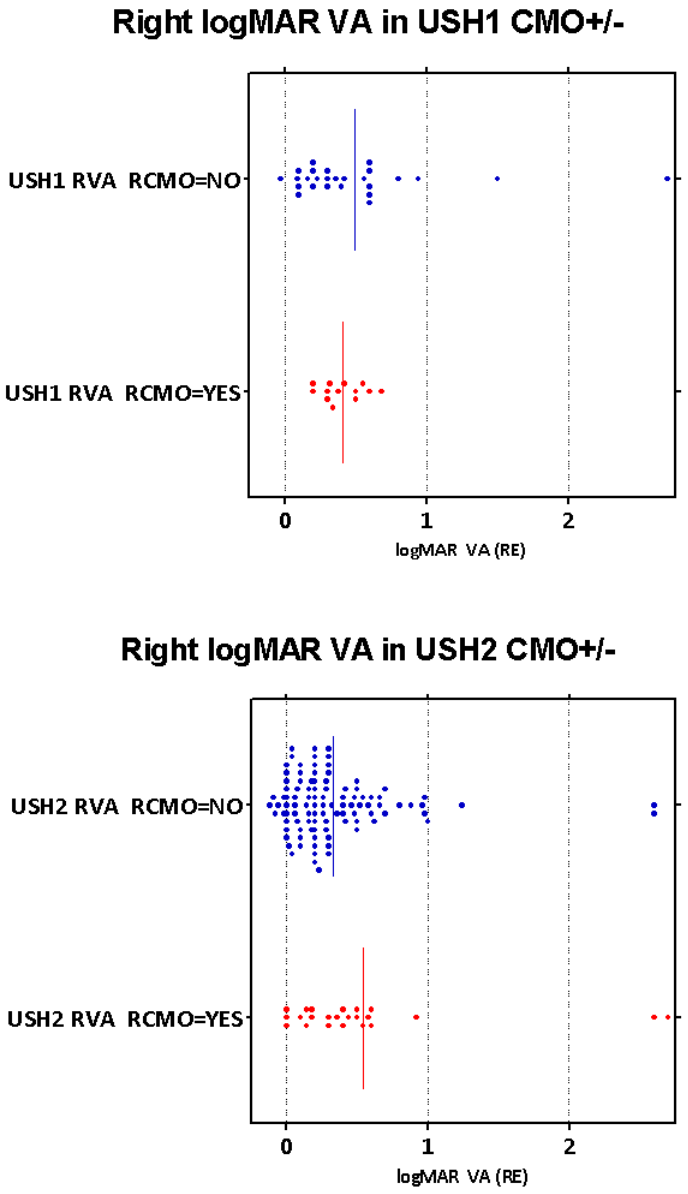

FIGURE 8.16: Scattergraph showing the logMAR VA for the RIGHT eyes in USH1 (top) and USH2 (bottom). Individuals with cystoid macular oedema are shown in red and those without in blue. Within each clinical group the difference between median visual acuity of those with/without CMO was not statistically significant. A number of individuals maintained good visual acuity despite having CMO

The median VA of USH2 individuals was worse in those with CMO at logMAR 0.4 (n=23) and in the absence of CMO was logMAR 0.2 (n=101) but this difference was not statistically significant (Mann Whitney test, P=0.11). This difference remained insignificant after the removal of outliers with poor VA (logMAR VA >1.0).

8.3.5 CMO per gene

Table 8.3 shows the proportions of individuals with CMO in each molecular subtype. CMO was identified in each molecular subtype.

TABLE 8.3: Table showing that CMO was found in all molecular subtypes

	GENE													
	MYO7A		USH1C		CDH23		PCDH15		USH2A		GPR98		USH3A	
	number	%	number	%	number	%	number	%	number	%	number	%	number	%
Cystoid Macular Oedema	7	36.8%	1	20.0%	3	50.0%	1	50.0%	18	19.8%	4	40.0%	0	.0%
NO Cystoid Macular Oedema	12	63.2%	4	80.0%	3	50.0%	1	50.0%	73	80.2%	6	60.0%	3	100.0%

8.4 Fundus Autofluorescence (AF)

Fundus AF images were obtained on 154 individuals in the NCUS and a further nine non-USH individuals. 16 individuals had such poor fundal fluorescence, no discernible retinal landmarks could be identified. The characteristics of these individuals with poor AF are described separately at the end of this section 8.4.6.

8.4.1 Foveal Hyperfluorescence

Foveal hyperfluorescence was a common finding, present in the majority of individuals with AF images. It was found to be highly symmetrical. Of all NCUS affected individuals with FAF images that were analysed (n=154), bilateral scans were available in over 95% of cases (n=147). The presence or absence of foveal hyperfluorescence was found to be 100% concordant between left and right eyes. For the purposes of clarity, the remainder of this subsection will consider analysis of variables related to the right eye only.

Foveal Hyperfluorescence - prevalence

Foveal hyperfluorescence was present in 58% (n=19) USH1 affected individuals, 53% (n=62) USH2 and was present in an individual with a diagnosis of RP (NCUS 491) who's affected sibling was an USH2 index case (NCUS 490) both belonging to Family 141. Of note, the USH2 sibling from this family did not manifest foveal hyperfluorescence. There was no significant difference between the proportions of those with foveal hyperfluorescence in USH1 vs USH2 (Fisher's exact test P=0.56). Of the two USH3 families, AF was of such low fluorescence the image could not be characterised in one individual (NCUS 82, Family 26, Age 48yrs); foveal hyperfluorescence was absent in the two siblings from the other USH3 family (NCUS 49 and 50, Family 16, Aged 22yrs and 25yrs respectively).

High resolution OCT imaging of foveal hyperfluorescence

Figure High resolution AF and OCT scanning of foveal hyperfluorescence revealed optically dense deposits identifiable in the inner retina; specifically around the photoreceptor and outer nuclear layer. The retinal pigment epithelium later appeared to be contiguous intact, suggesting that the origin of the signal may be inner retinal, rather than pigment epithelial.

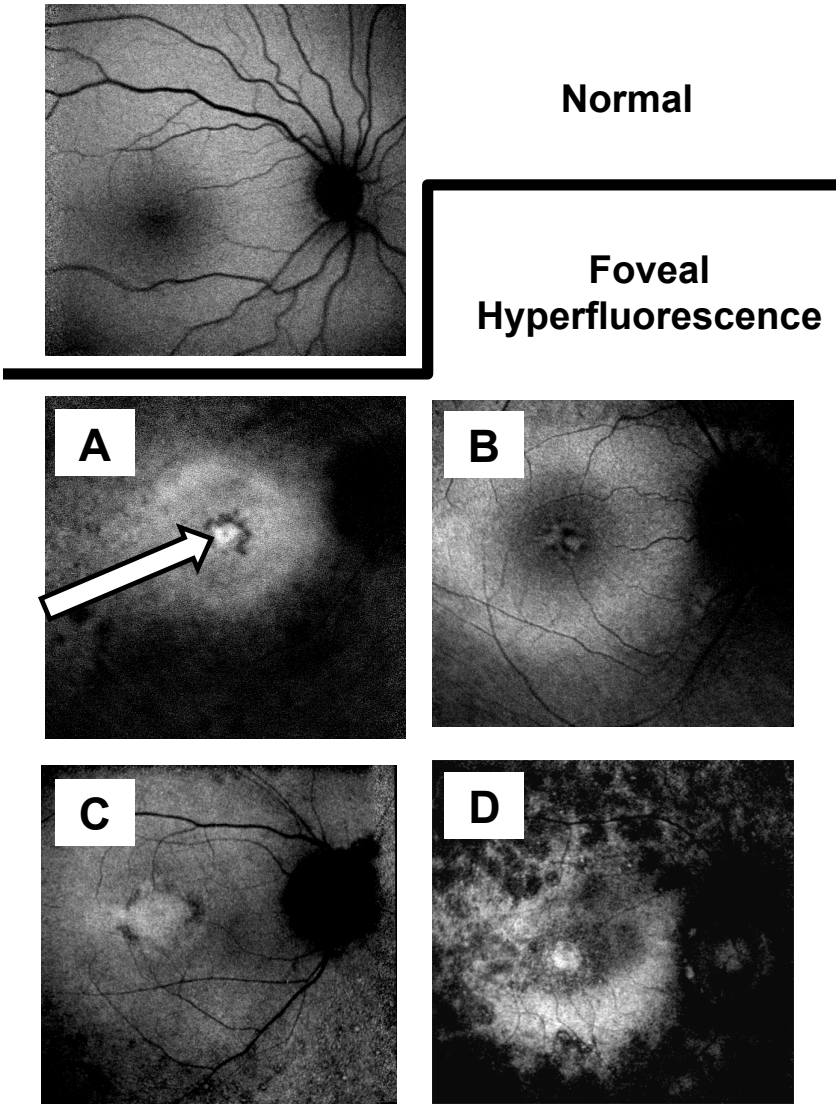

FIGURE 8.17: Image montage of fundus autofluorescence images. A normal AF image is shown above for reference. The images A through D demonstrate abnormal areas of hyperfluorescence at the fovea. All images also demonstrate varying amounts of patchy hypofluorescence around the vascular arcades. **Panel A**: Arrow indicates area of hyperfluorescence. **Panel B**: Discrete areas of hyperfluorescence within the foveal area. This 'petalloid' appearance was due to the presence of CMO **Panel C**: Area of contiguous hyperfluorescence at fovea associated with areas of parafoveal hyperfluorescence. **Panel D**: Area of contiguous hyperfluorescence at fovea associated with an annulus of parafoveal hyperfluorescence

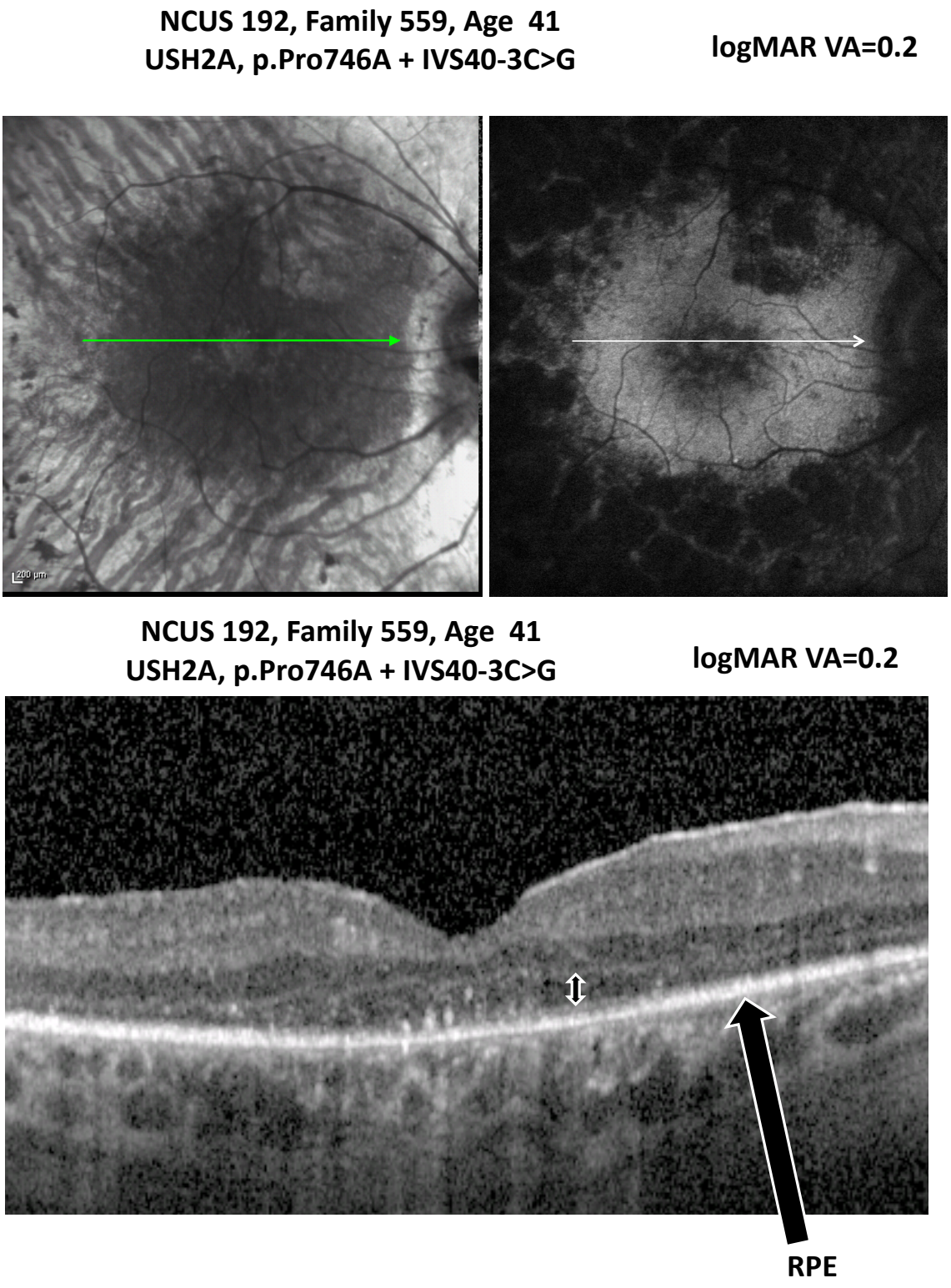

FIGURE 8.18: High resolution infrared image (top left) and autofluorescence image (top right). The horizontal arrows represent the point at which the high resolution OCT scan (bottom) was taken. Areas of hyperintense signal are seen in the inner retina corresponding top of the areas of foveal hyperfluorescence. The retinal pigment epithelim (RPE) apperas intact. The vertical arrow in the lower picture delimits the outer nuclear layer

Foveal Hyperfluorescence - association with visual acuity

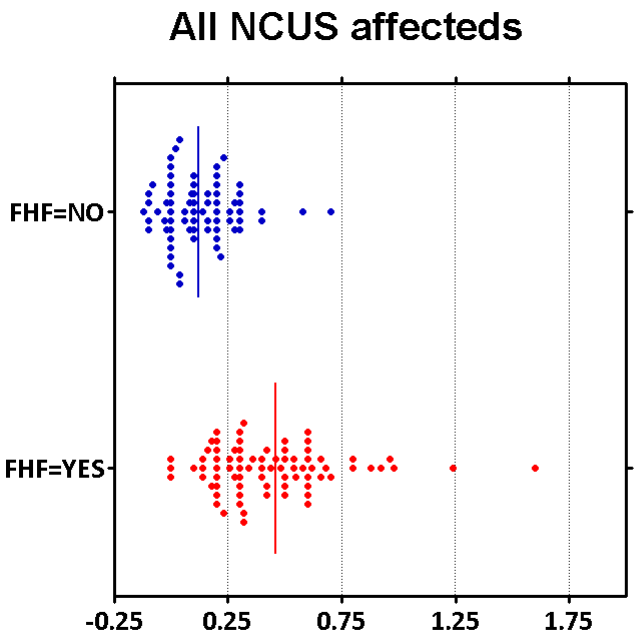

FIGURE 8.19: Scattergraph showing the logMAR VA (x-axis) in the right eyes of all NCUS affected individuals with and without foveal hyperfluorescence (FHF)

The median VA was significantly worse at logMAR=0.4 (n=80) amongst individuals who had foveal hyperfluorescence compared to those who did not (logMAR VA=0.1, n=70) (Mann Whitney test, P<0.0001).

Of those with foveal hyperfluorescence, there was no difference between median VA in USH1 (logMAR=0.42, n=19) vs. USH2 (logMAR=0.40, n=59).

However when considering the VA of those without foveal hyperfluorescence , the median VAs were significantly different between USH1(logMAR=0.23, n=12) vs. USH2 (logMAR=0.08, n=57). This difference is likely due to the baseline difference in VA already noted between USH1 and USH2 groups reported earlier.

Foveal Hyperfluorescence - association with age and CMO

Representative images are shown to illustrate the finding of foveal hyperfluorescence with CMO (Figure 8.21) and in the absence of CMO (Figure 8.22).

The median age of those with foveal hyperfluorescence was 43.5 yrs (n=80) which was significantly older that individuals in whom foveal hyperfluorescence was absent, who had a median age of 30 yrs (n=71). This difference was highly significant (Mann Whitney test, P<0.0001).

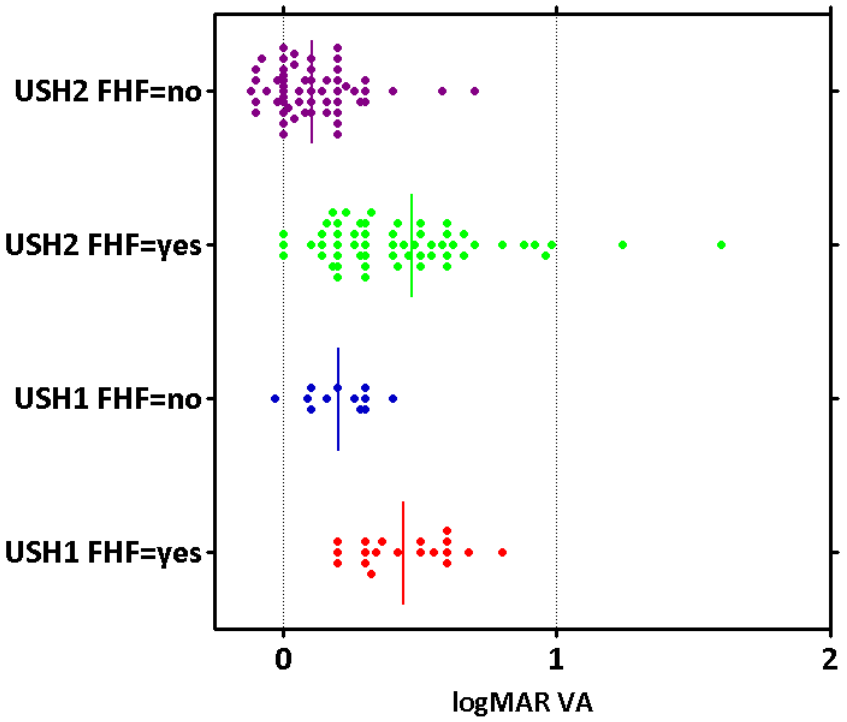

FIGURE 8.20: Scattergraph showing the logMAR VA in the right eyes of USH1 and USH2 individuals with and without foveal hyperfluorescence (FHF)

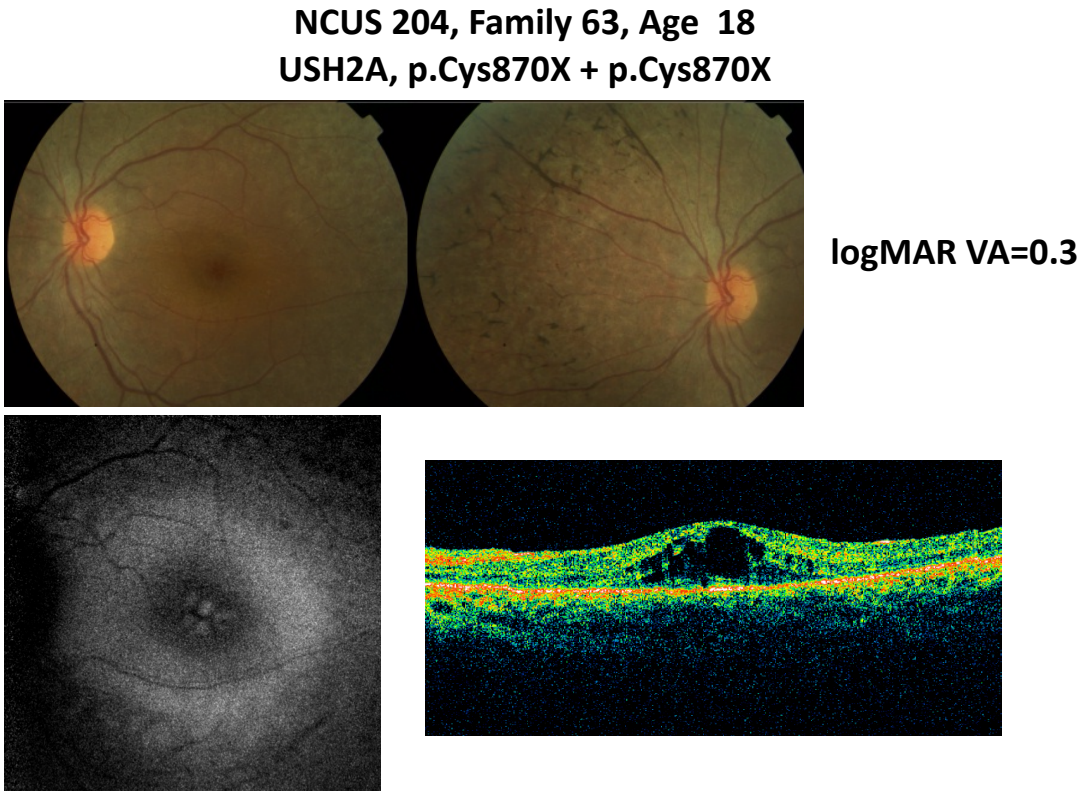

FIGURE 8.21: Montage of images from the left eye of an USH2 affected with foveal hyperfluorescence and cystoid macular oedema. Images are colour fundus photos (above), AF imaging (below right) and OCT3 scanning (below left)

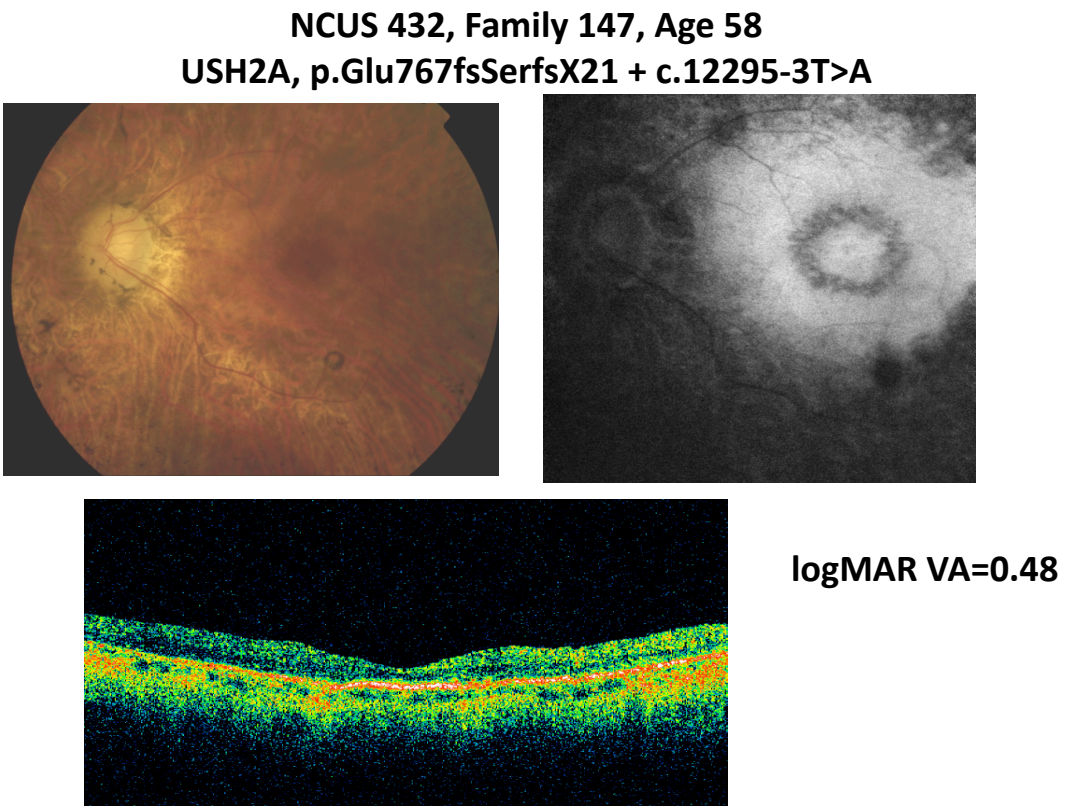

FIGURE 8.22: Montage of images from the left eye of an USH2 affected with foveal hyperfluorescence with no cystoid macular oedema. Images are colour fundus photos (above), AF imaging (below right) and OCT3 scanning (below left)

It can be stated that foveal hyperfluorescence is significantly correlated with poorer visual acuity and is found in higher prevalence in older patients with USH1, USH2 and an affected USH2 sibling with RP. As the pathogenesis of the hyperfluorescence is uncertain it remains unclear whether this finding is a cause of poor visual acuity or a secondary finding in the retinal pathogenesis of Usher syndrome.

As was shown earlier, when analysing USH1 and USH2 groups separately, there was no significant difference in median VA between those with or without CMO.

TABLE 8.4: Crosstab table showing number of individuals with foveal hyperfluorescence and cystoid macular oedema for all NCUS affecteds

		Foveal hyperfluorescence		
		yes	no	TOTAL
Cystoid Macular Oedema	yes	28	2	30
	no	46	57	103
	TOTAL	74	59	

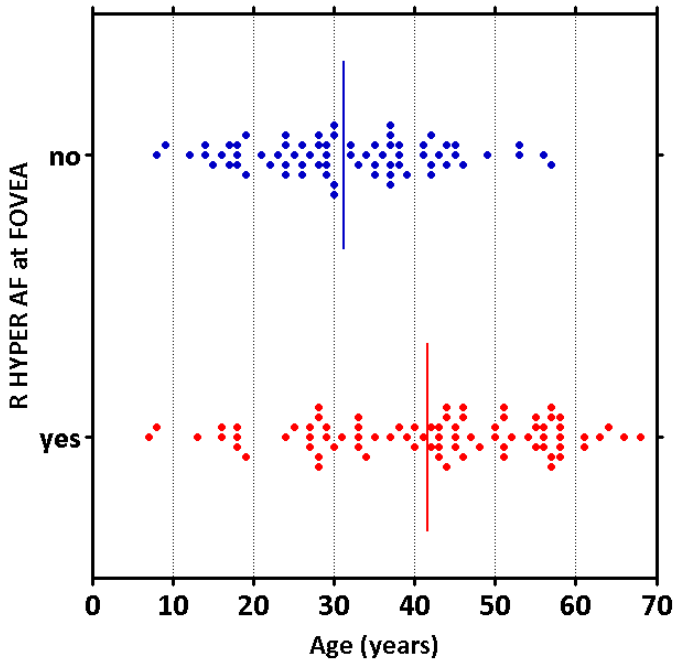

FIGURE 8.23: Scattergraph showing the assoiation between age and foveal hyperfluorescence

Table 8.23 shows that CMO accounts for 28/74 cases of foveal hyperfluorescence, but a larger proportion 46/74 had foveal hyperfluorescence in the absence of CMO. Interestingly, of the two individuals who had CMO but no foveal hyperfluorescence, one (NCUS 42, Family11, disease due to *MYO7A* gene) had been on long term oral acetazolamide therapy daily for many years to treat her chronic CMO.

TABLE 8.5: Crosstab tables showing number of individuals with foveal hyperfluorescence and cystoid macular oedema in USH1 and USH2 clinical groups

			Foveal hyperfluorescence		
			yes	no	TOTAL
USH1	Cystoid Macular Oedema	yes	11	1	**12**
		no	7	10	**17**
		TOTAL	**18**	**11**	

			Foveal hyperfluorescence		
			yes	no	TOTAL
USH2	Cystoid Macular Oedema	yes	17	1	**18**
		no	38	45	**83**
		TOTAL	**55**	**46**	

Foveal hyperfluorescence per gene

	Foveal hyperfluorescence		
GENE	**yes**	**no**	**TOTAL**
MYO7A	6	6	**12**
USH1C	2	4	**6**
CDH23	5	1	**6**
PCDH15	1	1	**2**
USH2A	48	40	**88**
GPR98	2	5	**7**
USH3A	0	2	**2**

FIGURE 8.24: Crosstab table showing number of individuals with foveal hyperfluorescence per disease causing gene

Table 8.24 shows the proportions of foveal hyperfluorescence per gene. No striking pattern is seen. foveal hyperfluorescence appears to be present/absent in roughly equal numbers and no obvious pattern is seen, however the small numbers of individuals in most molecular categories makes drawing statistical conclusions from these data difficult.

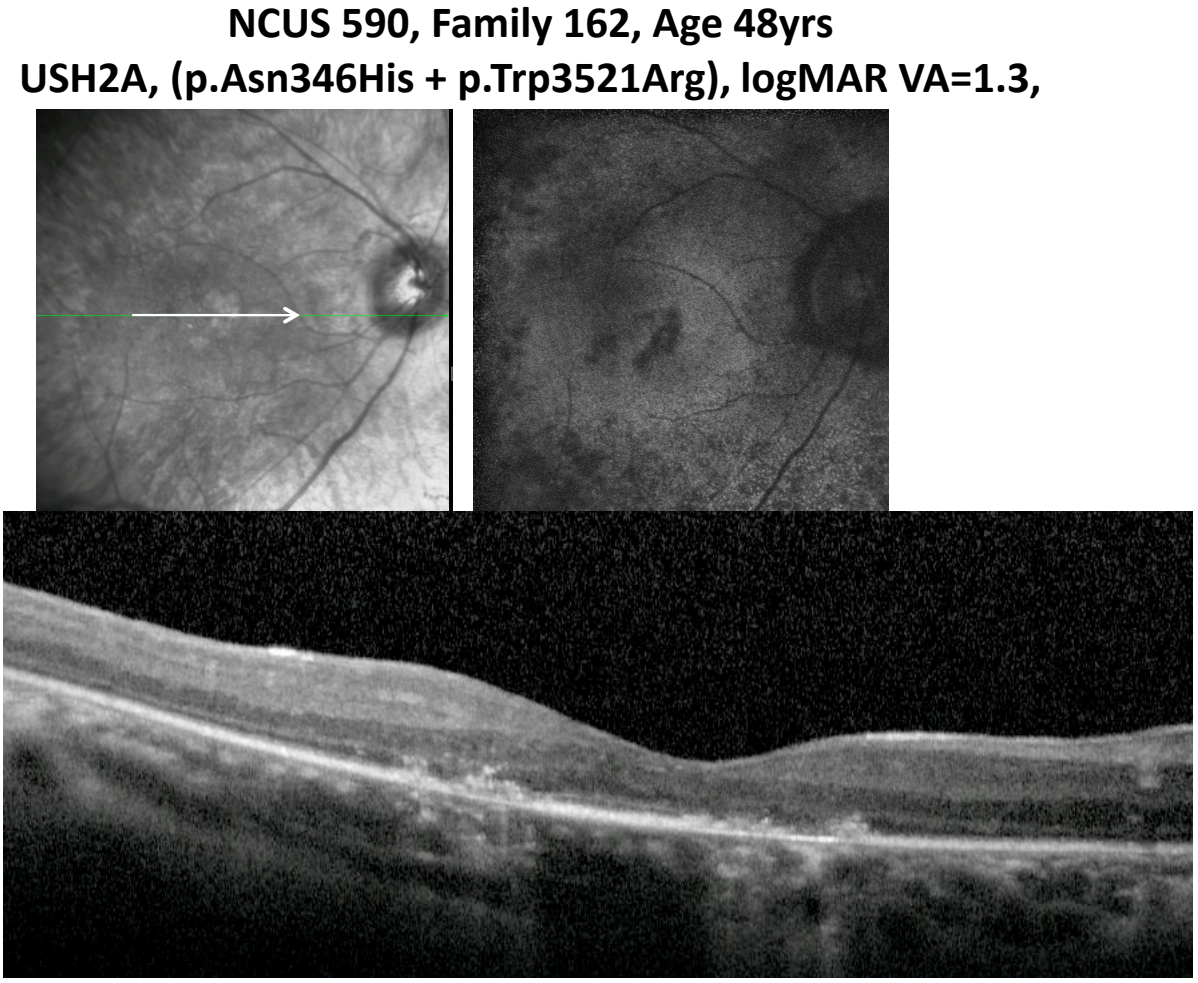

FIGURE 8.25: High resolution infrared image (top left) and autofluorescence image (top right). The horizontal arrows represent the point at which the high resolution OCT scan (bottom) was taken. Areas of hyperintense signal are seen in the inner retina on high resolution OCT scans

8.4.2 Parafoveal hypofluorescence

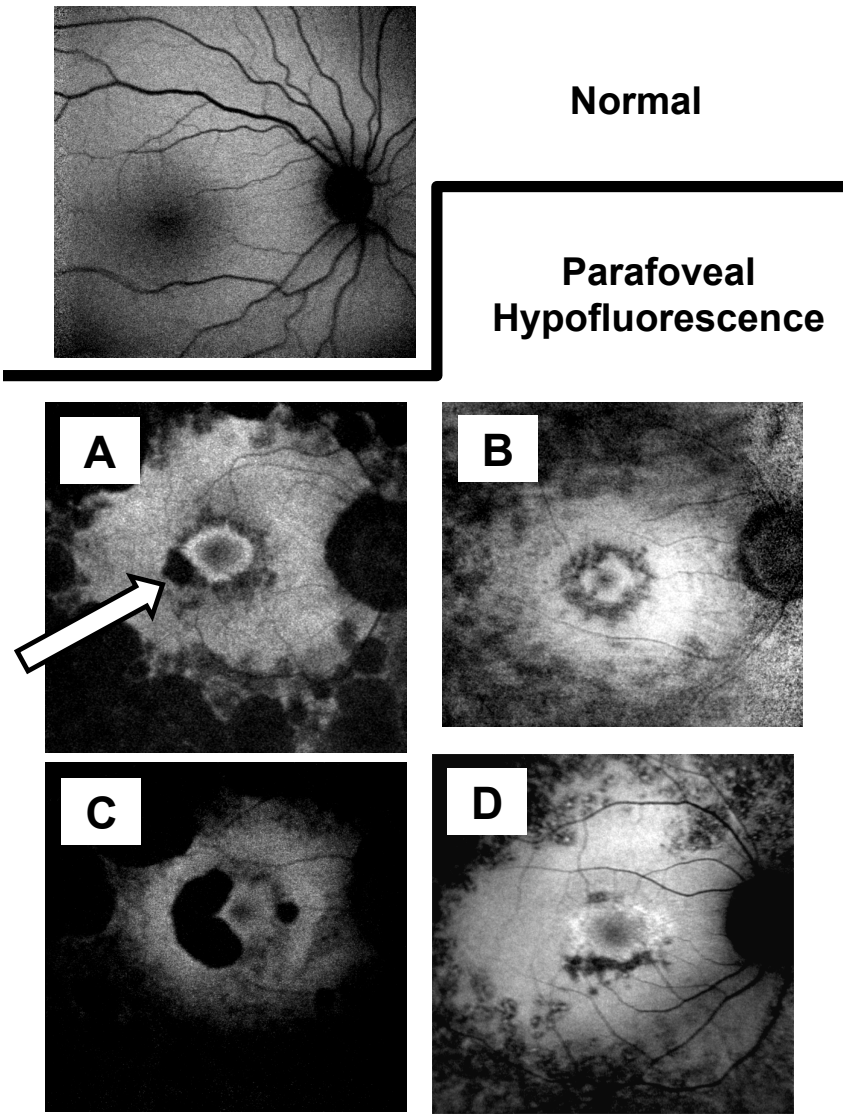

FIGURE 8.26: Image montage of fundus autofluorescence images. A normal AF image is shown above for reference. The panels A through D demonstrate abnormal areas of parafoveal hypofluorescence. All images also demonstrate varying amounts of patchy hypofluorescence around the vascular arcades and relatively preserved autofluorescence at the posterior poles. **Panel A**: Arrow indicates area of hypofluorescence (dark area) inferotemporal to right fovea which is continuous with an annulus of patchy hypofluorescence just external to a ring of hyperfluorescence (bright area). **Panels B** and **C**: Both show parafoveal hypofluorescence external to a hyperfluorescent ring.**Panel D**: Shows patchy areas of parafoveal hypofluorescence restricted to superiorly and inferior to a hyperfluorescent ring

Of all the AF images that were available for analysis from all NCUS affecteds (n=154), parafoveal hypofluorescence was identified in about a third (n=55). Similarly to hyperfoveal hyperfluorescence, it was a highly symmetrical finding. Of the individuals who had AF images for both eyes available for analysis (N=147), the presence of parafoveal

hypofluorescence had 100% concordance between left and right eyes. Due to the highly symmetrical nature of the finding, data is presented in relation to parafoveal hypofluorescence and related variables on the right eye only.

Parafoveal hypofluorescence - prevalence

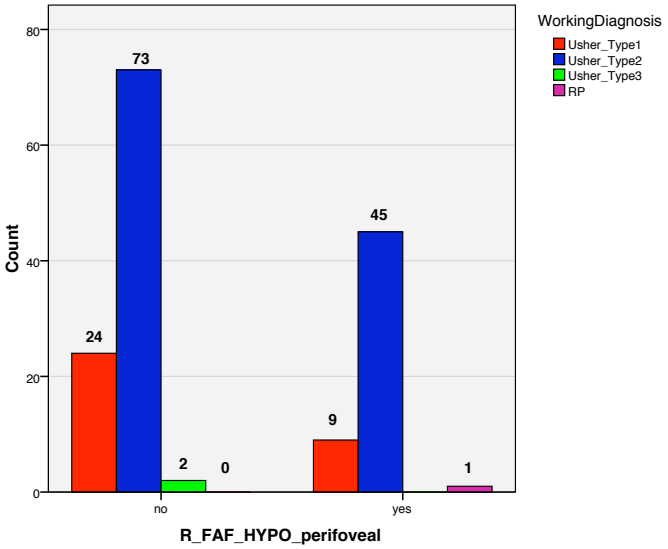

FIGURE 8.27: Barchart showing number of individuals with parafoveal hypofluorescence per subtype

Parafoveal hypofluorescence was identified in 27% (n=9) of USH1, 38% (n=45) of USH2 individuals. It was also identified in the individual with a diagnosis of RP (NCUS 491) who's affected sibling was an USH2 index case (NCUS 490) both belonging to Family 141. Of note, the USH2 sibling from this family did not manifest parafoveal hypofluorescence. There was no significant difference between the proportions of those with parafoveal hypofluorescence in USH1 vs USH2 (Fisher's exact test P=0.31).

Of the two USH3 families, AF was of such low fluorescence it could not be characterised in one individual (NCUS 82, Family 26, Age 48yrs) and parafoveal hypofluorescence was absent in the two siblings from the other USH3 family (NCUS 49 and 50, Family 16, Aged 22yrs and 25yrs respectively).

8.4.3 Parafoveal hypofluorescence - associations

Of the variables analysed only VA and CMO were correlated with parafoveal hypofluorescence. No correlation was identified between the presence of parafoveal hypofluorescence and visual acuity, disease duration, visual fields or foveal thickness.

Age vs. parafoveal hypofluorescence

For the NCUS cohort as a whole, the median age was significantly higher in those with parafoveal hypofluorescence (48yrs, n=53) compared to those who did not manifest parafoveal hypofluorescence (30yrs, n=98) (Mann Whitney test, P<0.0001).

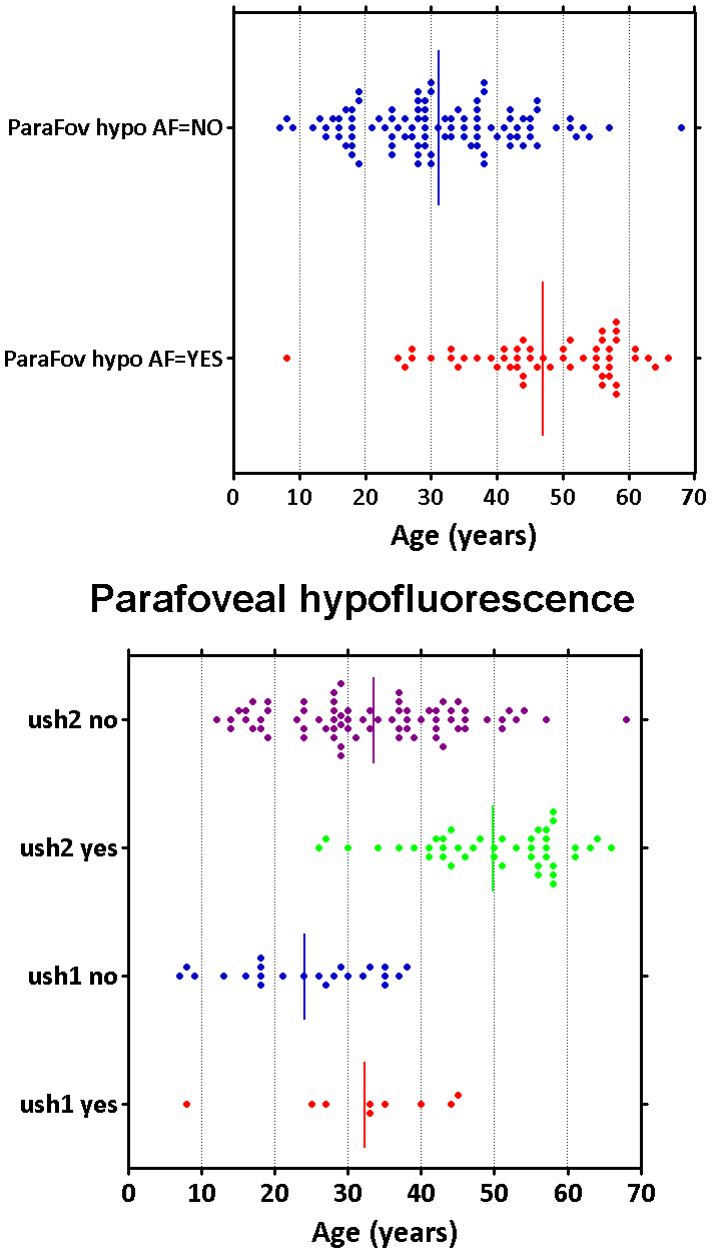

FIGURE 8.28: Scattergraphs of the relationship between age and the presence/absence of parafoveal hypofluorescence. The top figure shows the significantly older age of those manifesting parafoveal hypofluorescence. The lower figure represents the same data, but after subdividing in to USH1 and USH2. This shows that the majority of the age effect was contributed by the USH2 group

Figure 8.28 shows that parafoveal hypofluorescence was identified in an older group of USH1 and USH2 individuals, however this difference was only statistically significant for the USH2 group (Mann Whitney test, P=0.0001).

CMO vs. parafoveal hypofluorescence

TABLE 8.6: Incidence of parafoveal hypofluorescence and cystoid macular oedema for whole study group

		Perifoveal hypofluorescence		
		yes	no	TOTAL
Cystoid Macular Oedema	yes	7	23	**30**
	no	37	66	**103**
	TOTAL	**44**	**89**	

Table 8.6 highlights that parafoveal hypofluorescence was found more frequently amongst individuals without CMO although the difference between these proportions was not statistically significant (Fisher's exact test P=0.14). The relative proportions remained similar and did not achieve statistical significance after subdividing the NCUS cohort in to two groups of USH1 and USH2. The relative proportions following subdivision are shown in Table 8.7. Although not statistically significant, it is noteworthy that in contrast to foveal *hyper*fluoresence, parafoveal *hypo*fluorescence was *less* prevalent amongst individuals with CMO.

TABLE 8.7: Incidence of parafoveal hypofluorescence and cystoid macular oedema for USH1 and USH2

		Parafoveal hypofluorescence							
		Usher_Type1				Usher_Type2			
		yes		no		yes		no	
		(n)	%	(n)	%	(n)	%	(n)	%
CMO	yes	2	16.7%	10	83.3%	5	27.8%	13	72.2%
	no	6	35.3%	11	64.7%	30	36.1%	53	63.9%

Parafoveal hypofluorescence per disease causing gene

Table 8.8 shows that parafoveal hypofluorescence was identified in all molecular groups apart from *PCDH15* and *USH3A*.

TABLE 8.8: Parafoveal hypofluorescence per molecular group

	Parafoveal hypofluorescence		
GENE	**yes**	**no**	**TOTAL**
MYO7A	2	10	**12**
USH1C	1	5	**6**
CDH23	3	3	**6**
PCDH15	0	2	**2**
USH2A	37	51	**88**
GPR98	1	6	**7**
USH3A	0	2	**2**

8.4.4 AF hyperfluorescent rings

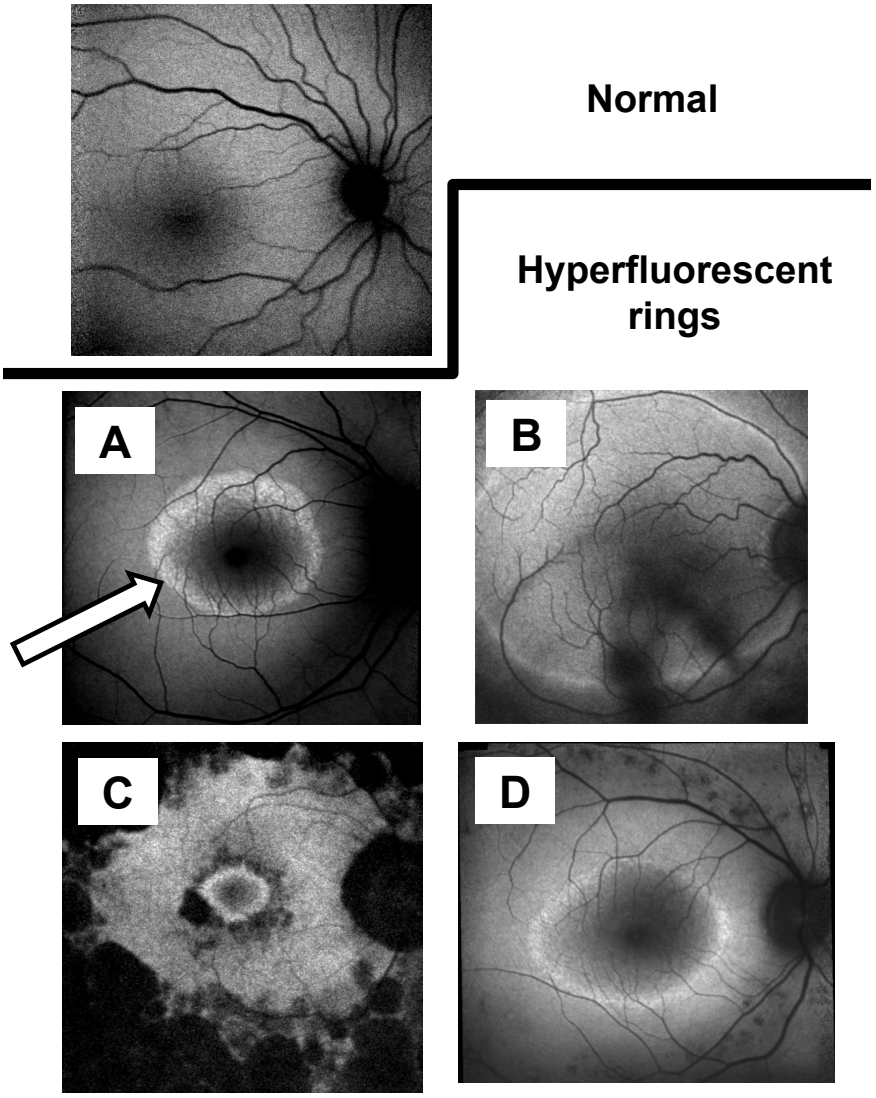

FIGURE 8.29: Montage of images showing hyperfluorescent rings seen on autofluorescence imaging

Prevalence of AF hyperfluorescent rings per subtype

Of the total number of AF images available for review (n=154), hyperfluorescent rings were a common finding present in 73% (n=112) of the NCUS cohort. The rings were only identified by AF imaging and did not generally correspond to any obvious visible features on slit lamp biomicroscopy.

Hyperfluorescent rings were found at a prevalence of 85% (n=28) in USH1 and 69% (n=81) in USH2 with the proportions being statistically similar between these two groups (Fisher's exact test P=0.12). Of the two USH3 families, AF was of such low signal the

image could not be characterised in one individual (NCUS 82, Family 26, Age 48yrs); the two siblings from the other (Family 16) both manifest hyperfluorescent rings at 22yrs and 25yrs.

Like other AF features described in earlier subsections, the presence of hyperfluorescent rings was highly symetrical. Of those with AF images available for analysis from both eyes (n=147) the presence of hyperfluorescent rings showed 100% concordance between left and right eyes.

Age vs. Prevalence of AF hyperfluorescent rings

Considering the NCUS cohort as a whole, the median age of those with hyperfluorescent rings was significantly younger at 30.5yrs (n=112) compared to those without hyperfluorescent rings 49yrs (n=42) (Mann Whitney test, P<0.0001).

TABLE 8.9: Number, percentage and median age of individuals who manifest hyperfluorescent rings on AF imaging when subdividing by clinical subtype

	Hyperfluorescent ring present?					
	NO			**YES**		
	(n)	% of subtype	Median age (years)	(n)	% of subtype	Median age (years)
Usher_Type1	5	*15.2%*	40.00	28	*84.8%*	26.00
Usher_Type2	37	*31.4%*	51.00	81	*68.6%*	36.50
Usher_Type3	0	*.0%*		2	*100.0%*	23.50
RP	0	*.0%*		1	*100.0%*	56.00

TABLE 8.10: Number, percentage and median age of individuals who manifest hyperfluorescent rings on AF imaging when subdividing by molecular diagnosis

		Hyperfluorescent ring present?					
		NO			**YES**		
		(n)	% per GENE	Median age (years)	(n)	% per GENE	Median age (years)
GENE	**MYO7A**	3	*25.0%*	38.00	9	*75.0%*	21.00
	USH1C	0	*.0%*		6	*100.0%*	35.00
	CDH23	1	*16.7%*	44.00	5	*83.3%*	27.00
	PCDH15	0	*.0%*		2	*100.0%*	12.00
	USH2A	28	*31.8%*	51.00	60	*68.2%*	31.50
	GPR98	3	*42.9%*	51.00	4	*57.1%*	37.00
	USH3A	0	*.0%*		2	*100.0%*	23.50

Table 8.11 represents the distribution of AF rings by molecular diangosis. Note that AF rings were found in each molecular subtype identified from this study. Although only small numbers of subjects were available for study in *USH1C*, (n=6) AF rings were present in all cases. They were also present with a striking and unique morphology in Family 142 who had an atypical phenotype due to mutations in the *USH1C* gene (discussed in a later chapter 10.1.1).

Amongst the most common molecular group *USH2A*, rings were identified in 68% (n=60/88) of cases.

TABLE 8.11: Table showing presence of AF rings by molecular diagnosis

		AF ring	
		no	yes
GENE	no AF data	(n)	(n)
MYO7A	11	3	9
USH1C	0	0	6
CDH23	0	1	5
PCDH15	2	0	2
USH2A	29	28	60
GPR98	4	3	4
USH3A	1	0	2

Hyperfluorescent rings - associations

Hyperfluorescent ring status - association with age and disease duration

Hyperfluorescent ring status refers to whether or not an individual manifests an hyperfluorescent ring on AF imaging. This is to be distinguished from **Hyperfluorescent ring area**, which is covered later.

The younger median age of those that manifest hyperfluorescent rings remained highly significant when comparing USH1 and USH2 groups separately (Mann Whitney test, P<0.0001) (see Table 8.9).

After further subdivision in to molecular groups (see Table 8.10), only the two largest groups, *MYO7A* and *USH2A* maintained a statistically significant difference of a younger median age for the subgroup with hyperfluorescent rings (Mann Whitney test, P<0.0001).

Hyperfluorescent ring status - association with visual acuity

In USH2 median VA was significantly better in those with hyperfluorescent rings logMAR=0.17 (n=81) than in those without logMAR=0.49 (n=37) (Mann Whitney test, P<0.0001). In USH1, although the median VA was considerably better at logMAR=0.3

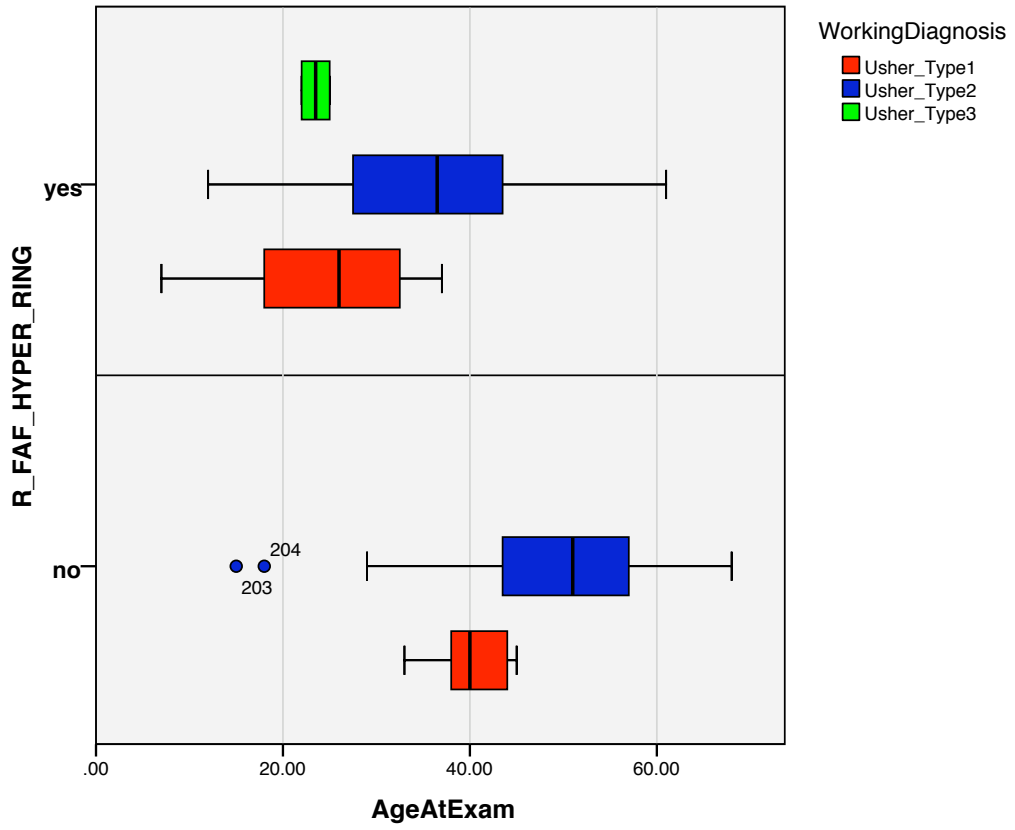

FIGURE 8.30: Boxplot and whisker representation showing the younger median age of those with manigest hyperfluorescent rings on AF imaging. The two outliers (NCUS 203 and 204) are siblings from Family 63

(n=28) in those with hyperfluorescent rings, due to the small number of individuals (n=5) who did not have hyperfluorescent rings with a median VA of 0.55, this difference was not statistically significant (Mann Whitney test, P=0.62).

Due to the younger median age of those with hyperfluorescent rings in both USH1 and USH2 subtypes, the better VA seen in these groups is perhaps not surprising.

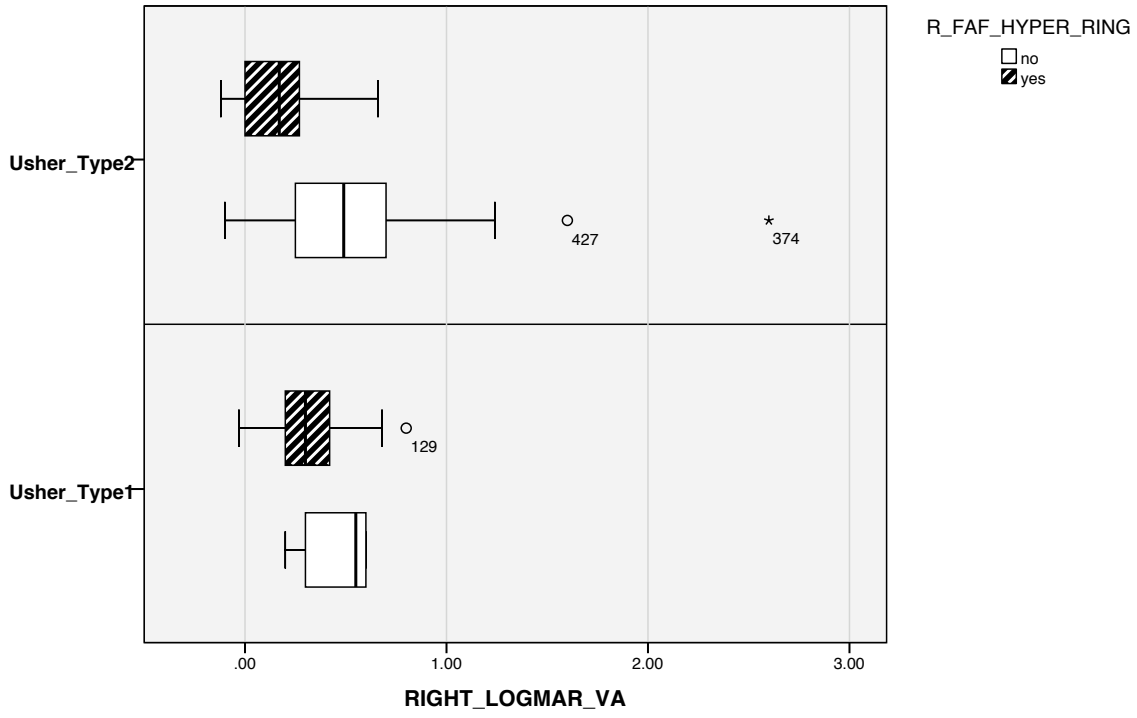

FIGURE 8.31: Boxplot and whisker showing the median, interquartile range and total range of visual acuity. Outliers are indicated by their NCUS ID number

Hyperfluorescent ring status - association with visual field parameters

Analysing all NCUS affecteds together, the presence of a hyperfluorescent ring correlated significantly and positively with all central, peripheral and total areas from each of the three visual field isopters V4e, II4e and I4e. Their correlation coefficients ranged from r=0.38 to r=0.81 (all P <0.05) indicated significant positive correlation between visual field and the presence or absence of a hyperfluorescent ring.

There was no evidence of correlation between hyperfluorescent ring presence and CMO status, age at first visual symptom or average macular thickness in the central $1mm^2$ (from OCT scans).

Hyperfluorescent ring AREA - laterality

There was a high degree of correlation between the AF ring area in the left vs the right eye (Spearman's rank coefficient 0.979, P <0.001). A linear regression model was highly significant at predicting left from right ring area (r2=0.992, 104 d.f., P <0.001).

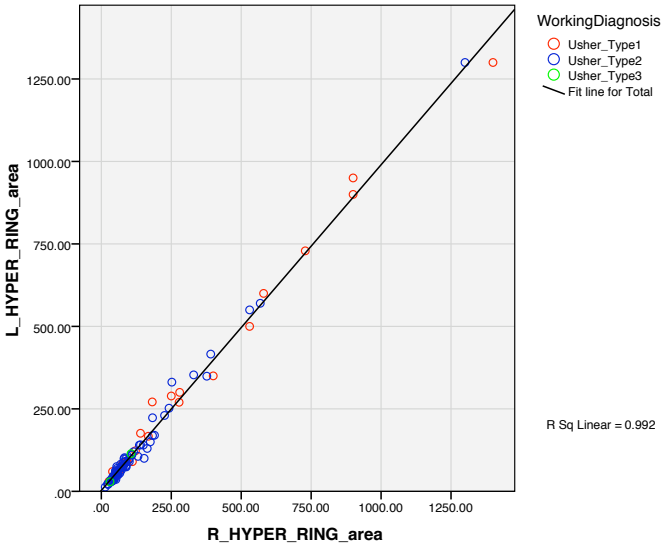

FIGURE 8.32: Scattergraph showing the high degree of correlation between right and left AF ring area. The linear regression line predicting left from right AF ring area is shown

Due to this high degree of symmetry between both eyes, subsequent analysis was performed using the one eye (the right eye) only.

Hyperfluorescent ring size

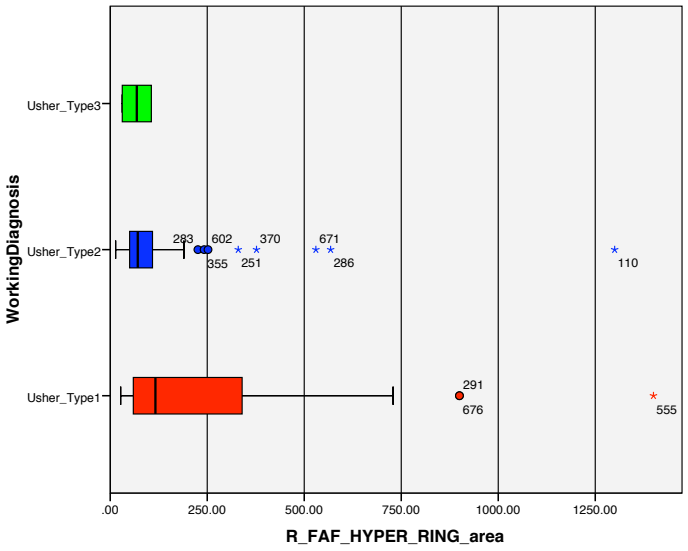

FIGURE 8.33: Boxplot and whisker showing AF ring area for each clinical subtype. The outliers are labelled with their NCUS ID number

There was a highly significant difference between median hyperfluorescent ring area between USH1 and USH2 clinical groups. The median hyperfluorescent ring area was 116.5 degrees squared (n=57) for USH1 and 71 degrees squared for USH2 (n-163) (Mann Whitney test, P<0.01). The mean and median ring area in the two siblings with USH3 (Family 49) was 68.5 degrees squared and thus comparable to the USH2 group.

Figure 8.33 highlights the disparity in not only the median ring sizes between USH1 and USH2, but also the narrow range of ring area observed in USH2, despite the greater number of individuals in the study and the wider spread of ring areas seen in USH1 despite having fewer individuals in this group.

As hyperfluorescent ring status has been shown to be associated with a younger median age and through recruitment bias in to this study, the USH1 population is of significantly younger median age than the USH2 population. It might be reasonable to assume that this larger ring area in USH1 might be due to this group having a younger median age. However, age alone is unlikely to be able to explain this difference due to the magnitude of this difference. This is illustrated in Figure 8.34 which shows age plotted against hyperfluorescent ring area.

p50 vs AF ring area

The p50 value indicating macular function on retinal elctrodiagnostics was highly correlated with AF ring area (r=0.712, P<0.0001).

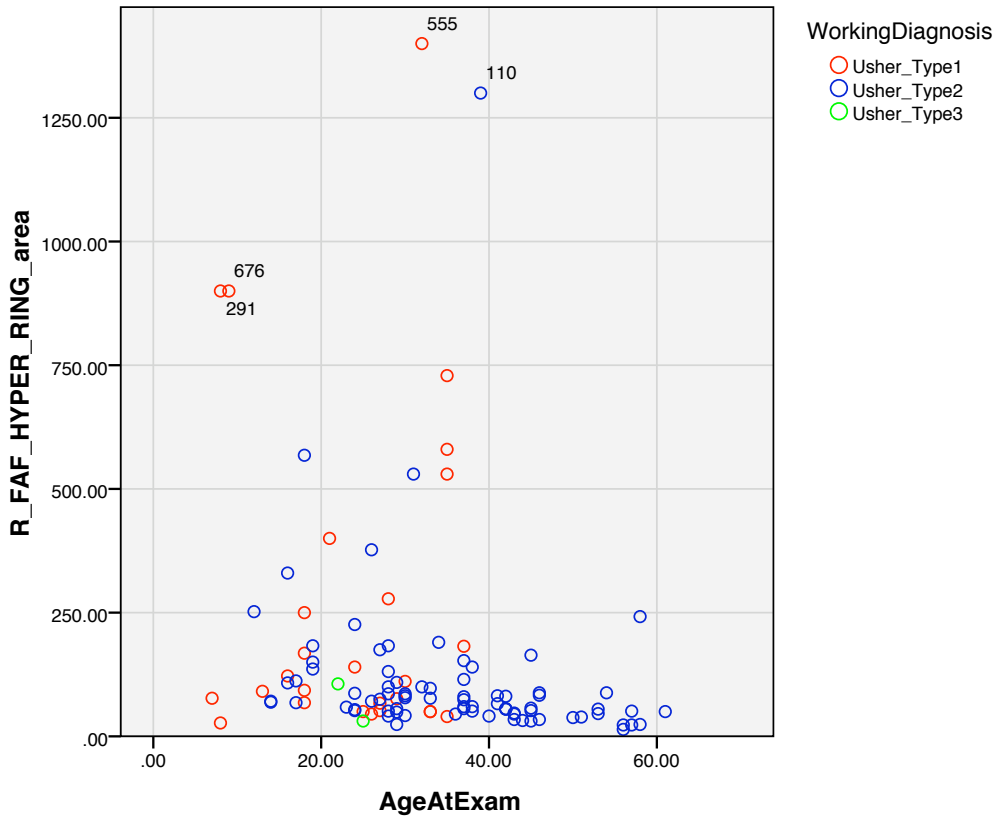

FIGURE 8.34: Scattergraph showing the relationship for AF ring area in the right eye with age. Note the general trend to smaller ring sizes with increasing age in USH2. Although not significant, there appears to be a trend toward larger AF ring size in USH1 with increasing age

A linear regression model for predicting AF ring area on p50 provided a good fit for the data (r2=0.26, 20 d.f., P=0.01).

When restricting this analysis to just *USH2A* molecular group a much better fit was achieved (r2=0.435, 31 d.f., P=0.003) which was able to achieve statistical significance of the gradient +61.963 (95% confidence intervals 29.033 to 94.892) but not the y-intercept.

y=61.963 (29.033 to 94.892) + c

8.4.5 Regression analysis for AF hyperfluorescent rings

Linear regression model for USH2: Age vs. AF ring area

Following from the finding that AF ring size correlated with age in USH2, this relationship was examined by constructing a linear regression model, which was highly significant in predicting ring size as a function of age.

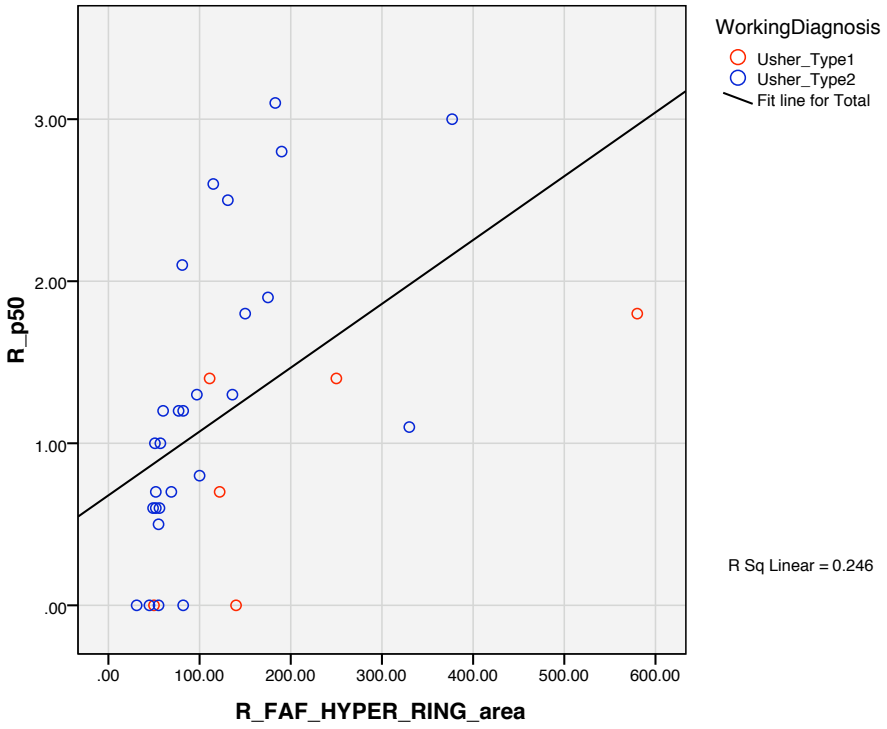

FIGURE 8.35: Scattergraph showing relationship and regression line of AF ring area vs p50 for all study participants with ERG data who manifested AF rings

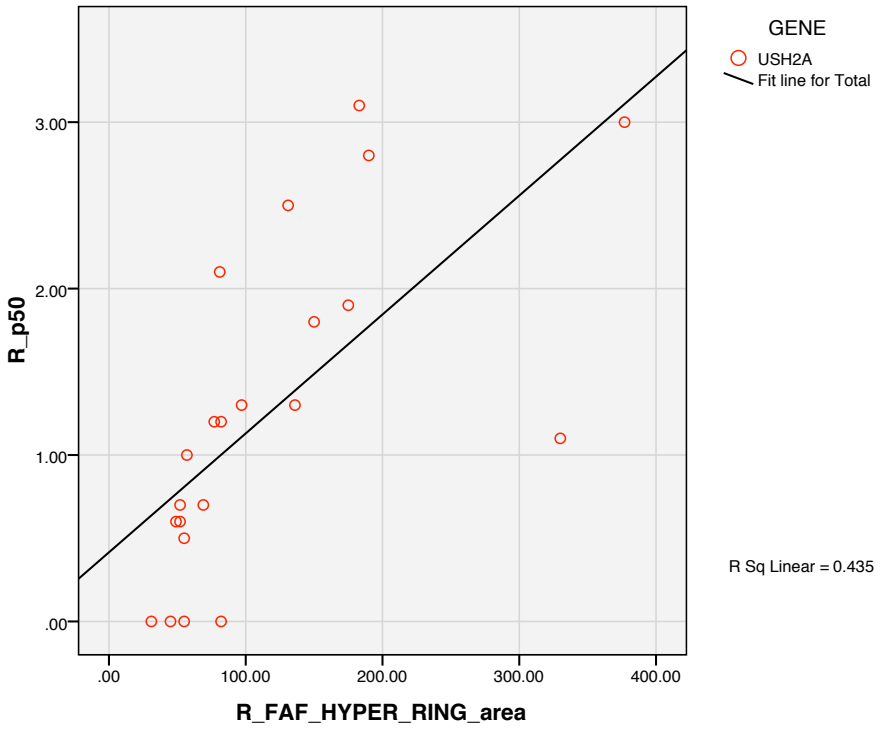

FIGURE 8.36: Scattergraph showing relationship and regression line of AF ring area vs p50 for individuals with a molecular diagnosis of *USH2A* with ERG data who manifested AF rings

The sample used were USH2 affected individuals with documented AF ring area of less than 600 degrees squared. One individual from this subset was excluded as they were an outlier (NCUS 110, Family 31) with a ring area much larger (1300 degrees squared) than the rest of this sample, the next largest ring area being 568 degrees squared. Of note, this outlier did not have a confirmed molecular diagnosis despite screening of the nine Usher genes.

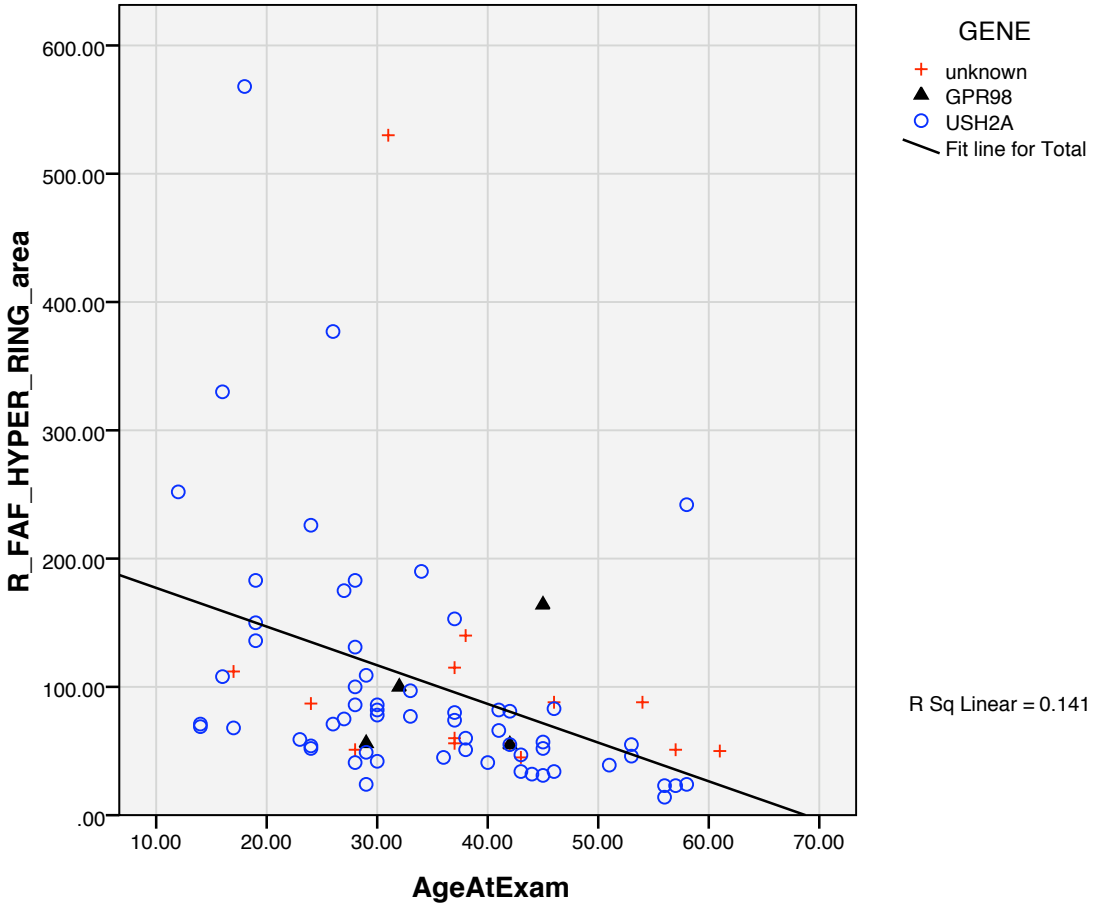

FIGURE 8.37: Scattergraph and linear regression line showing age vs. AF ring area for molecular groups with an USH2 phenotype

The regression model for this subset (Figure 8.37) was y=-2.694x + 206.668 (r2=0.141, 77 d.f., P <0.001). The model suggested that age as a variable may account for 14% of the decline in ring size seen. The rate of decline in ring size for per year for this model was 2.7 degrees squared per year (95% confidence intervals 1.2 - 4.2). The regression model suggested a ring area of 206.7 degrees squared (95% confidence intervals 143.3 - 270.0) when age=0 (P=0.0001).

The above subset was further reduced in size and genetic heterogeneity by only including individuals with USH2 and the *USH2A* molecular subtype, which improved the fit of the model.

Linear regression model for *USH2A* genotype: Age vs. AF ring area

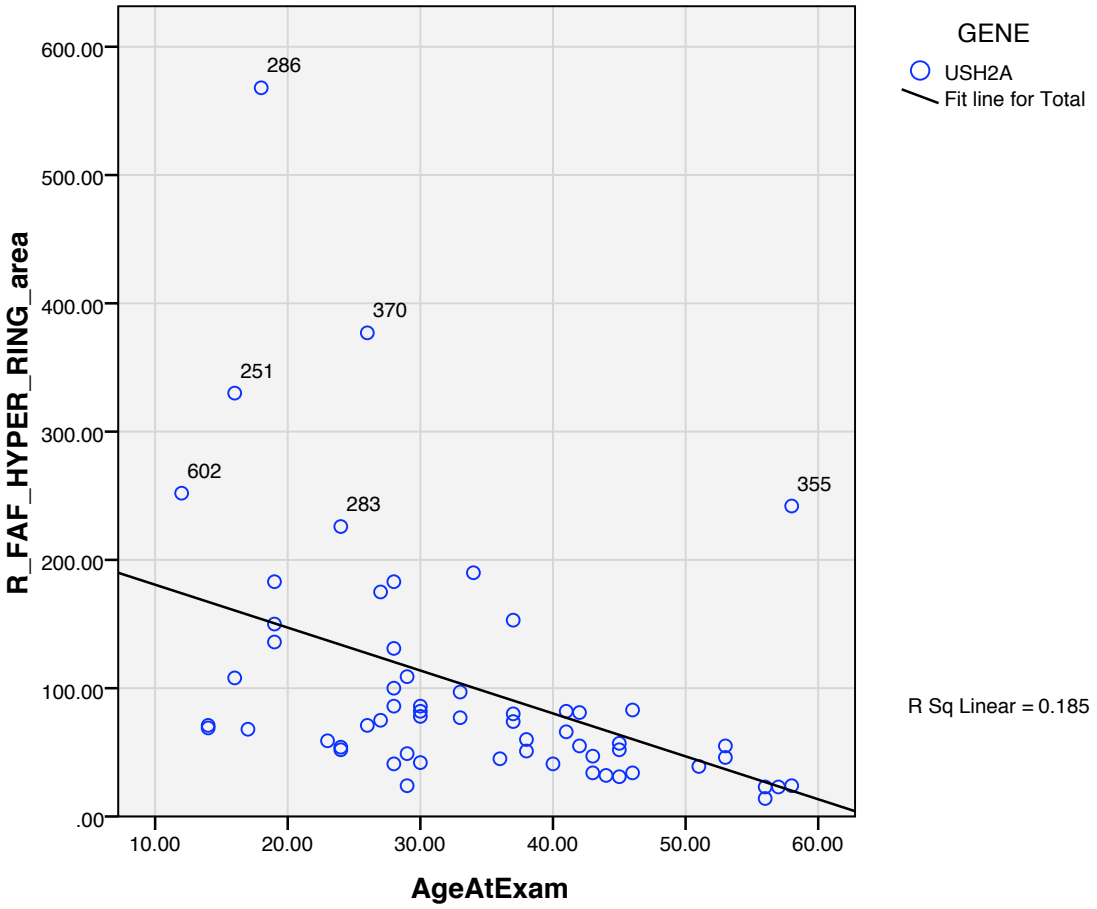

FIGURE 8.38: Scattergraph and linear regression line showing age vs. AF ring area and regression line for USH2A molecular group

Figure 8.38 shows the regression line through the data points. The model for the *USH2A* molecular subset was y=-2.895x + 212.412 (r2=0.185, 58 d.f., P <0.001). This model was a better fit for the data, that the previous model including individuals with a molecular diagnosis of *GPR98* or unknown genotype. The regression model suggested that age as a variable, may account for 19% of the decline in ring size seen and that ring size may decrease by 3 degrees (95% confidence intervals 1.3 - 4.5) squared per year. The regression model suggested a ring area of 212.4 degrees squared (95% confidence intervals 146.6 - 278.2) when age=0 (P=0.0001).

Age vs. AF ring area in *MYO7A*

Due to small sample size no statistically significant correlation or regression analysis was identified in the above subgroups. Figure 8.39 shows the scatterplot of age vs. AF ring area. Although statistically inconclusive, it is worth remarking that unlike the *USH2A* molecular group, the *MYO7A* group appear to show a positive correlation, that is larger ring sizes are noted in older individuals. Note the magnitude of the y-axis has changed to reflect the larger AF ring areas seen in this group.

Figure 8.37 shows a similar trend for *GPR98* molecular group, however as all points lie close to the *USH2A* cluster and regression line it would be unwise to make assumptions regarding trends in this small group.

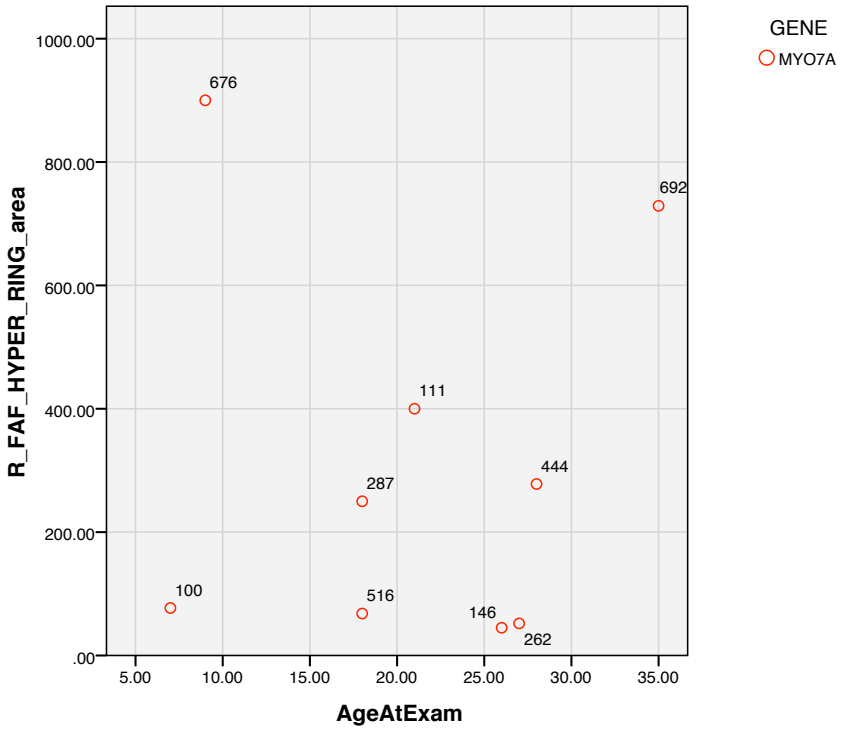

FIGURE 8.39: Scattergraph showing age vs. AF ring area and regression line for *MYO7A* molecular group

8.4.6 Poor AF signal precluding image acquisition

NCUS ID	Family ID	Diagnosis	Age	Disease duration	LogMAR VA in BEST eye	GVF V4e total in BEST eye	HRR test	HRR RG	HRR BY	CMO in either eye	GENE	Allele1	Allele1 path	Allele2	Allele2 path
578	161	USH1	44	36	0.46	63	abnormal	strong	strong	NO CMO	MYO7A	p.Arg669X	4	p.Lys542GlnfsX5	4
257	80	USH1	4		0.56		normal	normal	normal	NO CMO	MYO7A	p.Cys31X	4	p.Arg1883Gln	3
500	143	USH1	41	31	0.94	61	abnormal	strong	strong	NO CMO	MYO7A	p.Trp1431X	4	p.Ala826Thr	3
206	65	USH1	57	49	0.58	48				NO CMO	MYO7A	p.Tyr2015His	2.5	p.Tyr2015His	2.5
93	28	USH1	36	27	2.7	295	unable	unable	unable		MYO7A	c.3504-1G>C	4	p.Leu1858Pro	3
68	21	USH1	28	19	0.42	341	abnormal	mild	strong	CMO	MYO7A	p.Gly214Arg	3	p.Arg212His	3
182	49	USH1	44	38	1.3	0	unable	unable	unable	NO CMO	MYO7A	p.Pro2124LeufsX5	4	p.Arg1240Trp	3
292	87	USH1	5	1		14462	normal	normal	normal		PCDH15	p.Gly942Valfs22X	4	p.Gly942Valfs22X	4
311	92	USH2	16			19232									
193	60	USH2	53		0.3		abnormal	strong	strong	CMO	USH2A	His308SerfsX16	4	IVS47+1G>C	4
520	149	USH2	44	16	0.22	2398	normal	normal	normal	NO CMO					
385	111	USH2	54	37	0.18	270	abnormal	mild	strong	NO CMO	USH2A	p.Glu3305ArgfsX41	4	p.Asn346His	3
271	82	USH2	31	7	-0.09	300	abnormal	strong	strong	CMO	MASS1	p.Arg4802X	4		
631	169	USH2	15		0.3		abnormal	medium	medium	NO CMO					
312	92	USH2	12				normal	normal	normal						
82	26	USH3	48	37	2.7	0	unable	unable	unable	NO CMO	USH3A	p.Asn48Lys	3	p.Asn48Lys	3

FIGURE 8.40: Table listing details of individuals with poor signals on AF imaging

Figure 8.40 shows the clinical characteristics of the 16 individuals in whom poor AF precluded analysis of features. The majority of poor signal AF images precluding image acquisition were due to advanced disease (n=14) and two young individuals (both aged under 5 years), may have been influenced by difficulty in test cooperation.

The median age for this group was 38.5 years and most had poor VA (median logMAR 0.46), only four individuals had normal colour vision.

8.5 Discussion of results - central retinal function

8.5.1 VA summary

Data from this large prospective cohort study show that VA was significantly different between the two largest clinical groups USH1 and USH2.

VA - differences between USH1 and USH2

When considering median VA (without making allowances for age) the USH1 group were found to have significantly worse VA than the USH2 group, despite the latter having a significantly older median age. This is a significant finding and on its own would be sufficient to conclude that USH1 carries a worse visual prognosis than USH2.

To interrogate this relationship further, linear regression models were constructed to account for the effects of both age and disease duration. It is important to appreciate that as this data was from an observational cohort study, not longitudinal, the regression models should not be used to attempt to predict an individuals' VA in the future, as this would assume the rate and character of decline within each (genetically heterogeneous) clinical group is the same. They can however be used to make generalisations and to characterise apparent relationships from the data collected.

The apparent rate of decline in VA extrapolated from the cohort data suggested that this was similar between USH1 and USH2, however for a given age, VA was worse in USH1 compared to USH2 (significant difference in the elevation of regression lines).

It is possible that this difference in age vs. VA between USH1 and USH2 could be explainable by the earlier age of onset of visual symptoms in the USH1 group reported in the previous chapter? To answer this question, VA was modelled against disease duration, rather than age. The results suggest that despite efforts to correct for the different age of onset (on an individual basis) the USH1 group still appeared to have worse VA for a given age, as demonstrated by the statistically significant difference between the elevation of regression lines for disease duration vs. VA.

There are three possible explanations for this. Firstly that this result was achieved by chance, which statistically would be expected to occur in 0.14% of cases. Secondly assuming that the variable 'disease duration' represents an accurate representation of the length of time since the onset of retinal symptoms, this would imply that individuals with USH1 do not become aware of their symptoms until a relatively later stage compared to USH2, then declines at a comparable rate between both groups. Thirdly, as the variable for disease duration was derived from subjective data it is open to bias (some possible reasons for this are discussed in the summary section of the last chapter) it is possible that there was a difference in the subjective reporting of first visual symptoms between the USH1 or USH2 groups, such that ether USH1 reported symptoms later or USH2 reported symptoms earlier.

VA - comparison between molecular groups

The comparison of molecular groups showed that the VA and age in those with a molecular diagnosis of one of the four USH1 genes *MYO7A, USH1C, CDH23* and *PCDH15* was similar. Due in part to the small numbers in the above molecular groups, regression models were not statistically significant in interpreting the VA data controlling for the effect of age. The lack of significant difference in this sub-group of USH1 genes is informative. Due to the similar median ages of these four molecular groups, it suggests

that the VA prognosis is similar amongst these molecular groups, at least over the age ranges analysed. Due to the large number of private alleles and consequent allelic heterogeneity, no conclusions can be drawn regarding the VA within each of the molecular groups *MYO7A, USH1C, CDH23* and *PCDH15* groups.

Due to the much larger numbers in the largest molecular group *USH2A*, an attempt to reduce some of this allelic heterogeneity was made by performing sub-group analysis between individuals who carried the common p.Glu767SerfsX2 mutation in *USH2A*. As most of the p.Glu767SerfsX2 allele sub-group carried this allele with another disease causing change (only 7 individuals from 6 families were homozygous for p.Glu767SerfsX2) it does not negate the effect of allelic heterogeneity within the *USH2A* group, however it does represent an attempt to control for it. Comparison between those that carried the allele (n=61) and those that did not (n=56) suggesting that the VA phenotype in the p.Glu767SerfsX2 subgroup was not distinguishable from the remainder of the *USH2A* group, which represents an important finding.

VA - rate of decline in VA observed

The rate of deterioration in VA implied from observational data in this study was similar for the entire cohort and remained statistically similar after interpreting the data following subdivision on the basis of clinical subtype (USH1 vs USH2) and within the largest molecular group, *USH2A*. This rate was equivalent to 0.01 logMAR units per year, which equates to loosing a line of VA every decade.

Notably the USH2 group VA data showed that visual acuity remained well preserved in most individuals through adult life, with logMAR=0.5 at age 60.5 years (from the USH2 regression line). Using the USH2 regression line to comment on VA the within the observed age ranges we can see that visual acuity is good at the age of 18.8 years (logMAR VA=0) explaining the modest deterioration in VA for USH2 over adult life.

Although most of the USH1 VA data in this study was from younger individuals, a significant difference in elevation of the USH1 regression line overall suggests that for a given age, the VA was worse, however this increment could not be quantified (the y-intercept for the USH1 regression line could not confidently be predicted).

LogMAR=0 is equivalent to a visual acuity of 20/20, and is generally accepted as representing the lower limit of 'normal' visual acuity. USH2 regression line predicts a value of 18.8 years when logMAR=0 (6/6 or 20/20 Snellen equivalent).

In the previous chapter, the median reported age of onset of visual symptoms in USH2 was 17 years of age, which equates to a VA level of -0.02 from the USH2 regression line.

A useful statistic that can be delivered to patients with Usher syndrome is that from the observational data in this study, half of those with USH1 (including its largest constituent molecular group *MYO7A*) maintained driving vision until their mid thirties, and this figure was much later for those with USH2 (including its largest constituent molecular group *USH2A*) at the mid-fifties. If is important to note that 'driving vision' to satisfy the DVLA also requires that the minimum standards are met for visual field size and sensitivity and not just based on VA.

8.5.2 Cystoid Macular Oedema

This prospective study found the prevalence of CMO to be 25% for the whole cohort with 38% (n= 14/38) of USH1 and 22% (n=27/125) of USH2. This difference was approaching statistical significance, dependent on the statistical test used with two-tailed Chi Squared Test P=0.04 and with Fisher?s exact test P=0.07.

An important finding was that there appeared to be no relationship between age and presence of CMO as a study group overall and also when comparing USH1 and USH2 groups separately. Moreover there was also there was no apparent relationship between the presence of CMO on OCT scans and reduced visual acuity.

Earlier reports based on clinical examination alone found the prevalence of CMO in Usher syndrome to be much lower 8% [177] and 9% [27]. The advent of OCT imaging suggested that many cases of CMO in Usher syndrome were sub-clinical A recent retrospective study did not assess visual acuity. but found a 25% incidence of CMO in 76 USH2 individuals which is comparable to the USH2 group incidence in this study. A small but detailed study using OCT in molecularly diagnosed USH2 cases found CMO in 1 of 3 *GPR98* patients and 6 of 10 *USH2A* cases. Interestingly they also noted that despite the presence of CMO, all cases maintained good visual acuity of 20/30 (0.18 logMAR) or better. Previous studies in to other forms of RP have identified that retinal thickness does not always correlate with visual acuity [178] [179].

The pathogenesis of RP-related CMO remains unclear. Various theories exist to explain the pathogenesis in RP. Increased vascular permeability from the outer and inner blood-retinal barriers have been reported [180] [181] and studies have considered the role of antiretinal antibodies [182].

Acetazolamide therapy has been studied and in some cases of RP and Usher syndrome whilst it has been shown to decrease retinal thickness, this has not been strongly associated with a commensurate increase in visual acuity [183][184][185][186].

In eyes without retinal dystrophy it has been shown that the presence of cystic changes at the fovea may develop in to partial of full thickness macular holes [187], and such changes have been reported in Usher syndrome as well as noted in one individual in this study and one rationale for treating CMO might be to reduce the risk of structural damage to the macular.

But it is interesting to note that the CMO seen in Usher syndrome and other forms of RP appears not to affect visual acuity as much as other causes of CMO such as diabetes and secondary to ocular inflammation, which likely reflects differences in the pathogenesis of this common pathological finding.

8.5.3 AF imaging

Lipofuscin is a naturally occurring fluorophore that is generated from the continual lysosymal degredation of photoreceptor outer segments by the retinal pigment epithelium (RPE). AF imaging provides a non-invasive method of visualisation of the distribution of lipofuscin across the poster pole of the eye enabling an *in vivo* method of assessing the functioning of the RPE/photoreceptor complex.

Previous studies have documented the presence of parafoveal rings of hyperfluoresent/high-density in individuals with a variety of retinal dystrophies including RP [188][188][189–191], X-linked retinoschisis, Lebers congenital amaurosis (LCA) [192], cone-rod dystrophies [193, 194] pigmented paravenous retinochoroidal atrophy (PPRCA)[195], and Bests disease[196].

Work carried out alongside this study, including a subset of individuals with USH2 from this study has documented a decrease in the size of hyperflorescent rings over time in a subset of individuals with RP and USH2[190], which was associated with a decline in visual fields and macular function as assessed by electroretinography. Interestingly similar rings have been noted to possibly increase in area with time, in cone-rod dystrophy, where the primary site of disease is at the macular area [191].

This study contributes the largest cohort of AF images in a cohort individuals with Usher syndrome, most of which also have a molecular diagnosis.

Foveal hyperfluorescence

Foveal hyperfluorescence was a common finding amongst those with Usher syndrome type 1 and 2. Its presence was associated with poorer visual acuity. CMO was a major cause for foveal hyperfluorescence, however foveal hyperfluorescence was also identified

in approximately half of the cases where CMO was absent. Qualitatively, the foveal hyperfluoresence in the presence of CMO was generally of a softer less dense nature (e.g. Figure 8.29 Panel B) but in those cases of advanced disease in the absence of CMO the hyperfluoresence was generally of contiguous areas of high density hyperfluorescence (e.g. Figure 8.29 Panel A).

Whilst foveal hyperfluorescent signals can be caused by CMO in some cases the source of the hyperfluorescent signal in those eyes without CMO is unclear. One possibility is that the high density signal may be due to the deposition of fluorescent material such as lipofuscin. High resolution OCT scans taken appeared to reveal an optically dense material in the inner retina corresponding to areas of high density AF signal seen. Foveal autofluorescence is masked my the macular pigment in a normal eye, another possibility to account for the hyerfluorescent signal might be loss of this masking effect. One observation was that many of the individuals with advanced disease and foveal hyperfluorescence had a history of CMO in the past.

Ring size

This study documents that amongst the cohort of Usher syndrome clinical subtypes. The presence of AF rings was associated with younger age and better visual acuity. Rings were seen in all three clinical subtypes and in all molecular groups identified, representing a novel finding.

In all clinical subtypes AF rings were associated with better visual acuity and younger age, suggesting that they are likely to occur earlier rather than later in the retinal pathogenesis of Usher syndrome.

The relationship between decreasing ring size with advancing age was demonstrated for the USH2 clinical or USH2A molecular groups, with linear regression, however no such relationship could be made amongst the USH1 or MYO7A groups. Figure 8.34 demonstrates a slight preponderance of larger ring areas for USH1, but this difference was not statistically significant nor could a significant correlation being achieved. With longitudinal follow up of these USH1 individuals with large AF ring areas, it will be interesting to see if their ring size increases or decreases with time.

Another intresting observation was that AF rings in the USH2 molecular subtypes (*USH2A* and *GPR98*) were geographically located within the vascular arcades, however for the USH1 molecular subtypes the AF rings were generally much larger and located anterior to the vascular arcades. Interestingly the AF rings seen in the family with an atypical phenotype due to the *USH1C* gene had larger AF rings, extending in to the retinal periphery.

Parafoveal hypofluorescence

Previous studies on foveal pathology in Usher syndrome have noted the presence of clinically atrophic foveal lesions or 'bull's eye' macular lesions which were more prevalent in USH2 compared to USH1 [177, 197]. This study has characterized the atrophic lesions further with AF imaging. The areas of parafoveal atrophy highlighted by AF are likely to represent areas of RPE +/- photoreceptor death and therefore visually significant.

The combination of central hyperfluorescene and perifoveal hypofluorescence could be described as a 'bull's eye' picture. Moreover these lesions were more commonly, but not exclusively seen in the *USH2A* molecular group.

Serial AF images in one individual (Figure 8.41) document increase in the area of parafoveal hypofluorescence over a period of 4 years. These features appear to be more common later on in the retinal disease process.

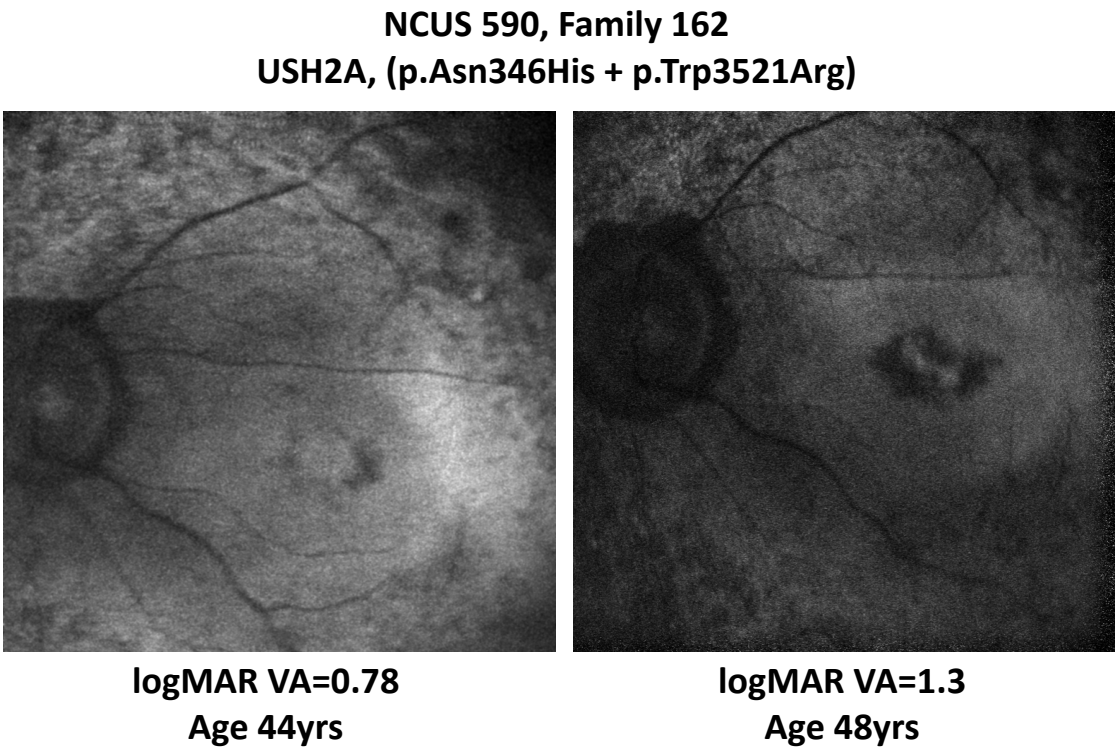

FIGURE 8.41: Serial AF images in the left eye of an individual with USH2 documenting significant progression of the area of parafoveal hypofluorescence over a 4 year period

The findings on autofluorescence in this study have demonstrated AF rings in all molecular subtypes, which is a common finding amongst RP and other forms of retinal dystrophy. The additional and frequent findings of foveal hyperfluorescence and parafoveal areas of hypofluorescence are much less common and whilst not pathognomic of Usher

syndrome appear to be more frequent in this disorder, which may suggest a common pathological aetiology in this disorder.

Chapter 9

Results - Peripheral retinal function

9.1 Visual field (VF) area

This chapter reports on the results of kinetic visual field testing using Goldmann visual fields. Three sizes of identical luminance were used to map the visual field at different levels of sensitivity. The largest target was V4e, the intermediate target was II4e and the smallest target I4e.

9.1.1 Left vs Right VF area

There was a high degree of left/right correlation between the visual field area recorded for each of the three isopters. The correlation coefficients for each of the three isopters were high (r=0.947 (largest), r=0.854 (intermediate), r=0.842 (smallest)) and all highly significant ($p<0.0001$) indicating a high degree of similarity between the visual fields in both eyes.

For the remainder of this chapter visual field analysis was undertaken using the value in the better eye (larger visual field area). This was similar to the analysis of visual acuity which analysed the better seeing eye.

9.2 VF area - regression analysis

When analysing the median visual field area in the better eye, there was no significant difference between USH1 and USH2 groups for any of the isopters (Mann Whitney test, P>0.3.

As visual field size is known to deteriorate with age this difference should be interpreted with caution as the median ages of these two groups were significantly different.

TABLE 9.1: Summary of linear regression analysis for age and disease duration vs. visual field data comparing USH1 and USH2 clinical groups. The gradient of the slopes and elevations of USH1 and USH2 regression lines were compared statistically. Each yes or no response is the answers to the question: "Is there a statistically significant difference between the USH1 vs. USH2 groups?"

		GRADIENT	ELEVATION
AGE	LARGEST (V4e)	no	yes
	INTERMEDIATE (II4e)	no	yes
	SMALLEST (I4e)	no	no

		GRADIENT	ELEVATION
DISEASE DURATION	LARGEST (V4e)	no	no
	INTERMEDIATE (II4e)	no	no
	SMALLEST (I4e)	no	no

To account for age, linear regression models were constructed for age vs. visual field area (calculated in degrees squared) and then using the natural log of visual field area. Due to the better fit of data for the logarithmic models, these results are presented.

A summary of the regression analysis is presented in Table 9.1.

When using linear regression models to predict visual field size as a function of *disease duration*, there was no significant difference between USH1 and USH2 groups. Graphically this can be seen by the similar gradient and elevations of the USH1 and USH2 regression lines.

When using linear regression to to predict visual field size as a function of *age*, only the *elevation* of the USH1 and USH2 regression lines for the largest and intermediate isopter sizes were statistically different, but for the smallest isopter the difference between the two groups was not.

As the gradient for all regresion models was statistically similar this suggests that the *rate* of observable decline was similar in USH1 and USH2 groups was also similar.

The following figures represent the regression plots against age and disease duration. Each page represents the same isopter size.

The regression equations are given below for USH1 and USH2 for the largest V4e isopter.

USH1: y= -0.097x + 10.021 (r2=0.478 , 41 d.f., P <0.0001)

95% confidence intervals for SLOPE (-0.129 to -0.065)

95% confidence intervals for Y-INTERCEPT (9.049 to 10.994)

USH2: y= -0.086x + 10.767 (r2=0.418 , 117 d.f., P <0.0001)

95% confidence intervals for SLOPE (-0.105 to -0.068)

95% confidence intervals for Y-INTERCEPT (9.989 to 11.545)

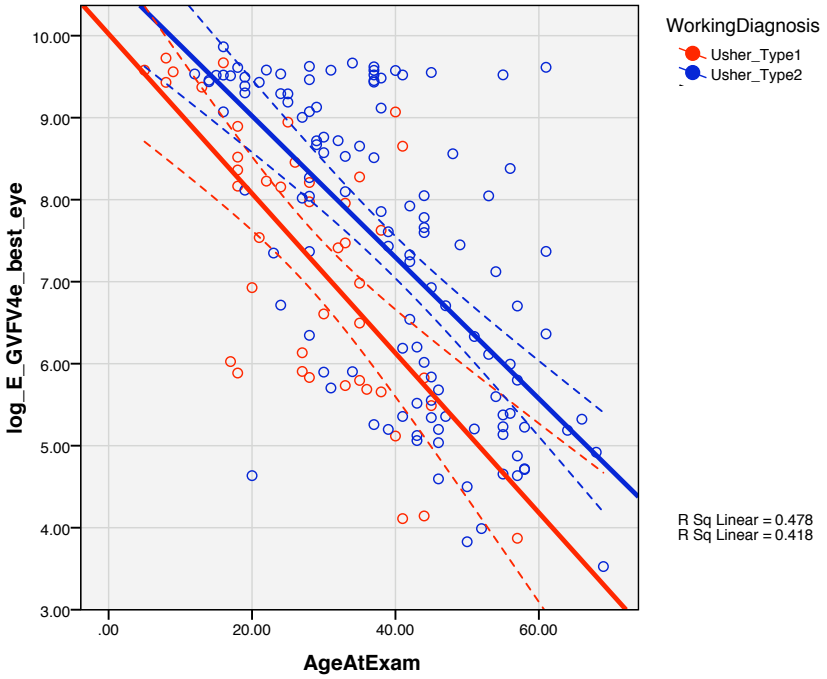

FIGURE 9.1: Scattergraph of Age vs. natural log of VF size for the LARGEST isopter (V4e) in the better eye for USH1 and USH2 groups. The linear regression models provided a significant fit for the data and are shown for USH1 and USH2, with their respective 95% confidence intervals shown by broken lines. The regression lines have the same gradient. The dotted lines either side of the regression lines do not overlap because the elevations of the lines are significantly different

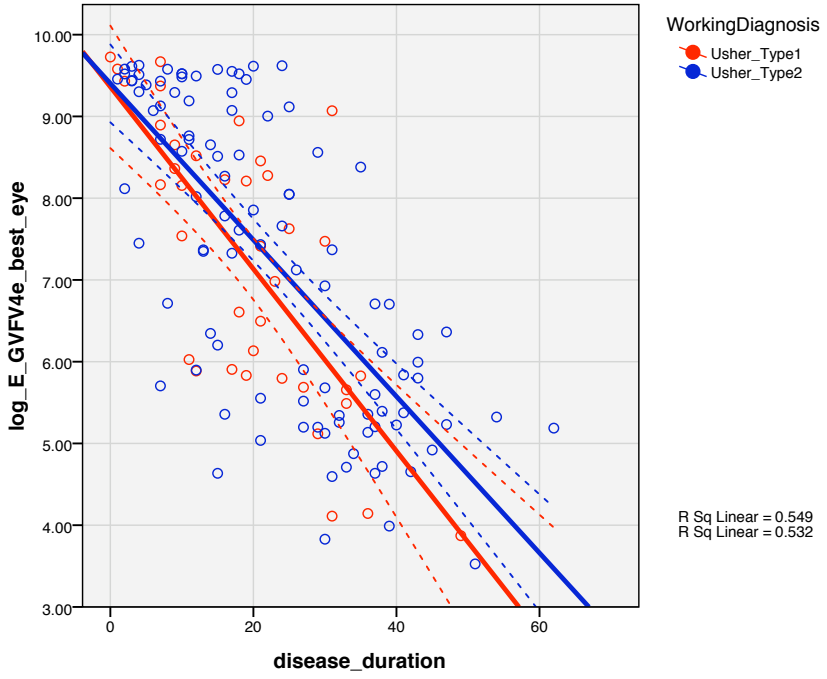

FIGURE 9.2: Scattergraph of DISEASE DURATION vs natural log of VF size for the LARGEST isopter (V4e) in the better eye for USH1 and USH2 groups. The linear regression models provided a significant fit for the data and are shown for USH1 and USH2, with their respective 95% confidence intervals shown by dotted lines. The regression lines have the same gradient and elevation resulting in significant overlap of the broken lines for each regression line.

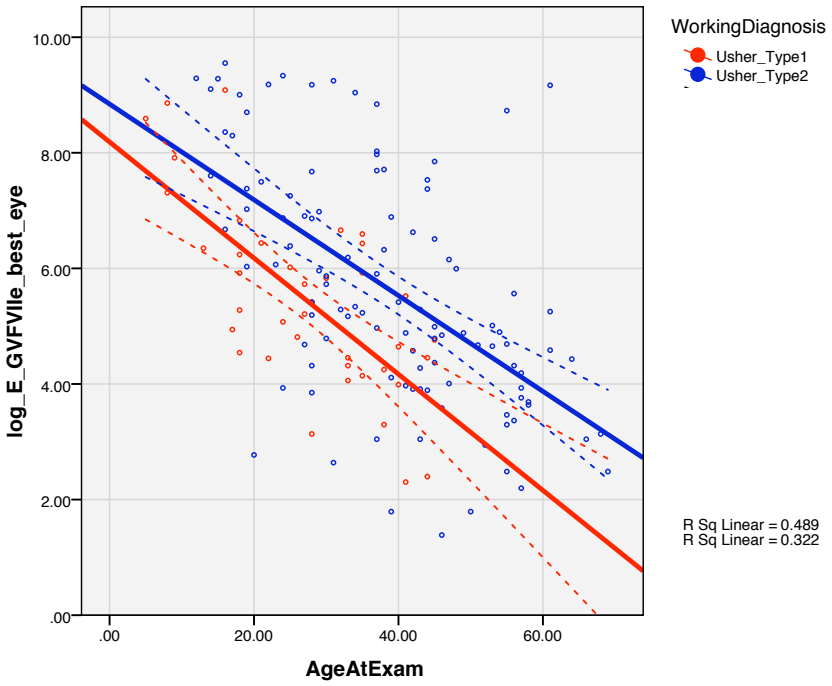

FIGURE 9.3: Scattergraph of Age vs. natural log of VF size for the INTERMEDIATE SIZE isopter (II4e) in the better eye for USH1 and USH2 groups. The linear regression models provided a significant fit for the data and are shown for USH1 and USH2, with their respective 95% confidence intervals shown by broken lines. The regression lines have the same gradient. The dotted lines either side of the regression lines do not significantly overlap because the elevations of the lines are significantly different

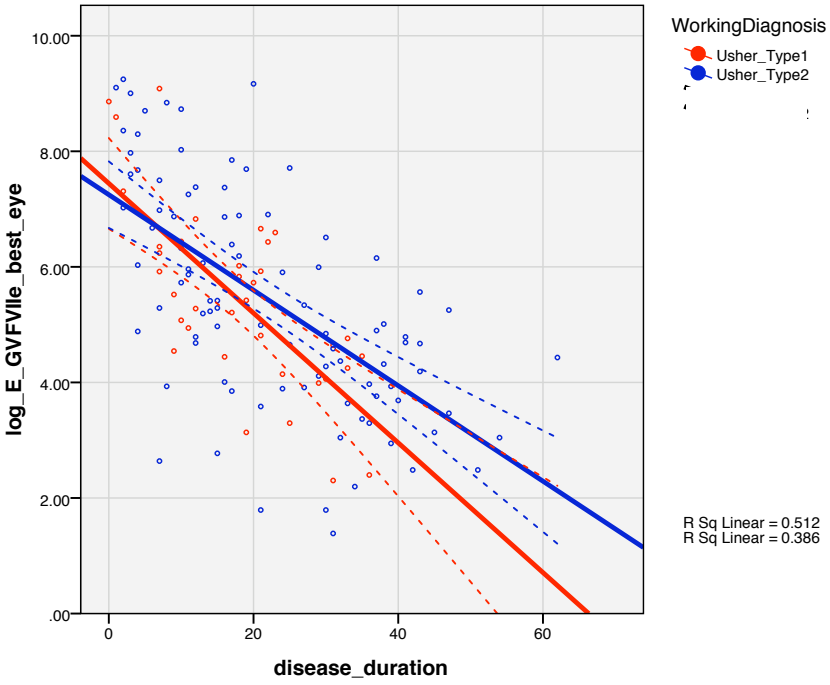

FIGURE 9.4: Scattergraph of Disease duration vs. natural log of VF size for the INTERMEDIATE SIZE isopter (II4e) in the better eye for USH1 and USH2 groups. The linear regression models provided a significant fit for the data and are shown for USH1 and USH2, with their respective 95% confidence intervals shown by broken lines. The regression lines have the same gradient and elevation resulting in significant overlap of the broken lines for each regression line.

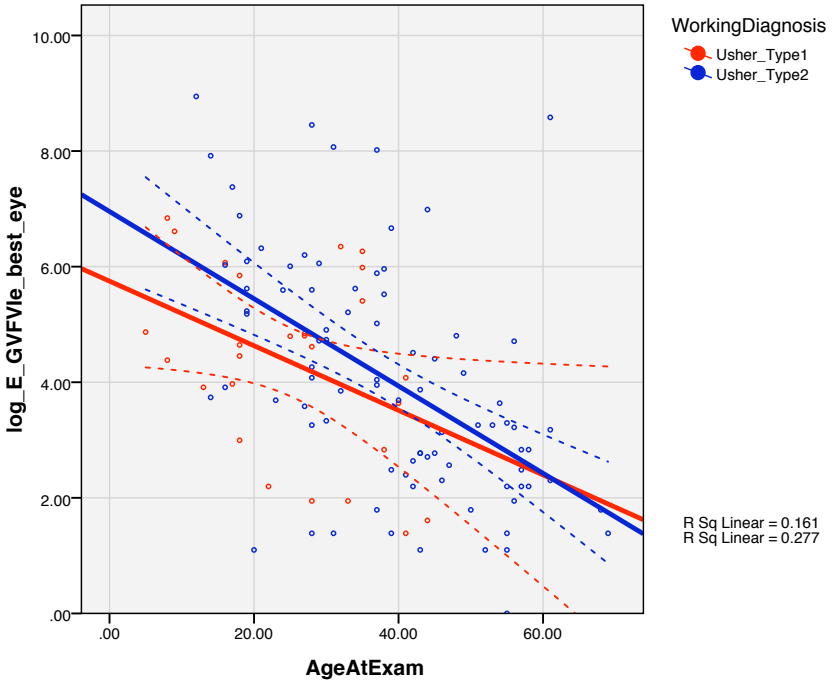

FIGURE 9.5: Scattergraph of Age vs. natural log of VF size for the SMALLEST isopter (I4e) in the better eye for USH1 and USH2 groups. The linear regression models provided a significant fit for the data and are shown for USH1 and USH2, with their respective 95% confidence intervals shown by broken lines. The regression lines have the same gradient and elevation resulting in significant overlap of the broken lines for each regression line

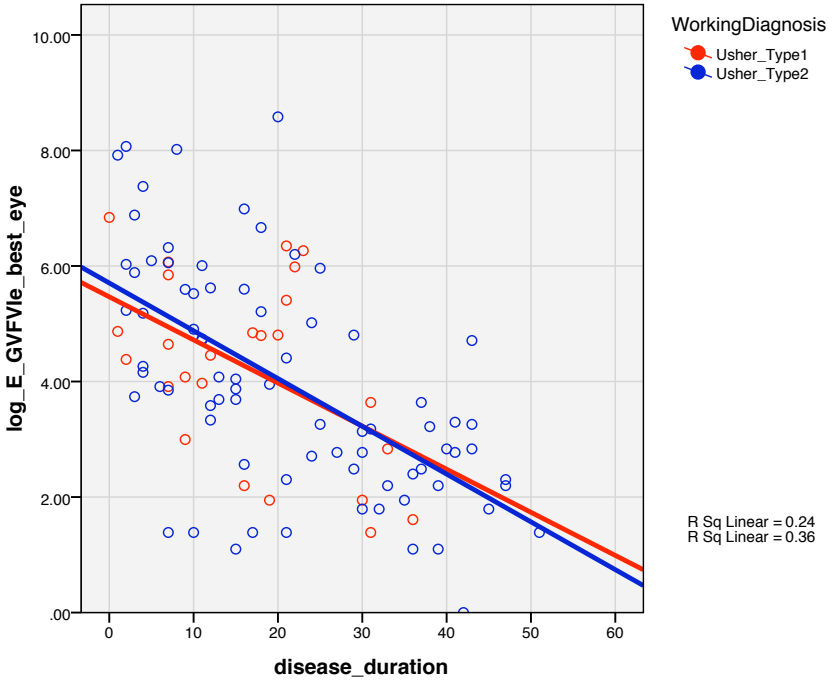

FIGURE 9.6: Scattergraph of Disease duration vs. natural log of VF size for the SMALLEST isopter (I4e) in the better eye for USH1 and USH2 groups. The linear regression models provided a significant fit for the data and are shown for USH1 and USH2. The 95% confidence intervals are not shown as the regression lines run a visibly similar course.

9.2.1 Molecular subtypes

There was a highly significant difference between the elevation of the regression lines (P<0.0001) but there was no statistically significant difference in their gradients.

Linear regression models were significant fit for the data and were effective at predicting visual field from age.

The lines were a better fit for *MYO7A* (r2=0.78 , 18 d.f., P <0.001) than for *USH2A* (r2=0.47 , 89 d.f., P <0.001).

If the overall elevations were identical, there is a less than 0.01% chance of randomly choosing data points with elevations this different.

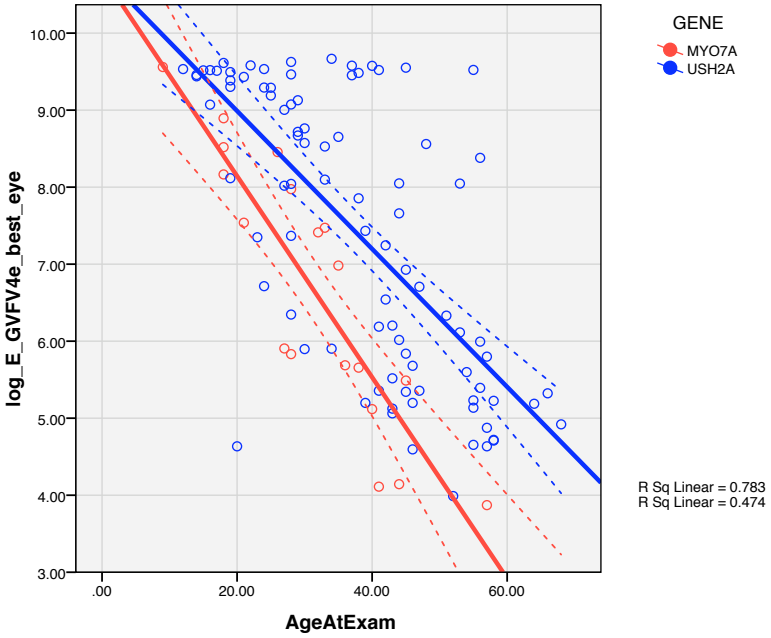

FIGURE 9.7: Regression models for age vs. visual field area for the LARGEST V4e isopter

9.3 Survival analysis

To quantify the data in terms of a tangible area of visual field size, the area of 10 degrees squared was taken as an end point. Survival curves were plotted for USH1 and USH2 groups as well as for their largest constituent molecular groups, *MYO7A* and *USH2A* respectively. The median survival point represents the age at which 50% of each population reduce the area of visual field to 10 degrees squared.

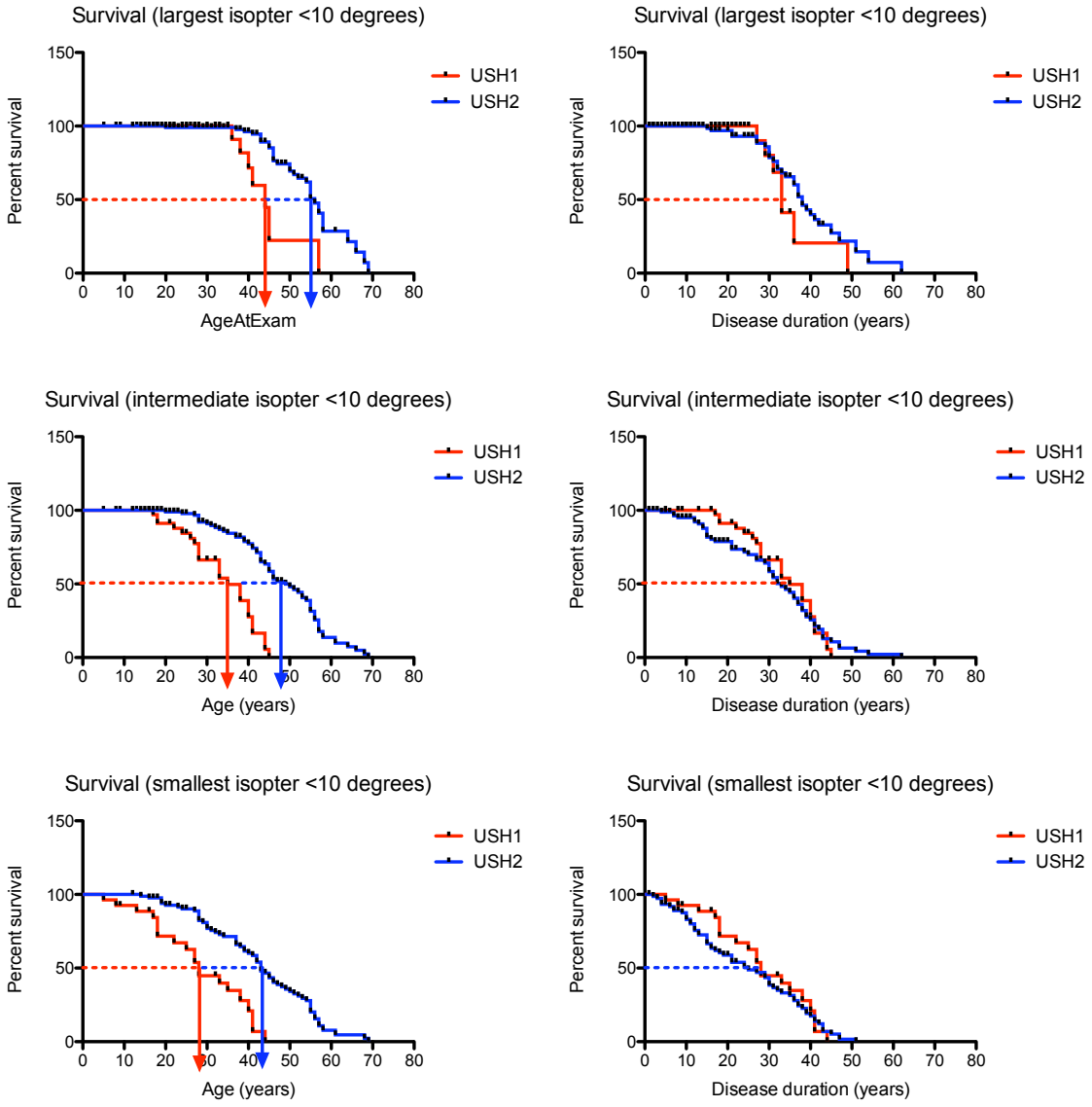

FIGURE 9.8: Survival curve analysis for USH1 and USH2 clinical groups. The end point used was a visual field size of 10 degrees squared or less. The three plots on the left represent the survival curves using the variable AGE and the plots on the right represent the variable DISEASE DURATION. The median survival points are indicated with dotted lines. The vertical arrows represent the median survival points for the two groups, but are only shown where the curves were statistically different from each other (P <0.0001)

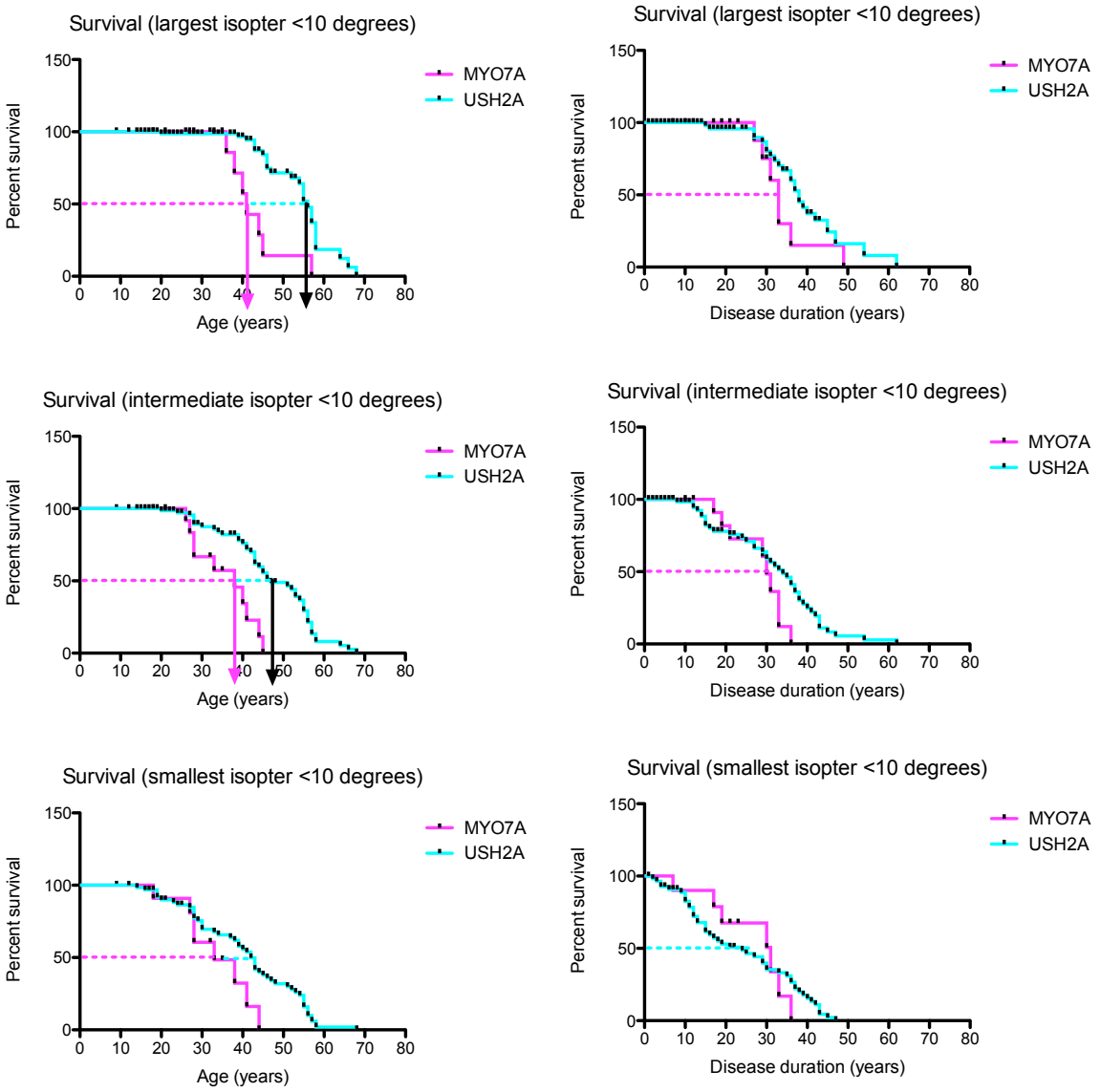

FIGURE 9.9: Survival curve analysis for USH2A and MYO7A molecular groups. The end point used was a visual field size of 10 degrees squared or less. The three plots on the left represent the survival curves using the variable AGE and the plots on the right represent the variable DISEASE DURATION. The median survival points are indicated with dotted lines. The arrows represent the median survival points for the two groups, but are only shown where the curves were statistically different from each other (P <0.0001)

9.4 Visual fields summary

TABLE 9.2: Summary of median survival points (age in years) for the time taken for USH1 and USH2 groups to drop their field size to 10 degrees squared

ISOPTER SIZE	USH1 (years)	USH2 (years)	Are curves significantly different?
LARGEST	44	56	YES P<0.0001
INTERMEDIATE	35	49	YES P<0.0001
SMALLEST	28	43	YES P<0.0001

TABLE 9.3: Summary of median survival points (age in years) for the time taken for *MYO7A* and *USH2A* molecular groups to drop their field size to 10 degrees squared

ISOPTER SIZE	MYO7A (years)	USH2A (years)	Are curves significantly different?
LARGEST	41	56	YES P<0.0001
INTERMEDIATE	38	47	YES P<0.0001
SMALLEST	33	42	NO (P=0.00502)

Previous studies comparing USH1 and USH2 clinical groups have documented that visual fields are worse for a given age in USH1 compared to USH2 [198]. Two longitudinal studies done on small numbers of molecularly subtyped individuals with *USH2A* reported that the rate of longitudinal visual field loss is similar in Usher syndrome to RP, and that visual field loss in USH2 appeared to correlate better with disease duration than with age [199][28].

Although this study is an observational cohort study and not longitudinal in design, the linear regression data suggests that for a given age, USH2 have a larger visual field area than USH1 for the larger targets, but for smaller targets this difference is less significant.

The survival curves support this data, also found a highly significant difference between USH1 and USH2 groups. The time taken for half of each cohort to drop their visual field size to 10 degrees squared occurred a decade earlier in USH1 (mid-forties) than USH2 for the largest isopter. This remained the case when repeating the analysis for the *MYO7A* and *USH2A* molecular groups. Statistically the difference between these two molecular groups was highly significant for the largest and intermediate isopter, and borderline significance (P=0.00502) for the smallest isopter.

The data from the survival curve analysis is of use when counselling patients with Usher syndrome.

Chapter 10

Non Usher families

10.1 Syndromic families with non-USH

10.1.1 Family with sector RP and hearing loss due to mutations in *USH1C*

This section reports Family 142, who were recruited in to the study. The index case had received a diagnosis of USH2 previously. As additional tests were performed outside the remit of the NCUS, the methodology relating to the relevant aspects of clinical analysis of this family is described in this section rather than in the main body of clinical methods.

Electrodiagnostic and Fine Matrix Mapping methods

(Dr Anthony Robson, Dr Graham Holder, Mr V Luong) Pattern and full-field electroretinograms (ERGs) were performed to incorporate existing International standards [200, 201]. One of the siblings underwent photopic and scotopic fine matrix mapping (FMM) performed according using previously described protocol [202–206]. The matrix of retinal luminance sensitivity at each test location was used to generate a surface or contour plot showing the size and location of luminance sensitivity gradients across the grid (contour steps: 0.1 log unit). The numerical matrices and luminance sensitivity contour plots were superimposed onto the AF images with custom image-analysis software. Accurate superimposition was achieved by aligning anatomic landmarks, such as the center of the optic disc and the fovea, with the corresponding perimetry landmarks, such as the center of the blind spot and fixation. Scotopic FMM was performed over identical retinal locations following pupil dilation (tropicamide 1%) and 40 min dark

adaptation. Fixation was monitored continuously. Photopic and scotopic threshold values were compared with those obtained in a control group of 10 normal individuals [189].

Audiovestibular phenotyping

(Dr Nell Rangesh and Prof Linda Luxon)

Audiological evaluation included pure tone audiometry, tympanometry, stapedial reflexes, transient evoked otoacoustic emissions recordings and auditory brain stem evoked responses using standard protocol [207][208][209][210] [207–210]. Subjective pure tone air and bone conduction thresholds were determined at 0.25, 0.5, 1, 2, 4, and 8 kHz using a GSI 61 audiometer (Guymark, Cradley Heath, UK) TDH39 supra aural earphones (Sennheiser U.K Ltd, High Wycombe, UK) and the British Society of Audiology (BSA) recommended procedure. Audiometric descriptors of mild, moderate, severe and profound hearing loss were calculated according to BSA descriptors (2004). Vestibular function was evaluated with infra-red videonystagmography, a rotary chair system (Neurokinetics, Pittsburgh USA) and vestibulo-ocular reflex responses (VOR) [209]. Binaural bithermal caloric testing was undertaken using the BSA recommended protocol (1999) and departmental normative data for peak slow component velocity were used to determine normality. Canal paresis (>17%) and directional preponderance (>16%) were calculated according to Jongkees formulae (Jongkees 1953) and vestibular hypofunction was defined by total eye velocity less than 78 degrees/sec. All parameters were defined by departmental normative data. Bilateral horizontal semicircular canal function was assessed using sinusoidal (60 degrees peak velocity and 0.05 Hz) and step rotation testing (acceleration 0-60 degrees/sec constant velocity in <1 sec.). A gain of less than 0.23 in either test or a time constant of less than 8 seconds on impulsive rotation was considered vestibular hypofunction.

Additional Molecular methods

Variants were annotated according to accession number GenBank:NM 153676.3. Analysis of putative splice site sequence changes was performed using the online splice site prediction software.

Clinical history

Family 142 consisted of the index case (NCUS 497) aged 42yrs, her affected sibling (NCUS 505) 40 yrs old and their parents, both of whom were of Caucasian European

origin. Their parents were both in their seventies and although they were not clinically examined they did not suffer from any visual problems. Molecular data were available from all four family members.

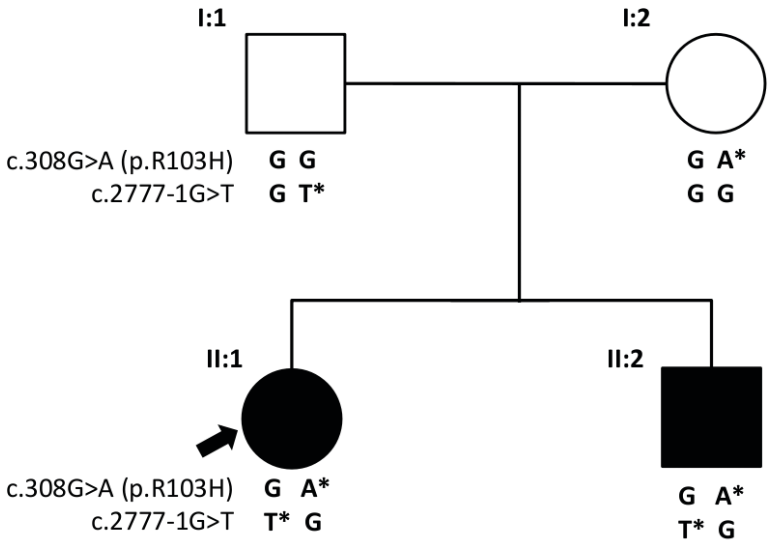

FIGURE 10.1: Pedigree of sector RP family with hearing loss. Black symbols represent affected siblings. The index case is indicated with a solid arrow. Mutations are indicated with a star

Both siblings were diagnosed with severe hearing loss at four years of age and had worn hearing aids since that time. Language acquisition and speech development were normal. There was no history of delay in motor milestones, consistent with normal vestibular function in infancy. When last examined, the affected siblings were 42 years and 40 years old and maintained good central visual acuity and color vision (Table 10.1).

TABLE 10.1: Table summarizing ophthalmic clinical findings of the two affected siblings NCUS 497 and 505

AFFECTED INDIVIDUAL	NCUS 497	NCUS 505
Gender	Female	Male
Age at examination	42	40
Age of onset of subjective nightblindness	Not aware of nightblindness	39
Age of onset of subjective visual field loss	22	Not aware of visual field loss
Best corrected logMAR visual acuity (right eye)	0.1	0.03
Best corrected logMAR visual acuity (left eye)	0.02	0.3
Color Vision (HRR plates)	Normal	Normal
Lens opacity (cataract)	Mild nuclear sclerotic cataract (not visually significant)	Trace of posterior subcapsular catarat (not visually significant)
Vitreous detachment	Yes	Yes

The elder sibling (NCUS 497) noticed visual field loss from age 22 years, but denied any night blindness at age 42 years of age. Her younger brother (NCUS 505) experienced no visual symptoms until the age of 39 years, when he became aware of night blindness and difficulties adjusting to changed lighting conditions, which prompted ophthalmic review. Unlike his elder sister, he was not aware of any visual field loss when last examined aged 40 years.

Despite their unusual sectorial retinal disease , the siblings had previously been diagnosed with Usher syndrome type 2 and had initially been recruited to a comprehensive clinical and molecular study of Usher syndrome.

Retinal phenotype

Both siblings demonstrated bilateral symmetrical areas of retinal and retinal pigment epithelial change restricted to the inferior fundus. In the more severely affected index case, the changes extended to the nasal retina (Figure 10.2). FAF imaging (Figure 10.2 middle row) revealed a thick curvilinear band of hyperfluoresence, which appeared to separate preserved central fluorescence from the abnormal areas of hypofluoresence corresponding to the abnormal areas of intraretinal pigment migration seen clinically (Figure 10.2 top row).

Interestingly this prominent hyperfluorescent band did not correspond to any obvious visible changes on fundoscopy. The inferior and nasal abnormal retinal areas corresponded to the superior and temporal areas of visual field loss noted on kinetic perimetry respectively. Bilateral vitreous separation and subclinical lens opacities were noted in both siblings, which were not visually significant. The photopic and scotopic sensitivity was tested psychophysically at specific retinal locations in the index case (Figure 10.5). Retinal sensitivity was relatively preserved within the central area of preserved autofluorescence. The thick band of hyperfluorescence was associated with a gradient of retinal sensitivity change, with retinal sensitivity being abnormally elevated outside the band (Figure 10.5 4c, 4d).

Photopic fine matrix mapping revealed normal thresholds over central (Figure 10.5) and the innermost eccentric locations (Figure 10.5). Thresholds increased gradually with eccentricity (within 2 SDs of the normal mean) and showed a steep gradient of sensitivity loss across the arc of high density (Figure 10.5). Cone system sensitivity showed the steepest gradient of loss over an area spatially associated with the hyperfluorescent arc seen on FAF imaging. Significant loss in rod system sensitivity occurred at a less eccentric location, internal to the arc (Figure 10.6 5d). Photopic thresholds peripheral to the arc of high density were elevated by approximately 2.2-2.6 log units (5.0-5.9

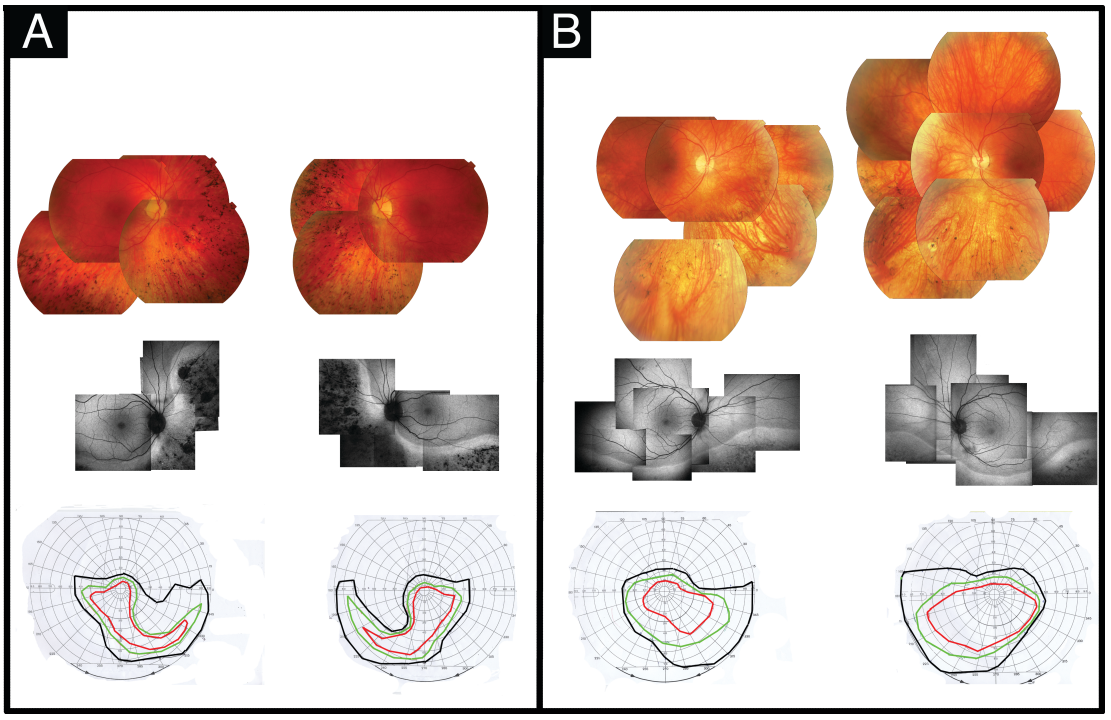

FIGURE 10.2: Composite of images from index case NCUS 497 (A) and NCUS 505 (B). In each panel images from the right eye are shown in the left-hand column and images from the left eye shown in the right-hand column. (top) Colour fundus photographs show bilateral symmetrical areas of retinal and retinal pigment epithelial changes restricted to the inferior and nasal areas of the fundus in both siblings. Retinal pigment epithelial (RPE) atrophy results in increased visibility of the underlying choroidal vasculature in affected areas, blood vessel attenuation and intraretinal 'bone-spicule' pigment migration. Outside these areas the blood vessels appeared to be of normal caliber. The fundus appearance is otherwise unremarkable (middle) Fundus autofluoresence imaging reveals a thick curvilinear hyperfluorescent band that appears to separate normal from abnormal retina. In both individuals the hyperfluorescent band runs outside the inferior vascular arcades. The band In the more severely affected index case NCUS 497 (A), takes a course nasal to the optic disc running superiorly in to the nasal retina, whereas in the less severely affected sibling NCUS 505 (B), the hyperfluorescent band and abnormal area is restricted to the inferior retina. In both siblings the abnormal areas are generally hypofluorescent with additional discrete areas of denser atrophy. (bottom) Goldmann visual fields relate to isopters V4e (largest target) in black, II4e isopter in green and I4e isopter (smallest target) in red. In the more severely affected index case NCUS 497 (A) there is a tongue of field loss in the mid-periphery of the superotemporal visual field, whilst in the less severely affected sibling NCUS 505 (B), only relatively minor visual field loss is evident in the superotemporal part of the visual field.

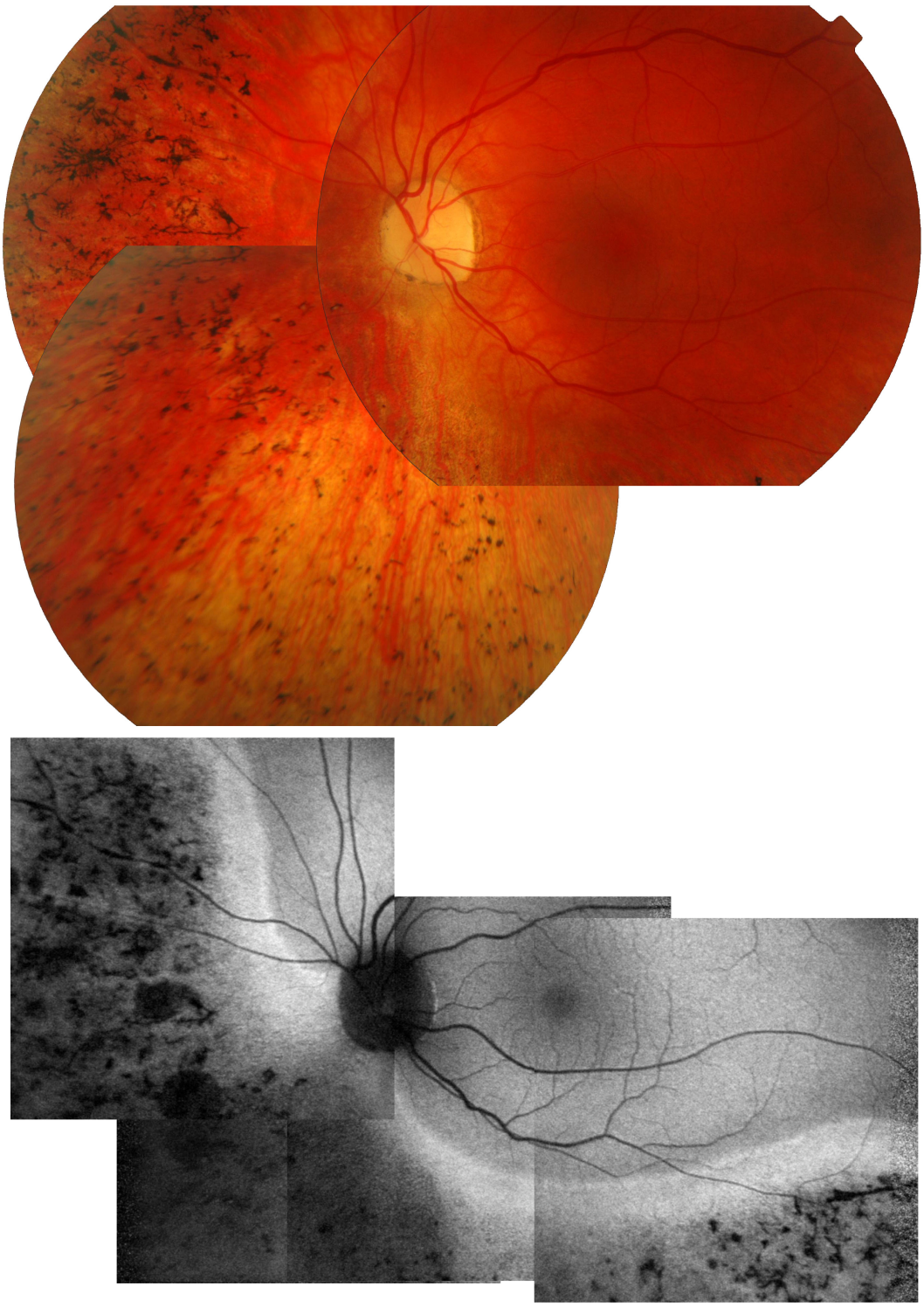

FIGURE 10.3: Left eye of Index case with colour fundus photos (above) and AF imaging (below)

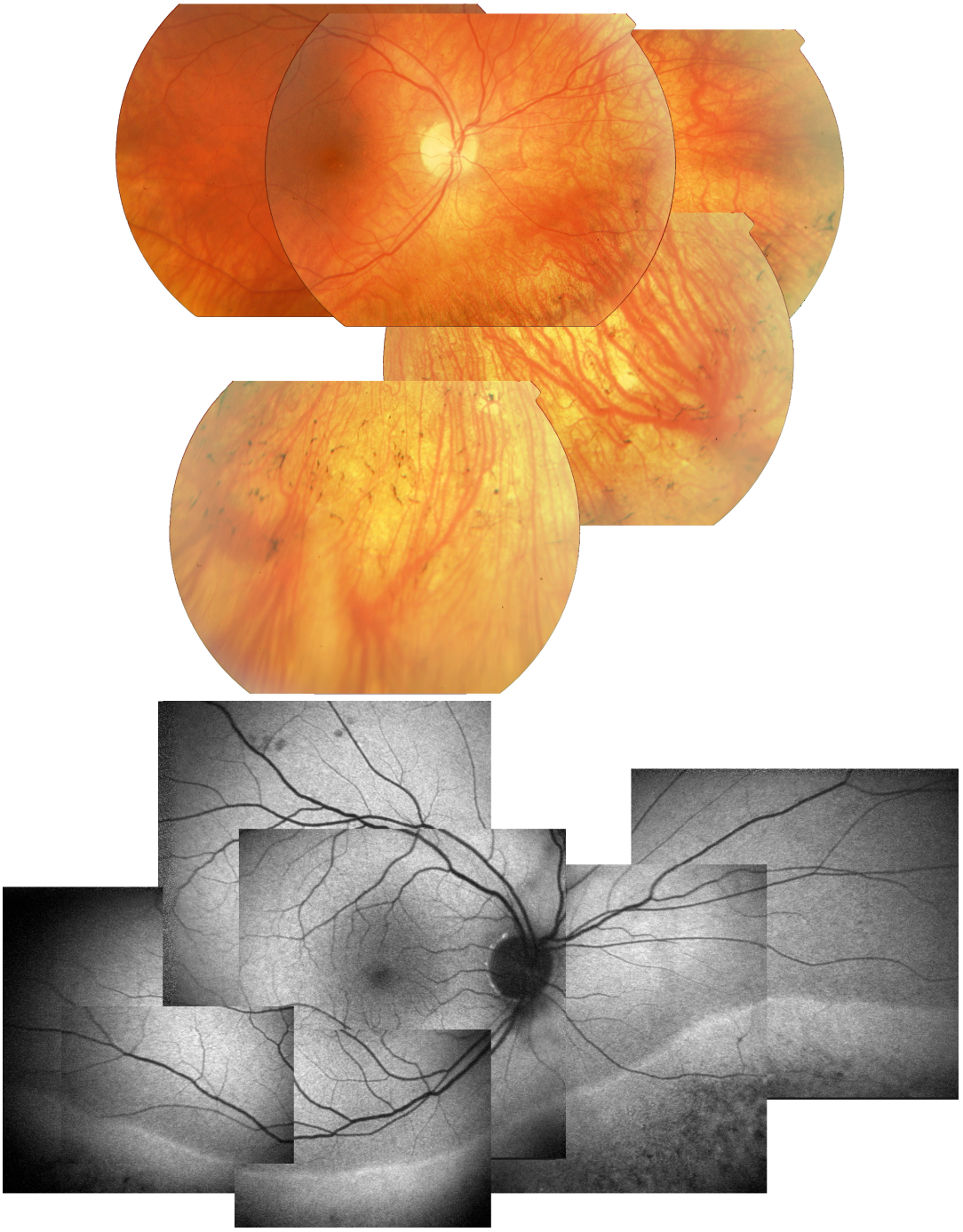

FIGURE 10.4: Right eye of affected sibling colour fundus photos (above) and AF imaging (below)

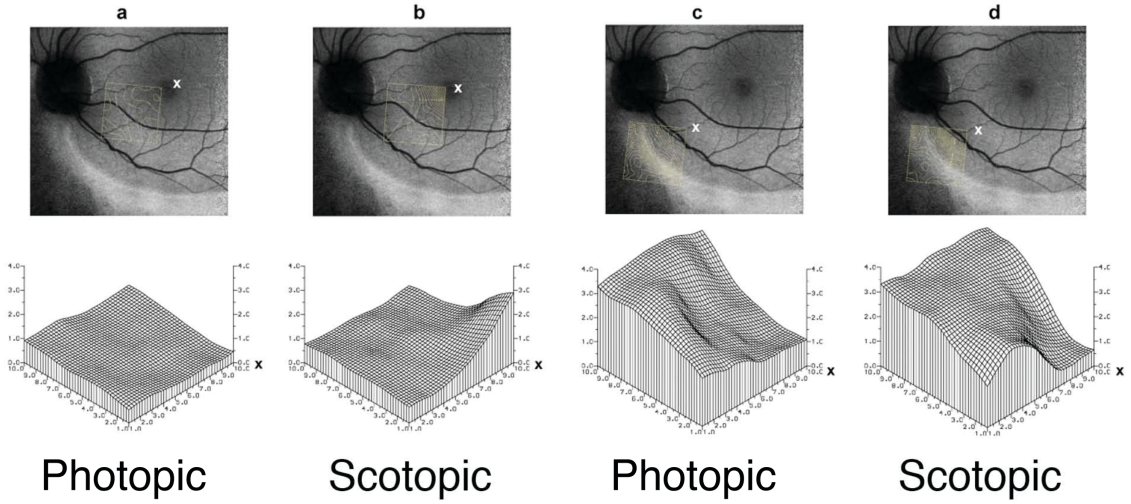

FIGURE 10.5: Contour plots (top row) and threshold plots (bottom row) obtained in the index case under photopic (a and c) and scotopic (b and d) conditions. Testing was performed at central (a and b) and eccentric (c and d) retinal locations. Labelling (x) illustrates correspondence between the orientation of contour and threshold plots. x-axis: retinal location (degrees); y-axis: threshold (log units).

SDs) above the normal mean, with milder elevation close to the optic disc. Thresholds eccentric to this region were elevated by approximately 2.1-2.45 log units (3.0-3.4 SDs) above the normal mean, with some sparing of sensitivity close to the optic disc.

Electrophysiological testing (Figure 10.6) demonstrated a normal PERG in both siblings indicating normal macular function, consistent with the preservation of photopic sensitivity demonstrated by the FMM. Full field ERGs suggested a relatively mild rod-cone dystrophy: scotopic ERGs were subnormal, consistent with rod photoreceptor dysfunction, and there was mild abnormality of cone response amplitude. There was no significant delay in rod or cone-mediated ERGs, in keeping with restricted disease. Both siblings demonstrated normal retinal and foveal architecture on OCT scanning, but both had areas of retinal thickening above the 95th centile compared to age matched controls, most obvious in the nasal half of the retina (Figure 10.7).

Audiovestibular phenotype

The index case had a moderate sensorineural hearing loss, which was bilateral and symmetrical (Figure **??**) Tympanometry and stapedial reflexes were normal but TEOAE responses were absent, characteristic of cochlear hearing loss. Auditory brain stem evoked responses were absent in spite of the moderate hearing loss, suggesting retrograde neural degenerative changes. Rotational tests showed vestibular hypofunction with a gain of 0.16 on sinusoidal rotation (normal limits: 0.39 +/- 0.16) and a right directional

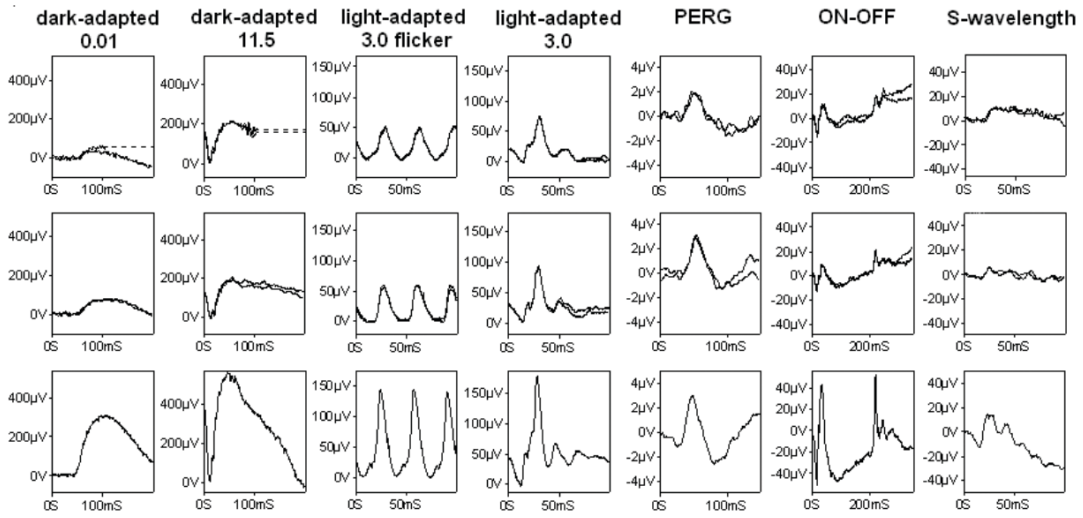

FIGURE 10.6: Full-field ERGs and pattern ERGs (PERG) from one eye of the affected sibling (row 1) and index case (row 2). Representative normal data appear in the bottom row.. All responses showed minimal inter-ocular asymmetry. PERGs were within normal limits for both siblings. Rod-mediated full field ERGs in affected sibling (row 1) were mildly subnormal; cone-mediated 30Hz flicker ERGs were mildly subnormal and of borderline timing, in keeping with a mild rod-cone dystrophy. In index case (row 2) Rod-mediated responses were mildly subnormal with b-waves of borderline timing; 30Hz flicker ERGs were mildly subnormal and of normal timing. Dark-adapted ERGs are shown for flash intensities of 0.01 and 11.5 cd.s.m-2; light-adapted ERGs for a flash intensity of 3.0 cd.s.m-2. ON-OFF ERGs used an orange stimulus (560 cd.m-2, duration 200ms) superimposed on a green background (150 cd.m-2). S-wavelength flash ERGs used a blue stimulus (445 nm, 80 cd/m2) on an orange background (620 nm, 560 cd/m2). Eye movement artefacts are replaced by broken lines.

preponderance of 22% (normal limits $\leq$ 20%) which was confirmed by caloric testing, which showed a significant right directional preponderance of 33% (normal limit $\leq$ 16%). Her younger sibling showed a similar symmetrical sensorineural hearing loss, but of severe degree with a steeper loss across the low frequencies but similar recovery at 4 kHz (Figure **??**) His transient evoked otoacoustic emissions and auditory brain stems responses were also absent. His vestibular function was within normal limits for sinusoidal rotation (0.25 Normal range 0.39+/-0.16) but showed mild hypofunction on impulsive rotation with a gain of 0.19 (normal range 0.39+/-0.16). He also had a mild directional preponderance of 20% (departmental norm $\leq$17%) on caloric testing.

USH1C mutations

Two USH1C mutations were identified, the previously reported c.308G(p.R103H) [64], and the novel c.2227-1Ginvariant splice site change. Both sibs were compound heterozygous for these two variants, which were inherited from each parent (Figure 10.1). Neither allele was found in 866 control chromosomes. Screening of *MYO7A, CDH23, PCDH15,*

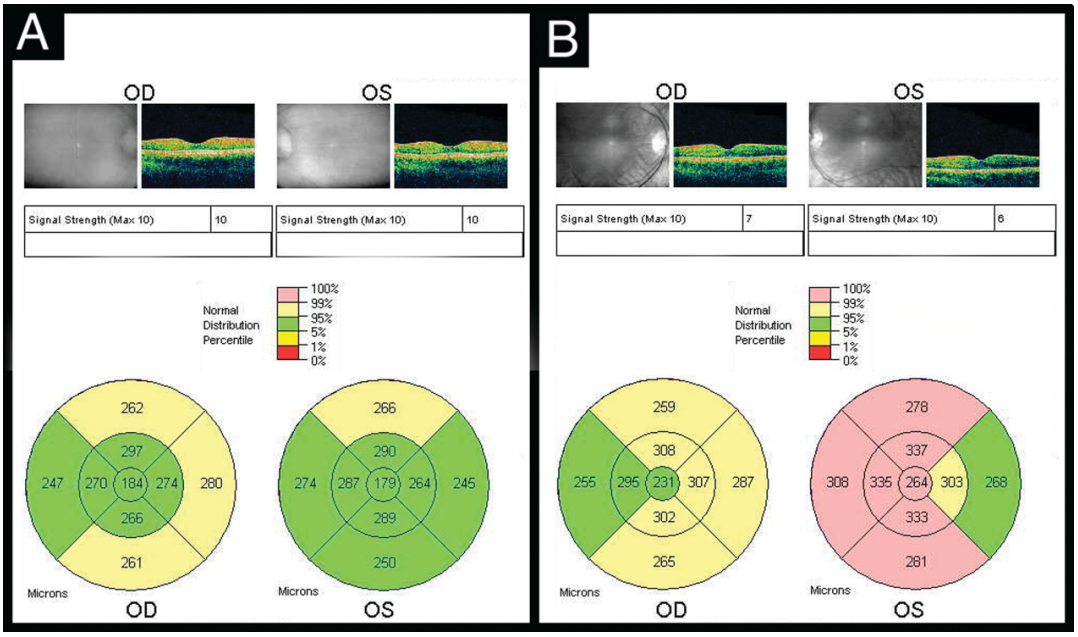

FIGURE 10.7: 6mm Optical Coherence Tomography (OCT3) scans centered at the fovea of the right eye (OD) and left eye (OS) of the index case (A) and her affected sibling (B). The upper images are representative cross sectional scans showing normal retinal architecture. The schematic below these images represent the average thickness (in microns) of each quadrant after subdivision by three concentric circles of 6mm, 3mm and 1mm compared against age matched normative data. This demonstrates the thickness of nasal retina to be above the 95th centile in both affected individuals.

USH2A, GPR98, WHRN, USH3A (the other seven genes associated with Usher syndrome) failed to reveal any putative pathogenic changes such as frameshift, splice site or rare missense changes.

Discussion

We report a sibship with sector RP with associated hearing loss due to mutations in the USH1C gene. To our knowledge this is the first reported case of sector RP associated with mutations in this gene. The finding of a discrete arcs or rings of hyperfluorescence has been reported in other forms of retinal dystrophy, and whilst they have no obvious correlation to changes observed with fundus biomicroscopy, they appear to be of functional significance [211–215].

The affected individuals reported here demonstrate an unusual pattern of FAF with a thick curvilinear band of hyperfluorescence separating preserved central fluorescence with abnormal areas of hyperfluorescence inferiorly and nasally. Previous reports of FAF in sector RP have described areas of hypofluoresence [216] as well as hyperfluorescent arcs bordering the area of dysfunction [195].

Photopic and scotopic fine matrix mapping in the affected individuals reported here revealed normal cone and rod system sensitivity over central macular locations. The constriction of hyperfluorescent rings seen on FAF imaging have been reported in RP due to mutations in one of the other genes associated with Usher syndrome (USH2A) and it has been suggested that progressive visual field loss may mirror constriction of the AF ring, led by encroaching rod dysfunction over more central and concentric macular areas [189, 211].

Both *USH1C* alleles carried by the affected siblings were inherited independently, absent in 866 control chromosomes and are likely to be pathogenic. The p.R103H allele has been previously reported in a family with Usher syndrome (USH1 phenotype) and was not found in another panel of 352 control chromosomes [64]. The novel c.2227-1G<T allele reported here is predicted to abolish the invariant AG dinucleotide splice acceptor site interfering with splicing at the intron 21/exon 22 junction. If exon 22 were to be skipped as predicted, the mature transcript would result in an inframe loss of 18 amino acids (743 to 760 inclusive). This is likely to have significant functional consequences, however further functional studies would be required to confirm the pathogenicity of this allele.

A full list of USH1C mutations can be found here at Usher group from Montpellier, France [217]. Null alleles in *USH1C* result in profound hearing loss and RP; less severe hypomorphic missense changes appear to spare retinal involvement but are still associated with profound hearing loss with normal [54], or unknown vestibular function [62]. The hearing loss in this sibship is less severe than previously reported in disease due to *USH1C*, which is typically profound, preventing the attainment of language. Both siblings used hearing aids since childhood but developed normal speech and language. The sector retinitis pigmentosa in this sibship also represents a milder retinal phenotype than other reported patients with mutation in *USH1C*, with regard to age of onset of symptoms, ERG amplitude and visual field area [218]. It is tempting to suggest that the milder retinal and audiovestibular phenotype reported in this sibship might represent a form of *USH1C* hypofunction affecting the retina and inner ear less severely than in cases of Usher syndrome due to mutations in *USH1C*.

Sector retinitis pigmentosa is a rare form of RP characterized by bilateral symmetrical retinal degeneration restricted to one area of the ocular fundus, usually the inferior nasal quadrant. Disease transmission is usually autosomal dominant although autosomal recessive transmission and X-linked cases have been reported [219–222]. Although clinical examination may suggest restricted disease, tests such as dark adaptation, fluorescein angiography and electrophysiological testing can reveal generalized rather than restricted retinal involvement ([220, 222–224]. In the literature, a case of sector RP with

prelingual hearing loss has been reported in a male individual with a retinal vasoproliferative tumor [225], however there was only a brief description of phenotype and no molecular diagnosis . The only molecular cause of sector RP reported to date has been due to mutations in the Rhodopsin (RHO) gene (OMIM 80380) which encodes human rhodopsin pigment of the retinal rods. Several missense mutations in RHO have been associated with the sector RP phenotype [219, 226, 227]

The *USH1C* gene (OMIM 605242) encodes a PDZ-containing protein called Harmonin or USH1C, which is expressed in alternatively spliced isoforms that make up three different sized subclasses [43, 44]. Mutations in this gene have been associated with Usher syndrome (the combination of generalized RP and hearing loss) [44] [92] [93–97], as well as with non-syndromic autosomal recessive hearing loss (DFNB18) [54, 62]. There appears to be some genotype-phenotype correlation with hypomorphic alleles causing hearing loss without RP, whilst more severe truncating mutations result in hearing loss and RP [54, 62]. The audiovestibular phenotype associated with mutations in *USH1C* is one of prelingual profound hearing loss with absent peripheral vestibular function when associated with RP [43, 44, 97], and with normal vestibular function when associated with non-syndromic hearing loss [54, 62]. The retinal phenotype is usually typical of RP with widespread fundus changes and visual problems from childhood.

Despite both siblings being of similar age and sharing the same two alleles in USH1C, the index case had a marginally worse retinal phenotype with mild vestibular hypofunction, whilst her sibling who was only 2 years her junior, had worse hearing loss, normal vestibular function, milder retinal phenotype and later age of onset of visual symptoms. No other putative pathogenic changes were identified in the other seven genes associated with Usher syndrome suggesting environmental or stochastic factors or genetic modifiers may influence disease severity. With regard to the retinal phenotype, it may be relevant that the index case had worked outdoors for most of her adult life, whilst her sibling with a milder retinal phenotype, reported less cumulative sunlight exposure. Phototoxicity as a modifier in accelerating retinal degeneration has been reported in sector RP due to a missense mutation in RHO [219]. Abnormal genetically encoded sensitivity to ultraviolet and blue light has also been proposed to explain inferior retinal changes [228]. Classically, RP is associated with generalized dysfunction, and therefore with peak-time shift, particularly in the 30Hz flicker ERG [229]. The absence of a marked cone flicker ERG delay in both affected siblings is consistent with restricted rather than generalized dysfunction, the latter commonly causing peak-time delay. Whilst an early form of slowly progressive generalized retinal dysfunction manifesting as sector RP cannot be excluded, at this stage is not suggested by the ERG characteristics.

In summary we report a sibship with sector retinitis pigmentosa, severe hearing loss associated with mutation in *USH1C*. There was evidence of mild vestibular hypofunction in one of the siblings and both siblings were able to develop speech. Both the retinal and audiovestibular phenotypes are much milder than in previously reported cases of *USH1C*-related nonsyndromic hearing loss or Usher syndrome type 1, representing a new spectrum of phenotype associated with mutations in the *USH1C* gene.

10.1.2 Alstrom syndrome - Family 133

The index case (NCUS 448) from Family 133 was a 41 year old male who attended for ophthalmic phenotyping for this study having received a diagnosis of Usher syndrome many years previously. At the time of examination, he had not been seen by an Ophthalmologist for over 5 years.

He gave a history of poor vision noted by his mother since 2 years of age and a history of nyctalopia from age 7 years. His primary visual problem during his school years was a reduction of central vision, followed by progressive deterioration in his peripheral visual field. On direct questioning he admitted to hemeralopia during his childhood. At age 12 he was moved from a mainstream school to a partially sighted school.

His hearing loss was noticed by teachers at school at age 18 and had been non-progressive in nature. At the time of his initial diagnosis of hearing loss, due to additional symptoms of weight gain, impotence and anxiety, a CT scan was arranged. At this time a diagnosis was made, (presumably central hypogonadism) for which thrice weekly male hormone replacement therapy was started and was ongoing.

He had three unaffected siblings and there was no family history of visual or audiovestibular dysfunction. In addition to the above, his medical history also included hypertension and hypercholesterolaemia for which he was on treatment and non-insulin dependant diabetes mellitus (diet controlled).

Examination revealed a blind left eye (no perception of light) and hand movements vision in the right eye. Visual field testing was not possible due to significant visual impairment.

Slit lamp biomicroscopy revealed dense nuclear scelerotic cataracts in both eyes preventing a useful fundal view. In the left eye there was irregular cortical opacification of the nasal half of the lens. A large sentinel vessel was seen on the temporal aspect of the iris and a pea-sized smooth dark swelling beneath the sclera was noted on the temporal aspect of the globe. Intraocular pressures was high in the left eye (45 mmHg) and within normal limits in the right (15 mmHg). Both anterior segments were quiet. Gonioscopy

in the left eye revealed an open drainage angle for all but the temporal 3 clock hours where the angle could not be visualised due to a hypermobile iris. No mass was seen on gonioscopy. There was no history of ocular pain on direct questioning.

B-mode ultrasound scans revealed bilateral atrophic temporal retinal detachments (probably longstanding) and no evidence of an intraocular lesion. Recent Chest X ray and liver funcion tests showed a mild rise in ALT levels. He was referred to a specialist ocular oncology unit for assessment of the left choroidal mass. Ocular neoplasia was excluded and a diagnosis of non-specific scleromalacia was made.

Clinically his symptoms were consstent with a diagnosis of Alstrom syndrome, a rare multisystem disorder and he was referred to a specialist physician. Subsequent molecular testing confirmed the diagnosis by identification of mutations in the *ALMS1* gene.

10.1.3 Unknown syndromic cause

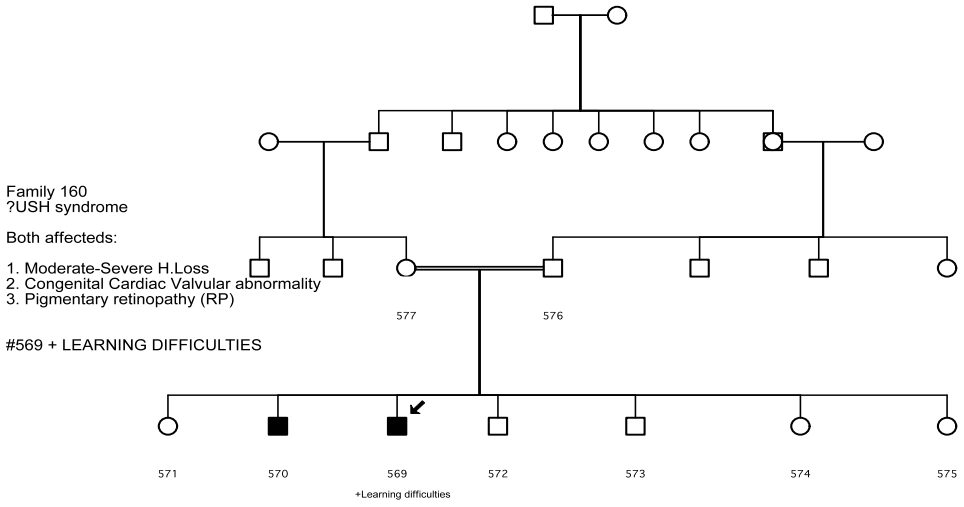

FIGURE 10.8: Pedigree for Family 160

Two siblings (NCUS 569 and 570) from Family 160 were recruited in the study having previously received a diagnosis of Usher syndrome. The two siblings were 19 and 21 years old respectively. They were the product of a 1st cousin consanguineous union and their grandparents were originally from Yemen (see Figure 10.8). There were five additional unaffected siblings, the youngest of which was 5 years old. Other than the sibling pair, there was no family history of cardiac, audiological or ophthalmic problems with neither of the affected siblings being known to have a history of rheumatic fever or infectious disease. There was difficulty in obtaining a clinical history as neither of the affected siblings used sign language. The index case had a diagnosis of learning difficulties. The affected older sibling was in college.

Both brothers had been treated for congenital cardiac valvular abnormalities of an unspecified nature. They were apparently under the care of a cardiologist and were not on any active treatment or known to have any active cardiac problems, however more detailed information was not available.

Both siblings had profound hearing loss, the younger index case apparently deriving some benefit from hearing aids (which were used bilaterally). Subjectively the hearing loss for both affected siblings was described as asymmetrical and non-progressive.

The index case had poor vision bilaterally (counting fingers vision OD, hand movements vision OS). The poor vision in the left eye was due to a previous retinal detachment which may have been post-traumatic in aetiology. Colour vision testing and visual field testing was not possible due to poor cooperation.

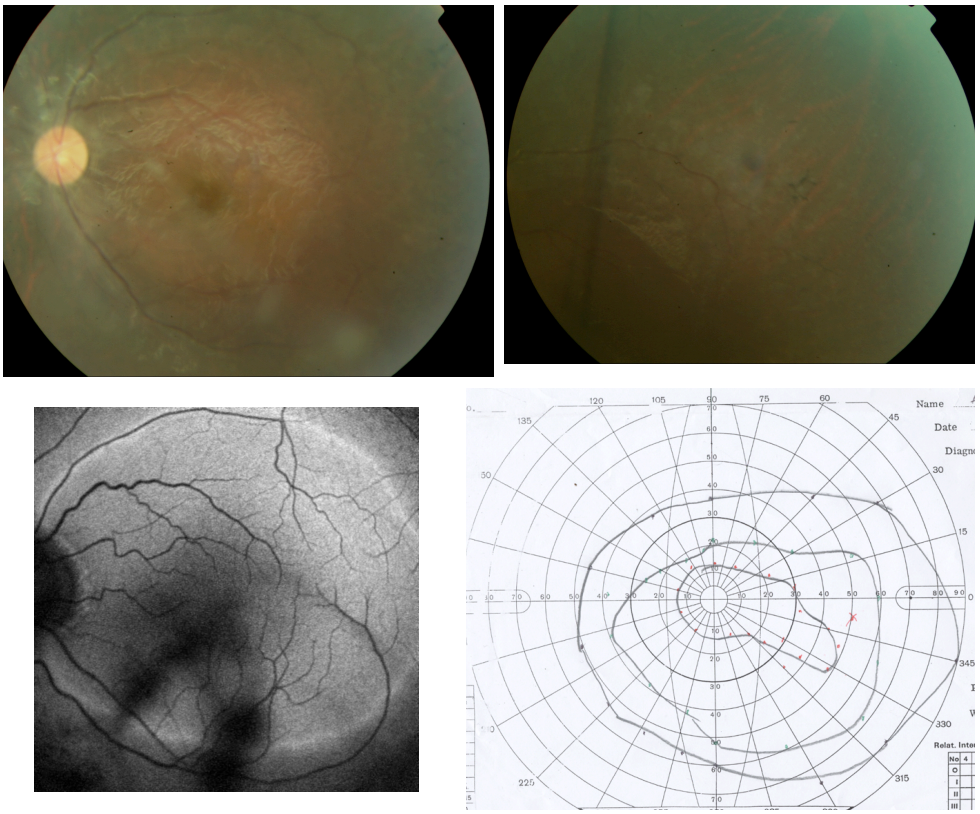

FIGURE 10.9: (Above) Colour fundus photos from the left eye of the affected sibling (NCUS 570). (Below left) Autofluorescence imaging from the left eye showing a hyperfluorescent ring just within the vascular arcades. (Below right) Goldmann visual fields for V4e, II4e and I4e isopters

The affected sibling had best corrected logMAR VA of 0.5 OD and 0.42 OS. No defects were noted on HRR colour vision testing. There was mild constriction of the V4e isopter with marked constriction of smaller isopters (see Figure 10.9).

On clinical examination, both siblings had normal anterior segments. The index case had a lens implant from previous cataract surgery and signs consistent with previous retinal detachment in the left eye. Both retina were flat.

Dilated fundoscopy in the right eye of the index case and both eyes in the affected sibling showed a similar pattern of modest mid-peripheral pigment migration and RPE changes in both fundi. The retinal periphery was notable by lack of peripheral retinal vasculature.

No cystic changes were noted on examination or OCT scanning. Fundal autofluorescence performed in the affected sibling revealed bilateral hyperfluorescent rings.

As part of a separate study genome wide linkage analysis was performed using the Affymetrix 50K SNP Chip platform which revealed homozygosity in the affected siblings for several regions outlined in table 3.2.

TABLE 10.2: Regions of homozygosity identified in the two affected siblings from Family 160

CHROMOSOME	ROW NUMBER FROM	ROW NUMBER TO	FROM	TO	SIZE	SIZE IN MEGABASES	candidate genes
5			18471442	23010149	4538707	4.54	cdh18, cdh12
8	3155	3257	131791884	135210399	3418515	3.42	
9	1078	1260	53.25	60.65	7.4	0	
9	1267	1483	70235778	81210361	10974583	10.97	RP11,
10	459	687	19482190	28237295	8755105	8.76	RP13, MYO3A
10	370	434	15861784	18459978	2598194	2.6	

10.1.4 Family 170

The index case NCUS 633 from Family 170 was unusual as her initial visual symptoms were of central visual dysfunction aged 10. Her visual acuity was poor bilaterally at logMAR 1.6 OD, 2.6 OS. Colour vision and visual field testing was not possible due to severe visual dysfunction. She had two paternal half siblings and there was no family history of visual or audiovestibular dysfunction.

On clinical examination she had nummular areas of retinal pigment migration across the posterior pole along with puctate areas of retinal pigment epithelial atrophy. Autofluorescence imaging revealed patchy areas of hyperfluoresnce acrro the posterior pole and macular area with peripheral hypofluorescence.

No supporting audiovestibular data was available on this individual but severe to profound hearing loss was suspected. Communication was by speech.

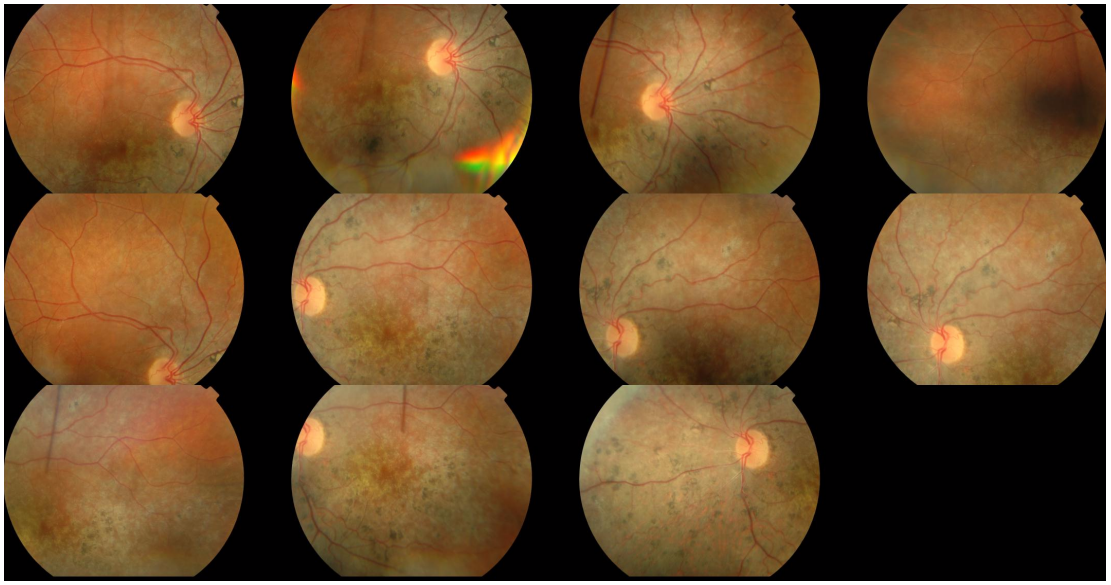

FIGURE 10.10: Colour fundus photographs from index case 633 from Family 170 showing the atypical nummular areas of retinal pigment migration across the posterior pole

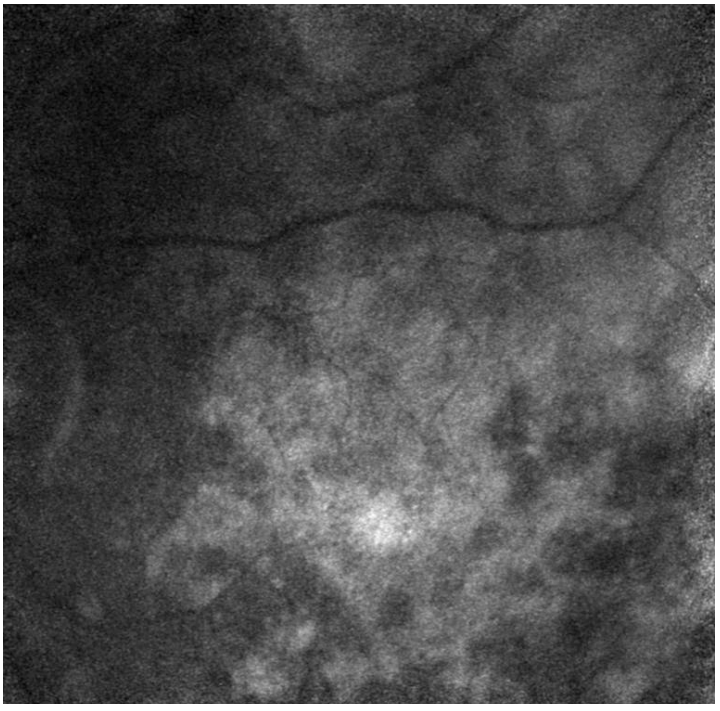

FIGURE 10.11: AF imaging from index case 633 from Family 170 showing patchy areas of hyper and hypofluorescence across the posterior pole

Compared to the rest of the affected individuals in this study, retinal phenotype and poor visual acuity at such a young age was atypical. No disease causing mutations were found in any of the Usher genes.

10.1.5 Atypical audiovestibular phenotypes

Three families (Family 124, 140 and 29) had pedigrees consistent with hearing and visual loss segregating as the same disorder. The index case from Family 124 had central vestibular hypofunction and a history of progressive hearing loss. The index cases from Family 140 and 29 both had atypical audiovestibular phenotypes in that both index cases communicated via speech but with profound hearing loss. They were both found to have audiograms highly atypical of Usher syndrome.

10.2 non-syndromic families with non-USH

10.2.1 Visual and hearing dysfunction segregating as separate disorders

Family 37 represents an example of two separate disorders segregating in the same family. Figure 10.12 shows the family pedigree which shows the segregation of autosomal dominant adult onset hearing loss from the paternal and likley autosomal dominant RP on the maternal side.

The index case (NCUS 501) from Family 144 had a retinal dystrophy which was atypical for RP consisting of an atrophic fundus. Hearing loss did not occur until adult life and although audiograms were reported as being consistent with an USH2 phenotype, they were atypical.

10.2.2 Hearing loss with no retinal phenotype

The index case in Family 502 was an 11 years old with moderate congenital hearing loss. Communication was by speech with the use of hearing aids. Referral to an ophthalmology service at around age 6 was prompted by his mother's concern regarding her child's visual function. He was prescribed glasses for a moderate refractive error and at some point during his work up had retinal electrodiagnostics. These showed equivoval results. On examination acuity was logMAR 0.2 OD and 0.3 OS. Slit lamp biomicroscopy was unremarkable and visual fields were full to all isopters tested. On

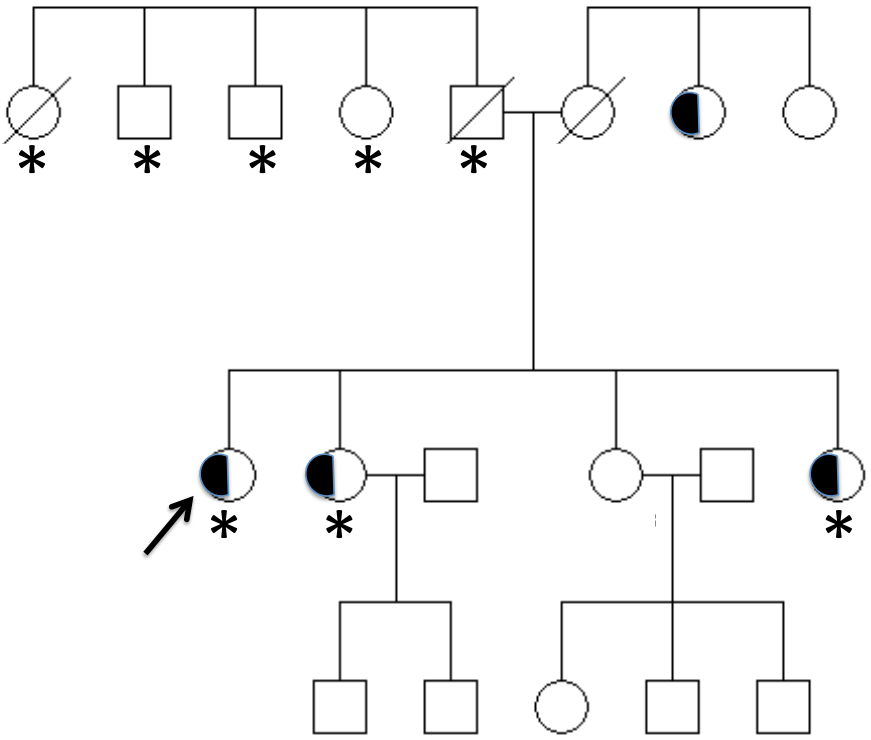

FIGURE 10.12: Pedigree of Family 37. Half circles represent a diagnosis of RP in childhood or early adulthood. Asterisks represent late onset deafness (40 years of age or greater). The arrow indicates the index case

direct questioning, no symptoms of nyctalopia or visual field loss were identified. Repeat retinal electrodiagnostics were performed and were entirely normal.

The index case of Family 167 was a 54 year old with a history of congenital or early childhood onset hearing and visual impairment. It appears that a diagnosis of Usher syndrome had been mentioned by a healthcare professional at some point, but never formally confirmed. This individual did not complete clincial phenotyping or undergo molecular analysis for this study as it came to light that their visual dysfunction was as a result of congenital cataracts and secondary glaucoma.

10.2.3 Atypical or acquired hearing loss

The remainder of non-USH families were either found to have acquired hearing loss or an atypical audiovestibular phenotype making a diagnosis of Usher syndrome unlikely, supported by the lack of putative pathogenic alleles identified in this cohort.

10.3 Summary of non-USH families

The importance of taking a detailed family history was illustrated by the segregation of two separate disorders in Family 37. Aside from this family, the remainder of the non-Usher families identified in this study were found to have retinal and/or audiovestibular phenotypes that were atypical. Of the 11 non-Usher families identified, only one was found to carry any putative pathogenic sequence variants in any of the known Usher genes. This suggests that Usher syndrome due to mutations in the Usher genes screened in this study produce phenotypes that are relatively similar. Specifically no cases of severe childhood visual dysfunction were identified.

Only one affected individual under the age of 20 years old with USH1 or USH2 had a visual acuity worse than logMAR=0.3 in their better seeing eye. This was a 4 year old child with disease due to *MYO7A* (Family 80) who had VA of 0.56 in both eyes. This suggests that if an affected person suspected of Usher syndrome has visual acuity worse than logMAR=0.6, they would be unlikely to have disease due to any of the known Usher genes.

However, the atypical phenotype identified in Family 142 with mutations in the *USH1C* gene also highlights the variation in phenotype that mutation in these genes can produce.

Chapter 11

Discussion

11.1 Review of thesis aims and findings

This study represents the largest prospective clinical and molecular cohort study in Usher syndrome to date.

Identify a cohort of genotyped individuals with Usher syndrome in the UK

This study has achieved its initial goal in recruiting 187 families with a diagnosis of Usher syndrome from the UK. 176 of these families were felt to have a clinical diagnosis of Usher syndrome and a molecular diagnosis was achieved in 80% of the 175 families who underwent molecular analysis.

The first and arguably the most important task to facilitate this study was the identification and recruitment of UK families with a diagnosis of Usher syndrome. Recruitment of families with a rare disease causing dual sensory impairment has its challenges and was slow to start.

The use of email and publicising the study on the internet via the charity Sense's website were helpful in getting news of the study out in to the deafblind community, which proved to be a critical factor in achieving our goals in terms of numbers of families recruited, as a quarter of all families self referred in to the study. Email proved to be a valuable tool and was the most frequently requested mode of contact for USH1 families and second only to voicephone in USH2 families. Moorfields Eye Hospital, a tertiary centre for ophthalmic care in the UK was a valuable resource in identifying families with Usher syndrome and provided just over half of all families.

Understand natural history of the disorder

One has to be careful in drawing conclusions from an observational cohort study such as this. However the large dataset collected in this prospective study has provided some insights in to the pathogenesis of Usher syndrome. 219 affected individuals from 187 families underwent ophthalmic phenotyping.

This study has shown that symptomatic onset of retinal disease occurs at a younger age in USH1 (median age 9 years old) and USH2 (median age 17 years old). Whilst the earlier onset of USH1 has been known for some time, the data from this study has shown that the early onset in USH1 was seen in all the four USH1 genes (*MYO7A, USH1C, CDH23* and *PCDH15*) and the wider range for the age of onset of visual symptoms in USH2 was reflected in both the USH2 molecular groups identified, *USH2A* and *GPR98*.

Only one affected individual under the age of 20 years old with USH1 or USH2 had a visual acuity worse than logMAR=0.3 in their better seeing eye. This was a 4 year old child with disease due to *MYO7A* (Family 80) who had VA of 0.56 in both eyes. From the dataset collected in this study, this suggests that if an affected person under the age of 20 years old suspected of Usher syndrome has visual acuity worse than logMAR=0.6, they would be unlikely to have disease due to any of the known Usher genes sequenced in this study, however as this study has not collected an exhaustive set of Usher patients this is simply an interesting observation, rather than a statement.

Facilitate subsequent longitudinal studies

The large cohort of prospectively phenotyped individuals with a molecular diagnosis will be a useful resource in the future for delineating genotype vs phenotype correlations by generating longitudinal data on the same study recruits.

Help devise a strategy for subsequent molecular analysis in the UK

We embarked on the National Collaborative Usher Study in order to determine the molecular epidemiology of Usher syndrome in the UK, and as a prerequisite to establishing a diagnostic service necessary for when trials and treatments become available. Molecular diagnosis in Usher syndrome is hindered by significant genetic heterogeneity, the large size of some of the Usher genes and the large number of missense changes in genes such as MYO7A and USH2A. Demonstrating variants that are truly pathogenic, rather than neutral, is often difficult. Although a number of molecular studies of Usher

cohorts have been published to date, none have been designed in a way that would systematically detect digenic inheritance and whether or not this is a significant or recurring phenomenon. Whilst a major undertaking in terms of time and expense, we decided to sequence all the known Usher genes in all subjects, regardless of clinical subtype in order to assess evidence for digenic inheritance and determine the extent of polymorphic sequence variation within the genes.

MYO7A was the most prevalent gene resulting in an USH1 phenotye and 75% USH2 was due to the *USH2A* gene which is similar to previous studies [162, 174, 230]. It was interesting to note that no mutations in the genes *USH1G* and *WHRN* were identified whilst *USH3A* mutations were only identified in two families suggesting that these genes are rare amongst the UK population.

It was anticipated that by looking at the spread of mutations and molecular groups, a molecular analysis protocol could be devised to screen for mutations in the UK population.

In the entire study, only a few common putative pathogenic alleles identified in three genes, the rest of mutations being private to families. The common allele *USH2A*:p.Glu767SerfsX21 accounted for over half of all families with USH2 and over a quarter of all families in the study, regardless of phenotype. The high prevalence of this allele has been widely reported in many different populations [161–163, 165, 166, 231, 232]. p.Cys419Phe in the same gene was identified in 6 families.

The third most prevalent allele among all families was the splice site change c.496+1G >A which has been previously reported and identified as a founder mutation in the French Canadian population [44, 94, 160]. Four sequence variants in the *USH2A* gene were each identified in four different families, but the overwhelming majority of remaining families carried private alleles. This presents significant challenges in terms of establishing a useful method of screening which is compounded by the large genomic size of many of the USH genes.

Mutation detection rate

We detected at least one pathogenic/likely pathogenic mutant allele in 86% of probands studied and found considerable genetic heterogeneity in the mutations involved. This suggest that there are unlikely to be any other Usher genes of *major* impact in the population, and that a significant proportion of mutations in the known genes remain undetected by current conventional sequencing methods, as only a single mutation was found in 30 families.

Although probands with a clinical classification of Usher syndrome type 1 were screened for all USH genes, the causative mutations were only found in USH1 genes. Screening of the USH2 genes in USH1 probands therefore can be expected to have a very low mutation yield and the clinical classification of type 1 Usher, is generally very robust as it correlates with a molecular diagnosis of type 1 Usher as well. Only only 1 out of 125 probands clinically classified as USH2, had a single nonsense mutation in MYO7A, an USH1 gene, and it is unclear as to whether this mutation is disease causing in this individual. In another family who entered the study with a diagnosis of Usher syndrome type 2/3, we identified two *USH1C* mutations and affected sibs were subsequently diagnosed as having sector RP and hearing loss [233] . Therefore we can recommend that screening *all* genes is unnecessary in most cases and molecular screening can be somewhat directed by clinical diagnosis. Segregation analysis using haplotypes is also a valuable tool for selecting candidate genes as shown by Roux et al. who detected putative disease-causing mutations in more than 90% of 34 USH1 families from France [64, 234].

The use of genotyping microarrays using arrayed primer extension is an available and cost effective tool to detect DNA sequence variants, however this technology is only successful in identifying *known* mutations. Given the large number of private alleles identified across all the Usher genes in our study, using genotyping microarrays is unlikely to yield a high degree of sensitivity. The drawbacks of such techniques may also affect specificity, for example if a deaf child was found to have one putative pathogenic allele in an Usher gene, this result on its own would be equivocal. However on balance this probably represents the most cost and time effective method of molecular diagnosis for Usher syndrome at this time.

MYO7A has been detected in nasal epithelium [141] and a recent report has identified mRNA expression of seven of the nine Usher genes in hair roots, representing a novel method of mutation detection [235]. This may provide a useful diagnostic tool in the future and is also the subject of further work carrying on from this study.

Relative involvement of Usher genes

In agreement with other studies [64, 110, 236], *MYO7A* was the most frequent cause of USH1, implicated in 53.2% of USH1 families. Surprisingly however, *USH1C* was the second most common USH1 gene, accounting for USH in 12.8% of USH1 cases. This is different from USH1 studies of 34 French USH1 patients [64], 33 of USA/UK patients [110] and 121 Spanish patients [237] populations, where USH1C was responsible for the disease in 6%, 7% and 1.5% of cases, respectively. However, our *USH1C* frequency is similar to the study of patients from Germany, Denmark and Switzerland where

USH1C was responsible for 12.5% ⩽ of cases [94]. USH1C:c.496+1G>A was not only the most frequent *USH1C* mutation (representing 75% of *USH1C* pathogenic alleles), it was also the most frequent USH1 mutation overall accounting for USH in 10.6% of USH1 families. The patients who harboured the mutation had the same disease-associated USH1C haplotype, but we cannot conclude that the mutation arose from a common ancestor as the haplotype consisted of only three informative and highly polymorphic SNPs. Proportions of CDH23 (11.1% of USH1 cases) and PCDH15 (6.7%) mutations were lower than previously reported by Roux et al. who reports PCDH15 and CDH23 account for 19% of cases each (Roux et al., 2006).

Mutations in *USH2A* were the major cause of USH2 in our cohort of 125 patients with at least one pathogenic/likely pathogenic variant found in 75.7% of USH2 families, a finding similar to previous studies which report *USH2A* is involved in 25 out of 33 (75%) USH2 cases[174], in 89 out of 118 (75.4%) USH patients [168] and 57-63 out of 100 (57%-63%) USH2 patients [238]. Apart from the common *USH2A*:p.Glu767SerfsX21 mutation, we identified a wide range of private mutations. Fifty (31.8%) pathogenic/UV4/UV3 USH2A alleles were not previously described. Data regarding the frequency of *GPR98* mutations is scarce, but it appears to be a less common cause of USH2. In our USH2 cohort, 6.25% of families segregated *GPR98* mutations, which is similar to the study in the French population where *GPR98* accounted for 5.6% of cases [239].

Investigate the possibility of digenic effects and unusual phenotypes

A strength of this study is the comprehensive nature of molecular testing. Sequencing all nine known Usher genes in each proband could be criticised as being excessive however it has enabled us to answer the important question as to whether pathogenic alleles in more than one of the known Usher genes might cause disease. We were unable to find any evidence of this in 186 families and this suggests that the likelihood of this is low. However, we cannot exclude the possibility that this is the case or indeed that sequence variants in other genes may play a disease modifying role in the pathogenesis of Usher syndrome. Another interesting discovery to come about as a result of our approach to molecular diagnosis was the identification of a family with the atypical phenotype of sectorial retinal disease (sector RP) and hearing loss less severe than usually associated with the *USH1C* gene. One explanation to the milder disease might be explained by the pathogenic alleles in this family being hypomorphic compared to the other truncating sequence variants that are usually associated with the USH1 phenotype. Prior to this finding the only reported molecular cause of sector RP was due to mutations in the *RHO* gene coding for the human rhodopsin pigment.

Identify which DNA sequence changes are disease causing

The relatively high proportion of single alleles identified in families with disease due to the most prevalent genes *USH2A* and *MYO7A*, suggest that sequencing methods alone failed to identify the second allele. The reasons for this are unclear but might be due to factors such as unidentified or missed heterozygous deletions, non-coding variants or other potentially digenic effects with as yet unknown genes.

The large number of families with no molecular diagnosis (n=30) despite this comprehensive molecular analysis strategy, suggest that more disease-causing genes are yet to be identified for this disorder. The challenges of determining the pathogenicity of the large number of rare DNA sequence variants assayed in a control population have also been demonstrated. Many of these sequence variants were missense changes that remain of uncertain pathogenicity. In silico analysis was helpful in conforming our suspicions for those missense changes felt to be likely to be disease causing (UV4) and those that were less likely to be so (UV3 and UV2), but due to the nature of in silico bioinformatics, we have still not been able to confidently determine whether many of the novel sequence variants found are disease causing. This will be the topic of further work and may involve other techniques. This brings to light an important factor to consider as we enter the age of next generation sequencing, when the generation of vast amounts of DNA sequence data is becoming exponentially more efficient and cheaper. The more DNA sequence variants we identify, the more we will have to test to determine whether they are disease causing or not. The increase in DNA sequencing power has not been matched by a commensurate increase in novel technologies to perform "arrayed" *in vitro* or *in vivo* studies and it is difficult to imaging how this problem will be resolved in the near future.

The molecular algorithmic system devised and implemented to help the grading of putative pathogenic alleles for this study is simple and quite transferable to other genetic studies of autosomal recessive disease. Using a benchmark minimum allele frequency is helpful for an ethnically homogenous population, but as we found in this study, rare ethnic population polymorphisms will be unrepresented in a homogenous control group. One benefit projects such as the 1000 Genomes Project and other future studies utilising next generation sequencing technologies will be to interrogate DNA variants in much larger ethnically diverse populations to help with this problem.

The pathogenicity grade of missense changes in this study was determined by their presence or absence in control chromosomes, other Usher families, or other Usher genes, in trans or in cis co-occurrence with a pathogenic mutation in the same gene and their haplotype. As the majority of mutations identified were private, their presence in the

control chromosomes with a frequency of less than 0.236% proved to be a good indicator of non-pathogenicity. Thirty-five out of 218 (16.1%) missense changes showed a frequency of over 0.236% in control chromosomes and were thus considered neutral. Eighty-six out of 218 (33.4%) missense changes were not found in 876 control chromosomes and additional 25 (11.5%) had a frequency below the benchmark of 0.236%, but were unlikely to be pathogenic as they did not segregate with disease or were found in patients with other more certain pathogenic changes.

Those families from this study that had no putative pathogenic DNA variants identified will undergo further molecular analysis including closer analysis of polymorphic markers and Multiplex Ligation-dependent Probe Amplification to detect deletions which may have been missed by direct sequencing.

Genetic counselling for individuals and families

Families involved in the study will have information regarding their molecular diagnosis fed back to them and have the option of attending for genetic counselling and discussion of results. As the results for this study were done as part of a research project and not conducted in an NHS reference laboratory this information will carry a caveat and would require confirmation in an accredited laboratory prior to any clinical decisions being made in relation to their molecular diagnosis. In the short term, we plan to feed back to each family the gene we believe their disease to be due to. We feel that giving patients more detailed information on sequence variants ever we are unsure as to whether they are pathogenic or not, may cause more confusion than is necessary.

Genotype vs. Phenotype: inform clinicians

An important finding to come out of this study was on retrospective questioning, onset of visual symptoms occurred at a significantly younger age in USH1 (median age 9 years old) compared to USH2 (median age 17 years old). In our data, no USH1 individuals reported onset of visual symptoms later than 14 years of age, suggesting that if a child with profound hearing loss does not develop any visual symptoms by their mid-teens they would be unlikely to go on to develop RP (i.e have USH1). This generalisation does not extend to individuals with mutations in USH1 genes that cause atypical phenotypes (e.g. the family with sector RP and hearing loss due to *USH1C* who had onset of symptoms much later in life), and so comes with a caveat. This information can be taken in to consideration by ophthalmic clinicians, who now have evidence to exclude a diagnosis of typical USH1 when assessing profoundly deaf adults who do not have any visual symptoms. Conversely one cannot confidently exclude the possibility of an

adult with moderate to severe hearing loss developing RP (i.e. USH2) on the basis of age alone, as some individuals did not experience visual symptoms until their thirties or forties. This also highlights the importance of specifically asking adults with RP for a history of hearing loss, as moderate hearing loss with a well concealed hearing aid may not be immediately apparent to the ophthalmic clinician on meeting a patient for the first time.

This study found that overall USH2 had significantly better median visual acuity than USH1 for any given age. A useful statistic that can be fed back to patients was that on average, central visual acuity good enough to meet the criteria for driving was maintained until mid-thirties for USH1 and mid-fifties for USH2. Restriction of visual fields similarly occurred at a younger age for USH1, with half of individuals maintaining a visual field of ten degrees squared (criteria for the legal definition of "blindness" or "severely visually impaired") by their mid-forties in USH1 and mid-fifties for USH2. These are useful statistics that can be delivered to patients who enquire about prognosis for central vision.

The clinical distinction between Usher syndrome clinical subtypes is made on the audiovestibular findings alone, however it appears that there are also similarities with regard to visual function shared by these two groups and their constituent molecular subsets. Similarity amongst the four USH1 genes and two USH2 genes with regard to onset of disease, visual acuity and visual fields was noted in this study.

The p.Glu767SerfsX21 sequence variant in *USH2A* was the most prevalent allele identified in this UK study. When comparing those individuals with disease due to *USH2A* and comparing those with this allele and those without, the only significantly different finding was a slightly earlier age of reported onset of visual symptoms. Visual acuity, visual fields, prevalence of cystoid macular oedema and AF features did not appear to be distinct to those with this genotype.

TABLE 11.1: Table documenting the clinical results from individuals with a molecular diagnosis of *USH2A* who carry the p.Glu767SerfsX21 allele and those that do not. The only statistical difference in any of the variables entered is the earlier age of onset of visual symptoms in those with the common allele

		p.Glu767SerfsX21 allele					
		NO			**YES**		
		Median	Mean	*(n)*	Median	Mean	*(n)*
Clinical	Age	41.00	41.38	*56*	34.00	37.05	*61*
	Disease duration	21	23	*56*	24	24	*61*
	VA in best eye	0.18	0.33	*56*	0.18	0.23	*61*
	Age of first visual symptom	18.00	18.64	*56*	15.00	14.63	*61*
CMO	Cystoid macular oedema in either eye			*9*			*9*
	No cystoid macular oedema			*35*			*38*
Visual fields	Ln(V4e) in best_eye	8.05	7.50	*56*	7.36	7.29	*61*
	Ln(II4e) in best_eye	4.89	5.39	*56*	5.41	5.78	*61*
	Ln(I4e) in best_eye	3.26	3.70	*56*	3.89	4.24	*61*
AF: HYPERfluorescent ring	no			*17*			*11*
	yes			*24*			*36*
AF: Perifoveal HYPOfluorscence	no			*21*			*30*
	yes			*20*			*17*
AF: Foveal HYPERluorescence	no			*16*			*25*
	yes			*25*			*22*

We have submitted our molecular findings to the online mutation USHbases database (https://grenada.lumc.nl/LOVD2/Usher$_m$*ontpellier*/*USHbases.html*) to aid other researchers in the same field and contribute to the wider body of knowledge regarding the molecular genetics of Usher syndrome.

Many of the participants in this study expressed willingness to return in the future for additional clinical investigations. This will afford the opportunity to collect longitudinal clinical data on this UK cohort of genotyped individuals with Usher syndrome, which will provide a clearer insight in the the clinical pathogenesis of this disorder.

Appendix A

Appendix Title Here

Publications arising from this study to date:

1. Comprehensive sequence analysis of nine Usher syndrome genes in the UK National Collaborative Usher Study. Le Quesne Stabej P, Saihan Z, Rangesh N, Steele-Stallard HB, Ambrose J, Coffey A, Emmerson J, Haralambous E, Hughes Y, Steel KP, Luxon LM, Webster AR, Bitner-Glindzicz M Journal of Medical Genetics, 2012 Jan;49(1):27-36. PMID: 22135276

2. Mutations in the USH1C gene associated with sector retinitis pigmentosa and hearing loss. Saihan Z, Stabej Ple Q, Robson AG, Rangesh N, Holder GE, Moore AT, Steel KP, Luxon LM, Bitner-Glindzicz M, Webster AR Retina. 2011 Sep;31(8):1708-16.

3. Update on Usher syndrome. Saihan Z, Webster AR, Luxon L, Bitner-Glindzicz M. Curr Opin Neurol. 2009 Feb;22(1):19-27. PMID: 19165952

4. Functional characteristics of patients with retinal dystrophy that manifest abnormal parafoveal annuli of high density fundus autofluorescence; a review and update. Robson AG, Michaelides M, Saihan Z, Bird AC, Webster AR, Moore AT, Fitzke FW, Holder GE. Doc Ophthalmol. 2008 Mar;116(2):79-89. Epub 2007 Nov 6. Review. PMID: 17985165

5. Development of a genotyping microarray for Usher syndrome. Cremers FP, Kimberling WJ, Klm M, de Brouwer AP, van Wijk E, te Brinke H, Cremers CW, Hoefsloot LH, Banfi S, Simonelli F, Fleischhauer JC, Berger W, Kelley PM, Haralambous E, Bitner-Glindzicz M, Webster AR, Saihan Z, De Baere E, Leroy BP, Silvestri G, McKay GJ, Koenekoop RK, Millan JM, Rosenberg T, Joensuu T, Sankila EM, Weil D, Weston MD, Wissinger B, Kremer H. J Med Genet. 2007 Feb;44(2):153-60. Epub 2006 Sep 8. PMID: 16963483

6. Functional characterisation and serial imaging of abnormal fundus autofluorescence in patients with retinitis pigmentosa and normal visual acuity. Robson AG, Saihan Z, Jenkins SA, Fitzke FW, Bird AC, Webster AR, Holder GE. Br J Ophthalmol. 2006 Apr;90(4):472-9. PMID: 16547330

Bibliography

[1] T P Nikolopoulos, D Lioumi, S Stamataki, and G M O'Donoghue. Evidence-based overview of ophthalmic disorders in deaf children: a literature update. *Otol Neurotol*, 27(2 Suppl 1):S1–24, discussion S20, Feb 2006. ISSN 1531-7129 (Print). doi: 10.1097/01.mao.0000185150.69704.18.

[2] M Vernon. Usher's syndrome–deafness and progressive blindness. clinical cases, prevention, theory and literature survey. *J Chronic Dis*, 22(3):133–151, Aug 1969. ISSN 0021-9681 (Print).

[3] J A Boughman, M Vernon, and K A Shaver. Usher syndrome: definition and estimate of prevalence from two high-risk populations. *J Chronic Dis*, 36(8):595–603, 1983. ISSN 0021-9681 (Print).

[4] J Grondahl. Estimation of prognosis and prevalence of retinitis pigmentosa and usher syndrome in norway. *Clin Genet*, 31(4):255–264, Apr 1987. ISSN 0009-9163 (Print).

[5] M L Marazita, L M Ploughman, B Rawlings, E Remington, K S Arnos, and W E Nance. Genetic epidemiological studies of early-onset deafness in the u.s. school-age population. *Am J Med Genet*, 46(5):486–491, Jun 1993. ISSN 0148-7299 (Print). doi: 10.1002/ajmg.1320460504.

[6] T Rosenberg, M Haim, A M Hauch, and A Parving. The prevalence of usher syndrome and other retinal dystrophy-hearing impairment associations. *Clin Genet*, 51(5):314–321, May 1997. ISSN 0009-9163 (Print).

[7] Ulrich H M Spandau and Klaus Rohrschneider. Prevalence and geographical distribution of usher syndrome in germany. *Graefes Arch Clin Exp Ophthalmol*, 240 (6):495–498, Jun 2002. ISSN 0721-832X (Print). doi: 10.1007/s00417-002-0485-8.

[8] von Graefe A. Vereinzelte beobachtungen und bemerkungen. exceptionelle verhalten des gesichtsfeldes bei pigmentenartung des netzhaut. *Arch. Klin. Ophthalmol*, 4:250–253, 1858.

[9] R Liebreich. Abkunft aus ehen unter blutsverwandten als grund von retinitis pigmentosa. *Dtsch. Klin.*, 1861.

[10] C.H. Usher. On the inheritance of retinitis pigmentosa, with notes of cases. *R. Lond. Ophthalmol Hosp Rep*, 19:130–236, 1914.

[11] M B Mets, N M Young, A Pass, and J B Lasky. Early diagnosis of usher syndrome in children. *Trans Am Ophthalmol Soc*, 98:237–242, 2000. ISSN 0065-9533 (Print).

[12] J Bell. *Retinitis pigmentosa and allied diseases*, volume 1. Cambridge Press, London, 1922.

[13] B HALLGREN. Retinitis pigmentosa combined with congenital deafness; with vestibulo-cerebellar ataxia and mental abnormality in a proportion of cases: A clinical and genetico-statistical study. *Acta Psychiatr Scand Suppl*, 34(138):1–101, 1959. ISSN 0065-1591 (Print).

[14] R J Smith, C I Berlin, J F Hejtmancik, B J Keats, W J Kimberling, R A Lewis, C G Moller, M Z Pelias, and L Tranebjaerg. Clinical diagnosis of the usher syndromes. usher syndrome consortium. *Am J Med Genet*, 50(1):32–38, Mar 1994. ISSN 0148-7299 (Print). doi: 10.1002/ajmg.1320500107.

[15] Omenn GS. Davenport SLH. The heterogeneity of usher syndrome. In *Vth International Conference Birth Defects*, 1977.

[16] C Petit. Usher syndrome: from genetics to pathogenesis. *Annu Rev Genomics Hum Genet*, 2:271–297, 2001. ISSN 1527-8204 (Print). doi: 10.1146/annurev.genom.2.1.271.

[17] J D Eudy, M D Weston, S Yao, D M Hoover, H L Rehm, M Ma-Edmonds, D Yan, I Ahmad, J J Cheng, C Ayuso, C Cremers, S Davenport, C Moller, C B Talmadge, K W Beisel, M Tamayo, C C Morton, A Swaroop, W J Kimberling, and J Sumegi. Mutation of a gene encoding a protein with extracellular matrix motifs in usher syndrome type iia. *Science*, 280(5370):1753–1757, Jun 1998. ISSN 0036-8075 (Print).

[18] T Joensuu, R Hamalainen, A E Lehesjoki, A de la Chapelle, and E M Sankila. A sequence-ready map of the usher syndrome type iii critical region on chromosome 3q. *Genomics*, 63(3):409–416, Feb 2000. ISSN 0888-7543 (Print). doi: 10.1006/geno.1999.6096.

[19] S Karjalainen, L Pakarinen, M Teräsvirta, H Kääriäinen, and E Vartiainen. Progressive hearing loss in usher's syndrome. *Ann Otol Rhinol Laryngol*, 98(11):863–6, Nov 1989.

[20] L Pakarinen, S Karjalainen, K O Simola, P Laippala, and H Kaitalo. Usher's syndrome type 3 in finland. *Laryngoscope*, 105(6):613–617, Jun 1995. ISSN 0023-852X (Print). doi: 10.1288/00005537-199506000-00010.

[21] Avital Adato, Sarah Vreugde, Tarja Joensuu, Nili Avidan, Riikka Hamalainen, Olga Belenkiy, Tsviya Olender, Batsheva Bonne-Tamir, Edna Ben-Asher, Carmen Espinos, Jose M Millan, Anna-Elina Lehesjoki, John G Flannery, Karen B Avraham, Shmuel Pietrokovski, Eeva-Marja Sankila, Jacques S Beckmann, and Doron Lancet. Ush3a transcripts encode clarin-1, a four-transmembrane-domain protein with a possible role in sensory synapses. *Eur J Hum Genet*, 10(6):339–350, Jun 2002. ISSN 1018-4813 (Print). doi: 10.1038/sj.ejhg.5200831.

[22] Randall R Fields, Guimei Zhou, Dali Huang, Jack R Davis, Claes Moller, Samuel G Jacobson, William J Kimberling, and Janos Sumegi. Usher syndrome type iii: revised genomic structure of the ush3 gene and identification of novel mutations. *Am J Hum Genet*, 71(3):607–617, Sep 2002. ISSN 0002-9297 (Print). doi: 10.1086/342098.

[23] S L Ness, T Ben-Yosef, A Bar-Lev, A C Madeo, C C Brewer, K B Avraham, R Kornreich, R J Desnick, J P Willner, T B Friedman, and A J Griffith. Genetic homogeneity and phenotypic variability among ashkenazi jews with usher syndrome type iii. *J Med Genet*, 40(10):767–772, Oct 2003. ISSN 1468-6244 (Electronic).

[24] C I Hope, S Bundey, D Proops, and A R Fielder. Usher syndrome in the city of birmingham–prevalence and clinical classification. *Br J Ophthalmol*, 81(1):46–53, Jan 1997. ISSN 0007-1161 (Print).

[25] A Kumar, G Fishman, and N Torok. Vestibular and auditory function in usher's syndrome. *Ann Otol Rhinol Laryngol*, 93(6 Pt 1):600–8, 1984.

[26] C G Moller, W J Kimberling, S L Davenport, I Priluck, V White, K Biscone-Halterman, L M Odkvist, P E Brookhouser, G Lund, and T J Grissom. Usher syndrome: an otoneurologic study. *Laryngoscope*, 99(1):73–79, Jan 1989. ISSN 0023-852X (Print). doi: 10.1288/00005537-198901000-00014.

[27] Ekaterini T Tsilou, Benjamin I Rubin, Rafael C Caruso, George F Reed, Anita Pikus, James F Hejtmancik, Fumino Iwata, Joy B Redman, and Muriel I Kaiser-Kupfer. Usher syndrome clinical types i and ii: could ocular symptoms and signs differentiate between the two types? *Acta Ophthalmol Scand*, 80(2):196–201, Apr 2002. ISSN 1395-3907 (Print).

[28] Alessandro Iannaccone, Stephen B Kritchevsky, Maria Laura Ciccarelli, Salvatore A Tedesco, Claudio Macaluso, William J Kimberling, and Grant W Somes. Kinetics of visual field loss in usher syndrome type ii. *Invest Ophthalmol Vis Sci*, 45(3):784–792, Mar 2004. ISSN 0146-0404 (Print).

[29] Mazal Cohen, Maria Bitner-Glindzicz, and Linda Luxon. The changing face of usher syndrome: clinical implications. *Int J Audiol*, 46(2):82–93, Feb 2007. ISSN 1499-2027 (Print). doi: 10.1080/14992020600975279.

[30] M L Tamayo, J E Bernal, G E Tamayo, J L Frias, G Alvira, O Vergara, V Rodriguez, J I Uribe, and J C Silva. Usher syndrome: results of a screening program in colombia. *Clin Genet*, 40(4):304–311, Oct 1991. ISSN 0009-9163 (Print).

[31] L Pakarinen, K Tuppurainen, P Laippala, M Mantyjarvi, and H Puhakka. The ophthalmological course of usher syndrome type iii. *Int Ophthalmol*, 19(5):307–311, 1995-1996. ISSN 0165-5701 (Print).

[32] C R Otterstedde, U Spandau, A Blankenagel, W J Kimberling, and C Reisser. A new clinical classification for usher's syndrome based on a new subtype of usher's syndrome type i. *Laryngoscope*, 111(1):84–86, Jan 2001. ISSN 0023-852X (Print). doi: 10.1097/00005537-200101000-00014.

[33] E L Berson. Retinitis pigmentosa. the friedenwald lecture. *Invest Ophthalmol Vis Sci*, 34(5):1659–1676, Apr 1993. ISSN 0146-0404 (Print).

[34] David S Williams. Usher syndrome: animal models, retinal function of usher proteins, and prospects for gene therapy. *Vision Res*, 48(3):433–441, Feb 2008. ISSN 0042-6989 (Print). doi: 10.1016/j.visres.2007.08.015.

[35] H M Fortnum, A Q Summerfield, D H Marshall, A C Davis, and J M Bamford. Prevalence of permanent childhood hearing impairment in the united kingdom and implications for universal neonatal hearing screening: questionnaire based ascertainment study. *BMJ*, 323(7312):536–40, Sep 2001.

[36] unpecified. *Genes and disease*. NCBI, c.2009. URL http://www.ncbi.nlm.nih.gov/books/bv.fcgi?call=bv.View..ShowTOC&rid=gnd.TOC&depth=2.

[37] A C Davis. *Hearing in adults*. Whurr, 1995.

[38] M Bitner-Glindzicz. Hereditary deafness and phenotyping in humans. *Br Med Bull*, 63:73–94, 2002.

[39] W J Kimberling, C G Moller, S Davenport, I A Priluck, P H Beighton, J Greenberg, W Reardon, M D Weston, J B Kenyon, and J A Grunkemeyer. Linkage of

usher syndrome type i gene (ush1b) to the long arm of chromosome 11. *Genomics*, 14(4):988–994, Dec 1992. ISSN 0888-7543 (Print).

[40] H Chaib, J Kaplan, S Gerber, C Vincent, H Ayadi, R Slim, A Munnich, J Weissenbach, and C Petit. A newly identified locus for usher syndrome type i, ush1e, maps to chromosome 21q21. *Hum Mol Genet*, 6(1):27–31, Jan 1997. ISSN 0964-6906 (Print).

[41] D Weil, P Kussel, S Blanchard, G Levy, F Levi-Acobas, M Drira, H Ayadi, and C Petit. The autosomal recessive isolated deafness, dfnb2, and the usher 1b syndrome are allelic defects of the myosin-viia gene. *Nat Genet*, 16(2):191–193, Jun 1997. ISSN 1061-4036 (Print). doi: 10.1038/ng0697-191.

[42] M Hmani, A Ghorbel, A Boulila-Elgaied, Z Ben Zina, W Kammoun, M Drira, M Chaabouni, C Petit, and H Ayadi. A novel locus for usher syndrome type ii, ush2b, maps to chromosome 3 at p23-24.2. *Eur J Hum Genet*, 7(3):363–367, Apr 1999. ISSN 1018-4813 (Print). doi: 10.1038/sj.ejhg.5200307.

[43] M Bitner-Glindzicz, K J Lindley, P Rutland, D Blaydon, V V Smith, P J Milla, K Hussain, J Furth-Lavi, K E Cosgrove, R M Shepherd, P D Barnes, R E O'Brien, P A Farndon, J Sowden, X Z Liu, M J Scanlan, S Malcolm, M J Dunne, A Aynsley-Green, and B Glaser. A recessive contiguous gene deletion causing infantile hyperinsulinism, enteropathy and deafness identifies the usher type 1c gene. *Nat Genet*, 26(1):56–60, Sep 2000. ISSN 1061-4036 (Print). doi: 10.1038/79178.

[44] E Verpy, M Leibovici, I Zwaenepoel, X Z Liu, A Gal, N Salem, A Mansour, S Blanchard, I Kobayashi, B J Keats, R Slim, and C Petit. A defect in harmonin, a pdz domain-containing protein expressed in the inner ear sensory hair cells, underlies usher syndrome type 1c. *Nat Genet*, 26(1):51–55, Sep 2000. ISSN 1061-4036 (Print). doi: 10.1038/79171.

[45] Z M Ahmed, S Riazuddin, S L Bernstein, Z Ahmed, S Khan, A J Griffith, R J Morell, T B Friedman, S Riazuddin, and E R Wilcox. Mutations of the protocadherin gene pcdh15 cause usher syndrome type 1f. *Am J Hum Genet*, 69(1):25–34, Jul 2001. ISSN 0002-9297 (Print). doi: 10.1086/321277.

[46] K N Alagramam, H Yuan, M H Kuehn, C L Murcia, S Wayne, C R Srisailpathy, R B Lowry, R Knaus, L Van Laer, F P Bernier, S Schwartz, C Lee, C C Morton, R F Mullins, A Ramesh, G Van Camp, G S Hageman, R P Woychik, and R J Smith. Mutations in the novel protocadherin pcdh15 cause usher syndrome type 1f. *Hum Mol Genet*, 10(16):1709–1718, Aug 2001. ISSN 0964-6906 (Print).

[47] H Bolz, B von Brederlow, A Ramirez, E C Bryda, K Kutsche, H G Nothwang, M Seeliger, M del C-Salcedo Cabrera, M C Vila, O P Molina, A Gal, and C Kubisch. Mutation of cdh23, encoding a new member of the cadherin gene family, causes usher syndrome type 1d. *Nat Genet*, 27(1):108–112, Jan 2001. ISSN 1061-4036 (Print). doi: 10.1038/83667.

[48] J M Bork, L M Peters, S Riazuddin, S L Bernstein, Z M Ahmed, S L Ness, R Polomeno, A Ramesh, M Schloss, C R Srisailpathy, S Wayne, S Bellman, D Desmukh, Z Ahmed, S N Khan, V M Kaloustian, X C Li, A Lalwani, S Riazuddin, M Bitner-Glindzicz, W E Nance, X Z Liu, G Wistow, R J Smith, A J Griffith, E R Wilcox, T B Friedman, and R J Morell. Usher syndrome 1d and nonsyndromic autosomal recessive deafness dfnb12 are caused by allelic mutations of the novel cadherin-like gene cdh23. *Am J Hum Genet*, 68(1):26–37, Jan 2001. ISSN 0002-9297 (Print). doi: 10.1086/316954.

[49] Dominique Weil, Aziz El-Amraoui, Saber Masmoudi, Mirna Mustapha, Yoshiaki Kikkawa, Sophie Laine, Sedigheh Delmaghani, Avital Adato, Sellama Nadifi, Zeineb Ben Zina, Christian Hamel, Andreas Gal, Hammadi Ayadi, Hiromichi Yonekawa, and Christine Petit. Usher syndrome type i g (ush1g) is caused by mutations in the gene encoding sans, a protein that associates with the ush1c protein, harmonin. *Hum Mol Genet*, 12(5):463–471, Mar 2003. ISSN 0964-6906 (Print).

[50] Erwin van Wijk, Ronald J E Pennings, Heleen te Brinke, Annemarie Claassen, Helger G Yntema, Lies H Hoefsloot, Frans P M Cremers, Cor W R J Cremers, and Hannie Kremer. Identification of 51 novel exons of the usher syndrome type 2a (ush2a) gene that encode multiple conserved functional domains and that are mutated in patients with usher syndrome type ii. *Am J Hum Genet*, 74(4):738–744, Apr 2004. ISSN 0002-9297 (Print). doi: 10.1086/383096.

[51] Michael D Weston, Mirjam W J Luijendijk, Kurt D Humphrey, Claes Moller, and William J Kimberling. Mutations in the vlgr1 gene implicate g-protein signaling in the pathogenesis of usher syndrome type ii. *Am J Hum Genet*, 74(2):357–366, Feb 2004. ISSN 0002-9297 (Print). doi: 10.1086/381685.

[52] Inga Ebermann, Hendrik P N Scholl, Peter Charbel Issa, Elvir Becirovic, Jurgen Lamprecht, Bernhard Jurklies, Jose M Millan, Elena Aller, Diana Mitter, and Hanno Bolz. A novel gene for usher syndrome type 2: mutations in the long isoform of whirlin are associated with retinitis pigmentosa and sensorineural hearing loss. *Hum Genet*, 121(2):203–211, Apr 2007. ISSN 0340-6717 (Print). doi: 10.1007/s00439-006-0304-0.

[53] X Z Liu, J Walsh, P Mburu, J Kendrick-Jones, M J Cope, K P Steel, and S D Brown. Mutations in the myosin viia gene cause non-syndromic recessive deafness. *Nat Genet*, 16(2):188–190, Jun 1997. ISSN 1061-4036 (Print). doi: 10.1038/ng0697-188.

[54] Zubair M Ahmed, Tenesha N Smith, Saima Riazuddin, Tomoko Makishima, Manju Ghosh, Sirosh Bokhari, Puthezhath S N Menon, Dilip Deshmukh, Andrew J Griffith, Sheikh Riazuddin, Thomas B Friedman, and Edward R Wilcox. Nonsyndromic recessive deafness dfnb18 and usher syndrome type ic are allelic mutations of ushic. *Hum Genet*, 110(6):527–531, Jun 2002. ISSN 0340-6717 (Print). doi: 10.1007/s00439-002-0732-4.

[55] L M Astuto, J M Bork, M D Weston, J W Askew, R R Fields, D J Orten, S J Ohliger, S Riazuddin, R J Morell, S Khan, S Riazuddin, H Kremer, P van Hauwe, C G Moller, C W R J Cremers, C Ayuso, J R Heckenlively, K Rohrschneider, U Spandau, J Greenberg, R Ramesar, W Reardon, P Bitoun, J Millan, R Legge, T B Friedman, and W J Kimberling. Cdh23 mutation and phenotype heterogeneity: a profile of 107 diverse families with usher syndrome and nonsyndromic deafness. *Am J Hum Genet*, 71(2):262–275, Aug 2002. ISSN 0002-9297 (Print). doi: 10.1086/341558.

[56] Tamar Ben-Yosef, Seth L Ness, Anne C Madeo, Adi Bar-Lev, Jessica H Wolfman, Zubair M Ahmed, Robert J Desnick, Judith P Willner, Karen B Avraham, Harry Ostrer, Carole Oddoux, Andrew J Griffith, and Thomas B Friedman. A mutation of pcdh15 among ashkenazi jews with the type 1 usher syndrome. *N Engl J Med*, 348(17):1664–1670, Apr 2003. ISSN 1533-4406 (Electronic). doi: 10.1056/NEJMoa021502.

[57] Philomena Mburu, Mirna Mustapha, Anabel Varela, Dominique Weil, Aziz El-Amraoui, Ralph H Holme, Andreas Rump, Rachel E Hardisty, Stephane Blanchard, Roney S Coimbra, Isabelle Perfettini, Nick Parkinson, Ann-Marie Mallon, Pete Glenister, Mike J Rogers, Adam J Paige, Lee Moir, Jo Clay, Andre Rosenthal, Xue Zhong Liu, Gonzalo Blanco, Karen P Steel, Christine Petit, and Steve D M Brown. Defects in whirlin, a pdz domain molecule involved in stereocilia elongation, cause deafness in the whirler mouse and families with dfnb31. *Nat Genet*, 34(4):421–428, Aug 2003. ISSN 1061-4036 (Print). doi: 10.1038/ng1208.

[58] C Rivolta, E A Sweklo, E L Berson, and T P Dryja. Missense mutation in the ush2a gene: association with recessive retinitis pigmentosa without hearing loss. *Am J Hum Genet*, 66(6):1975–1978, Jun 2000. ISSN 0002-9297 (Print). doi: 10.1086/302926.

[59] Babak Jian Seyedahmadi, Carlo Rivolta, Julia A Keene, Eliot L Berson, and Thaddeus P Dryja. Comprehensive screening of the ush2a gene in usher syndrome type ii and non-syndromic recessive retinitis pigmentosa. *Exp Eye Res*, 79(2): 167–173, Aug 2004. ISSN 0014-4835 (Print). doi: 10.1016/j.exer.2004.03.005.

[60] X Z Liu, S H Blanton, M Bitner-Glindzicz, A Pandya, B Landa, B MacArdle, K Rajput, S Bellman, B T Webb, X Ping, R J Smith, and W E Nance. Haplotype analysis of the ush1d locus and genotype-phenotype correlations. *Clin Genet*, 60 (1):58–62, Jul 2001. ISSN 0009-9163 (Print).

[61] Julie M Bork, Robert J Morell, Shaheen Khan, Sheikh Riazuddin, Edward R Wilcox, Thomas B Friedman, and Andrew J Griffith. Clinical presentation of dfnb12 and usher syndrome type 1d. *Adv Otorhinolaryngol*, 61:145–152, 2002. ISSN 0065-3071 (Print).

[62] Xiao Mei Ouyang, Xia Juan Xia, Elisabeth Verpy, Li Lin Du, Arti Pandya, Christine Petit, Thomas Balkany, Walter E Nance, and Xue Zhong Liu. Mutations in the alternatively spliced exons of ush1c cause non-syndromic recessive deafness. *Hum Genet*, 111(1):26–30, Jul 2002. ISSN 0340-6717 (Print). doi: 10.1007/s00439-002-0736-0.

[63] Zubair M Ahmed, Saima Riazuddin, Jamil Ahmad, Steve L Bernstein, Yan Guo, Muhammad F Sabar, Paul Sieving, Sheikh Riazuddin, Andrew J Griffith, Thomas B Friedman, Inna A Belyantseva, and Edward R Wilcox. Pcdh15 is expressed in the neurosensory epithelium of the eye and ear and mutant alleles are responsible for both ush1f and dfnb23. *Hum Mol Genet*, 12(24):3215–3223, Dec 2003. ISSN 0964-6906 (Print). doi: 10.1093/hmg/ddg358.

[64] A-F Roux, V Faugere, S Le Guedard, N Pallares-Ruiz, A Vielle, S Chambert, S Marlin, C Hamel, B Gilbert, S Malcolm, and M Claustres. Survey of the frequency of ush1 gene mutations in a cohort of usher patients shows the importance of cadherin 23 and protocadherin 15 genes and establishes a detection rate of above 90 *J Med Genet*, 43(9):763–768, Sep 2006. ISSN 1468-6244 (Electronic). doi: 10.1136/jmg.2006.041954.

[65] Sandie Le Guedard, Valerie Faugere, Sue Malcolm, Mireille Claustres, and Anne-Francoise Roux. Large genomic rearrangements within the pcdh15 gene are a significant cause of ush1f syndrome. *Mol Vis*, 13:102–107, 2007. ISSN 1090-0535 (Electronic).

[66] X Z Liu, C Hope, C Y Liang, J M Zou, L R Xu, T Cole, R F Mueller, S Bundey, W Nance, K P Steel, and S D Brown. A mutation (2314delg) in the usher syndrome

type iia gene: high prevalence and phenotypic variation. *Am J Hum Genet*, 64(4): 1221–1225, Apr 1999. ISSN 0002-9297 (Print).

[67] S Bernal, C Meda, T Solans, C Ayuso, B Garcia-Sandoval, D Valverde, E Del Rio, and M Baiget. Clinical and genetic studies in spanish patients with usher syndrome type ii: description of new mutations and evidence for a lack of genotype–phenotype correlation. *Clin Genet*, 68(3):204–214, Sep 2005. ISSN 0009-9163 (Print). doi: 10.1111/j.1399-0004.2005.00481.x.

[68] Tomas Fernandez-Alfonso and Timothy A Ryan. The efficiency of the synaptic vesicle cycle at central nervous system synapses. *Trends Cell Biol*, 16(8):413–420, Aug 2006. ISSN 0962-8924 (Print). doi: 10.1016/j.tcb.2006.06.007.

[69] Batiste Boeda, Aziz El-Amraoui, Amel Bahloul, Richard Goodyear, Laurent Daviet, Stephane Blanchard, Isabelle Perfettini, Karl R Fath, Spencer Shorte, Jan Reiners, Anne Houdusse, Pierre Legrain, Uwe Wolfrum, Guy Richardson, and Christine Petit. Myosin viia, harmonin and cadherin 23, three usher i gene products that cooperate to shape the sensory hair cell bundle. *EMBO J*, 21(24): 6689–6699, Dec 2002. ISSN 0261-4189 (Print).

[70] Jan Reiners, Boris Reidel, Aziz El-Amraoui, Batiste Boeda, Irene Huber, Christine Petit, and Uwe Wolfrum. Differential distribution of harmonin isoforms and their possible role in usher-1 protein complexes in mammalian photoreceptor cells. *Invest Ophthalmol Vis Sci*, 44(11):5006–5015, Nov 2003. ISSN 0146-0404 (Print).

[71] Avital Adato, Vincent Michel, Yoshiaki Kikkawa, Jan Reiners, Kumar N Alagramam, Dominique Weil, Hiromichi Yonekawa, Uwe Wolfrum, Aziz El-Amraoui, and Christine Petit. Interactions in the network of usher syndrome type 1 proteins. *Hum Mol Genet*, 14(3):347–356, Feb 2005. ISSN 0964-6906 (Print). doi: 10.1093/hmg/ddi031.

[72] Jan Reiners, Erwin van Wijk, Tina Marker, Ulrike Zimmermann, Karin Jurgens, Heleen te Brinke, Nora Overlack, Ronald Roepman, Marlies Knipper, Hannie Kremer, and Uwe Wolfrum. Scaffold protein harmonin (ush1c) provides molecular links between usher syndrome type 1 and type 2. *Hum Mol Genet*, 14(24):3933–3943, Dec 2005. ISSN 0964-6906 (Print). doi: 10.1093/hmg/ddi417.

[73] Mathias Senften, Martin Schwander, Piotr Kazmierczak, Concepcion Lillo, Jung-Bum Shin, Tama Hasson, Gwenaelle S G Geleoc, Peter G Gillespie, David Williams, Jeffrey R Holt, and Ulrich Muller. Physical and functional interaction between protocadherin 15 and myosin viia in mechanosensory hair cells. *J Neurosci*, 26(7):2060–2071, Feb 2006. ISSN 1529-2401 (Electronic). doi: 10.1523/JNEUROSCI.4251-05.2006.

[74] Erwin van Wijk, Bert van der Zwaag, Theo Peters, Ulrike Zimmermann, Heleen Te Brinke, Ferry F J Kersten, Tina Marker, Elena Aller, Lies H Hoefsloot, Cor W R J Cremers, Frans P M Cremers, Uwe Wolfrum, Marlies Knipper, Ronald Roepman, and Hannie Kremer. The dfnb31 gene product whirlin connects to the usher protein network in the cochlea and retina by direct association with ush2a and vlgr1. *Hum Mol Genet*, 15(5):751–765, Mar 2006. ISSN 0964-6906 (Print). doi: 10.1093/hmg/ddi490.

[75] Hannie Kremer, Erwin van Wijk, Tina Marker, Uwe Wolfrum, and Ronald Roepman. Usher syndrome: molecular links of pathogenesis, proteins and pathways. *Hum Mol Genet*, 15 Spec No 2:R262–70, Oct 2006. ISSN 0964-6906 (Print). doi: 10.1093/hmg/ddl205.

[76] Tina Maerker, Erwin van Wijk, Nora Overlack, Ferry F J Kersten, Joann McGee, Tobias Goldmann, Elisabeth Sehn, Ronald Roepman, Edward J Walsh, Hannie Kremer, and Uwe Wolfrum. A novel usher protein network at the periciliary reloading point between molecular transport machineries in vertebrate photoreceptor cells. *Hum Mol Genet*, 17(1):71–86, Jan 2008. ISSN 0964-6906 (Print). doi: 10.1093/hmg/ddm285.

[77] Avital Adato, Gaelle Lefevre, Benjamin Delprat, Vincent Michel, Nicolas Michalski, Sebastien Chardenoux, Dominique Weil, Aziz El-Amraoui, and Christine Petit. Usherin, the defective protein in usher syndrome type iia, is likely to be a component of interstereocilia ankle links in the inner ear sensory cells. *Hum Mol Genet*, 14(24):3921–3932, Dec 2005. ISSN 0964-6906 (Print). doi: 10.1093/hmg/ddi416.

[78] N A Adams, Ahmed Awadein, and Hassanain S Toma. The retinal ciliopathies. *Ophthalmic Genet*, 28(3):113–125, Sep 2007. ISSN 1381-6810 (Print). doi: 10.1080/13816810701537424.

[79] T P Dryja, S M Adams, J L Grimsby, T L McGee, D H Hong, T Li, S Andréasson, and E L Berson. Null rpgrip1 alleles in patients with leber congenital amaurosis. *Am J Hum Genet*, 68(5):1295–8, May 2001. doi: 10.1086/320113.

[80] A Meindl, K Dry, K Herrmann, F Manson, A Ciccodicola, A Edgar, M R Carvalho, H Achatz, H Hellebrand, A Lennon, C Migliaccio, K Porter, E Zrenner, A Bird, M Jay, B Lorenz, B Wittwer, M D'Urso, T Meitinger, and A Wright. A gene (rpgr) with homology to the rcc1 guanine nucleotide exchange factor is mutated in x-linked retinitis pigmentosa (rp3). *Nat Genet*, 13(1):35–42, May 1996. doi: 10.1038/ng0596-35.

[81] O E Blacque and M R Leroux. Bardet-biedl syndrome: an emerging pathomechanism of intracellular transport. *Cell Mol Life Sci*, 63(18):2145–61, Sep 2006. doi: 10.1007/s00018-006-6180-x.

[82] Maxence V Nachury, Alexander V Loktev, Qihong Zhang, Christopher J Westlake, Johan Peränen, Andreas Merdes, Diane C Slusarski, Richard H Scheller, J Fernando Bazan, Val C Sheffield, and Peter K Jackson. A core complex of bbs proteins cooperates with the gtpase rab8 to promote ciliary membrane biogenesis. *Cell*, 129(6):1201–13, Jun 2007. doi: 10.1016/j.cell.2007.03.053.

[83] Z Y Chen, T Hasson, P M Kelley, B J Schwender, M F Schwartz, M Ramakrishnan, W J Kimberling, M S Mooseker, and D P Corey. Molecular cloning and domain structure of human myosin-viia, the gene product defective in usher syndrome 1b. *Genomics*, 36(3):440–448, Sep 1996. ISSN 0888-7543 (Print). doi: 10.1006/geno.1996.0489.

[84] D Weil, S Blanchard, J Kaplan, P Guilford, F Gibson, J Walsh, P Mburu, A Varela, J Levilliers, and M D Weston. Defective myosin viia gene responsible for usher syndrome type 1b. *Nature*, 374(6517):60–61, Mar 1995. ISSN 0028-0836 (Print). doi: 10.1038/374060a0.

[85] M D Weston, P M Kelley, L D Overbeck, M Wagenaar, D J Orten, T Hasson, Z Y Chen, D Corey, M Mooseker, J Sumegi, C Cremers, C Moller, S G Jacobson, M B Gorin, and W J Kimberling. Myosin viia mutation screening in 189 usher syndrome type 1 patients. *Am J Hum Genet*, 59(5):1074–1083, Nov 1996. ISSN 0002-9297 (Print).

[86] X Z Liu, C Hope, J Walsh, V Newton, X M Ke, C Y Liang, L R Xu, J M Zhou, D Trump, K P Steel, S Bundey, and S D Brown. Mutations in the myosin viia gene cause a wide phenotypic spectrum, including atypical usher syndrome. *Am J Hum Genet*, 63(3):909–912, Sep 1998. ISSN 0002-9297 (Print). doi: 10.1086/302026.

[87] Z B Zina, S Masmoudi, H Ayadi, F Chaker, A M Ghorbel, M Drira, and C Petit. From dfnb2 to usher syndrome: variable expressivity of the same disease. *Am J Med Genet*, 101(2):181–183, Jun 2001. ISSN 0148-7299 (Print).

[88] X Z Liu, J Walsh, Y Tamagawa, K Kitamura, M Nishizawa, K P Steel, and S D Brown. Autosomal dominant non-syndromic deafness caused by a mutation in the myosin viia gene. *Nat Genet*, 17(3):268–9, Nov 1997. doi: 10.1038/ng1197-268.

[89] Xue Zhong Liu. The clinical presentation of dfnb2. *Adv Otorhinolaryngol*, 61:120–3, 2002.

[90] F Gibson, J Walsh, P Mburu, A Varela, K A Brown, M Antonio, K W Beisel, K P Steel, and S D Brown. A type vii myosin encoded by the mouse deafness gene shaker-1. *Nature*, 374(6517):62–4, Mar 1995. doi: 10.1038/374062a0.

[91] X Liu, B Ondek, and D S Williams. Mutant myosin viia causes defective melanosome distribution in the rpe of shaker-1 mice. *Nat Genet*, 19(2):117–8, Jun 1998. doi: 10.1038/470.

[92] M M DeAngelis, T L McGee, B J Keats, R Slim, E L Berson, and T P Dryja. Two families from new england with usher syndrome type ic with distinct haplotypes. *Am J Ophthalmol*, 131(3):355–358, Mar 2001. ISSN 0002-9394 (Print).

[93] Sevtap Savas, Ben Frischhertz, Mary Z Pelias, Mark A Batzer, Prescott L Deininger, and Bronya B Keats. The ush1c 216g–¿a mutation and the 9-repeat vntr(t,t) allele are in complete linkage disequilibrium in the acadian population. *Hum Genet*, 110(1):95–97, Jan 2002. ISSN 0340-6717 (Print). doi: 10.1007/s00439-001-0653-7.

[94] I Zwaenepoel, E Verpy, S Blanchard, M Meins, E Apfelstedt-Sylla, A Gal, and C Petit. Identification of three novel mutations in the ush1c gene and detection of thirty-one polymorphisms used for haplotype analysis. *Hum Mutat*, 17(1):34–41, 2001. ISSN 1098-1004 (Electronic). doi: 10.1002/1098-1004(2001)17:1⟨34::AID-HUMU4⟩3.0.CO;2-O.

[95] D C Blaydon, R F Mueller, T P Hutchin, B P Leroy, S S Bhattacharya, A C Bird, S Malcolm, and M Bitner-Glindzicz. The contribution of ush1c mutations to syndromic and non-syndromic deafness in the uk. *Clin Genet*, 63(4):303–307, Apr 2003. ISSN 0009-9163 (Print).

[96] Jennifer Lentz, Sevtap Savas, San-San Ng, Grace Athas, Prescott Deininger, and Bronya Keats. The ush1c 216g–¿a splice-site mutation results in a 35-base-pair deletion. *Hum Genet*, 116(3):225–227, Feb 2005. ISSN 0340-6717 (Print). doi: 10.1007/s00439-004-1217-4.

[97] X M Ouyang, J F Hejtmancik, S G Jacobson, X J Xia, A Li, L L Du, V Newton, M Kaiser, T Balkany, W E Nance, and X-Z Liu. Ush1c: a rare cause of ush1 in a non-acadian population and a founder effect of the acadian allele. *Clin Genet*, 63 (2):150–153, Feb 2003. ISSN 0009-9163 (Print).

[98] Jan Siemens, Piotr Kazmierczak, Anna Reynolds, Melanie Sticker, Amanda Littlewood-Evans, and Ulrich Muller. The usher syndrome proteins cadherin 23 and harmonin form a complex by means of pdz-domain interactions. *Proc Natl*

Acad Sci U S A, 99(23):14946–14951, Nov 2002. ISSN 0027-8424 (Print). doi: 10.1073/pnas.232579599.

[99] Zubair M Ahmed, Richard Goodyear, Saima Riazuddin, Ayala Lagziel, P Kevin Legan, Martine Behra, Shawn M Burgess, Kathryn S Lilley, Edward R Wilcox, Sheikh Riazuddin, Andrew J Griffith, Gregory I Frolenkov, Inna A Belyantseva, Guy P Richardson, and Thomas B Friedman. The tip-link antigen, a protein associated with the transduction complex of sensory hair cells, is protocadherin-15. *J Neurosci*, 26(26):7022–7034, Jun 2006. ISSN 1529-2401 (Electronic). doi: 10.1523/JNEUROSCI.1163-06.2006.

[100] Piotr Kazmierczak, Hirofumi Sakaguchi, Joshua Tokita, Elizabeth M Wilson-Kubalek, Ronald A Milligan, Ulrich Müller, and Bechara Kachar. Cadherin 23 and protocadherin 15 interact to form tip-link filaments in sensory hair cells. *Nature*, 449(7158):87–91, Sep 2007. doi: 10.1038/nature06091.

[101] Ayala Lagziel, Zubair M Ahmed, Julie M Schultz, Robert J Morell, Inna A Belyantseva, and Thomas B Friedman. Spatiotemporal pattern and isoforms of cadherin 23 in wild type and waltzer mice during inner ear hair cell development. *Dev Biol*, 280 (2):295–306, Apr 2005. ISSN 0012-1606 (Print). doi: 10.1016/j.ydbio.2005.01.015.

[102] Agnieszka K Rzadzinska, Adam Derr, Bechara Kachar, and Konrad Noben-Trauth. Sustained cadherin 23 expression in young and adult cochlea of normal and hearing-impaired mice. *Hear Res*, 208(1-2):114–21, Oct 2005. doi: 10.1016/j.heares.2005.05.008.

[103] Jan Siemens, Concepcion Lillo, Rachel A Dumont, Anna Reynolds, David S Williams, Peter G Gillespie, and Ulrich Müller. Cadherin 23 is a component of the tip link in hair-cell stereocilia. *Nature*, 428(6986):950–5, Apr 2004. doi: 10.1038/nature02483.

[104] Zubair M Ahmed, Saima Riazuddin, Sandar Aye, Rana A Ali, Hanka Venselaar, Saima Anwar, Polina P Belyantseva, Muhammad Qasim, Sheikh Riazuddin, and Thomas B Friedman. Gene structure and mutant alleles of pcdh15: nonsyndromic deafness dfnb23 and type 1 usher syndrome. *Hum Genet*, 124(3):215–223, Oct 2008. ISSN 1432-1203 (Electronic). doi: 10.1007/s00439-008-0543-3.

[105] L Doucette, ND Merner, S Cooke, E Ives, D Galutira, V Walsh, T Walsh, L Maclaren, T Cater, B Fernandez, JS Green, ER Wilcox, L Shotland, XC Li, M Lee, MC King, and TL Young. Profound, prelingual nonsyndromic deafness maps to chromosome 10q21 and is caused by a novel missense mutation in the usher syndrome type if gene pcdh15. *Eur J Hum Genet*, Dec 2008. doi: 10.1038/ejhg.2008.231.

[106] Stuart W Webb, Nicolas Grillet, Leonardo R Andrade, Wei Xiong, Lani Swarthout, Charley C Della Santina, Bechara Kachar, and Ulrich Müller. Regulation of pcdh15 function in mechanosensory hair cells by alternative splicing of the cytoplasmic domain. *Development*, 138(8):1607–17, Apr 2011. doi: 10.1242/dev.060061.

[107] Elena Aller, Teresa Jaijo, Gema García-García, M José Aparisi, David Blesa, Manuel Díaz-Llopis, Carmen Ayuso, and José M Millán. Identification of large rearrangements of the pcdh15 gene by combined mlpa and a cgh: large duplications are responsible for usher syndrome. *Invest Ophthalmol Vis Sci*, 51(11):5480–5, Nov 2010. doi: 10.1167/iovs.10-5359.

[108] Elisa Caberlotto, Vincent Michel, Isabelle Foucher, Amel Bahloul, Richard J Goodyear, Elise Pepermans, Nicolas Michalski, Isabelle Perfettini, Olinda Alegria-Prévot, Sébastien Chardenoux, Marcio Do Cruzeiro, Jean-Pierre Hardelin, Guy P Richardson, Paul Avan, Dominique Weil, and Christine Petit. Usher type 1g protein sans is a critical component of the tip-link complex, a structure controlling actin polymerization in stereocilia. *Proc Natl Acad Sci U S A*, 108(14):5825–30, Apr 2011. doi: 10.1073/pnas.1017114108.

[109] E Kalay, A P M de Brouwer, R Caylan, S B Nabuurs, B Wollnik, A Karaguzel, J G A M Heister, H Erdol, F P M Cremers, C W R J Cremers, H G Brunner, and H Kremer. A novel d458v mutation in the sans pdz binding motif causes atypical usher syndrome. *J Mol Med*, 83(12):1025–1032, Dec 2005. ISSN 0946-2716 (Print). doi: 10.1007/s00109-005-0719-4.

[110] Xiao Mei Ouyang, Denise Yan, Li Lin Du, J Fielding Hejtmancik, Samuel G Jacobson, Walter E Nance, An Ren Li, Simon Angeli, Muriel Kaiser, Valerie Newton, Steve D M Brown, Thomas Balkany, and Xue Zhong Liu. Characterization of usher syndrome type i gene mutations in an usher syndrome patient population. *Hum Genet*, 116(4):292–299, Mar 2005. ISSN 0340-6717 (Print). doi: 10.1007/s00439-004-1227-2.

[111] Xiaoqing Liu, Oleg V Bulgakov, Keith N Darrow, Basil Pawlyk, Michael Adamian, M Charles Liberman, and Tiansen Li. Usherin is required for maintenance of retinal photoreceptors and normal development of cochlear hair cells. *Proc Natl Acad Sci U S A*, 104(11):4413–4418, Mar 2007. ISSN 0027-8424 (Print). doi: 10.1073/pnas.0610950104.

[112] N Hilgert, K Kahrizi, N Dieltjens, N Bazazzadegan, H Najmabadi, R J H Smith, and G Van Camp. A large deletion in gpr98 causes type iic usher syndrome in male and female members of an iranian family. *J Med Genet*, 46(4):272–6, Apr 2009. doi: 10.1136/jmg.2008.060947.

[113] Martin E Hemler. Tetraspanin functions and associated microdomains. *Nat Rev Mol Cell Biol*, 6(10):801–11, Oct 2005. doi: 10.1038/nrm1736.

[114] H T Maecker, S C Todd, and S Levy. The tetraspanin superfamily: molecular facilitators. *FASEB J*, 11(6):428–42, May 1997.

[115] Guilian Tian, Yun Zhou, Dagmar Hajkova, Masaru Miyagi, Astra Dinculescu, William W Hauswirth, Krzysztof Palczewski, Ruishuang Geng, Kumar N Alagramam, Juha Isosomppi, Eeva-Marja Sankila, John G Flannery, and Yoshikazu Imanishi. Clarin-1, encoded by the usher syndrome iii causative gene, forms a membranous microdomain: possible role of clarin-1 in organizing the actin cytoskeleton. *J Biol Chem*, 284(28):18980–93, Jul 2009. doi: 10.1074/jbc.M109.003160.

[116] Z M Ahmed, S Riazuddin, S N Khan, P L Friedman, S Riazuddin, and T B Friedman. Ush1h, a novel locus for type i usher syndrome, maps to chromosome 15q22-23. *Clin Genet*, 75(1):86–91, Jan 2009. ISSN 1399-0004 (Electronic). doi: 10.1111/j.1399-0004.2008.01038.x.

[117] Sylvie Gerber, Dominique Bonneau, Brigitte Gilbert, Arnold Munnich, Jean-Louis Dufier, Jean-Michel Rozet, and Josseline Kaplan. Ush1a: chronicle of a slow death. *Am J Hum Genet*, 78(2):357–359, Feb 2006. ISSN 0002-9297 (Print). doi: 10.1086/500275.

[118] Raffi Tonikian, Yingnan Zhang, Stephen L Sazinsky, Bridget Currell, Jung-Hua Yeh, Boris Reva, Heike A Held, Brent A Appleton, Marie Evangelista, Yan Wu, Xiaofeng Xin, Andrew C Chan, Somasekar Seshagiri, Laurence A Lasky, Chris Sander, Charles Boone, Gary D Bader, and Sachdev S Sidhu. A specificity map for the pdz domain family. *PLoS Biol*, 6(9):e239, Sep 2008. ISSN 1545-7885 (Electronic). doi: 10.1371/journal.pbio.0060239.

[119] Michal I Milewski, Andrea Lopez, Monika Jurkowska, Jessica Larusch, and Garry R Cutting. Pdz-binding motifs are unable to ensure correct polarized protein distribution in the absence of additional localization signals. *FEBS Lett*, 579 (2):483–487, Jan 2005. ISSN 0014-5793 (Print). doi: 10.1016/j.febslet.2004.11.106.

[120] Benjamin Delprat, Vincent Michel, Richard Goodyear, Yasuhiro Yamasaki, Nicolas Michalski, Aziz El-Amraoui, Isabelle Perfettini, Pierre Legrain, Guy Richardson, Jean-Pierre Hardelin, and Christine Petit. Myosin xva and whirlin, two deafness gene products required for hair bundle growth, are located at the stereocilia tips and interact directly. *Hum Mol Genet*, 14(3):401–410, Feb 2005. ISSN 0964-6906 (Print). doi: 10.1093/hmg/ddi036.

[121] Waldo Herrera, Tomas S Aleman, Artur V Cideciyan, Alejandro J Roman, Eyal Banin, Tamar Ben-Yosef, Leigh M Gardner, Alexander Sumaroka, Elizabeth A M Windsor, Sharon B Schwartz, Edwin M Stone, Xue-Zhong Liu, William J Kimberling, and Samuel G Jacobson. Retinal disease in usher syndrome iii caused by mutations in the clarin-1 gene. *Invest Ophthalmol Vis Sci*, 49(6):2651–2660, Jun 2008. ISSN 0146-0404 (Print). doi: 10.1167/iovs.07-1505.

[122] A J Hudspeth. How hearing happens. *Neuron*, 19(5):947–50, Nov 1997.

[123] U Müller and A Littlewood-Evans. Mechanisms that regulate mechanosensory hair cell differentiation. *Trends Cell Biol*, 11(8):334–42, Aug 2001.

[124] Melissa A Vollrath, Kelvin Y Kwan, and David P Corey. The micromachinery of mechanotransduction in hair cells. *Annu Rev Neurosci*, 30:339–65, 2007. doi: 10.1146/annurev.neuro.29.051605.112917.

[125] A el Amraoui, I Sahly, S Picaud, J Sahel, M Abitbol, and C Petit. Human usher 1b/mouse shaker-1: the retinal phenotype discrepancy explained by the presence/absence of myosin viia in the photoreceptor cells. *Hum Mol Genet*, 5(8): 1171–1178, Aug 1996. ISSN 0964-6906 (Print).

[126] T Hasson, J Walsh, J Cable, M S Mooseker, S D Brown, and K P Steel. Effects of shaker-1 mutations on myosin-viia protein and mrna expression. *Cell Motil Cytoskeleton*, 37(2):127–138, 1997. ISSN 0886-1544 (Print). doi: 10.1002/(SICI)1097-0169(1997)37:2⟨127::AID-CM5⟩3.0.CO;2-5.

[127] Z M Ahmed, S Riazuddin, S Riazuddin, and E R Wilcox. The molecular genetics of usher syndrome. *Clin Genet*, 63(6):431–444, Jun 2003. ISSN 0009-9163 (Print).

[128] Vincent Michel, Richard J Goodyear, Dominique Weil, Walter Marcotti, Isabelle Perfettini, Uwe Wolfrum, Corné J Kros, Guy P Richardson, and Christine Petit. Cadherin 23 is a component of the transient lateral links in the developing hair bundles of cochlear sensory cells. *Dev Biol*, 280(2):281–94, Apr 2005. doi: 10.1016/j.ydbio.2005.01.014.

[129] Ulrich Muller. Cadherins and mechanotransduction by hair cells. *Curr Opin Cell Biol*, 20(5):557–566, Oct 2008. ISSN 0955-0674 (Print). doi: 10.1016/j.ceb.2008.06.004.

[130] Joann McGee, Richard J Goodyear, D Randy McMillan, Eric A Stauffer, Jeffrey R Holt, Kirsten G Locke, David G Birch, P Kevin Legan, Perrin C White, Edward J Walsh, and Guy P Richardson. The very large g-protein-coupled receptor vlgr1: a component of the ankle link complex required for the normal development of

auditory hair bundles. *J Neurosci*, 26(24):6543–6553, Jun 2006. ISSN 1529-2401 (Electronic). doi: 10.1523/JNEUROSCI.0693-06.2006.

[131] Nicolas Michalski, Vincent Michel, Amel Bahloul, Gaëlle Lefèvre, Jérémie Barral, Hideshi Yagi, Sébastien Chardenoux, Dominique Weil, Pascal Martin, Jean-Pierre Hardelin, Makoto Sato, and Christine Petit. Molecular characterization of the ankle-link complex in cochlear hair cells and its role in the hair bundle functioning. *J Neurosci*, 27(24):6478–88, Jun 2007. doi: 10.1523/JNEUROSCI.0342-07.2007.

[132] P Küssel-Andermann, A El-Amraoui, S Safieddine, S Nouaille, I Perfettini, M Lecuit, P Cossart, U Wolfrum, and C Petit. Vezatin, a novel transmembrane protein, bridges myosin viia to the cadherin-catenins complex. *EMBO J*, 19(22): 6020–9, Nov 2000. doi: 10.1093/emboj/19.22.6020.

[133] F Di Palma, R H Holme, E C Bryda, I A Belyantseva, R Pellegrino, B Kachar, K P Steel, and K Noben-Trauth. Mutations in cdh23, encoding a new type of cadherin, cause stereocilia disorganization in waltzer, the mouse model for usher syndrome type 1d. *Nat Genet*, 27(1):103–107, Jan 2001. ISSN 1061-4036 (Print). doi: 10.1038/83660.

[134] Kenneth R Johnson, Leona H Gagnon, Lisa S Webb, Luanne L Peters, Norman L Hawes, Bo Chang, and Qing Yin Zheng. Mouse models of ush1c and dfnb18: phenotypic and molecular analyses of two new spontaneous mutations of the ush1c gene. *Hum Mol Genet*, 12(23):3075–3086, Dec 2003. ISSN 0964-6906 (Print). doi: 10.1093/hmg/ddg332.

[135] Yoshiaki Kikkawa, Hiroshi Shitara, Shigeharu Wakana, Yuki Kohara, Toyoyuki Takada, Mieko Okamoto, Choji Taya, Kazusaku Kamiya, Yasuhiro Yoshikawa, Hisashi Tokano, Ken Kitamura, Kunihiko Shimizu, Yuichi Wakabayashi, Toshihiko Shiroishi, Ryo Kominami, and Hiromichi Yonekawa. Mutations in a new scaffold protein sans cause deafness in jackson shaker mice. *Hum Mol Genet*, 12(5):453–61, Mar 2003.

[136] Jan Reiners, Kerstin Nagel-Wolfrum, Karin Jurgens, Tina Marker, and Uwe Wolfrum. Molecular basis of human usher syndrome: deciphering the meshes of the usher protein network provides insights into the pathomechanisms of the usher disease. *Exp Eye Res*, 83(1):97–119, Jul 2006. ISSN 0014-4835 (Print). doi: 10.1016/j.exer.2005.11.010.

[137] T Self, M Mahony, J Fleming, J Walsh, S D Brown, and K P Steel. Shaker-1 mutations reveal roles for myosin viia in both development and function of cochlear hair cells. *Development*, 125(4):557–566, Feb 1998. ISSN 0950-1991 (Print).

[138] U Wolfrum and A Schmitt. Rhodopsin transport in the membrane of the connecting cilium of mammalian photoreceptor cells. *Cell Motil Cytoskeleton*, 46(2): 95–107, Jun 2000. ISSN 0886-1544 (Print). doi: 10.1002/1097-0169(200006)46: 2⟨95::AID-CM2⟩3.0.CO;2-Q.

[139] D G Hunter, G A Fishman, R S Mehta, and F L Kretzer. Abnormal sperm and photoreceptor axonemes in usher's syndrome. *Arch Ophthalmol*, 104(3):385–9, Mar 1986.

[140] S D Barrong, M H Chaitin, S J Fliesler, D E Possin, S G Jacobson, and A H Milam. Ultrastructure of connecting cilia in different forms of retinitis pigmentosa. *Arch Ophthalmol*, 110(5):706–710, May 1992. ISSN 0003-9950 (Print).

[141] U Wolfrum, X Liu, A Schmitt, I P Udovichenko, and D S Williams. Myosin viia as a common component of cilia and microvilli. *Cell Motil Cytoskeleton*, 40(3): 261–271, 1998. ISSN 0886-1544 (Print). doi: 10.1002/(SICI)1097-0169(1998)40: 3⟨261::AID-CM5⟩3.0.CO;2-G.

[142] Jan Reiners, Tina Marker, Karin Jurgens, Boris Reidel, and Uwe Wolfrum. Photoreceptor expression of the usher syndrome type 1 protein protocadherin 15 (ush1f) and its interaction with the scaffold protein harmonin (ush1c). *Mol Vis*, 11:347–355, 2005. ISSN 1090-0535 (Electronic).

[143] Jan Reiners and Uwe Wolfrum. Molecular analysis of the supramolecular usher protein complex in the retina. harmonin as the key protein of the usher syndrome. *Adv Exp Med Biol*, 572:349–353, 2006. ISSN 0065-2598 (Print).

[144] Samuel G Jacobson, Artur V Cideciyan, Tomas S Aleman, Alexander Sumaroka, Alejandro J Roman, Leigh M Gardner, Haydn M Prosser, Monalisa Mishra, N Torben Bech-Hansen, Waldo Herrera, Sharon B Schwartz, Xue-Zhong Liu, William J Kimberling, Karen P Steel, and David S Williams. Usher syndromes due to myo7a, pcdh15, ush2a or gpr98 mutations share retinal disease mechanism. *Hum Mol Genet*, 17(15):2405–2415, Aug 2008. ISSN 1460-2083 (Electronic). doi: 10.1093/hmg/ddn140.

[145] Carlo Rivolta, Eliot L Berson, and Thaddeus P Dryja. Paternal uniparental heterodisomy with partial isodisomy of chromosome 1 in a patient with retinitis pigmentosa without hearing loss and a missense mutation in the usher syndrome type ii gene ush2a. *Arch Ophthalmol*, 120(11):1566–1571, Nov 2002. ISSN 0003-9950 (Print).

[146] A P Strachan, T Read. *Human Molecular Genetics 2*. Garland Science, 1999.

[147] W H Li and L A Sadler. Low nucleotide diversity in man. *Genetics*, 129(2):513–23, Oct 1991.

[148] M Cargill, D Altshuler, J Ireland, P Sklar, K Ardlie, N Patil, N Shaw, C R Lane, E P Lim, N Kalyanaraman, J Nemesh, L Ziaugra, L Friedland, A Rolfe, J Warrington, R Lipshutz, G Q Daley, and E S Lander. Characterization of single-nucleotide polymorphisms in coding regions of human genes. *Nat Genet*, 22 (3):231–8, Jul 1999. doi: 10.1038/10290.

[149] R Sachidanandam, D Weissman, S C Schmidt, J M Kakol, L D Stein, G Marth, S Sherry, J C Mullikin, B J Mortimore, D L Willey, S E Hunt, C G Cole, P C Coggill, C M Rice, Z Ning, J Rogers, D R Bentley, P Y Kwok, E R Mardis, R T Yeh, B Schultz, L Cook, R Davenport, M Dante, L Fulton, L Hillier, R H Waterston, J D McPherson, B Gilman, S Schaffner, W J Van Etten, D Reich, J Higgins, M J Daly, B Blumenstiel, J Baldwin, N Stange-Thomann, M C Zody, L Linton, E S Lander, D Altshuler, and International SNP Map Working Group. A map of human genome sequence variation containing 1.42 million single nucleotide polymorphisms. *Nature*, 409(6822):928–33, Feb 2001. doi: 10.1038/35057149.

[150] David A Hinds, Laura L Stuve, Geoffrey B Nilsen, Eran Halperin, Eleazar Eskin, Dennis G Ballinger, Kelly A Frazer, and David R Cox. Whole-genome patterns of common dna variation in three human populations. *Science*, 307(5712):1072–9, Feb 2005. doi: 10.1126/science.1105436.

[151] M Genuardi, S Carrara, M Anti, M Ponz de Leòn, and A Viel. Assessment of pathogenicity criteria for constitutional missense mutations of the hereditary non-polyposis colorectal cancer genes mlh1 and msh2. *Eur J Hum Genet*, 7(7):778–82, 1999. doi: 10.1038/sj.ejhg.5200363.

[152] D Frishman and P Argos. Incorporation of non-local interactions in protein secondary structure prediction from the amino acid sequence. *Protein Eng*, 9(2): 133–42, Feb 1996.

[153] Xiaohong Li, Steven G Self, Patricia C Galipeau, Thomas G Paulson, and Brian J Reid. Direct inference of snp heterozygosity rates and resolution of loh detection. *PLoS Comput Biol*, 3(11):e244, Nov 2007. doi: 10.1371/journal.pcbi.0030244.

[154] J C Stephens, J A Schneider, D A Tanguay, J Choi, T Acharya, S E Stanley, R Jiang, C J Messer, A Chew, J H Han, J Duan, J L Carr, M S Lee, B Koshy, A M Kumar, G Zhang, W R Newell, A Windemuth, C Xu, T S Kalbfleisch, S L Shaner, K Arnold, V Schulz, C M Drysdale, K Nandabalan, R S Judson, G Ruano, and G F Vovis. Haplotype variation and linkage disequilibrium in 313 human genes. *Science*, 293(5529):489–93, Jul 2001. doi: 10.1126/science.1059431.

[155] Mary-Anne Enoch, Pei-Hong Shen, Ke Xu, Colin Hodgkinson, and David Goldman. Using ancestry-informative markers to define populations and detect population stratification. *J Psychopharmacol*, 20(4 Suppl):19–26, Jul 2006. doi: 10.1177/1359786806066041.

[156] S. Turnpenny, P. Ellard. *Emery's Elements of Medical Genetics*. Number 12th edition. Elsevier, London, 2005.

[157] Zippora Brownstein, Tamar Ben-Yosef, Orit Dagan, Moshe Frydman, Dvorah Abeliovich, Michal Sagi, Fabian A Abraham, Riki Taitelbaum-Swead, Mordechai Shohat, Minka Hildesheimer, Thomas B Friedman, and Karen B Avraham. The r245x mutation of pcdh15 in ashkenazi jewish children diagnosed with nonsyndromic hearing loss foreshadows retinitis pigmentosa. *Pediatr Res*, 55(6):995–1000, Jun 2004. ISSN 0031-3998 (Print). doi: 10.1203/01.PDR.0000125258.58267.56.

[158] Noa Auslender, Dikla Bandah, Leah Rizel, Doron M Behar, Mordechai Shohat, Eyal Banin, Stavit Allon-Shalev, Reuven Sharony, Dror Sharon, and Tamar Ben-Yosef. Four ush2a founder mutations underlie the majority of usher syndrome type 2 cases among non-ashkenazi jews. *Genet Test*, 12(2):289–294, Jun 2008. ISSN 1090-6576 (Print). doi: 10.1089/gte.2007.0107.

[159] Inga Ebermann, Robert K Koenekoop, Irma Lopez, Lara Bou-Khzam, Renee Pigeon, and Hanno J Bolz. An ush2a founder mutation is the major cause of usher syndrome type 2 in canadians of french origin and confirms common roots of quebecois and acadians. *Eur J Hum Genet*, 17(1):80–84, Jan 2009. ISSN 1476-5438 (Electronic). doi: 10.1038/ejhg.2008.143.

[160] Inga Ebermann, Irma Lopez, Maria Bitner-Glindzicz, Carolyn Brown, Robert Karel Koenekoop, and Hanno Jorn Bolz. Deafblindness in french canadians from quebec: a predominant founder mutation in the ush1c gene provides the first genetic link with the acadian population. *Genome Biol*, 8(4):R47, 2007. ISSN 1465-6914 (Electronic). doi: 10.1186/gb-2007-8-4-r47.

[161] B Dreyer, L Tranebjaerg, T Rosenberg, M D Weston, W J Kimberling, and O Nilssen. Identification of novel ush2a mutations: implications for the structure of ush2a protein. *Eur J Hum Genet*, 8(7):500–506, Jul 2000. ISSN 1018-4813 (Print). doi: 10.1038/sj.ejhg.5200491.

[162] M D Weston, J D Eudy, S Fujita, S Yao, S Usami, C Cremers, J Greenberg, R Ramesar, A Martini, C Moller, R J Smith, J Sumegi, and W J Kimberling. Genomic structure and identification of novel mutations in usherin, the gene responsible for usher syndrome type iia. *Am J Hum Genet*, 66(4):1199–1210, Apr 2000. ISSN 0002-9297 (Print).

[163] B Dreyer, L Tranebjaerg, V Brox, T Rosenberg, C Moller, M Beneyto, M D Weston, W J Kimberling, C W Cremers, X Z Liu, and O Nilssen. A common ancestral origin of the frequent and widespread 2299delg ush2a mutation. *Am J Hum Genet*, 69(1):228–234, Jul 2001. ISSN 0002-9297 (Print).

[164] B P Leroy, J A Aragon-Martin, M D Weston, D A Bessant, C Willis, A R Webster, A C Bird, W J Kimberling, A M Payne, and S S Bhattacharya. Spectrum of mutations in ush2a in british patients with usher syndrome type ii. *Exp Eye Res*, 72(5):503–509, May 2001. ISSN 0014-4835 (Print). doi: 10.1006/exer.2000.0978.

[165] Elena Aller, Carmen Najera, Jose Maria Millan, Juan S Oltra, Herminio Perez-Garrigues, Concepcion Vilela, Amparo Navea, and Magdalena Beneyto. Genetic analysis of 2299delg and c759f mutations (ush2a) in patients with visual and/or auditory impairments. *Eur J Hum Genet*, 12(5):407–410, May 2004. ISSN 1018-4813 (Print). doi: 10.1038/sj.ejhg.5201138.

[166] X M Ouyang, J F Hejtmancik, S G Jacobson, A R Li, L L Du, S Angeli, M Kaiser, T Balkany, and X Z Liu. Mutational spectrum in usher syndrome type ii. *Clin Genet*, 65(4):288–293, Apr 2004. ISSN 0009-9163 (Print). doi: 10.1046/j.1399-0004.2004.00216.x.

[167] E Aller, T Jaijo, M Beneyto, C Najera, S Oltra, C Ayuso, M Baiget, M Carballo, G Antinolo, D Valverde, F Moreno, C Vilela, D Collado, H Perez-Garrigues, A Navea, and J M Millan. Identification of 14 novel mutations in the long isoform of ush2a in spanish patients with usher syndrome type ii. *J Med Genet*, 43(11): e55, Nov 2006. ISSN 1468-6244 (Electronic). doi: 10.1136/jmg.2006.041764.

[168] Bo Dreyer, Vigdis Brox, Lisbeth Tranebjaerg, Thomas Rosenberg, Andre M Sadeghi, Claes Moller, and Oivind Nilssen. Spectrum of ush2a mutations in scandinavian patients with usher syndrome type ii. *Hum Mutat*, 29(3):451, Mar 2008. ISSN 1098-1004 (Electronic). doi: 10.1002/humu.9524.

[169] Frans P M Cremers, William J Kimberling, Maigi Kulm, Arjan P de Brouwer, Erwin van Wijk, Heleen te Brinke, Cor W R J Cremers, Lies H Hoefsloot, Sandro Banfi, Francesca Simonelli, Johannes C Fleischhauer, Wolfgang Berger, Phil M Kelley, Elene Haralambous, Maria Bitner-Glindzicz, Andrew R Webster, Zubin Saihan, Elfride De Baere, Bart P Leroy, Giuliana Silvestri, Gareth J McKay, Robert K Koenekoop, Jose M Millan, Thomas Rosenberg, Tarja Joensuu, Eeva-Marja Sankila, Dominique Weil, Mike D Weston, Bernd Wissinger, and Hannie Kremer. Development of a genotyping microarray for usher syndrome. *J Med Genet*, 44(2):153–160, Feb 2007. ISSN 1468-6244 (Electronic). doi: 10.1136/jmg.2006.044784.

[170] Office for National Statistics. Office for national statistics; census, april 2001. URL http://www.statistics.gov.uk/cci/nugget.asp?id=455.

[171] S Rozen and H Skaletsky. Primer3 on the www for general users and for biologist programmers. *Methods Mol Biol*, 132:365–86, 2000.

[172] N Drasdo and C M Haggerty. A comparison of the british number plate and snellen vision tests for car drivers. *Ophthalmic Physiol Opt*, 1(1):39–54, 1981.

[173] Mehdi Sadeghi, Edward S Cohn, William J Kelly, William J Kimberling, Lisbeth Tranebjoerg, and Claes Moller. Audiological findings in usher syndrome types iia and ii (non-iia). *Int J Audiol*, 43(3):136–143, Mar 2004. ISSN 1499-2027 (Print).

[174] David Baux, Lise Larrieu, Catherine Blanchet, Christian Hamel, Safouane Ben Salah, Anne Vielle, Brigitte Gilbert-Dussardier, Muriel Holder, Patrick Calvas, Nicole Philip, Patrick Edery, Dominique Bonneau, Mireille Claustres, Sue Malcolm, and Anne-Francoise Roux. Molecular and in silico analyses of the full-length isoform of usherin identify new pathogenic alleles in usher type ii patients. *Hum Mutat*, 28(8):781–789, Aug 2007. ISSN 1098-1004 (Electronic). doi: 10.1002/humu.20513.

[175] Ronald J E Pennings, Heleen Te Brinke, Michael D Weston, Annemarie Claassen, Dana J Orten, Henriette Weekamp, Annelies Van Aarem, Patrick L M Huygen, August F Deutman, Lies H Hoefsloot, Frans P M Cremers, Cor W R J Cremers, William J Kimberling, and Hannie Kremer. Ush2a mutation analysis in 70 dutch families with usher syndrome type ii. *Hum Mutat*, 24(2):185, Aug 2004. ISSN 1098-1004 (Electronic). doi: 10.1002/humu.9259.

[176] C Espinos, J M Millan, M Beneyto, and C Najera. Epidemiology of usher syndrome in valencia and spain. *Community Genet*, 1(4):223–228, 1998. ISSN 1422-2795 (Print). doi: 10.1159/000016167.

[177] G A Fishman, R J Anderson, B L Lam, and D J Derlacki. Prevalence of foveal lesions in type 1 and type 2 usher's syndrome. *Arch Ophthalmol*, 113(6):770–3, Jun 1995.

[178] H Hirakawa, H Iijima, T Gohdo, and S Tsukahara. Optical coherence tomography of cystoid macular edema associated with retinitis pigmentosa. *Am J Ophthalmol*, 128(2):185–91, Aug 1999.

[179] Michael A Sandberg, Robert J Brockhurst, Alexander R Gaudio, and Eliot L Berson. The association between visual acuity and central retinal thickness in retinitis pigmentosa. *Invest Ophthalmol Vis Sci*, 46(9):3349–54, Sep 2005. doi: 10.1167/iovs.04-1383.

[180] G A Fishman, J Cunha-Vaz, and T Salzano. Vitreous fluorophotometry in patients with retinitis pigmentosa. *Arch Ophthalmol*, 99(7):1202–7, Jul 1981.

[181] K S Mallick, R C Zeimer, G A Fishman, N P Blair, and R J Anderson. Transport of fluorescein in the ocular posterior segment in retinitis pigmentosa. *Arch Ophthalmol*, 102(5):691–6, May 1984.

[182] J R Heckenlively, B L Jordan, and N Aptsiauri. Association of antiretinal antibodies and cystoid macular edema in patients with retinitis pigmentosa. *Am J Ophthalmol*, 127(5):565–73, May 1999.

[183] Mohamed A Genead, Gerald A Fishman, and J Jason McAnany. Efficacy of topical dorzolamide for treatment of cystic macular lesions in a patient with enhanced s-cone syndrome. *Doc Ophthalmol*, Sep 2010. doi: 10.1007/s10633-010-9247-9.

[184] Gerald A Fishman and Marsha A Apushkin. Continued use of dorzolamide for the treatment of cystoid macular oedema in patients with retinitis pigmentosa. *Br J Ophthalmol*, 91(6):743–5, Jun 2007. doi: 10.1136/bjo.2006.107466.

[185] Sandeep Grover, Marsha A Apushkin, and Gerald A Fishman. Topical dorzolamide for the treatment of cystoid macular edema in patients with retinitis pigmentosa. *Am J Ophthalmol*, 141(5):850–8, May 2006. doi: 10.1016/j.ajo.2005.12.030.

[186] V C Greenstein, K Holopigian, E Siderides, W Seiple, and R E Carr. The effects of acetazolamide on visual function in retinitis pigmentosa. *Invest Ophthalmol Vis Sci*, 34(1):269–73, Jan 1993.

[187] B Haouchine, P Massin, and A Gaudric. Foveal pseudocyst as the first step in macular hole formation: a prospective study by optical coherence tomography. *Ophthalmology*, 108(1):15–22, Jan 2001.

[188] Petra Popović, Martina Jarc-Vidmar, and Marko Hawlina. Abnormal fundus autofluorescence in relation to retinal function in patients with retinitis pigmentosa. *Graefes Arch Clin Exp Ophthalmol*, 243(10):1018–27, Oct 2005. doi: 10.1007/s00417-005-1186-x.

[189] Anthony G Robson, Catherine A Egan, Vy A Luong, Alan C Bird, Graham E Holder, and Frederick W Fitzke. Comparison of fundus autofluorescence with photopic and scotopic fine-matrix mapping in patients with retinitis pigmentosa and normal visual acuity. *Invest Ophthalmol Vis Sci*, 45(11):4119–25, Nov 2004. doi: 10.1167/iovs.04-0211.

[190] Anthony G Robson, Michel Michaelides, Zubin Saihan, Alan C Bird, Andrew R Webster, Anthony T Moore, Fred W Fitzke, and Graham E Holder. Functional characteristics of patients with retinal dystrophy that manifest abnormal parafoveal annuli of high density fundus autofluorescence; a review and update. *Doc Ophthalmol*, 116(2):79–89, Mar 2008. ISSN 0012-4486 (Print). doi: 10.1007/s10633-007-9087-4.

[191] A G Robson, M Michaelides, V A Luong, G E Holder, A C Bird, A R Webster, A T Moore, and F W Fitzke. Functional correlates of fundus autofluorescence abnormalities in patients with rpgr or rims1 mutations causing cone or cone rod dystrophy. *Br J Ophthalmol*, 92(1):95–102, Jan 2008. doi: 10.1136/bjo.2007.124008.

[192] Hendrik P N Scholl, N H Victor Chong, Anthony G Robson, Graham E Holder, Anthony T Moore, and Alan C Bird. Fundus autofluorescence in patients with leber congenital amaurosis. *Invest Ophthalmol Vis Sci*, 45(8):2747–52, Aug 2004. doi: 10.1167/iovs.03-1208.

[193] S M Downes, G E Holder, F W Fitzke, A M Payne, M J Warren, S S Bhattacharya, and A C Bird. Autosomal dominant cone and cone-rod dystrophy with mutations in the guanylate cyclase activator 1a gene-encoding guanylate cyclase activating protein-1. *Arch Ophthalmol*, 119(1):96–105, Jan 2001.

[194] S M Downes, A M Payne, R E Kelsell, F W Fitzke, G E Holder, D M Hunt, A T Moore, and A C Bird. Autosomal dominant cone-rod dystrophy with mutations in the guanylate cyclase 2d gene encoding retinal guanylate cyclase-1. *Arch Ophthalmol*, 119(11):1667–73, Nov 2001.

[195] M Fleckenstein, P Charbel Issa, H A Fuchs, R P Finger, H-M Helb, H P N Scholl, and F G Holz. Discrete arcs of increased fundus autofluorescence in retinal dystrophies and functional correlate on microperimetry. *Eye (Lond)*, 23(3):567–75, Mar 2009. doi: 10.1038/eye.2008.59.

[196] Martina Jarc-Vidmar, Aleksandra Kraut, and Marko Hawlina. Fundus autofluorescence imaging in best's vitelliform dystrophy. *Klin Monbl Augenheilkd*, 220 (12):861–7, Dec 2003. doi: 10.1055/s-2003-812555.

[197] S Walia, GA Fishman, and M Hajali. Prevalence of cystic macular lesions in patients with usher ii syndrome. *Eye*, Apr 2008. ISSN 1476-5454 (Electronic). doi: 10.1038/eye.2008.105.

[198] A Edwards, G A Fishman, R J Anderson, S Grover, and D J Derlacki. Visual acuity and visual field impairment in usher syndrome. *Arch Ophthalmol*, 116(2): 165–168, Feb 1998. ISSN 0003-9950 (Print).

[199] Gerald A Fishman, Simge Bozbeyoglu, Robert W Massof, and William Kimberling. Natural course of visual field loss in patients with type 2 usher syndrome. *Retina*, 27(5):601–608, Jun 2007. ISSN 0275-004X (Print). doi: 10.1097/01.iae.0000246675.88911.2c.

[200] Graham E Holder, Mitchell G Brigell, Marko Hawlina, Thomas Meigen, Vaegan, Michael Bach, and International Society for Clinical Electrophysiology of Vision. Iscev standard for clinical pattern electroretinography–2007 update. *Doc Ophthalmol*, 114(3):111–6, May 2007. doi: 10.1007/s10633-007-9053-1.

[201] M F Marmor, A B Fulton, G E Holder, Y Miyake, M Brigell, M Bach, and International Society for Clinical Electrophysiology of Vision. Iscev standard for full-field clinical electroretinography (2008 update). *Doc Ophthalmol*, 118(1):69–77, Feb 2009. doi: 10.1007/s10633-008-9155-4.

[202] E L Chuang, D M Sharp, F W Fitzke, C M Kemp, A L Holden, and A C Bird. Retinal dysfunction in central serous retinopathy. *Eye (Lond)*, 1 (Pt 1):120–5, 1987.

[203] J C Chen, F W Fitzke, D Pauleikhoff, and A C Bird. Functional loss in age-related bruch's membrane change with choroidal perfusion defect. *Invest Ophthalmol Vis Sci*, 33(2):334–40, Feb 1992.

[204] M C Westcott, D F Garway-Heath, F W Fitzke, D Kamal, and R A Hitchings. Use of high spatial resolution perimetry to identify scotomata not apparent with conventional perimetry in the nasal field of glaucomatous subjects. *Br J Ophthalmol*, 86(7):761–6, Jul 2002.

[205] Hendrik P N Scholl, Caren Bellmann, Samantha S Dandekar, Alan C Bird, and Frederick W Fitzke. Photopic and scotopic fine matrix mapping of retinal areas of increased fundus autofluorescence in patients with age-related maculopathy. *Invest Ophthalmol Vis Sci*, 45(2):574–83, Feb 2004.

[206] Michel Michaelides, Sharon A Jenkins, Milam A Brantley, Jr, Richard M Andrews, Naushin Waseem, Vy Luong, Kevin Gregory-Evans, Shomi S Bhattacharya, Fred W Fitzke, and Andrew R Webster. Maculopathy due to the r345w substitution in fibulin-3: distinct clinical features, disease variability, and extent of retinal dysfunction. *Invest Ophthalmol Vis Sci*, 47(7):3085–97, Jul 2006. doi: 10.1167/iovs.05-1600.

[207] D T Kemp, S Ryan, and P Bray. A guide to the effective use of otoacoustic emissions. *Ear Hear*, 11(2):93–105, Apr 1990.

[208] M Cohen and D Prasher. The value of combining auditory brainstem responses and acoustic reflex threshold measurements in neuro-otological diagnosis. *Scand Audiol*, 17(3):153–62, 1988.

[209] L Pollak, L M Luxon, and D O Haskard. Labyrinthine involvement in behçet's syndrome. *J Laryngol Otol*, 115(7):522–9, Jul 2001.

[210] B Ceranić and L M Luxon. Progressive auditory neuropathy in patients with leber's hereditary optic neuropathy. *J Neurol Neurosurg Psychiatry*, 75(4):626–30, Apr 2004.

[211] A G Robson, Z Saihan, S A Jenkins, F W Fitzke, A C Bird, A R Webster, and G E Holder. Functional characterisation and serial imaging of abnormal fundus autofluorescence in patients with retinitis pigmentosa and normal visual acuity. *Br J Ophthalmol*, 90(4):472–9, Apr 2006. doi: 10.1136/bjo.2005.082487.

[212] Samantha S Dandekar, Sharon A Jenkins, Tunde Peto, Hendrik P N Scholl, Kulwant S Sehmi, Fred W Fitzke, Alan C Bird, and Andrew R Webster. Autofluorescence imaging of choroidal neovascularization due to age-related macular degeneration. *Arch Ophthalmol*, 123(11):1507–13, Nov 2005. doi: 10.1001/archopht.123.11.1507.

[213] F G Holz, C Bellmann, M Margaritidis, F Schütt, T P Otto, and H E Völcker. Patterns of increased in vivo fundus autofluorescence in the junctional zone of geographic atrophy of the retinal pigment epithelium associated with age-related macular degeneration. *Graefes Arch Clin Exp Ophthalmol*, 237(2):145–52, Feb 1999.

[214] A von Rückmann, F W Fitzke, and A C Bird. Distribution of pigment epithelium autofluorescence in retinal disease state recorded in vivo and its change over time. *Graefes Arch Clin Exp Ophthalmol*, 237(1):1–9, Jan 1999.

[215] F C Delori, C K Dorey, G Staurenghi, O Arend, D G Goger, and J J Weiter. In vivo fluorescence of the ocular fundus exhibits retinal pigment epithelium lipofuscin characteristics. *Invest Ophthalmol Vis Sci*, 36(3):718–29, Mar 1995.

[216] Catherine B Meyerle, Yale L Fisher, and Richard F Spaide. Autofluorescence and visual field loss in sector retinitis pigmentosa. *Retina*, 26(2):248–50, Feb 2006.

[217] D Baux, V Faugere, L Larrieu, S Le Guedard-Mereuze, D Hamroun, C Beroud, S Malcolm, M Claustres, and AF Roux. Umd-ushbases: a comprehensive set of

databases to record and analyse pathogenic mutations and unclassified variants in seven usher syndrome causing genes. *Hum Mutat*, 29(8):E76–E87, May 2008. ISSN 1098-1004 (Electronic). doi: 10.1002/humu.20780.

[218] David S Williams, Tomas S Aleman, Concepción Lillo, Vanda S Lopes, Louise C Hughes, Edwin M Stone, and Samuel G Jacobson. Harmonin in the murine retina and the retinal phenotypes of ush1c-mutant mice and human ush1c. *Invest Ophthalmol Vis Sci*, 50(8):3881–9, Aug 2009. doi: 10.1167/iovs.08-3358.

[219] J R Heckenlively, J A Rodriguez, and S P Daiger. Autosomal dominant sectoral retinitis pigmentosa. two families with transversion mutation in codon 23 of rhodopsin. *Arch Ophthalmol*, 109(1):84–91, Jan 1991.

[220] K A Hellner and J Rickers. Familiary bilateral segmental retinopathia pigmentosa. *Ophthalmologica*, 166(5):327–41, 1973.

[221] M T Contestabile, R Plateroti, S C Carlesimo, F Suppressa, G F Lepore, and E D'Alba. Atypical retinitis pigmentosa: a report of three cases. *Ann Ophthalmol*, 24(9):325–34, Sep 1992.

[222] A E Krill, D Archer, and D Martin. Sector retinitis pigmentosa. *Am J Ophthalmol*, 69(6):977–87, Jun 1970.

[223] A I Geltzer and E L Berson. Fluorescein angiography of hereditary retinal degenerations. *Arch Ophthalmol*, 81(6):776–82, Jun 1969.

[224] F A Abraham, M Ivry, and R Tsvieli. Sector retinitis pigmentosa: a fluorescein angiographic study. *Ophthalmologica*, 172(4):287–97, 1976.

[225] Saatci A Osman, Yaman Aylin, Gul Arikan, and Harika Celikel. Photodynamic treatment of a secondary vasoproliferative tumour associated with sector retinitis pigmentosa and usher syndrome type i. *Clin Experiment Ophthalmol*, 35(2):191–193, Mar 2007. ISSN 1442-6404 (Print). doi: 10.1111/j.1442-9071.2007.01440.x.

[226] E M Stone, A E Kimura, B E Nichols, P Khadivi, G A Fishman, and V C Sheffield. Regional distribution of retinal degeneration in patients with the proline to histidine mutation in codon 23 of the rhodopsin gene. *Ophthalmology*, 98(12):1806–13, Dec 1991.

[227] G A Fishman, E M Stone, L D Gilbert, and V C Sheffield. Ocular findings associated with a rhodopsin gene codon 106 mutation. glycine-to-arginine change in autosomal dominant retinitis pigmentosa. *Arch Ophthalmol*, 110(5):646–53, May 1992.

[228] L Schwartz, P Y Boëlle, F D'hermies, G Ledanois, and J Virmont. Blue light dose distribution and retinitis pigmentosa visual field defects: an hypothesis. *Med Hypotheses*, 60(5):644–9, May 2003.

[229] E L Berson. Retinitis pigmentosa and allied diseases: applications of electroretinographic testing. *Int Ophthalmol*, 4(1-2):7–22, Aug 1981.

[230] Ronald J E Pennings, Vedat Topsakal, Lisa Astuto, Arjan P M de Brouwer, Marietta Wagenaar, Patrick L M Huygen, William J Kimberling, August F Deutman, Hannie Kremer, and Cor W R J Cremers. Variable clinical features in patients with cdh23 mutations (ush1d-dfnb12). *Otol Neurotol*, 25(5):699–706, Sep 2004. ISSN 1531-7129 (Print).

[231] Carmen Najera, Magdalena Beneyto, Jose Blanca, Elena Aller, Ana Fontcuberta, Jose Maria Millan, and Carmen Ayuso. Mutations in myosin viia (myo7a) and usherin (ush2a) in spanish patients with usher syndrome types i and ii, respectively. *Hum Mutat*, 20(1):76–77, Jul 2002. ISSN 1098-1004 (Electronic). doi: 10.1002/humu.9042.

[232] M L Tamayo, G Lopez, N Gelvez, D Medina, W J Kimberling, V Rodriguez, G E Tamayo, and J E Bernal. Genetic counseling in usher syndrome: linkage and mutational analysis of 10 colombian families. *Genet Couns*, 19(1):15–27, 2008. ISSN 1015-8146 (Print).

[233] Zubin Saihan, Polona Le Quesne Stabej, Anthony G Robson, Nell Rangesh, Graham E Holder, Anthony T Moore Frcophth, Karen P Steel, Linda M Luxon, Maria Bitner-Glindzicz, and Andrew R Webster. Mutations in the ush1c gene associated with sector retinitis pigmentosa and hearing loss. *Retina*, Apr 2011. doi: 10.1097/IAE.0b013e31820d3fd1.

[234] Anne-Françoise Roux, Valérie Faugère, Christel Vaché, David Baux, Thomas Besnard, Susana Léonard, Catherine Blanchet, Christian Hamel, Michel Mondain, Brigitte Gilbert-Dussardier, Patrick Edery, Didier Lacombe, Dominique Bonneau, Muriel Holder-Espinasse, Umberto Ambrosetti, Hubert Journel, Albert David, Geneviève Lina-Granade, Sue Malcolm, and Mireille Claustres. Four year follow-up of diagnostic service in ush1 patients. *Invest Ophthalmol Vis Sci*, Mar 2011. doi: 10.1167/iovs.10-6869.

[235] Hiroshi Nakanishi, Masafumi Ohtsubo, Satoshi Iwasaki, Yoshihiro Hotta, Kunihiro Mizuta, Hiroyuki Mineta, and Shinsei Minoshima. Hair roots as an mrna source for mutation analysis of usher syndrome-causing genes. *J Hum Genet*, Jul 2010. doi: 10.1038/jhg.2010.83.

[236] A K Bharadwaj, J P Kasztejna, S Huq, E L Berson, and T P Dryja. Evaluation of the myosin viia gene and visual function in patients with usher syndrome type i. *Exp Eye Res*, 71(2):173–181, Aug 2000. ISSN 0014-4835 (Print). doi: 10.1006/exer.2000.0863.

[237] María José Aparisi, Gema García-García, Teresa Jaijo, Regina Rodrigo, Claudio Graziano, Marco Seri, Tulay Simsek, Enver Simsek, Sara Bernal, Montserrat Baiget, Herminio Pérez-Garrigues, Elena Aller, and José María Millán. Novel mutations in the ush1c gene in usher syndrome patients. *Mol Vis*, 16:2948–54, 2010.

[238] Terri L McGee, Babak Jian Seyedahmadi, Meredith O Sweeney, Thaddeus P Dryja, and Eliot L Berson. Novel mutations in the long isoform of the ush2a gene in patients with usher syndrome type ii or non-syndromic retinitis pigmentosa. *J Med Genet*, 47(7):499–506, Jul 2010. doi: 10.1136/jmg.2009.075143.

[239] Larrieu L Baux D Claustres M Roux AF Besnard T, Vaché C. Implication of gpr98 in usher syndrome type 2. In *International Symposium on Usher Syndrome and related Diseases.*, page 69, May May 2010.